



UNIVERSITÀ  
DEGLI STUDI  
DI PADOVA

UNIVERSITÀ DEGLI STUDI DI PADOVA  
Dipartimento di Salute della Donna e del Bambino

SCUOLA DI DOTTORATO DI RICERCA IN MEDICINA DELLO SVILUPPO E  
SCIENZE DELLA PROGRAMMAZIONE SANITARIA  
INDIRIZZO: Emato-oncologia, Genetica, Malattie Rare e Medicina Predittiva  
CICLO XXIX

**IDENTIFICATION OF ANNEXIN 2A AS A FUNDAMENTAL  
MEDIATOR OF GLIOBLASTOMA CELL DISSEMINATION  
AND POTENTIAL THERAPEUTIC TARGET**

**Coordinatore:** Ch.mo Prof. Carlo Giaquinto

**Supervisore:** Ch.mo Prof. Giuseppe Basso

**Tutor:** Dr. Luca Persano

**Dottorando:** Francesca Maule

## **TABLE OF CONTENTS**

### **1. TABLE OF CONTENTS**

### **2. SUMMARY**

### **3. SOMMARIO**

### **4. INTRODUCTION**

4.1 Gliomas and Glioblastoma Multiforme.

4.2 Glioblastoma multiforme Treatment.

4.3 Mechanisms of Glioblastoma Cell Migration and Invasion.

4.4 Annexin 2A in Tumorigenesis and Cancer Progression.

### **5. MAIN AIMS OF THE STUDY**

### **6. RESULTS**

6.1 ANXA2 expression correlates with glioma grade and patient outcome.

6.2 ANXA2 inhibition dramatically affects gene expression profile of GBM cells.

6.3 GBM cell migration and invasion are sustained by ANXA2.

6.4 ANXA2 impairment induces differentiation and inhibits proliferation of GBM cells.

6.5 An ANXA2<sup>down</sup> signature predicts GBM patient survival.

6.6 ANXA2-dependent gene signature mapping for drug repositioning.

### **7. DISCUSSION**

### **8. FUTURE PROSPECTIVES**

### **9. MATERIALS AND METHODS**

### **10. REFERENCES**

### **11. SUPPLEMENTARY TABLES**

11.1 Newman-Keuls multiple comparisons test from GSE4290.

11.2 Clinical characteristics of glioma patients included in survival and multivariate analyses.

**11.3** Differentially expressed genes in common between TCGA and GSE13041 datasets derived from comparison between ANXA2 Very Low and ANXA2 High patients.

**11.4** Primary GBM cells used in the study.

**11.5** Differentially expressed genes between Isotype and anti-ANXA2 antibody treated GBM cells.

**11.6** Summary of Log-rank analysis for ANXA2-dependent Risk Score on TCGA, GSE13041, GSE17536, E-MTAB-365 and GSE31210 cohorts of cancer patients.

**11.7** Differentially expressed genes between SiNEG and SiANXA2 transfected GBM cells.

**11.8** Antibodies used in this study.

**11.9** Sequence of primers used in this study.

## **12. ABBREVIATIONS USED IN THE TEXT**

## 2. SUMMARY

Glioblastoma multiforme (GBM) is the most devastating tumor of the brain, characterized by an almost inevitable tendency to recur after intensive treatments and a fatal prognosis. Indeed, despite recent technical improvements in GBM surgery, the complete eradication of cancer cell disseminated outside the tumor mass still remains a crucial issue for glioma patients management. In my PhD project, we identified Annexin 2A (ANXA2) as an important intracellular cytoskeletal protein expressed also on the surface of various types of cancer cells. Initially, we show that ANXA2 is over-expressed in IV grade GBM at various levels when compared to lower stage tumors. More importantly, we demonstrated that low/absent expression of ANXA2 identifies a subgroup of GBM patients endowed with better prognosis, suggesting that ANXA2 expression can be considered as an independent prognostic factor in glioma. We then analyzed the transcriptional changes associated to different levels of ANXA2 expression. In particular, we generated a series of ANXA2 dependent transcriptional signatures based on the comparison between ANXA2<sup>hi</sup> versus ANXA2<sup>lo</sup> expressing GBM patients from the TCGA and GSE13041 datasets (719 differentially expressed genes in common between the two cohorts), modulated transcripts after ANXA2 neutralization by specific antibody (855 differentially expressed genes) and the expression profiles of ANXA2 silenced cells respect to relative controls (3592 differentially expressed genes) in our primary GBM cell cultures. Interestingly, Gene Set Enrichment Analysis (GSEA) on the three different signatures obtained, revealed a negative enrichment of cell migration and mesenchymal transition related genes. These data strongly suggested the important role played by ANXA2 in GBM cell behavior and aggressiveness, allowing us to further setup strategies to specifically modulate its functions and dependent intracellular signaling. For this reason, we further analyzed ANXA2 functional activity *in vitro* in primary GBM cell cultures, demonstrating as ANXA2 is a major sustainer of GBM cell aggressiveness by regulating cellular invasion and motility together with cancer cell proliferation and differentiation status. Moreover, based on gene expression data of ANXA2 neutralized cells, we were able to test the prognostic potential of an ANXA2<sup>down</sup> signature in multiple cancer datasets, demonstrating that expression of genes regulated by ANXA2 fluctuations predict cancer patients outcome by themselves.

Finally, we then functionally mapped an ANXA2-dependent gene signature (TCGA and GSE13041 datasets analysis) by exploiting the Connectivity Map bioinformatic tool in order to identify compounds and approved drugs able to revert this signature of GBM aggressiveness. The compounds, significantly predicted to be able to counteract the ANXA2-dependent transcriptional signature, were analyzed for their ability to inhibit GBM cell invasion *in vitro* in primary GBM cultures. Finally, we applied ANXA2 dependent transcriptional signatures, previously generated from our primary GBM cells, to the QUADrATiC tool, which was allowed the exploration of a larger database of reference cell lines and perturbagens.

### 3. SOMMARIO

Il Glioblastoma Multiforme (GBM) è il tumore cerebrale più aggressivo, caratterizzato da una prognosi infausta e dall'inevitabile tendenza a ricadere anche in seguito ad un trattamento intensivo. Nonostante i recenti miglioramenti tecnici nella chirurgia del GBM, la sua completa rimozione rimane ad oggi uno dei maggiori problemi legati all'insuccesso terapeutico di questi pazienti. Questo studio si focalizza sulla caratterizzazione di annessina 2A (ANXA2), proteina presente in diversi compartimenti delle cellule normali e ritrovata anche sulla superficie di diversi tipi di cellule tumorali. Con lo sviluppo di questo progetto, abbiamo dimostrato che ANXA2 è espressa ad alti livelli nei gliomi di IV grado rispetto ai gliomi di grado minore e che una bassa/nulla espressione di ANXA2 identifica un sottogruppo di pazienti caratterizzati da una prognosi migliore, suggerendo come l'espressione di ANXA2 possa essere considerata un fattore prognostico indipendente nei gliomi.

Successivamente, con lo scopo di analizzare i cambiamenti trascrizionali associati ai differenti livelli di espressione di ANXA2, abbiamo generato una signature trascrizionale ANXA2-dipendente utilizzando i dati provenienti dai dataset pubblici TCGA e GSE13041 e basata sul confronto tra pazienti esprimenti alti livelli di ANXA2 e pazienti esprimenti bassi livelli di questa proteina (719 geni differenzialmente espressi in comune tra le due coorti). Sono state quindi generate due signature ANXA2-dipendenti basate rispettivamente sui trascritti modulati in seguito alla neutralizzazione di ANXA2 con anticorpo specifico (855 geni differenzialmente espressi) e tramite silenziamento (3592 geni differenzialmente espressi), in colture primarie di GBM. L'analisi di gene set enrichment (GSEA) condotta sulle tre signature, ha rivelato un arricchimento negativo di geni legati ai processi di migrazione cellulare e transizione epitelio-mesenchimale. Questi dati hanno fortemente suggerito l'importante ruolo svolto da ANXA2 nel comportamento e nell'aggressività delle cellule di GBM, portandoci pertanto a programmare differenti strategie per modulare le sue funzioni e le vie di segnale intracellulare ad essa correlate. Per questo motivo, è stata condotta una serie di analisi funzionali in vitro in cellule primarie di GBM, dimostrando come ANXA2 sia un principale mediatore dell'aggressività di questo tumore attraverso la regolazione di processi quali motilità cellulare, proliferazione e differenziamento.

Inoltre, basandoci sul profilo d'espressione genica di cellule di GBM in cui abbiamo inibito la funzione di ANXA2, abbiamo validato il potenziale prognostico di una signature "ANXA2down" (basata sui geni maggiormente down-regolati in cellule di GBM trattate con anticorpo neutralizzante ANXA2) in diversi dataset pubblici, dimostrando come l'espressione di geni regolati dai livelli di ANXA2 sia in grado di predire l'andamento dei pazienti.

Infine, la signature precedentemente generata dai dataset TCGA e GSE13041 è stata mappata funzionalmente utilizzando il tool bioinformatico Connectivity Map con lo scopo di identificare composti in grado di revertire tale signature. I composti identificati sono stati analizzati successivamente per la loro abilità di inibire il processo di invasione in vitro in colture primarie di GBM. Inoltre, le signature ANXA2-dipendenti, ottenute dalle precedenti analisi (cellule inibite/silenziate per ANXA2), sono state applicate al tool QUADrATiC. Ciò ha permesso di approfondire i risultati grazie all'utilizzo di un database più ampio che si basa sullo studio di un numero maggiore di composti approvati in numerose linee cellulari.

## 4. INTRODUCTION

### 4.1 Gliomas and Glioblastoma Multiforme.

Gliomas are primary brain tumors that arise from neural cells called glial cells [1]. As described by the World Health Organization (WHO) classification [2], malignant diffuse gliomas are comprised of astrocytic, oligodendroglial, and mixed oligoastrocytic neoplasms based on morphology, and then are further subdivided by tumor grade based on additional histological features in the tumor. Lower grade tumors (such as grade I-II tumors) are characterized by well differentiated cells while nuclear atypias and mitotic activity are required criteria for grade III lesions. The presence of necrosis or microvascular proliferation is required for the diagnosis of grade IV astrocytomas, named glioblastoma multiforme (GBM). While 90-95% of GBM arise de novo and are considered “primary,” about 5-10% arise from lower-grade gliomas in younger patients and are termed “secondary” [3].

Glioblastoma multiforme is the most common primary malignant brain tumor in the adult [4]. Together with grade III anaplastic astrocytoma, these tumors embrace the clinical entity termed “malignant glioma”. Extensive genomic characterization gave a high resolution picture of the molecular alterations underlying this tumor providing the emerging view that “GBM” represents several histologically similar but molecularly heterogeneous diseases. Indeed, World Health Organization classification has recently incorporated molecular information into diagnoses, which is made by both identifying and characterizing the physical appearance and growth rate as well as genetic features. The use of “integrated” phenotypic and genotypic parameters for CNS tumor classification adds a level of objectivity and narrowly defined diagnostic entities than in prior classifications, which in turn should lead to greater diagnostic accuracy as well as improved patient management and more accurate determinations of prognosis and treatment response [5].

GBM is a highly heterogeneous tumor with individual histologic hallmarks including high cell density, intratumoral necrosis, vascular hyperplasia and invasion through brain parenchyma [6]. Symptoms of disease depend on the specific location of the tumor, and diagnosis is most commonly made following surgical resection. The prognosis for patients with GBM is often very poor (only 2% of patients aged 65 years or older, and only 30% of those under the age of 45 years at diagnosis, survive for 2 years or more), and treatments to cure this cancer have yet to be devised.



Due to its cellular heterogeneity and the intrinsic ability of invading neighboring normal tissues, GBM is almost incurable. Despite decades of efforts in trying to improve surgical approaches and chemotherapy protocols, GBM patients display a median survival of only 17 months [7, 8]. Tumor cells remaining at the edge of the cavity after surgical removal of the mass appear to be resistant to the gold standard treatments, since the majority of GBM rapidly recur within 2-3cm of the original tumor site, giving rise to cancers with an even more aggressive and resistant phenotype (Figure 1). There are at least four different reasons possibly contributing to the recurrent phenotype of GBM tumors and their resistance to therapy:

1. Brain is a terminally differentiated organ with low or absent cellular turnover that impede the application of ablative therapies [6].
2. GBM masses can often localize and invade functional brain areas that make impossible for the surgeons to totally remove pathologic and cancer infiltrated tissues, without affecting cognitive processes or motor activities, thus unequivocally affecting patient's outcome [9].
3. Blood Brain Barrier (BBB) protects the CNS, preventing many systemically administered chemotherapeutics to reach tumor sites. For this reason, many chemotherapeutic strategies, that have shown to be effective in other malignancies, could not be applicable in the context of primary brain tumors [6].
4. GBM are characterized by a variety of genetic abnormalities. This heterogeneity may raise a therapeutic challenge, because cells bearing different abnormalities might differently respond to therapy.
5. GBM is one of the tumors in which cancer stem cells (CSCs) were identified. These stem-like cells, called glioma stem cells (GSCs), express both neuronal and astroglial markers of differentiation, together with several key determinants of neural stem cell fate. These findings confirmed that brain tumors contain transformed, undifferentiated neural precursors, indicating that GSCs have the ability to self-renew, proliferate and express typical markers of stem cells, such as the cell surface marker CD133, normally expressed on highly clonogenic and multipotent stem cells in human central nervous system (CNS) precursors [10]. GSCs are thought to be responsible for maintaining these tumors after therapy and repopulating them after gross total resection. Therefore these cells are important targets for treatment. Several embryonic signaling pathways, such as Notch, Hedgehog, and Hif-1 $\alpha$  have been reported to

help maintain these GSCs and thus provide potential targets for treating these extremely malignant cancer cells [11].

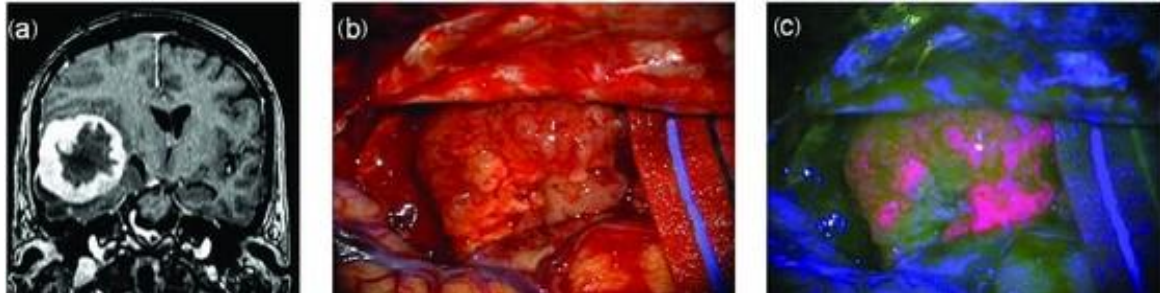


**Figure 1.** F 63/Y, preoperative MRI scan showing a large temporal high grade glioma (a). Intraoperative view: tumor resection under white (b) and blue (c) light till the complete removal of lesion. Histological report: glioblastoma (astrocytoma grade IV sec WHO). Reproduced from “Della Puppa A, et al. 5-Aminolevulinic Acid Fluorescence in High Grade Glioma Surgery: Surgical Outcome, Intraoperative Findings, and Fluorescence Patterns, Hindawi Publishing Corporation BioMed Research International Volume 2014” [12].

#### 4.2 Glioblastoma Multiforme Treatment.

Since GBM presents different phenotypic patterns and molecular signaling activation in distinct regions of the tumor mass, the pathological characterization can be influenced by the site of sample collected by the surgeon throughout the tumor [13]. In this context, O(6)-methylguanine-DNA methyltransferase (MGMT) protein expression and promoter methylation status are considered important prognostic factors [14]. This issue becomes particularly crucial because in the modern neuro-oncological setting, several diagnostic and prognostic markers are commonly analyzed to predict tumor grade and the consequential therapeutic approach. In addition, biomarkers are pivotal in the selection of glioma patients for their recruitment into clinical trials following surgery. In this sense, site of the tumor sample collection could represent a remarkable bias for both selection and stratification of patients. Due to its great heterogeneity, the current standard of care for GBM management is a multimodal approach comprising of maximal safe surgical resection, post-operative radiation therapy (RT), and concurrent and adjuvant temozolomide (TMZ). It is widely accepted that surgery alone cannot cure GBM because of tumor dissemination, however it provides fast mass reduction, with reported survival consequences [8]. Chemotherapy also has major limitations since most drugs cannot cross the blood brain barrier and the penetration into brain cells is limited.

Degree of tumor removal has been shown to strongly influence overall survival of patients [15]. Although maximal resection (MR) could be achieved only in a quote of patients ( $\approx 40\%$ ), it seems to significantly increase their survival by allowing a more efficient removal of disseminated tumor cells [16, 17]. Nevertheless, MR is challenging to accomplish, because of the complexity in recognizing tumor boundaries at GBM margins [9]. Moreover, relevance of extent of resection in surgical management of these tumors is clearly supported by the knowledge that almost all GBM patients experience recurrence within 2-3cm from previous surgical cavity, despite achievement of MR and multimodal treatments [18, 19].

For this reason, 5-aminolevulinic acid (5-ALA) staining of tumors cells during surgery has been recently adopted to intra-operatively identify GBM cells as fluorescent, with documented survival benefits [20, 21]. 5-ALA-derived fluorescence accumulates in distinct GBM regions and make tumour cells easily identifiable during surgery [22], with 100% predictive value in 5-ALA bright fluorescence areas [16, 23]. After maximal surgical resection, standard treatment consists of 6 weeks of radiotherapy (dose: 60Gy), together with concomitant chemotherapy with TMZ ( $75\text{mg}/\text{m}^2$  daily). Once chemo-radiotherapy is complete, a minimum of 6 months of adjuvant treatment with TMZ is started (dose:  $150\text{-}200\text{mg}/\text{m}^2$  for 5 days every 28 days) [8].

TMZ is a monofunctional methylating agent which is spontaneously activated in aqueous solution into the dacarbazine metabolite 5-(3-methyl-1-triazeno)imidazole-4-carboxamide. When TMZ is combined with radiotherapy in patients with newly diagnosed GBM, survival is significantly prolonged [8]. It exerts its anticancer property by adding methyl adducts to DNA, which eventually leads to apoptosis. TMZ achieves its cytotoxic effect mainly by methylating guanine residues in DNA at O6 position. This adduct can be removed by the DNA repair protein O6-methylguanine-DNA-methyltransferase (MGMT), which is heterogeneously expressed in GBM [4, 24, 25].

Recently, two phase III clinical trials investigated the addition of bevacizumab to standard treatment with TMZ. GBM promotes secretion of vascular endothelial growth factor (VEGF), which induces vascularization and increases capillary permeability of the blood brain barrier, subsequently causing extracellular edema [26, 27]. Bevacizumab (BV) is a humanized monoclonal antibody targeting VEGF and was first approved in the US for glioblastoma in 2009 [28]. Blocking the VEGF pathway restores the abnormal tumor vasculature to a more normal state, reducing vascular permeability and the regional cerebral blood volume around

the tumor in addition to decreasing peritumoral edema [29]. Although the addition of BV to the conventional standard therapy for newly diagnosed glioblastoma prolonged the progression-free survival time and the performance status of patients, it failed to extend overall survival time. Since recurrence of malignant glioma is often local, a further consideration can be done about loco-regional therapies. Gliadel wafers are a biodegradable polymer containing 3.85% carmustine (1,3-bis[2-chloroethyl]-1-nitrosourea [BCNU]), which are implanted in the resection cavity, delivering carmustine directly at the time of surgery. BCNU may alkylate the nucleoprotein and interfere with the DNA synthesis and repair, and the carbonylation of nucleoprotein lysine residues can also decrease RNA and protein synthesis [30]. However, use of carmustine wafers is currently a content of controversy. Westphal et al believed that local chemotherapy with carmustine wafers offers a survival benefit to patients with newly diagnosed GBM [31]. Affronti et al also emphasized that the BCNU wafer therapy is well tolerated and has a survival benefit compared with radiation alone [32]. Conversely, De Bonis et al showed that there was no significant improvement in the outcome by adding BCNU wafers and the toxicity after Gliadel use was significantly higher [33]. Currently, treatment with BCNU wafers has been excluded in some clinical trials of new chemotherapies because of the potential toxicities and lack of reliable survival statistics [34]. At present, several clinical studies have looked at the use of various pharmacological compounds such as integrin inhibitors (cilengitide), other antiangiogenics (cediranib), and vaccines against the epidermal growth factor receptor (EGFR), which is aberrantly expressed/activated in 30% of patients. Another innovative strategy is the application of the NovoTTF-110A device for several hours daily, which delivers alternating intermediate-frequency electrical fields (100-300kHz) as an adjunct to standard treatment. Immunotherapy has not demonstrated yet any conclusive results to date [35].

All these data highlight the urgent need for the identification of additional strategies to counteract the intrinsic GBM drug resistance. In this context, the Connectivity Map database is a powerful bioinformatic tool for drug repositioning, able to identify perturbagens predicted to revert the gene signature of a specific cancer to a less aggressive or drug-sensitive transcriptional profile [36, 38]. The recently developed QUADrATiC tool allows the exploration of a larger database of reference cell lines and perturbagens, making it attractive for a drug repurposing approach also against GBM [39].

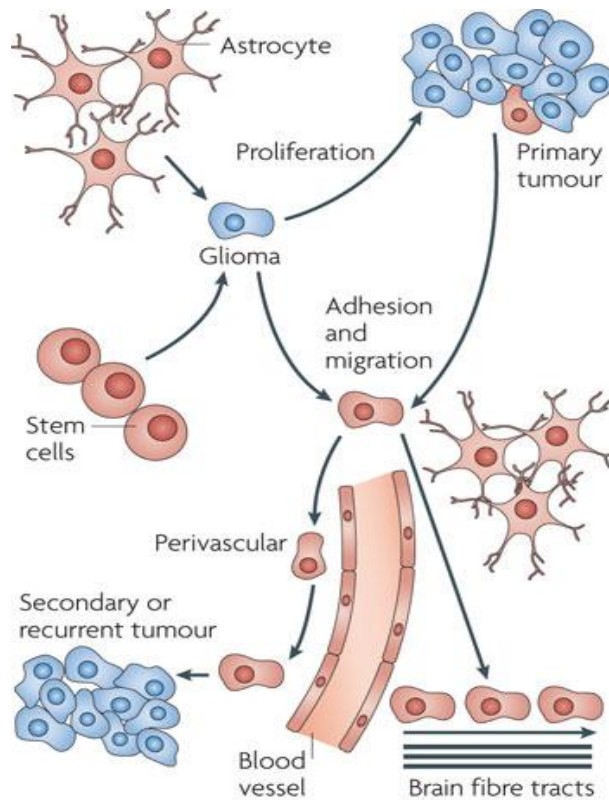
### **4.3 Mechanisms of Glioblastoma Cell Migration and Invasion.**

One of the characteristics of malignant gliomas that makes them universally fatal is their ability to infiltrate normal brain parenchyma. The rapid proliferation of GBM cells changes the tumor microenvironment, which becomes hypoxic, acidic, and poor of glucose and other nutrients. Tumor cells must adapt to these changes to survive and thus they shift from a proliferative to a migratory phenotype in order to reach a more favourable environment. Moreover, over time secreted cytokines diffuse and generate concentration gradients that are sensed by GBM cells, leading to the detachment and migration of these cells away from the primary tumor [40].

While other aggressive cancers metastasize by travelling through the circulatory or lymphatic systems to organs, high-grade glioma cells rarely metastasize outside of the brain and instead actively migrate through two types of extracellular space: 1) the perivascular space that is found around all blood vessels, and 2) the spaces in between the neurons and glial cells which makes up the brain parenchyma and white matter fiber tracts. The mechanisms underlying migration and invasion of GBM cells are complex and involve a number of sequential steps that require the adhesion of tumour cells to resident cells or matrix components, remodelling and degradation of this matrix and successful invasion of the infiltrating cells into the modified region (Figure 2).

First, tumor cells become morphologically polarized and develop membrane protrusions allowing the cells to reach forward and attach to the extracellular matrix (ECM). During this process, invasive cells alter the cell shape and volume in order to move through differently sized spaces, including the extremely small spaces in normal brain [41]. In addition to gaining mobility, invasive glioma cells must be able to interact with multiple components of the ECM, which provides ligands that tumor cells can anchor to. Several studies have shown that tumors influence the nearby stromal cells, causing reorganization of the structure and composition of the ECM. These changes in the ECM then further enhance tumor growth and invasion [42]. The ECM is composed of a network of fibrous proteins, glycoproteins and proteoglycans which form a scaffold to which cancer cells adhere [43]. While all tissues contain ECM, the composition, dimension and elasticity of the ECM differs between tissue types depending on tissue function [44]. ECM integrity is important in maintaining tissue-specific function, therefore, loss of ECM integrity results in the release of ECM-bound signalling molecules and changes in the tensional forces exerted on the cell [45]. Signalling

molecules and biomechanical perturbation trigger intracellular signalling cascades that change gene expression which facilitate either ECM degradation or synthesis of ECM components [46]. Generally, cells are inherently motile, but this is tightly regulated in various stages, such as embryological development, and in physiological responses, such as wound healing and immune-response. In GBM cells, motility becomes dys-regulated allowing them to be highly migratory [47]. Besides being able to migrate, these cells must be able to get through the physical barrier, ECM, by degrading its constituting proteins in order to create a path for invasion. Remodelling and degradation of ECM encompasses both secretion of altered matrix components and proteolytic modification of the existing matrix by proteases whose expression and activity is regulated by a number of interactive factors [48]. Finally, the migration and thus completed invasion of the GBM cells into the modified region is stimulated by a vast variety of soluble factors that are secreted either by the tumour cells themselves or by the surrounding stroma. These factors act in an autocrine or paracrine fashion, inducing cell migration and proteolytic activity. Alternatively, tumour cells may communicate with specific distant targets through secreted microvesicles that contain growth factors and receptors, functional mRNAs, and miRNAs [49-51]. For all these reasons, any imbalance in the expression of proteases, receptors and soluble factors could dramatically impact the complex process of cancer cell invasion.



Nature Reviews | Cancer

**Figure 2.** Mechanisms of glioblastoma cell migration and invasion. Reproduced from “Christian C. Naus & Dale W. Laird, Implications and challenges of connexin connections to cancer, Nature Reviews Cancer, June 2010” [52].

#### 4.4 Annexin2A in Tumorigenesis and Cancer Progression.

Annexin A2 gene (also called p36, annexin II, ANXA2, calpactin I, lipocortin II, chromobindin VIII, or placental anticoagulant protein IV) [53], is located on chromosome 15q22.2 and its transcription and translation give a 36kDa protein [54] expressed in many cellular types including: endothelial cells, macrophages, mononuclear cells and also cancerous cells. ANXA2 contains three distinct functional regions: the N-terminal region, the C-terminal region, and the core region. The N-terminal region contains the tissue plasminogen activator (tPA)- [55] and S100/A10 (also called p11)-binding sites [56]. The C-terminal region contains the F-actin- [57], heparin- [58] and plasminogen-binding sites [59]. The core region of ANXA2 contains the calcium and phospholipid-binding site [60]. The core domain contains four repeats, and each repeat features five alpha-helices that give rise to two annexin-type calcium-binding sites with the sequence GxGT-[38 residues]-D/E. ANXA2 is activated in a calcium-dependent manner and undergoes a conformational change that exposes a

hydrophobic amino acid to form a heterotetramer with p11 that shows a high affinity for phospholipids [61]. ANXA2 exists both as a monomer and a heterotetramer. The ANXA2 monomer is an intracellular 38kDa protein while the ANXA2 heterotetramer, consisting of two subunits of monomers and two subunits of p11 proteins (also known as S100A10), localized to the plasma membrane (Figure 3) [62].

Many studies have reported increased expression of ANXA2 in cancer tissues compared with normal tissues [63, 64] and the up-regulation of ANXA2 expression in pancreatic, colorectal, and brain tumors was directly correlated with advanced clinical stage [65, 66]. In particular, ANXA2 has been detected at high levels in fetal brain during the period when radial glia proliferate, instead of normal adult brain where it was not detected, suggesting that its expression might be important during brain development and differentiation of brain stem cells [66]. Higher ANXA2 expression was also observed in metastatic breast cancer and colon cancer cells compared with the non-metastatic cells [67]. Furthermore, a recent study demonstrated a correlation between high ANXA2 levels and a more aggressive prostate cancer phenotype [68]. Despite various researches confirming either an up or down regulation of ANXA2 in various tumour types, the exact mechanism that regulates its expression at both gene and protein level are poorly understood. Several studies suggest that ANXA2 plays an essential role in regulating cancer cell adhesion [69, 72], cytoskeleton structures and actin remodeling, which are both essential processes for cancer cell migration [61, 73].

ANXA2 binds with plasminogen and tissue plasminogen activator on the cell surface, which leads to the conversion of plasminogen to plasmin, which plays a key role in the activation of metalloproteinases and degradation of extracellular matrix components, essential for metastatic progression. Indeed, ANXA2 is a well-known facilitator of ECM degradation through its ability to simultaneously interact with the cytoskeletal, membrane and extracellular matrix components, thereby providing a structural link between ECM components and proteolytic enzymes [74, 76], reviewed by Roda et al. [77].

Initial evidence for the involvement of ANXA2 in tumor adhesion was discovered in RAW117 large cell lymphoma cells [78]. This study demonstrated that the binding of RAW117 tumor cells to endothelial cells (ECs) was mediated by ANXA2 expressed on the surface of RAW117, and this binding was inhibited by specific antibodies against ANXA2, reinforcing the role of ANXA2 in the tumor cell adhesion process. Recently, other studies have demonstrated that the adhesion between breast cancer cells and ECs is mediated by



interactions between ANXA2 and S100A10. ANXA2 expressed on the surface of breast cancer cells interacts with S100A10 located on microvascular ECs, facilitating the process by which cancer cells form cell-cell contact with microvascular ECs [79]. The contribution of ANXA2 to tumor invasion and metastasis by interacting with its potential invasion-associated protease proteins as well as the actin cytoskeleton, has been reported in many advanced human tumors. In breast cancer, for example, ANXA2 was found to be over-expressed in the highly invasive cell line MDA-MB-231 compared with a poorly invasive cell line MCF-7 [63]. In MCF-7/ADR cells, the administration of adriamycin increased the expression of ANXA2 consistent with the enhancement in cell proliferation and invasion, suggesting the involvement of ANXA2 in cancer cell invasion [80]. Shiozawa et al. (2008) also reported that ANXA2 regulates the adhesion and migration of prostate cancer cells to osteoblasts and endothelial cells [81].

In addition, the reduction in ANXA2 expression by siRNA or neutralizing antibodies significantly inhibited the motility and invasion of ovarian cancer cells [82]. A study by Zhao et al. [83] reported that ANXA2 interaction with a member of the immunoglobulin family (HAb18G/CD187) promotes invasion and migration of human hepatocellular carcinoma cells (FHCC-98 cells) *in vitro*. ANXA2 catalyzes the conversion through the interaction with tPA, thus efficiently enforcing the effects of plasmin on tumor angiogenesis and tissue remodeling, MMPs, latent growth factor activation and ECM degradation leading to tumor progression and metastasis [53, 84, 85]. Together these studies indicate that ANXA2 plays an important role in promoting adhesion, migration and subsequent metastasis of cancer cells. While the majority of ANXA2 is found in the heterotetrameric form associated with the membrane and the actin cytoskeleton, monomeric ANXA2 is found in the nucleus [86]. Here, ANXA2 has been shown to play an important role in DNA synthesis and mRNA transport and translation after identification of a small population existing in the nucleus and a NES in the N-terminus of this protein that regulates its nuclear export [86, 87]. Increasing evidence points to the participation of the multifunctional protein ANXA2 in mRNA localization as well as the translation of certain mRNAs on cytoskeleton-bound polysomes, and thereby in the regulation of the biosynthesis of specific proteins, such as c-Myc and ANXA2 itself, which are linked to cellular transformation. ANXA2 is most likely activated by signaling pathways, which result in its post-translational modifications and modulate its binding to various ligands. Positive and polar residues in helices C-D in domain IV of ANXA2 bind to cis-acting elements in the

3'-UTRs of its cognate, c-myc, collagen prolyl 4-hydroxylase- $\alpha$ (I) and N-methyl-D-aspartate R1 mRNAs, thus contributing to post-transcriptional regulation of the expression of specific genes [88, 89].

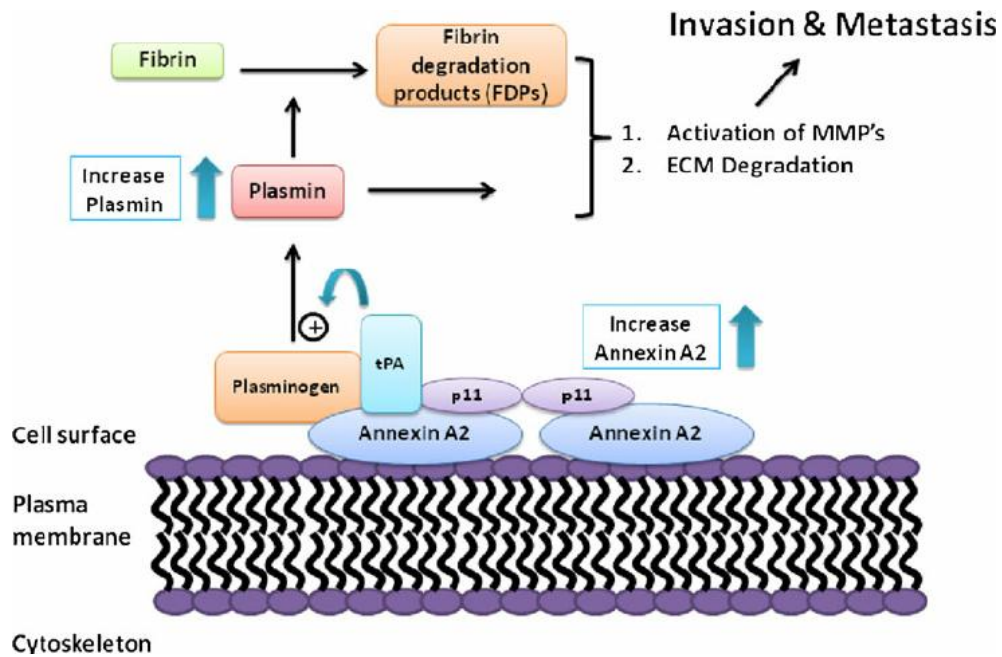


**Figure 3.** Proposed mechanism of ANXA2 promoting cancer metastasis in the plasminogen activation system. ANXA2 heterotetramer on the cell surface binds to t-PA and activates plasminogen conversion to plasmin. Plasmin results in activation of MMPs and lead to ECM degradation. Increased ANXA2 expression results in increased plasmin generation and enhances cancer invasion and metastasis. Reproduced from “Lokman NA1, Ween MP, Oehler MK, Ricciardelli C. The role of annexin A2 in tumorigenesis and cancer progression. *Cancer Microenviron*, 2011” [82].

## 5. MAIN AIMS OF THE STUDY

Glioblastoma multiforme (GBM) is the most devastating tumor of the brain, characterized by an almost inevitable tendency to recur after intensive treatments and a fatal prognosis, with a patients median survival of only 17 months. Indeed, despite recent improvements in GBM surgery, the complete eradication of cancer cell disseminated outside the tumor mass still remains a crucial issue for glioma patients management. These considerations make particularly relevant the identification of new targets and compounds able to counteract the severe effects of GBM cell invasion and dissemination. In this context, ANXA2 has been recently associated with cell dissemination and metastasis in many cancer types, thus making it an attractive putative regulator of cell invasion and potential therapeutic target also in GBM.

The main aims of this study are:

1. To better understand the biological and clinical significance of ANXA2 expression in GBM.
2. To investigate a possible ANXA2 signature with prognostic value.
3. To setup different strategies to target ANXA2 (neutralizing antibodies, siRNA, drugs) and evaluate the effects on GBM cells.
4. To *in vitro* screen a selection of compounds generated by the Connectivity Map bioinformatic tool based on the effects on established primary GBM cells in terms of cell proliferation, motility and invasion.

## 6.1 RESULTS

### 6.1 ANXA2 expression correlates with glioma grade and patient outcome.

To evaluate the impact of ANXA2 expression on glioma aggressiveness, we firstly performed ANXA2 IHC on a series of 89 gliomas. IHC staining disclosed that ANXA2 protein levels are significantly higher in GBM ( $p < 0.0001$ ) compared to less aggressive tumors (Figure 4A, 4B). To validate our results, we next retrieved ANXA2 gene expression values from GSE4290 [90] and GSE7696 [91] glioma patients cohorts confirming a significant over-expression of ANXA2 transcript in gliomas relative to control tissues and its progressive increase with tumor grade (Figure 4C, 4D and Supplementary Table 1). We then correlated ANXA2 IHC scores with clinical outcome of patients in terms of progression-free and overall survival (PFS and OS). In particular, glioma patients with “Very Low” ANXA2 IHC score ( $< 25^{\circ}$  percentile) show a significantly prolonged PFS and OS when compared with remaining “ANXA2 High” patients (Table 1 and Figure 5A-5D). Since this result could be partially biased by an unbalanced distribution of low grade tumors (grade II-III and secondary) in the ANXA2 Very Low subgroup, we then analyzed the impact of ANXA2 IHC score only in GBM patients. Importantly, GBM patients with an ANXA2 Very Low score ( $< 25^{\circ}$  percentile) display a significant increase in PFS and OS compared to all other GBMs (Figure 4E, 4F, Table 1 and Figure 5E, 5F), thus strengthening the correlation of ANXA2 with GBM aggressiveness. In order to validate these results, we analyzed ANXA2 gene expression data from two independent cohorts of GBM patients (the TCGA dataset [92, 93] and GSE13041 [94]) and correlated its expression to patient outcome. Log-rank analysis confirmed that GBM patients expressing “Very Low” levels of ANXA2 mRNA ( $< 25^{\circ}$  percentile) survived significantly longer in terms of OS (Figure 4G, 4H and Table 1) and PFS (Table 1 and Figure 6).

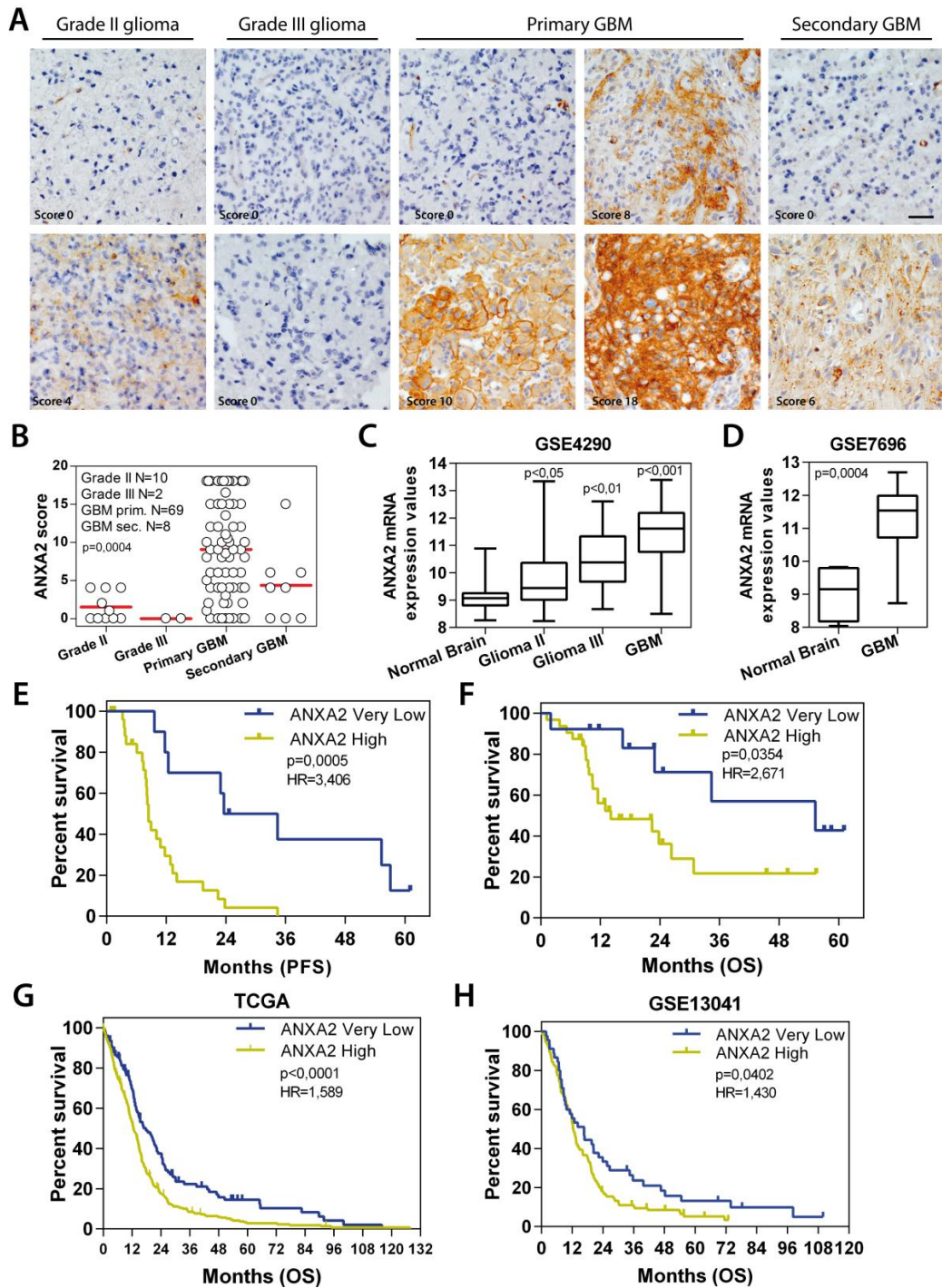


**Figure 4.** ANXA2 is over-expressed in GBM and positively correlates with bad prognosis. (A) Representative ANXA2 IHC staining performed on grade II, III and IV gliomas and secondary GBMs. Original magnification 20x; bar: 50 $\mu$ m. (B) ANXA2 protein expression levels represented as IHC scores in 10 grade II gliomas, 2 grade III gliomas, 69 GBM and 8 secondary GBM samples. (C and D) Box plots showing ANXA2 gene expression in samples retrieved from GSE4290 and GSE7696 datasets respectively. p values have been calculated relative to Normal Brain samples. (E and F) Kaplan Meier curves showing the impact of ANXA2 IHC score on GBM patient outcome in terms of progression-free (PFS) (E) and overall survival (OS) (F). (G and H) Validation of prognostic potential of ANXA2 mRNA expression in TCGA (G; N=519 patients) and GSE13041 (H; N=191) datasets.

**Table 1.** Summary of Log-rank analysis results on patients groups.

<i>Tumour type (origin of data)</i>	<i>Survival</i>	<i>ANXA2 status</i>	<i>Median Survival (months)</i>	<i>Log-rank (Mantel-Cox) p value</i>	<i>Hazard Ratio (logrank) High/Very Low</i>
<i>Gliomas from IHC</i>	PFS	ANXA2 High	9.6	<0.0001	3.888
		ANXA2 Very Low	34.6		
	OS	ANXA2 High	22.9	0.0282	3.018
		ANXA2 Very Low	N.D.		
<i>GBM from IHC</i>	PFS	ANXA2 High	8.4	0.0005	3.406
		ANXA2 Very Low	29		
	OS	ANXA2 High	14.1	0.0354	2.671
		ANXA2 Very Low	55.3		
<i>GBM from TCGA</i>	PFS	ANXA2 High	8.3	<0.0001	1.651
		ANXA2 Very Low	10.89		
	OS	ANXA2 High	12.6	<0.0001	1.589
		ANXA2 Very Low	17.76		
<i>GBM from GSE13041</i>	OS	ANXA2 High	12.5	0.0402	1.43
		ANXA2 Very Low	16.6		

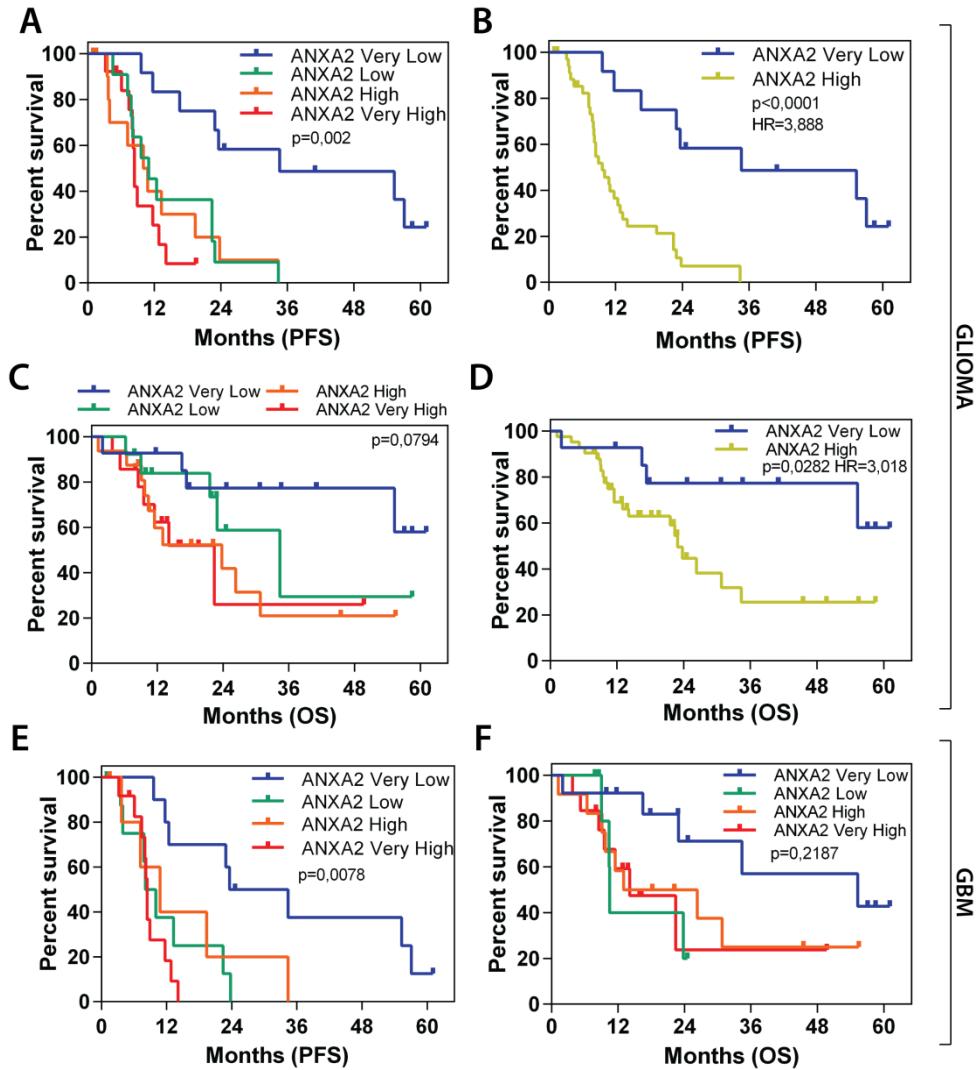


**Figure 5.** ANXA2 protein expression impacts glioma patient survival. (A-D) Kaplan Meier curves showing PFS and OS of glioma patients divided in four subgroups (A and C) depending on ANXA2 IHC score (ANXA2 Very Low: IHC score <25° percentile; ANXA2 Low: IHC score <50° percentile; ANXA2 High: IHC score <75° percentile; ANXA2 Very High: IHC score ≥75° percentile). Right panels reports PFS (B) and OS (D) of glioma patients divided in two subgroups depending on ANXA2 IHC score (ANXA2 Very Low: IHC score <25° percentile; ANXA2 High: IHC score >25° percentile). (E and F) Kaplan Meier curves showing PFS (E) and OS (F) of GBM patients divided in four quartiles on the basis of ANXA2 IHC score as previously reported.

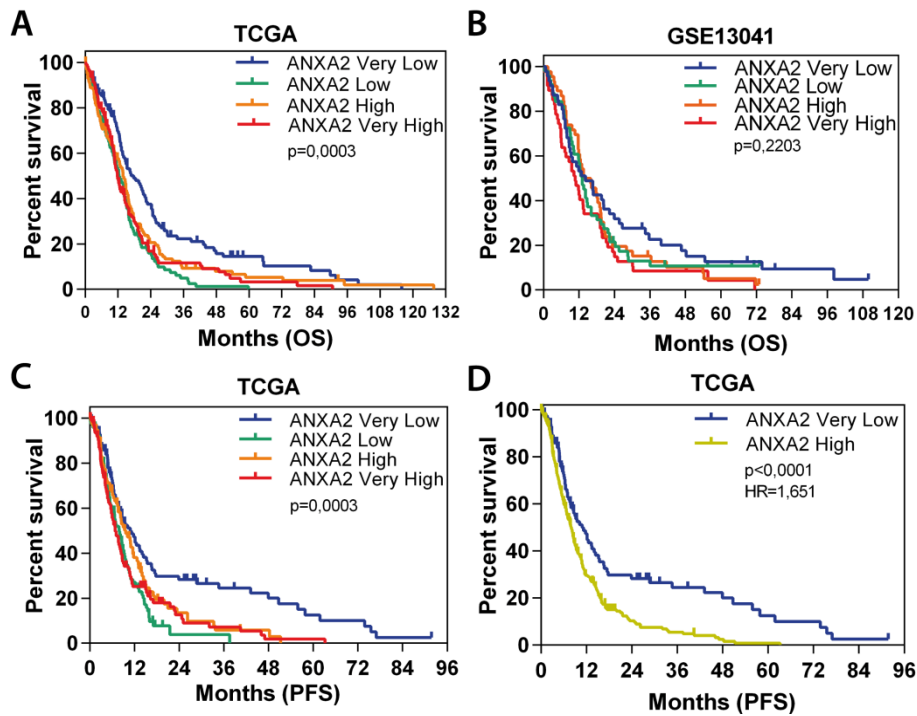


**Figure 6.** ANXA2 mRNA expression impacts GBM patient survival. (A and B) Kaplan Meier curves showing OS of GBM patients retrieved from TCGA (A; N=519 patients) [92, 93] or GSE13041 (B; N=191 patients) [94] datasets. GBM patients have been divided in four quartiles on the basis of ANXA2 mRNA expression levels as previously described. (C and D) Kaplan Meier curves showing PFS of GBM patients from TCGA divided in four quartiles (C) or in two subgroups (D; < or  $\geq 25^{\text{th}}$  percentile) on the basis of ANXA2 mRNA expression levels.



Then, we assessed the prognostic potential of ANXA2 IHC score in our cohort of patients (Supplementary Table 2) by Cox-regression (multivariate) analysis which demonstrated that ANXA2 IHC score is an independent prognostic factor for PFS (p=0.041; Table 2). Intriguingly, when considering only GBMs, ANXA2 score retains an even stronger prognostic value for PFS (p=0.029; Table 2).

**Table 2. Multivariate analysis**

<i>Variables</i>	<i>Progression Free Survival</i>		<i>Overall Survival</i>	
	<i>Univariate (p value)</i>	<i>Multivariate (p value)</i>	<i>Univariate (p value)</i>	<i>Multivariate (p value)</i>
<b>Glioma (grade II-IV and secondary)</b>				
<i>Sex</i>	0.268	0.606	0.016 *	0.090
<i>Age (≤60; &gt;60 years)</i>	0.881	0.720	0.194	0.355
<i>Performance Score (≤1; &gt;1)</i>	0.004 *	0.020 *	<0.001 *	0.005 *
<i>MGMT promoter (methylated or not)</i>	0.391	0.891	0.148	0.694
<i>IDH mutation</i>	0.026 *	0.876	0.001 *	0.968
<i>ANXA2 IHC score (≤4; &gt;4)</i>	0.001 *	0.041 *	0.016 *	0.404
<b>Glioblastoma (only grade IV)</b>				
<i>Sex</i>	0.836	0.555	0.107	0.106
<i>Age (≤60; &gt;60 years)</i>	0.878	0.498	0.867	0.564
<i>Performance Score (≤1; &gt;1)</i>	0.007 *	0.054	<0.001 *	0.019 *
<i>MGMT promoter (methylated or not)</i>	0.488	0.892	0.246	0.934
<i>IDH mutation</i>	0.230	0.679	0.049 *	0.975
<i>ANXA2 IHC score (≤4; &gt;4)</i>	0.008 *	0.029 *	0.035 *	0.607

\* highlight significant p values<0.05

## **6.2 ANXA2 inhibition dramatically affects gene expression profile of GBM cells.**

Starting from previous results, we analyzed TCGA and GSE13041 datasets in order to compare the gene expression profile of ANXA2 Very Low and ANXA2 High GBMs. We identified 421 up-regulated and 298 down-regulated genes in common between the two cohorts of patients and significantly associated to an “ANXA2-high expression phenotype” differentially expressed genes between ANXA2 High versus ANXA2 Low tumors with 25<sup>o</sup> percentile of ANXA2 expression as cut-off (Figure 7A and Supplementary Table 3). Interestingly, Gene Set Enrichment Analysis (GSEA) of differentially expressed genes revealed a positive enrichment for cell migration and epithelial to mesenchymal transition (EMT) signatures in ANXA2 High GBMs (Figure 7B). Moreover, it showed ANXA2 High GBMs as positively and negatively enriched for genes related to the “Mesenchymal” and “Proneural” molecular subtypes respectively (Figure 7B).

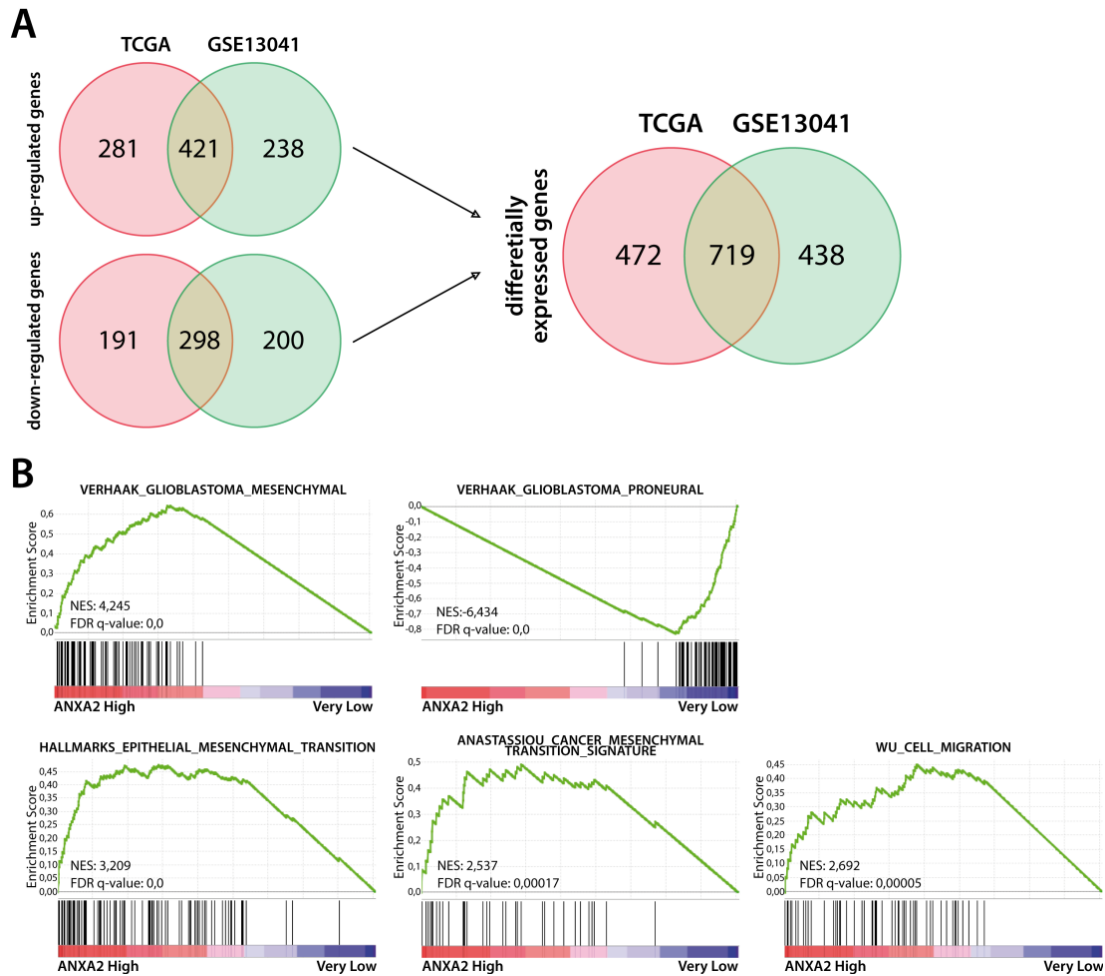


**Figure 7.** GSEA analysis of differentially expressed genes in ANXA2 High vs. ANXA2 Very Low GBM patients. (A) Venn diagrams reporting the number of differentially expressed genes between GBM tumours expressing high levels (ANXA2 High;  $\geq 25^{\circ}$  percentile) or very low (ANXA2 Very Low;  $< 25^{\circ}$  percentile) levels of ANXA2 mRNA in patients retrieved from TCGA (orange) or GSE13041 (green) datasets. (B) GSEA of commonly up-regulated genes in ANXA High patients from TCGA and GSE13041 datasets showing positive enrichment for genes of the Mesenchymal molecular subtype [95], EMT and cell migration, and negative enrichment for genes of the Proneural molecular subtype [95]. Plots were generated by c2 curated gene sets in the GSEA MSigDatabase. The green curves show the enrichment score and reflects the degree to which each gene (black vertical lines) is represented at the top or bottom of the ranked gene list. The heat map indicates the relative abundance (red to blue) of the genes specifically enriched in the ANXA2 High as compared with the ANXA2 Very Low GBM patients.

In order to better characterize the link between ANXA2 levels and GBM transcriptional profile, we retrieved gene expression data from GBM cells treated with an ANXA2 neutralizing antibody, previously reported to efficiently inhibit ANXA2 activity [96, 97]. To this end, we derived a series of primary GBM cultures from patient biopsies (Supplementary Table 4) and selected ANXA2 highly expressing GBM cells by WB (ANXA2<sup>hi</sup>; Figure 8).



**Figure 8.** ANXA2 protein expression in primary GBM cell cultures. Western Blot analysis of ANXA2 protein expression in seven primary GBM cells used in this study.  $\beta$ -Actin expression has been used as loading control. 10 $\mu$ g of protein lysate has been loaded in each lane.

ANXA2<sup>hi</sup> cells were then treated with the ANXA2-neutralizing antibody and their transcriptional profile analyzed by Affymetrix chips. Supervised analysis retrieved 855 differentially expressed probes between anti-ANXA2 and Isotype control-treated GBM cells (634 down- and 221 up-regulated; Figure 9A and Supplementary Table 5). Interestingly, ANXA2-inhibited cells showed a negative enrichment for EMT and metastasis genes (Figure 9B), confirming previous results from TCGA and GSE13041 datasets (Figure 7). Moreover, anti-ANXA2-treated cells were negatively enriched for genes correlated to a “stem cell/undifferentiated phenotype”, suggesting that ANXA2 modulation would potentially impact also cellular differentiation (Figure 9B, lower panels). To account for further effects mediated by ANXA2, we generated an enrichment map based on gene ontology (GO) analysis of differentially expressed genes, which clearly showed that ANXA2 blockade is sufficient to significantly down-regulate genes clustering in cell cycle, DNA replication, chromosome segregation and microtubule organization gene families, thus pointing ANXA2 also as a potential modulator of GBM cell proliferation (Figure 9C). Analysis of up-regulated genes revealed no association to specific enrichment modules or gene sets; however, GO analysis showed a general up-regulation of genes actively involved in the control of the transcriptional machinery (data not shown). Finally, to account for a potential molecular subtype shift after ANXA2 inhibition, HutuP174 primary GBM cells (isotype- or ANXA2

antibody-treated) were assigned to their specific molecular subtype according to the Verhaak classifier [95]. As a result, HuTuP174 were classified as “classical”, without shifting their assigned subtype after ANXA2 inhibition (data not shown). To validate these data we evaluated the expression of selected genes in GBM cells silenced for ANXA2 (Figure 9D) or transiently over-expressing ANXA2 mRNA (Figure 9E). As a result, ANXA2 silencing was able to dramatically down-regulate a series of genes down-modulated by ANXA2 antibody treatment (Supplementary Table 5) and particularly involved in the regulation of cell cycle, cell migration and ECM remodeling (Figure 9F). Conversely, the expression of these genes was significantly augmented by ANXA2 over-expression in ANXA2<sup>low</sup> cells (Figure 9G).

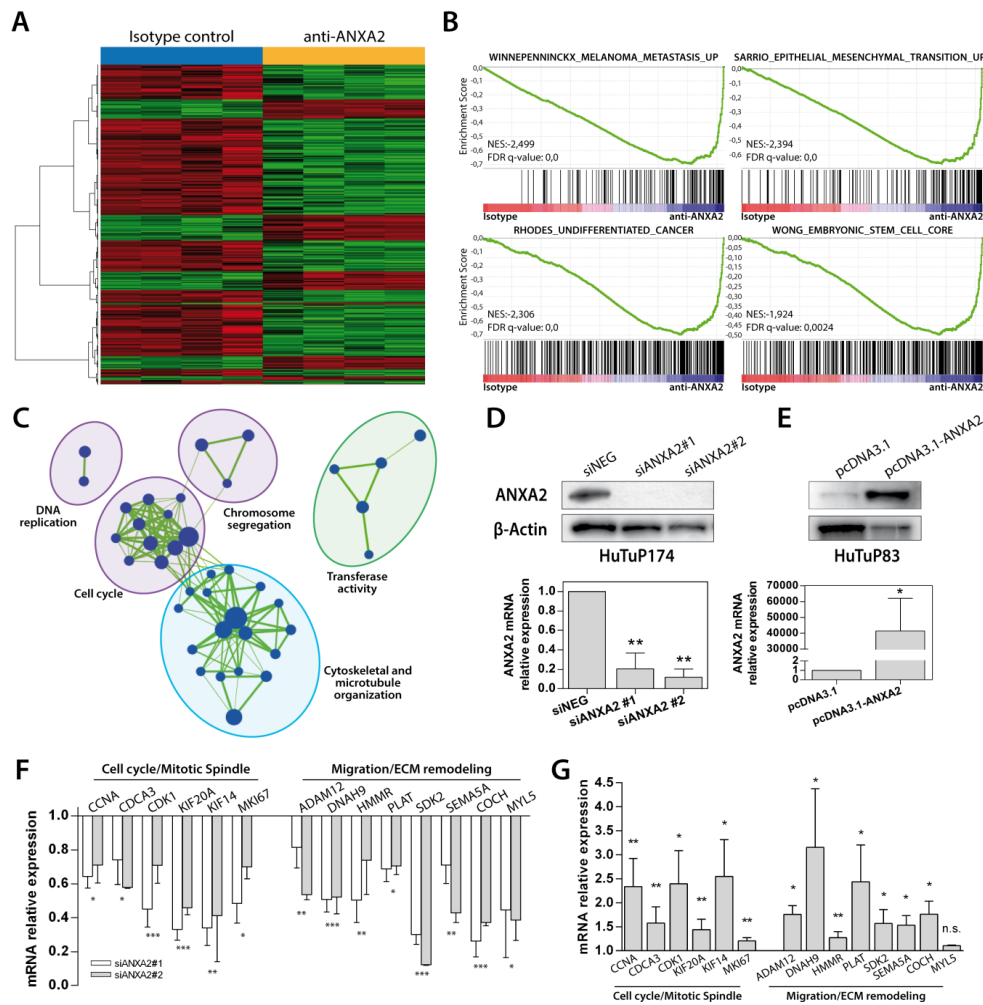


**Figure 9.** ANXA2 inhibition down-regulates the expression of genes involved in metastasis, EMT, cytoskeletal remodeling and cell cycle. (A) Heat map generated by supervised analysis of HuTuP174 primary GBM cells treated with a monoclonal anti-ANXA2 antibody for 48h (4 isotype vs. 4 ANXA2 antibody-treated cells) using the 855 differentially expressed probe sets (IFDR<0.05). (B) Representative GSEA enrichment plots demonstrating that probes down-regulated after ANXA2 inhibition are enriched for genes involved in the metastatic and EMT processes (upper panels), and a stem-like/undifferentiated phenotype (lower panels). Plot were generated by c2 curated gene sets in the GSEA MSigDatabase. The green curves show the enrichment score and reflects the degree to which each gene (black vertical lines) is represented at the top or bottom of the ranked gene list. The heat map indicates the relative abundance (red to blue) of the genes specifically enriched in the anti-ANXA2-treated as compared with the isotype control-treated cells. (C) Enrichment Map based on results of c5 Gene Ontology GSEA-MSigDB, generated using Enrichment Map Cytoscape plug-in. Node represents the functional gene sets and the size is proportional to the size of gene set. Edge thickness is proportional to the overlap between the gene sets. We show only gene sets that are enriched with a  $fdr < 5\%$  and only gene sets with a size between 15 and 500 genes were analyzed. Gene sets with common biological function are grouped in cluster and labeled with Gene Ontology terms. Green indicate negative enrichment in ANXA2 antibody-treated cells. (D and E) Evaluation of ANXA2 protein (upper panels) and mRNA (lower panels) expression in GBM cells after ANXA2 gene silencing (two different siRNAs against ANXA2 mRNA vs. siNEG in HuTuP174 GBM cells) or ANXA2 over-expression (HuTuP83) respectively by transient transfection procedures. (F and G) Validation of the transcriptional expression of a series of genes, selected from down-regulated genes after anti-ANXA2 treated cells, involved in cell cycle (CCNA, CDCA3, CDK1, KIF20A, KIF14 and MKI67) and cell migration (ADAM12, DNAH9, HMMR, PLAT, SDK2, SEMA5A, COCH, MYL5) cellular processes in ANXA2 silenced (HuTuP174) and ANXA2 over-expressing (HuTuP83) GBM cells respectively. \* $p < 0.05$ , \*\* $p < 0.01$ , \*\*\* $p < 0.001$ , n.s. not significant by one-way ANOVA or paired t-test.

### 6.3 GBM cell migration and invasion are sustained by ANXA2.

In order to functionally validate the role of ANXA2 as master sustainer of GBM cell dissemination, we modulated ANXA2 activity/expression in primary cells (Supplementary Table 4) and evaluated their migratory and invasive properties. Inhibition of ANXA2 by neutralizing antibody resulted in a dramatic impairment of GBM cell migration during scratch assays. In particular, the inhibitory effect on cell migration was detectable early after treatment (24h), being progressively stronger at later timepoints (Figure 10A, 10D). This effect was confirmed also by ANXA2 silencing (Figure 10B, 10E). In both conditions, we did not observe impairment of GBM cell viability (data not shown). Conversely, ANXA2 over-expression significantly enhanced the migratory properties of cells endowed with low motility (Figure 10C, 10F).

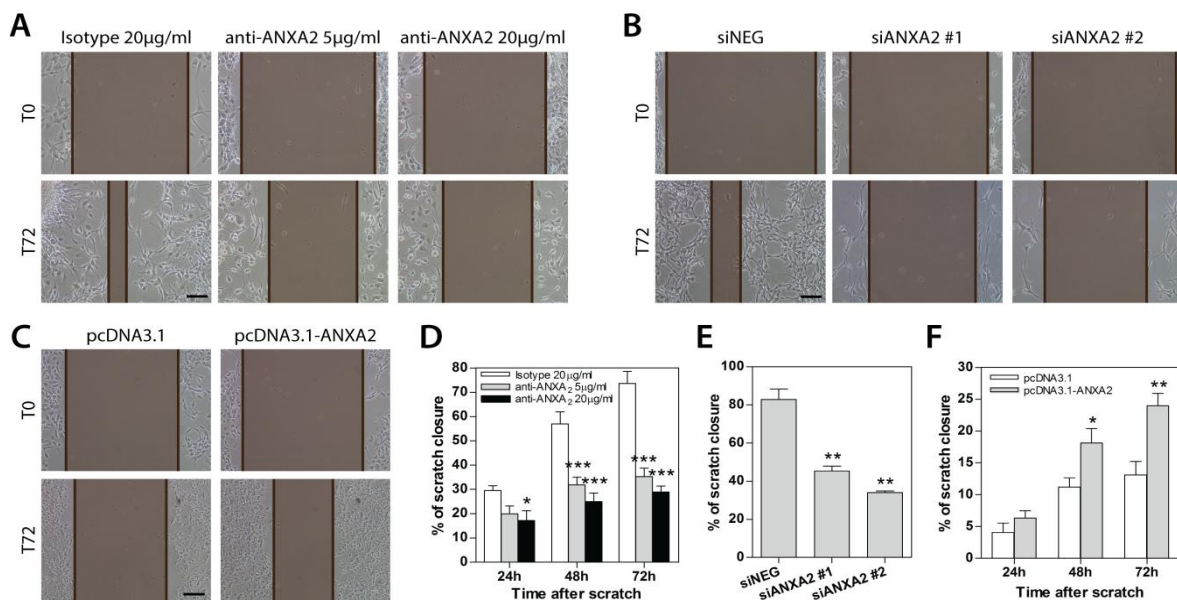


**Figure 10.** Modulation of ANXA2 activity or expression levels impacts primary GBM cell migration. (A, B and C) Representative images showing the ability of GBM cells to close the wound within 72h after scratching the cell monolayer during scratch assays. These have been performed on primary GBM cells treated with a monoclonal anti-ANXA2 antibody (A; HuTuP175), silenced for ANXA2 (B; HuTuP174) or ANXA2 over-expressing (C; HuTuP83) cells. The distance between the two edges of the scratch is marked in brown and has been quantified by using Adobe Photoshop CS6. Original magnification 10x; bar: 50µm. (D, E and F) Bar graphs showing relative quantification of the distance between scratch edges in anti-ANXA2 antibody-treated (D; N=6 for HuTuP107, HuTuP174 and HuTuP175), ANXA2-silenced (E; N=3 for HuTuP174) or ANXA2 over-expressing (F; N=3 for HuTuP83) primary GBM cells at the indicated timepoints. The migration ability of GBM cells after ANXA2 silencing is reported only at 72h. \*p<0.05; \*\*p<0.01; \*\*\*p<0.001 by one-way ANOVA or paired t-test.

We then tested the invasion ability of ANXA2<sup>hi</sup> cells in a basement membrane-like matrigel assay with cells plated on the top of a thin layer of semisolid medium. In this condition, HuTuP174 GBM cells grew as clonal spheres and inhibition of ANXA2 by antibody treatment counteracted their invasive properties in a dose dependent manner (Figure 11A, 11B). Importantly, the highest dose of antibody completely halted cell invasion until one week after treatment, with GBM cells being restricted in the spheres without any spreading (Figure 11A, 11B). We then confirmed these data in two additional primary GBM cultures endowed with reticulate growth (HuTuP13 and 176) which showed a dramatic reduction of the number and length of branches and the amount of invading cells (Figure 11C, 11D). As a further validation, ANXA2 inhibition/silencing were both able to halve the number of ANXA2<sup>hi</sup> GBM cells able to pass through a basal membrane extract (BME)-coated transwell (CultreCoat® Cell Invasion assay) within 48h (Figure 11E, 11F). Moreover, ANXA2 over-expression significantly increased GBM cell invasion (Figure 11G).



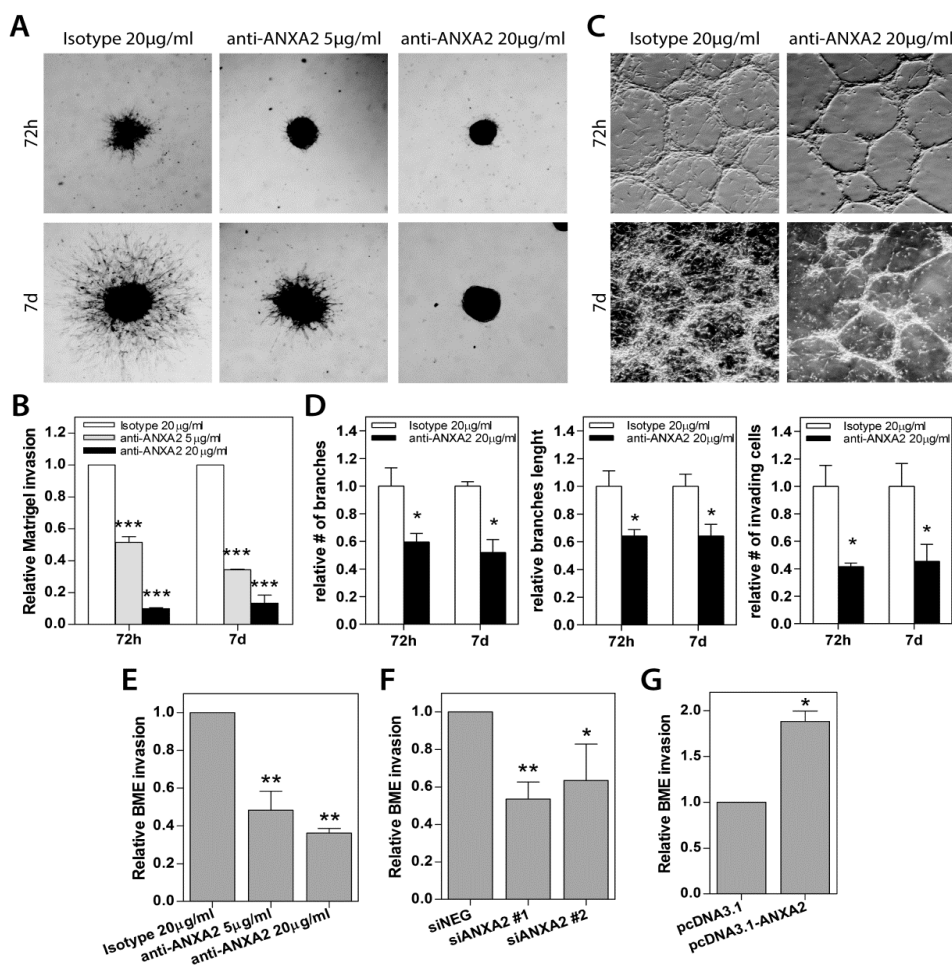


**Figure 11.** Modulation of ANXA2 activity or expression levels impacts primary GBM cell invasion. (A) Representative images of primary GBM cells growing as spheres (HuTuP174) on Matrigel-coated dishes and treated with anti-ANXA2 antibody until the indicated timepoints. Original magnification 4x. (B) Relative quantification of the length of the protrusions invading the matrix and spreading away from the spheres showed in (A). Bar graphs showing relative invasion of primary GBM cells after ANXA2 inhibition (C; N=3 for HuTuP13 and HuTuP175), gene silencing (D; N=3 for HuTuP13 and HuTuP174) or over-expression (E; N=4 for HuTuP83) as quantified by Cultrecoats® BME-based assays as described in the Methods section. \* $p < 0,05$ ; \*\* $p < 0,01$ ; \*\*\* $p < 0,001$  by one-way ANOVA or paired t-test.

To definitely assess the inhibitory effects exerted by ANXA2 blockade on the dissemination of GBM cells, we analyzed the impact of ANXA2 antibody treatment *in vivo* on GBM primary cells (EGFP expressing HuTuP13 cells) xeno-transplanted in the chick embryo chorioallantoic membrane (CAM). After 72h from initial treatment (2µg antibody/egg/day), isotype treated cells actively dispersed in the CAM, moving away from the initial site of cell deposition (Figure 12A, upper panels). On the contrary, ANXA2 inhibited cells formed restricted cellular masses, confined in the deposition site, without any spreading (Figure 12A,

lower panels). As a result, control cells disseminated covering a 60-fold larger area than ANXA2 antibody treated cells (Figure 12B), demonstrating that ANXA2 inhibition is able to completely block GBM cell invasiveness also in an *in vivo* setting.

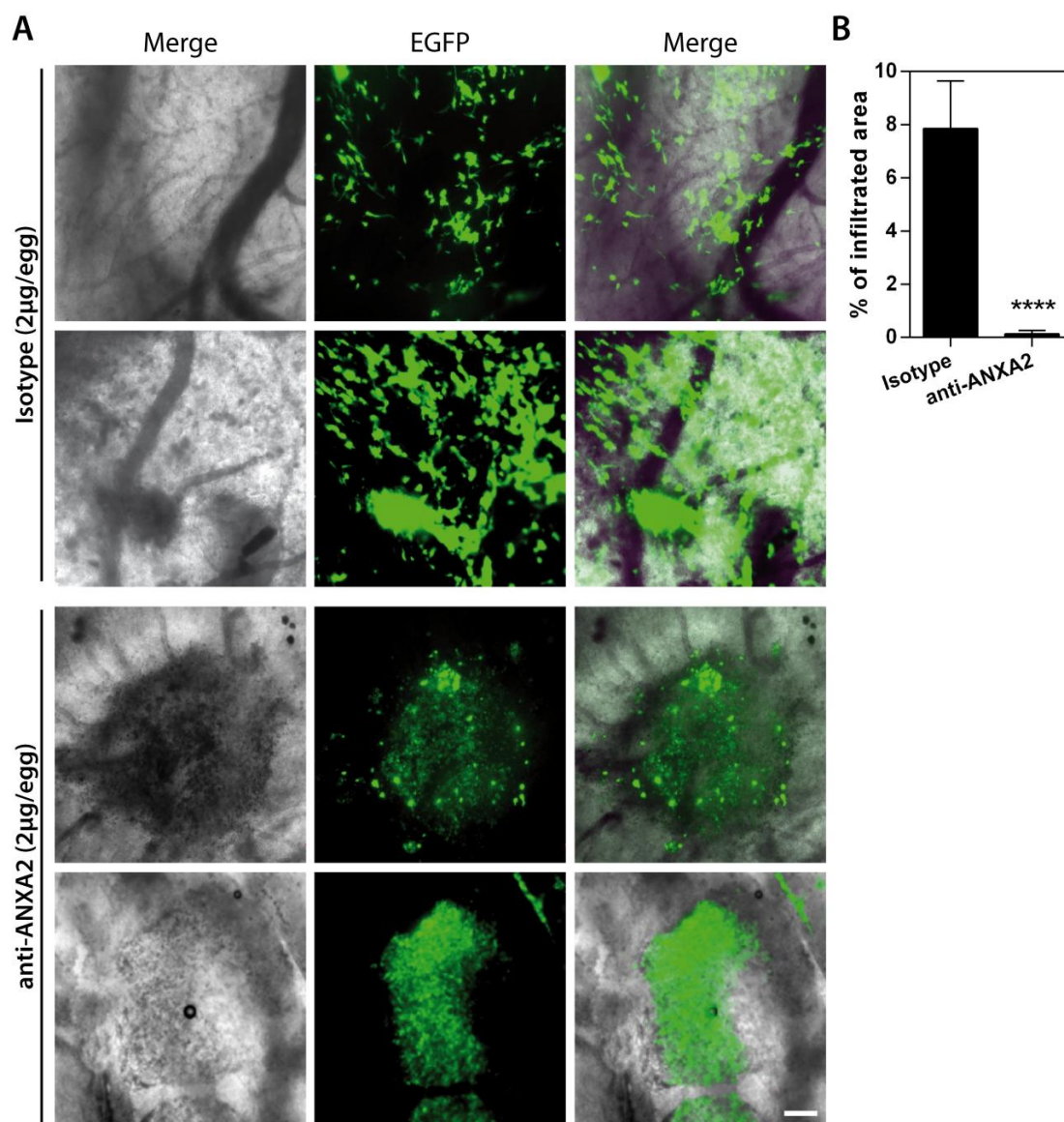


**Figure 12.** ANXA2 inhibition reduces GBM cell dissemination *in vivo* in the CAM invasion assay. (A and B) Representative images showing the migration/invasion of HuTuP13-EGFP primary GBM cells (green) inside the observation area after 3 days of treatment with 2µg of isotype control (upper panels) or ANXA2 antibody (lower panels) (2µg/egg/day) (A) and quantification of the area covered by cells relative to the entire observation space (24,7mm<sup>2</sup>; B). Original magnification 20x; bar: 200µm. \*\*\*\*p<0.0001 by t-test.

Cellular migration/invasion is usually mediated by re-organization of cytoskeletal actin fibers and their link to ECM through focal adhesions (FAs) [98, 99]. In this context, it has been previously reported that ANXA2 binds to filamentous (F)-actin [97]. For this reason, we analyzed the possible involvement of ANXA2 in cytoskeletal remodeling, as suggested by GO analysis (Figure 9C). Phalloidin staining revealed that ANXA2<sup>hi</sup> GBM cells are characterized by cytoskeletal fibers assembled in FA-like structures, indicative of a migrating phenotype (Figure 13A, 13B, 13D). Conversely, ANXA2 inhibited/silenced cells displayed a dramatic redistribution of F-actin fibers and an almost complete loss of FAs (Figure 13A, 13B, 13D), without affecting distribution of microtubules (data not shown). ANXA2 over-expression in ANXA2<sup>low</sup> GBM cells increased the number of FAs (Figure 13C, 13D), thus reinforcing the hypothesis of ANXA2 as a major player in the control of cytoskeletal dynamics.

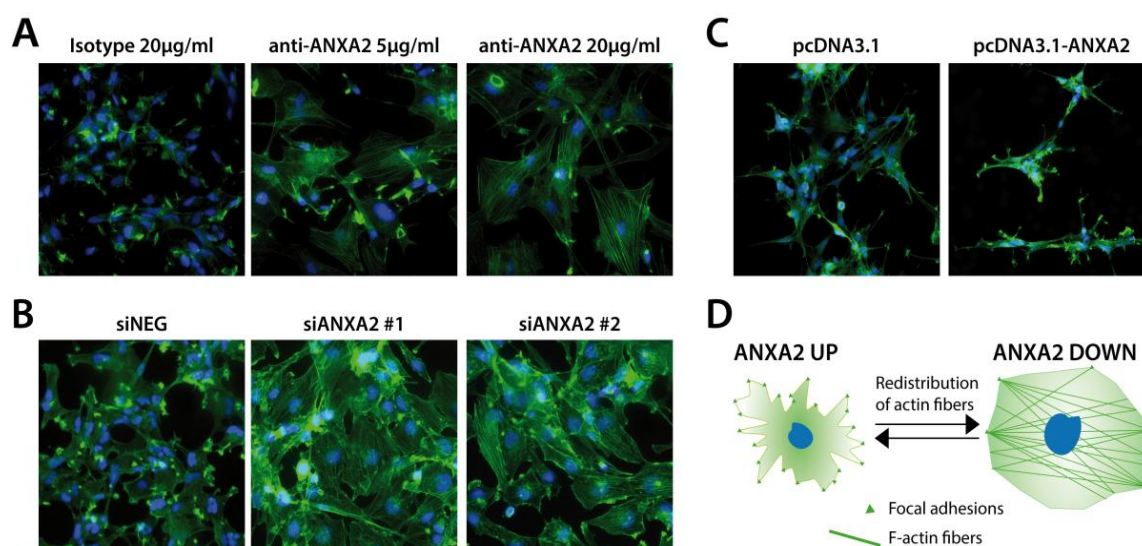


**Figure 13.** Modulation of ANXA2 levels is accompanied by dramatic cytoskeletal remodeling. (A-C) Representative immunofluorescence images of GBM cells after ANXA2 inhibition, gene silencing or over-expression respectively and stained with a FITC-labeled phalloidin probe in order to reveal the distribution of F-actin (green). Cell nuclei have been counterstained with DAPI (blue). Original magnification 20x. (D) Cartoon resembling the major morphological and cytoskeletal changes associated to the modulation of ANXA2 in GBM cells.

#### **6.4 ANXA2 impairment induces differentiation and inhibits proliferation of GBM cells.**

GSEA and GO analysis suggested a potential role of ANXA2 in the control of cell phenotype and proliferation (Figure 9B, 9C). According to this hypothesis, ANXA2 blockade significantly reduced the number of cells expressing the stem cell marker Sox2, nevertheless without affecting the expression of Nestin and CD133 (Figure 14A-14C). Conversely, ANXA2 inhibition was responsible of a significant increase of the number of cells expressing the astrocytic differentiation markers GFAP and S100 (Figure 14D, 14E and Figure 15A). Nevertheless, we did not observe induction of cell differentiation toward other neural lineages such as neurons or oligodendrocytes, since examined cells showed very low or absent expression of the neuronal marker microtubule associated protein 2 (MAP2; Figure 15B) and oligodendrocyte specific protein (OSP; Figure 15C). These effects increased in ANXA2-silenced GBM cells, which displayed a significant reduction of Nestin<sup>+</sup> and CD133<sup>+</sup> cells instead of Sox2 (Figure 14F-14J and Figure 15D, 15E).

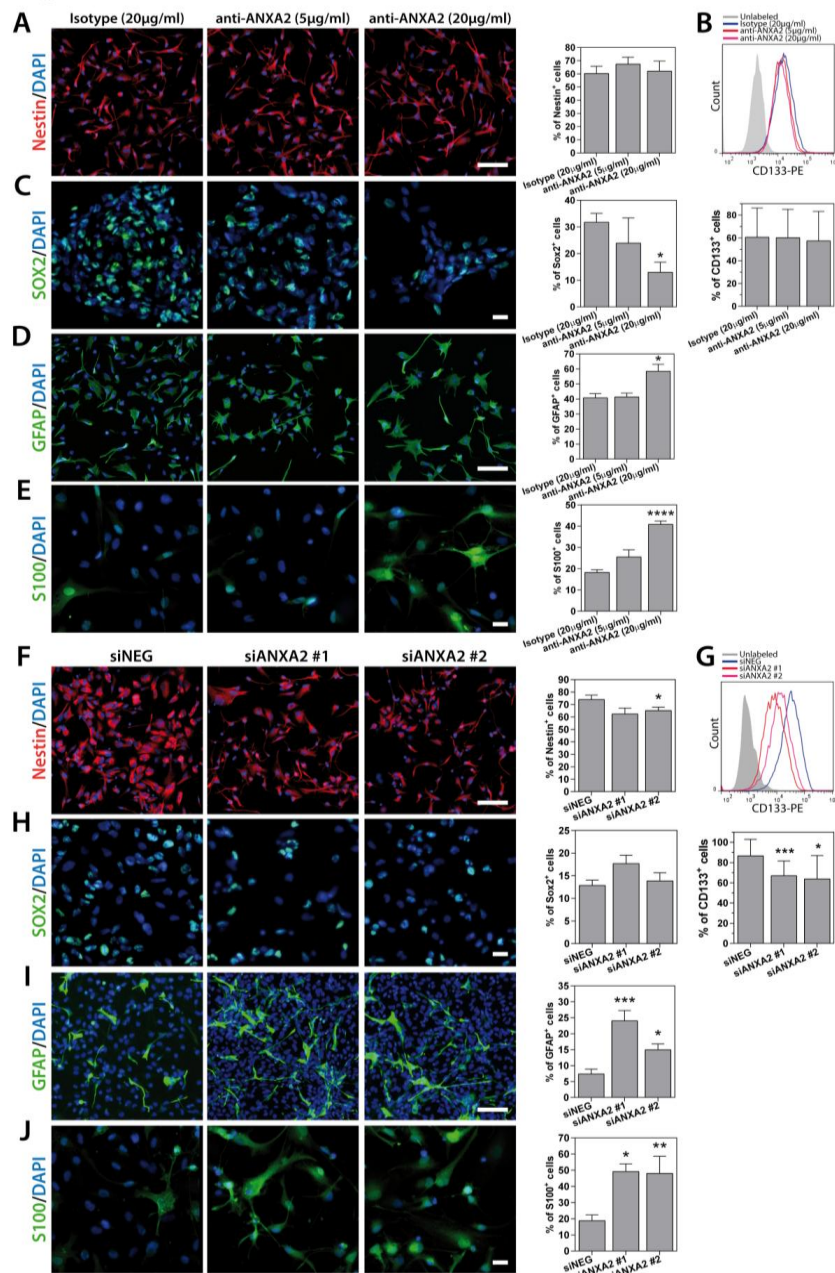


**Figure 14.** Analysis of primary GBM cell phenotype after ANXA2 inhibition or gene silencing. (A-E) Representative immunofluorescence images showing primary GBM cells (HuTuP175) treated with anti-ANXA2 monoclonal antibody or isotype control antibody and stained with anti-Nestin (A; red), anti-Sox2 (C; green), anti-GFAP (D; green) or anti-S100 (E; green) antibodies, and relative quantification of positive cells (right panels). (B) Representative plot showing overlay of CD133<sup>+</sup> cell populations in control and ANXA2 antibody treated cells (HuTuP13; upper panel) and relative quantification (N=5 for HuTuP13, HuTuP82 and HuTuP175; lower panel). (F-J) Representative immunofluorescence images showing primary GBM cells (HuTuP13) silenced for ANXA2 and stained with anti-Nestin (F; red) or anti-Sox2 (H; green), anti-GFAP (I; green) or anti-S100 (J; green) antibodies and relative quantification of positive cells (right panels). (G) Representative plot showing overlay of CD133<sup>+</sup> cell populations in siNEG and siANXA2 transfected cells (HuTuP13; upper panel) and relative quantification (N=9 for HuTuP13 and HuTuP82; lower panel). For all stainings GBM cell nuclei have been counterstained with DAPI (blue). Percentages of positive cells have been calculated as number of positive cells/number of DAPI<sup>+</sup> nuclei per microscopic field. At least 8 fields per condition have been analyzed. Original magnification 10-20x. Bar: 50µm. \*p<0.05;\*\*\*p<0.001 by one-way ANOVA analysis. Significance is reported relative to control (isotype treated or siNEG transfected) GBM cells.

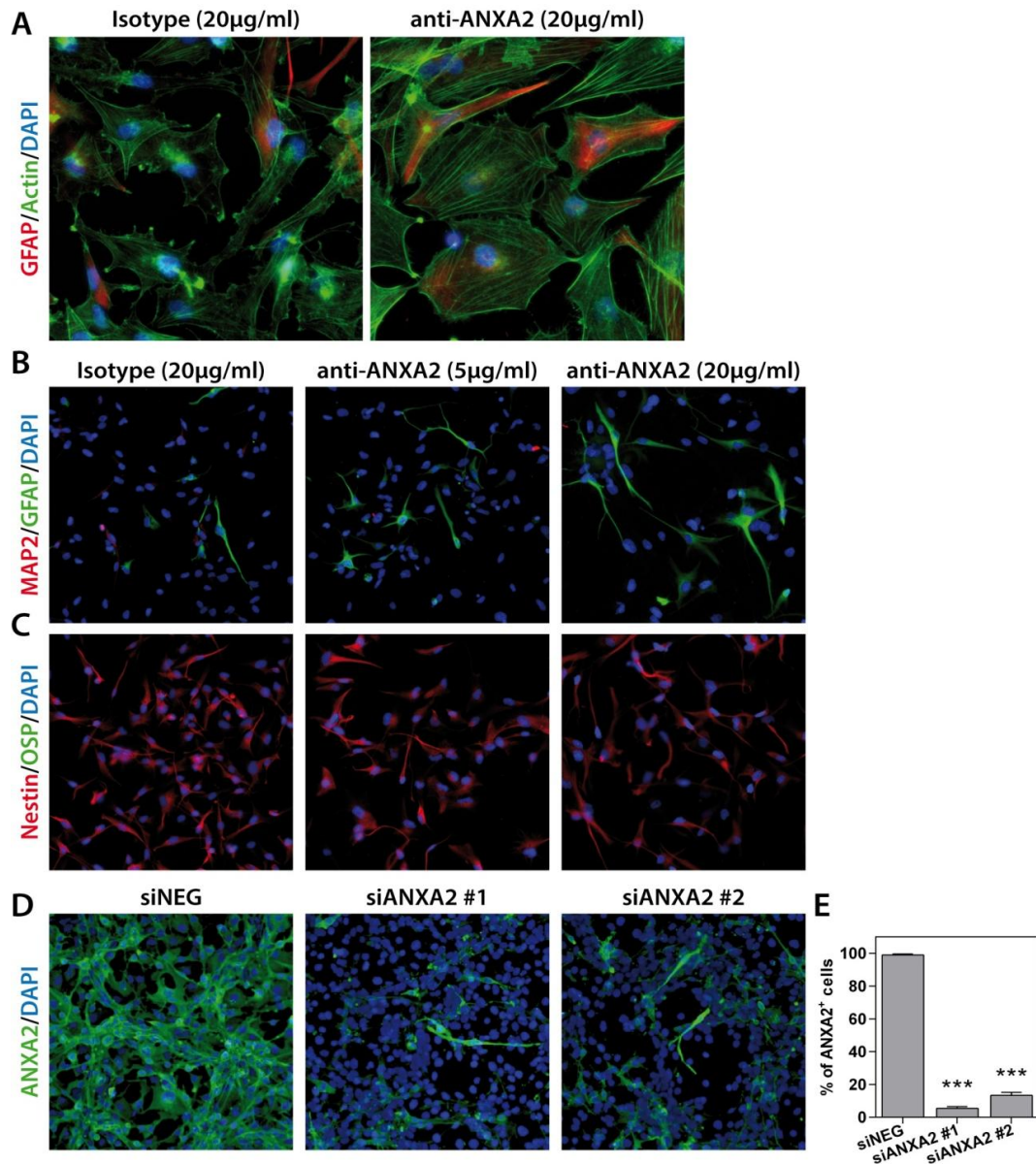


**Figure 15.** Immunofluorescence analysis of ANXA2 inhibited/silenced GBM cells. (A-C) Representative immunofluorescence images of GBM cells treated either with isotype or ANXA2 antibody and double stained for GFAP (red)/phalloidin (green) (A), MAP2 (red)/GFAP (green) (B) and Nestin (red)/OSP (green) (C). Images show a peculiar distribution of GFAP and Actin fibers within the cell cytoplasm. (D and E) Representative immunofluorescence images showing primary GBM cells (HuTuP13) silenced for ANXA2 and stained with anti-ANXA2 antibody (green; D) and bar graph reporting relative quantification of ANXA2<sup>+</sup> cells (E). Cell nuclei have been counterstained with DAPI (blue). Original magnification 10-20x. \*\*\*p<0.001 by one-way ANOVA analysis.

In line with these results, ANXA2 blockade/silencing strongly inhibited GBM cell proliferation. Indeed, the number of cells and the expression of the proliferation marker Ki67 were significantly reduced after ANXA2 knockdown (Figure 16A-16D and Figure 17). To better characterize these effects, we performed a PI-based cell cycle analysis on both antibody treated and silenced cells. We measured a significant reduction of cells in the G1 phase and a parallel accumulation of cells in the S phase of the cell cycle (Figure 16E, 16F), suggesting that impairment of ANXA2 is sufficient to partially arrest GBM cells at the S-G2/M cell cycle checkpoint. As a confirmation, experiments of BrdU uptake clearly showed a significant decrease of its incorporation within 96h in the same cells (Figure 16G, 16H). On the other hand, ANXA2 over-expression did not affect neither phenotype, nor cell cycle dynamics of GBM cells (data not shown), suggesting that ANXA2 would be necessary for the maintenance of a proliferative and in some way “less differentiated” cell phenotype, but its accumulation is not sufficient to perturb these systems by itself.

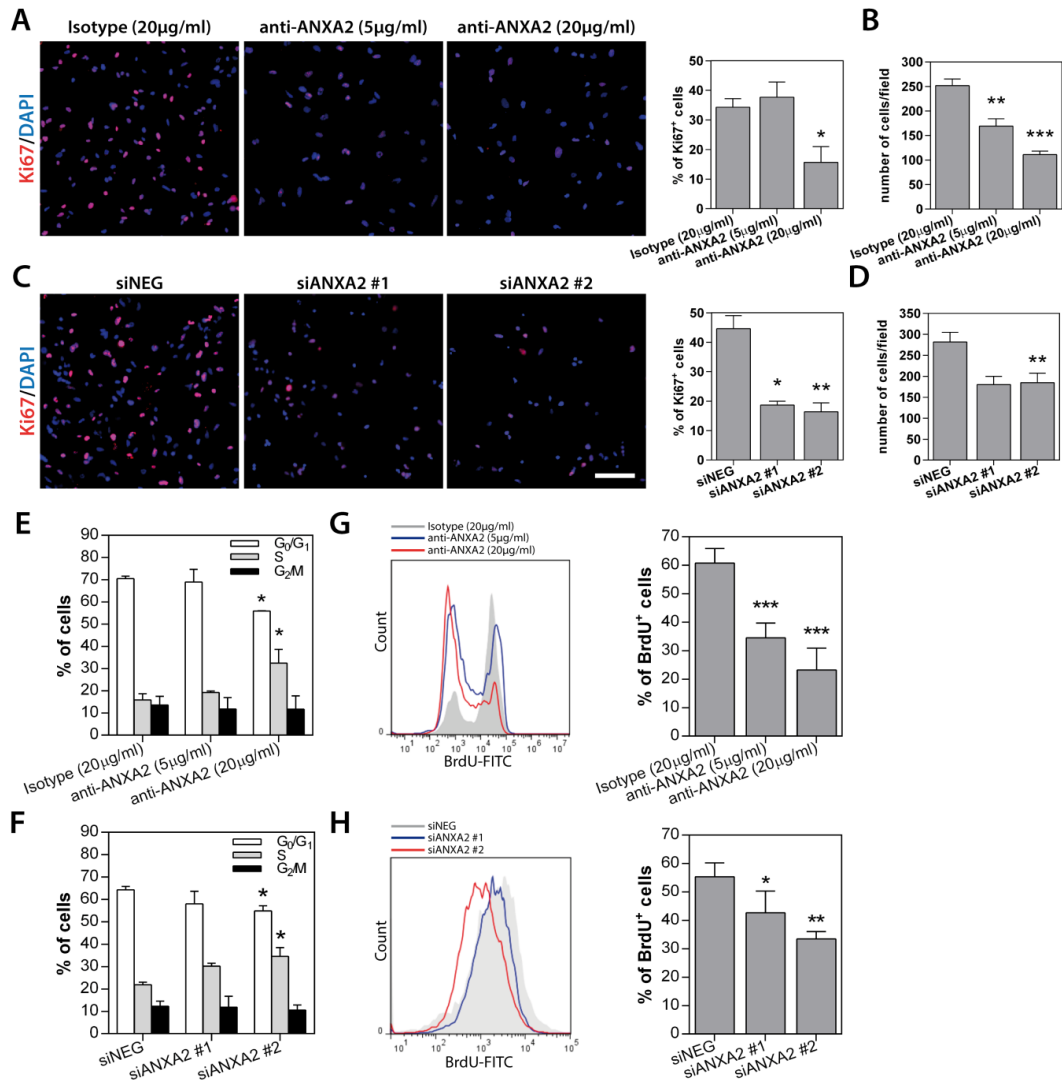


**Figure 16.** ANXA2 inhibition or gene silencing strongly reduces GBM cell proliferation by inducing a partial block at the S-G<sub>2</sub>/M checkpoint. (A-D) Representative immunofluorescence images of primary GBM cells treated with anti-ANXA2 antibody (HuTuP175) or silenced for ANXA2 (HuTuP13) and stained with anti-Ki67 (red) monoclonal antibody. Right panels show relative quantification of Ki67<sup>+</sup> cells (A and C) or quantification of DAPI<sup>+</sup> nuclei per microscopic field depending on the experimental condition (B and D). Percentages of Ki67<sup>+</sup> cells have been calculated as number of positive cells/number of DAPI<sup>+</sup> nuclei per microscopic field. At least 8 fields per condition have been analyzed. Original magnification 10x. Bar: 50 μm (E and F) Bar graph summarizing cell cycle analyses of ANXA2-neutralized or -silenced GBM cells (HuTuP13, HuTuP82 and HuTuP174). (G and H) Representative graphs showing BrdU incorporation analysis performed on HuTuP174 GBM cells after anti-ANXA2 antibody treatment or HuTuP53 GBM cells after ANXA2 silencing respectively. Right panels show bar graphs reporting relative quantifications. BrdU analyses have been performed on HuTuP13, HuTuP53, HuTuP82 and HuTuP174 primary GBM cells. \*p<0.05; \*\*p<0.01; \*\*\*p<0.001 by one-way ANOVA. Significance is reported relative to control (isotype treated or siNEG transfected) GBM cells.



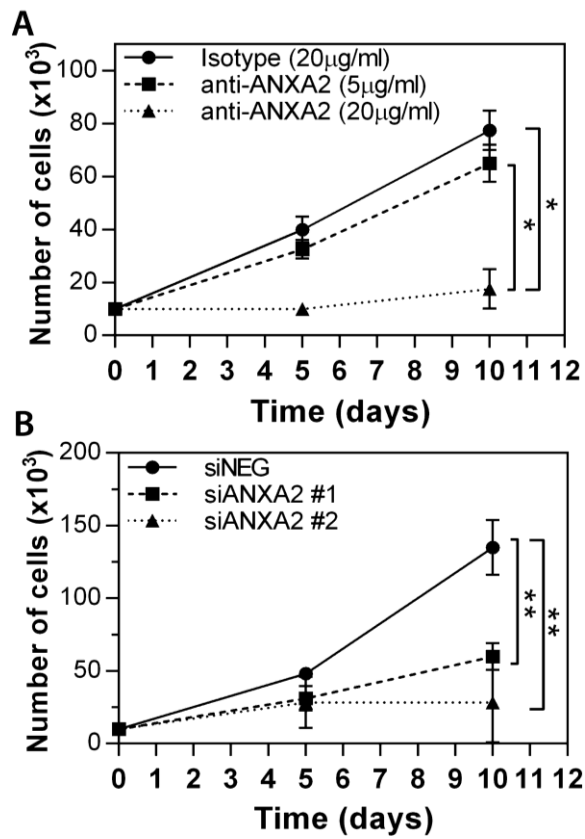


**Figure 17.** Long term anti-proliferative effects of ANXA2 inhibition/silencing in GBM cells. Growth curves generated by cell count (trypan blue exclusion) at different time-points after ANXA2 inhibition (HuTuP175; A) or gene silencing (HuTuP13; B). \* $p < 0.05$ , \*\* $p < 0.001$  by one-way ANOVA analysis.

### **6.5 An ANXA2<sup>down</sup> signature predicts GBM patient survival.**

To finally test the clinical relevance of the multiple effects exerted by ANXA2 modulation, we investigated the correlation of an ANXA2-dependent gene signature (ANXA2<sup>down</sup>), with clinical outcome in TCGA and GSE13041 datasets. We used the ANXA2<sup>down</sup> gene signature, based on the most down-regulated probes after ANXA2 antibody treatment, to divide patients into two equal groups on the basis of the median expression of the signature in the bulk GBM tumors. We observed a significant positive correlation between ANXA2<sup>down</sup> signature and survival (PFS and OS) in GBM patients from both datasets (Figure 18A-18C and Supplementary Table 6). In addition, we analyzed the potential correlation of the ANXA2<sup>down</sup> signature with clinical outcome also in other publicly available solid tumor datasets including colon cancer (GSE17536; [100]), breast cancer (E-MTAB-365; [101]) and lung adenocarcinoma (GSE31210; [102]). Of note, the signature significantly correlated with disease-specific (DSS) and relapse-free survival (RFS) in colon and breast cancer respectively (Figure 18D, 18E), showing a partial association with RFS also in lung adenocarcinoma (Figure 18F). These findings indicate that genes directly or indirectly regulated by ANXA2 retain a consistent prognostic relevance and that ANXA2 is endowed with the ability to participate in multiple cancer processes, fundamental for tumor survival, thus being a potential therapeutic target in GBM.

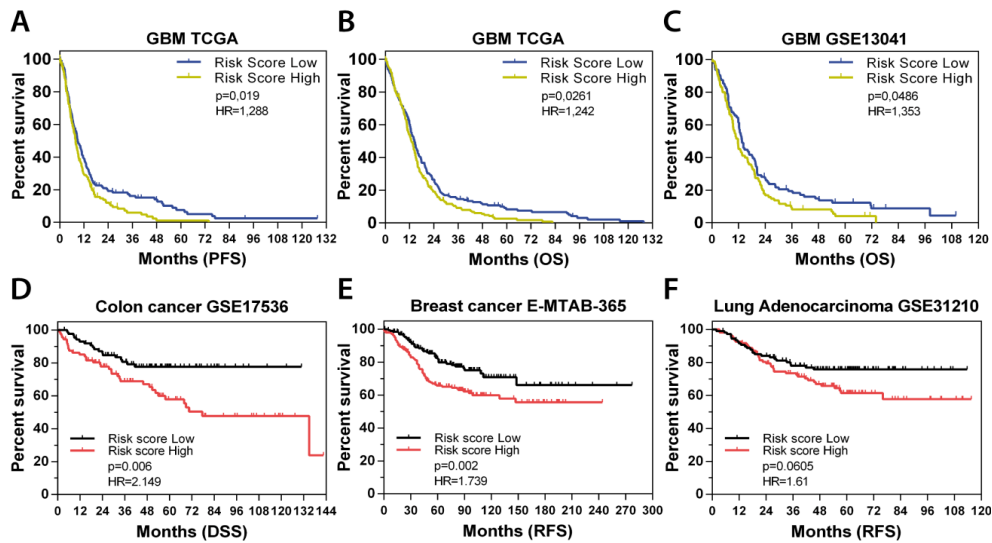


**Figure 18.** The ANXA2<sup>down</sup> signature predicts GBM patient survival. (A-C) Kaplan Meier curves showing the prognostic potential of the ANXA2<sup>down</sup> gene signature applied on GBM patients from TCGA (PFS and OS in A and B respectively) and the GSE13041 (OS in C) datasets. (D-F) Kaplan Meier curves showing the application of the ANXA2<sup>down</sup> gene signature on different solid tumors datasets including GSE17536 (disease specific survival-DSS in colon cancer patients in D), E-MTAB-365 (relapse free survival-RFS of breast cancer patients in E) and GSE31210 (RFS of lung adenocarcinoma patients in F). Hazard Ratios have been calculated as Risk Score Low/High.

Interestingly, we also examined the effects produced by intensive treatment protocols (defined as more than one cycle of single or concurrent chemo- and radiotherapy) in GBM patient subgroups generated on the basis of ANXA2 expression in the TCGA dataset. Our analyses show that aggressive treatment prolonged survival only in ANXA2 High tumors (HR=0,475; Figure 19A) rather than ANXA2 Very Low GBMs (HR=0,74; Figure 19B), resembling previous data on the Mesenchymal or Proneural subclasses respectively [95].

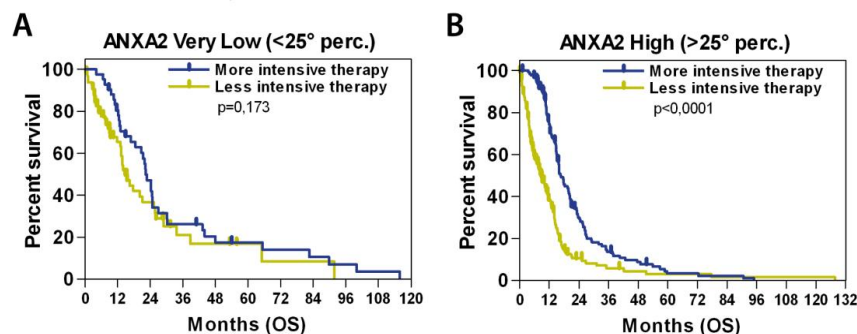


**Figure 19.** Impact of aggressive treatment on GBM patients depending on ANXA2 expression. Kaplan Meier curves reporting OS of GBM patients either treated with a single cycle of mono or concurrent therapy (Less Intensive), or by additional cycles of treatment (More Intensive) depending on their transcriptional expression of ANXA2 (< or  $\geq$ 25<sup>o</sup> percentile in A and B respectively).

## **6.6 ANXA2-dependent gene signature mapping for drug repositioning.**

In order to identify compounds and approved drugs able to revert the pro-oncogenic function of ANXA2 on GBM aggressiveness, we functionally mapped the ANXA2-dependent gene signature that we previously generated from TCGA and GSE13041 datasets by exploiting the Connectivity Map bioinformatic tool [37]. Top nine drugs, significantly predicted to be able to counteract the ANXA2-dependent transcriptional signature, were further selected for their activity on multiple cell types ( $n \geq 3$ ) (Figure 20A, 20B) and then analyzed for their ability to inhibit cell proliferation, motility and invasion also in primary GBM cultures *in vitro*.

First, MTT assay was performed on a panel of three different primary GBM cultures to determine the optimal concentration to be used in subsequent experiments on GBM (HuTuP174, HuTuP175, HuTuP176; Supplementary Table 4). Indeed, MTT metabolic assay allowed us to determine the potential anti-proliferative effects of compounds at different concentration and, in order to evaluate the anti-migratory and invasive effects of selected compounds we fixed as optimal concentration the IC20 for each drug (Figure 20C).

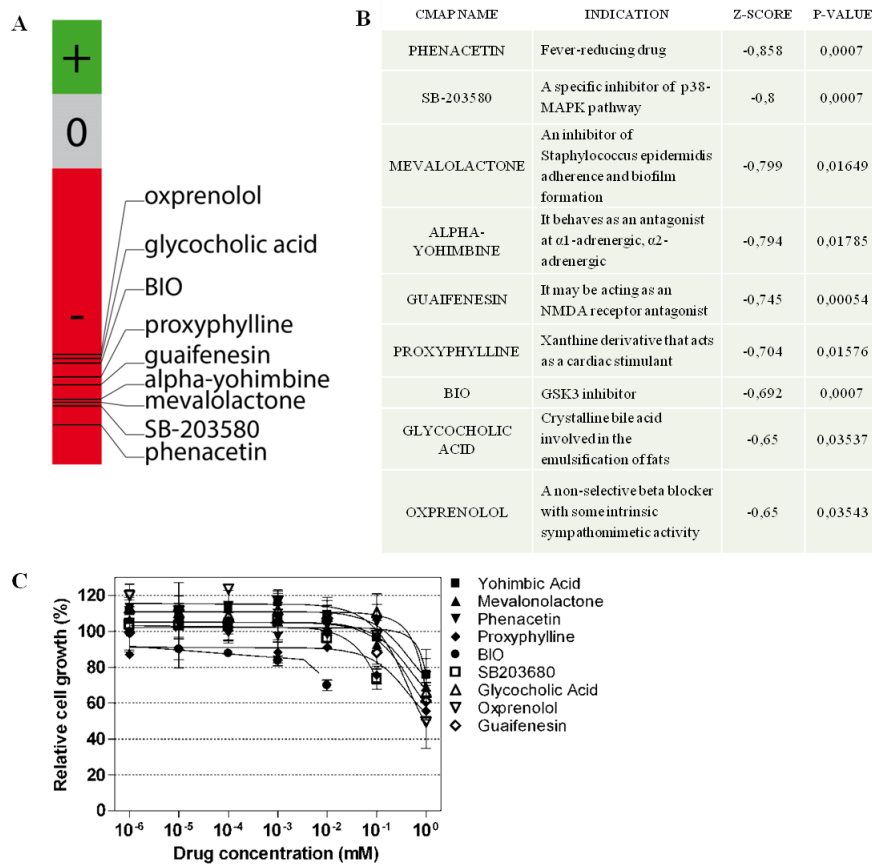


**Figure 20.** (A) Connectivity Map results. Only compounds with a negative score are represented in red. (B) The connections and perturbation stabilities of the nine significant drugs obtained for ANXA2-dependent transcriptional signature. (C) MTT assay on GBM cells. Starting from 10mM, scalar doses have been applied on three GBM patient cells, in order to determine the IG20 of the tested drugs, after 72h of treatment.

The 9 compounds selected were then tested in primary GBM culture to evaluate their ability to impair cells migratory and invasive properties. The treatment with Oxprenolol, BIO and SB203580 resulted in a dramatic inhibition of GBM cell migration during scratch assays and, in particular, the inhibitory effect on cell motility was detectable after 72h from treatment. Indeed, the treatment with these compounds prevented scratch closure of GBM cells, nevertheless without reducing their viability (Figure 21A, 21B) thus demonstrating the specific effects of these drugs on cell migration. The other six compounds tested did not show significant effects on GBM cell migration capacity (Figure 21C) so we excluded them from subsequent analysis.

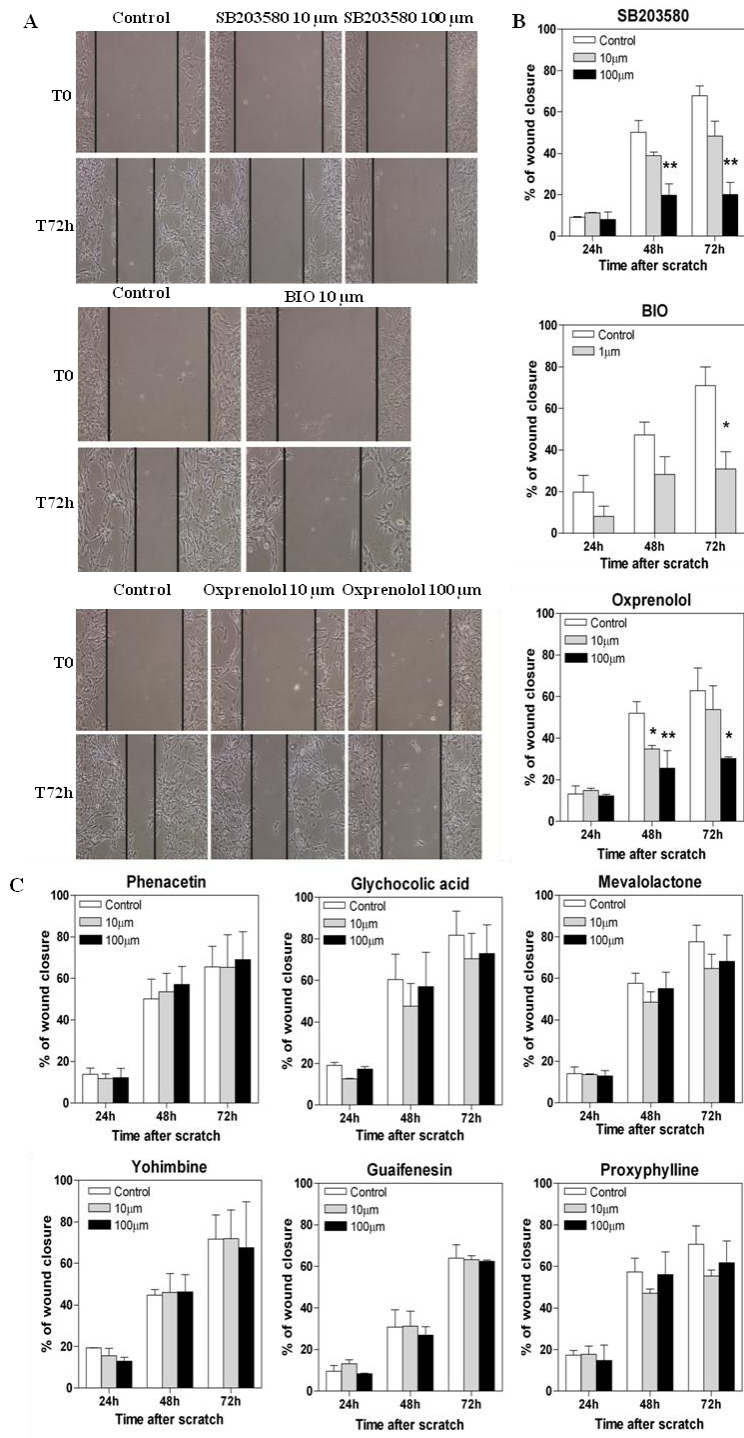


**Figure 21.** Treatment with SB203580, BIO and Oxprenolol impacts primary GBM cell migration compared to other compounds (A) Representative images showing the ability of primary GBM cells to close the wound within 72h after scratching the cell monolayer during scratch assays, after the treatment with SB203580, BIO and Oxprenolol. The distance between the two edges of the scratch is marked in brown and has been quantified by using Adobe Photoshop CS6. Original magnification 10x; bar: 50μm. (B, C) Bar graphs showing relative quantification of the distance between scratch edges in compounds-treated primary GBM cells at the indicated timepoints. \*p<0.05; \*\*p<0.01; \*\*\*p<0.001 by one-way ANOVA or paired t-test.

Therefore, we chose Oxprenolol, BIO and SB203580, which were resulted more efficient in previously scratch assays, to test the invasion ability of GBM cells in a basement membrane-like matrigel assay. In this condition, GBM cells grew as spheres and the treatment counteracted their invasive properties in a dose dependent manner (Figure 22). Importantly, the highest dose of compounds completely halted cell invasion until 72h after treatment, with GBM cells being restricted in the spheres without any spreading (Figure 22A, left panels).

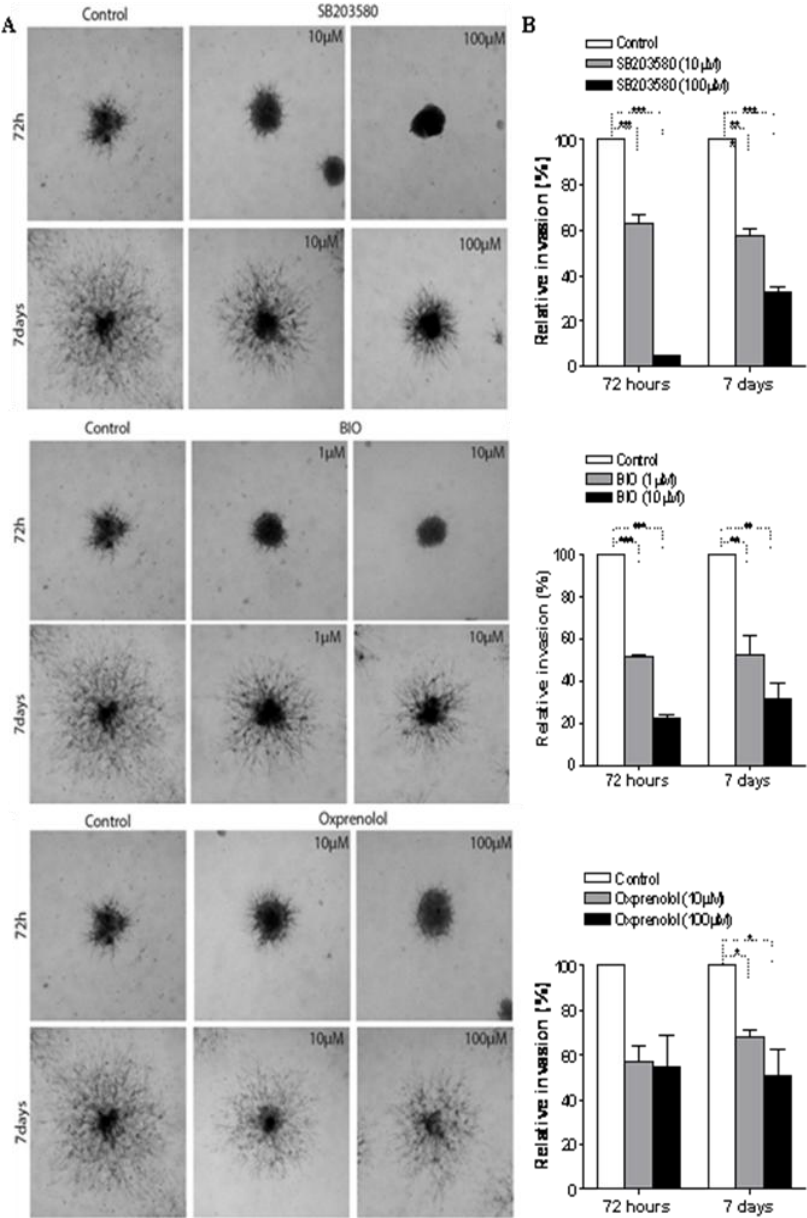


**Figure 22.** SB203580, BIO and Oxprenolol activity impacts primary GBM cell invasion. (A, left panels) Representative images of primary GBM cells growing as spheres on Matrigel-coated dishes and treated with compounds until the indicated timepoints. Original magnification 4x. (B, right panels) Relative quantification of the length of the protrusions invading the matrix and spreading away from the spheres showed in (A).

We then analyzed the possible effect of Oxprenolol, BIO and SB203580 in cytoskeletal remodeling as we did for ANXA2 inhibition and silencing. Indeed, phalloidin staining revealed that GBM cells are characterized by cytoskeletal fibers assembled in FA-like structures, indicative of a migrating phenotype (Figure 23, upper panels). Conversely, treated cells displayed a dramatic redistribution of F-actin fibers and an almost complete loss of FAs (Figure 23, lower panels) concordantly with the migration/invasion inhibition that we registered in the above described assays.

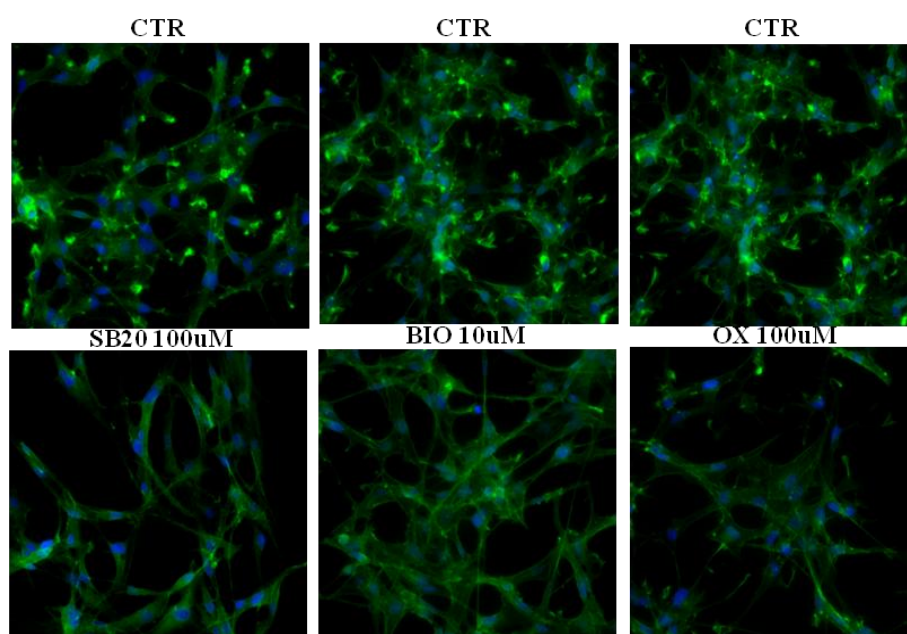


**Figure 23.** Treatment with SB203580, BIO and Oxprenolol induces a dramatic cytoskeletal remodeling. Representative immunofluorescence images of GBM cells after treatment of compounds and stained with a FITC-labeled phalloidin probe in order to reveal the distribution of F-actin (green). Cell nuclei have been counterstained with DAPI (blue). Original magnification 20x.

To go deeper in unveiling the specific role of ANXA2 in GBM, we generated an ANXA2 dependent transcriptional signature based on the expression profiles of ANXA2 silenced cells respect to relative controls. ANXA2<sup>hi</sup> cells were transfected with small interfering RNAs (siRNAs) against ANXA2 as well as with a non targeting siRNA (siNEG) and their transcriptional profile analyzed by Affymetrix chips. Supervised analysis on the specific signatures retrieved 3592 differentially expressed probes between siANXA2 or control-transfected GBM cells (1846 up- and 1746 down-regulated; Figure 24A and Supplementary Table 7). Interestingly, GSEA on ANXA2-silenced cells showed a negative enrichment for EMT and metastasis genes compared to control cells (Figure 24B), confirming previous gene



expression results obtained after ANXA2 neutralization by specific antibody (Figure 9). Moreover, GSEA on ANXA2-silenced cells revealed a negative enrichment also of genes related to stemness and cancer undifferentiated status (Figure 24B), highlighting the role of ANXA2 in controlling GBM differentiation.

To expand the results obtained by the Connectivity Map bioinformatic tool, we submitted to the QUADrATiC software [39] the ANXA2 dependent transcriptional signatures that we previously generated from ANXA2 treated- or transfected GBM cells, in order to identify perturbagens and FDA approved drugs able to reproduce the transcriptional effects mediated by ANXA2 activity down-modulation. Specifically, we retrieved 14 compounds significantly predicted ( $p < 0.05$ ) to be able to reproduce the transcriptional effects mediated by ANXA2 neutralizing antibody and 77 compounds significantly predicted to be able to reproduce the transcriptional effects obtained by ANXA2 specific silencing. Looking for a shared mechanism between the two signatures obtained, we intercrossed the two drug lists and found 7 common compounds (Figure 24C). In particular, we identified the proteasome inhibitor Bortezomib as the most significant drug, and two cationic ion pump inhibitors (Digitoxin and Qubain) that are analogues of the previously tested Oxprenolol which demonstrated to be able to inhibit GBM cells invasion potential.

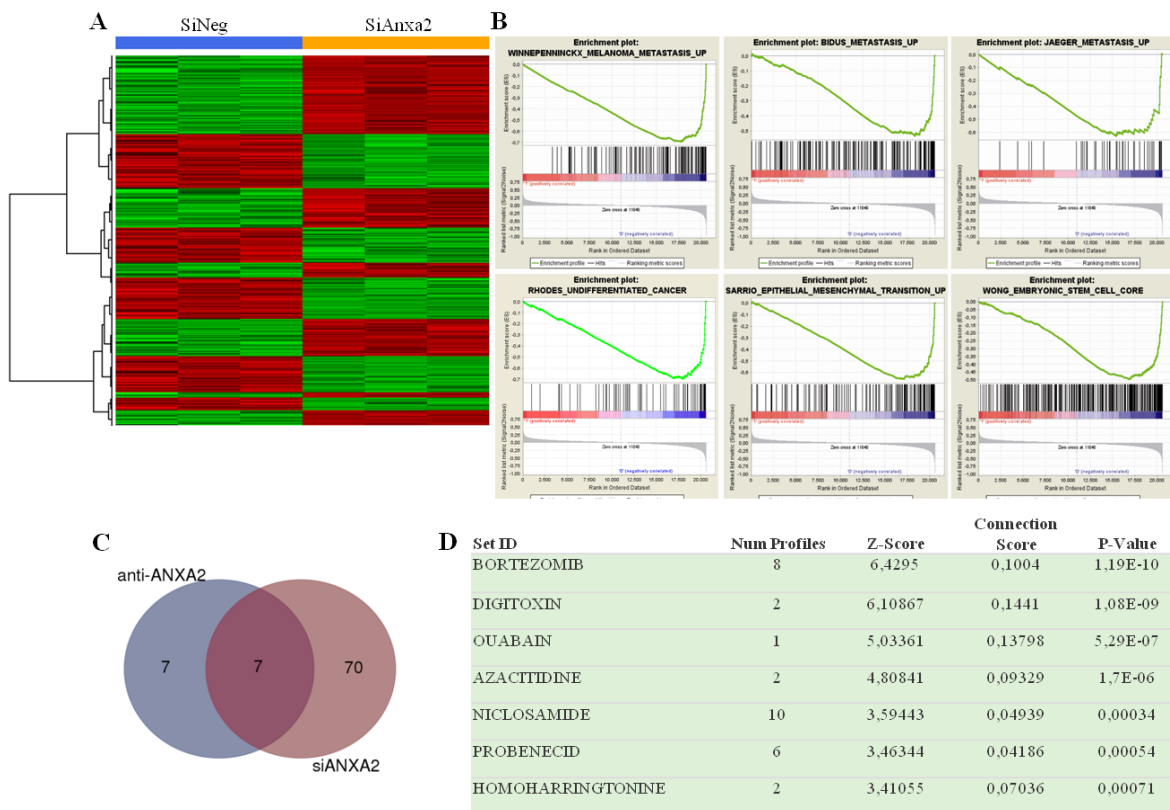


**Figure 24.** (A) Heat map generated by supervised analysis of HuTuP174 primary GBM cells silenced with small interfering RNAs (siRNAs) against ANXA2 for 48h (3 non targeting siRNA (siNEG) vs. 3 SiANXA2 silenced cells) using the 3592 differentially expressed probe sets (IFDR<0.05). (B) Representative GSEA enrichment plots demonstrating that probes down-regulated after ANXA2 silencing are enriched for genes involved in the metastatic process (upper panels), and a stem-like/undifferentiated phenotype (lower panels). Plot were generated by c2 curated gene sets in the GSEA MSigDatabase. The green curves show the enrichment score and reflects the degree to which each gene (black vertical lines) is represented at the top or bottom of the ranked gene list. The heat map indicates the relative abundance (red to blue) of the genes specifically enriched in the SiANXA2-silenced as compared with the SiNEG-silenced cells. (C) Venn diagram representative of the intersection between the compound lists obtained by functional mapping of ANXA2-neutralized and ANXA2-silenced cells specific signature on the QUADrATiC tool. (D) The connections and perturbation stabilities of the seven significant drugs obtained from the intersection.

## 7. DISCUSSION.

Most GBM tumors recur within 2 cm from the original tumor margin. This peculiar characteristic of GBM rely on brain cancer cell ability to invade the surrounding normal brain tissues, thus escaping from surgical removal and localized radiotherapy [103]. In this context, we and others recently exploited 5-ALA in order to properly identify and characterize dispersed GBM cells at the tumor margin, demonstrating that some of these cells are still endowed with stem-like characteristics, potentially hampering treatments [22, 104, 105]. In this discouraging landscape, a more comprehensive knowledge of the mechanisms involved in GBM cell spreading becomes particularly relevant.

Agreeing to this view, we chose to elucidate the potential involvement of ANXA2 in regulating GBM cell dissemination. Indeed, ANXA2 has been proved to sustain EMT and invasion of pancreatic ductal adenocarcinoma [106], induce hepatocellular carcinoma and breast cancer metastasis [72, 83] and was found up-regulated in highly invasive carcinomas [63, 107, 108]. Moreover, ANXA2 has been correlated to the observed hyperfibrinolysis-dependent bleeding in acute promyelocytic leukemia [109]. Here, we show that ANXA2 is significantly over-expressed in GBM in three independent cohorts of patients (Figure 4A-4D) and that ANXA2 expression can be considered as an independent prognostic factor in glioma [97, 110, 112]. More importantly, we demonstrate that low/absent expression of ANXA2 identifies a subgroup of GBM patients endowed with better prognosis in three different cohorts of GBM patients (Figure 4E–4H), with ANXA2 IHC score retaining a strong prognostic value for PFS in multivariate analysis (Table 2).

Since ANXA2 has been involved in multiple cellular functions including vesicle trafficking, cell division, calcium signalling and cellular growth [113], we analyzed a gene expression profile correlated to low ANXA2 expression in GBM tumors and characterized the transcriptional changes associated to its inhibition in GBM cells *in vitro*. Importantly, besides its reported role in cell migration and invasion, GSEA pointed out the existence of a positive and negative correlation between genes associated to high ANXA2 expression and the “Mesenchymal” and “Proneural” molecular subtypes [95] respectively. This information is particularly relevant, since GBMs belonging to the Proneural subtype display clinical and molecular features often associated to less aggressive tumors and long surviving patients [95, 114, 117]. On the other hand, tumors from the Mesenchymal molecular subgroup are

characterized by high expression of EMT markers such as MET and CD44, reminiscent of dedifferentiated aggressive tumors [95]. We also confirmed these findings by GSEA of ANXA2-inhibited GBM cells, which shows a significant negative enrichment of gene signatures associated to undifferentiated cancer and stem cell phenotype (Figure 9B), suggesting the potential involvement of ANXA2 also as a modulator of differentiation in GBM cells. Interestingly, we also examined the effects produced by intensive treatment protocols (defined as more than one cycle of single or concurrent chemo- and radiotherapy) in GBM patient subgroups generated on the basis of ANXA2 expression in the TCGA dataset. Our analyses show that aggressive treatment prolonged survival only in ANXA2 High tumors (HR=0,475; Figure 19A) rather than ANXA2 Very Low GBMs (HR=0,74; Figure 19B), resembling previous data on the Mesenchymal or Proneural subclasses respectively [95]. These latter results underline the potential and visionary clinical relevance of the assessment of ANXA2 expression in suggesting differential therapeutic strategies in GBM.

All these analyses recreate a complex scenario in which ANXA2 seems to sustain GBM cell aggressiveness at multiple levels. In addition, enrichment map generated by GO analysis of differentially expressed genes upon ANXA2 inhibition, points out a potential participation of ANXA2 also in the regulation of cytoskeletal organization and cell cycle dynamics (Figure 9C). Here we show that reduction of ANXA2 activity is sufficient to: i) dramatically impair GBM cell invasiveness; ii) induce a strong rearrangement of cytoskeletal structures; iii) inhibit cell proliferation. Although studies already reported that ANXA2 knockdown negatively affects invasiveness and proliferation of human and rodent glioma cell lines *in vitro* [118] and *in vivo* [97], to the best of our knowledge, we report for the first time the effects mediated by ANXA2 inhibition in patient-derived primary GBM cells, thus strengthening our conclusions. In particular, our data clearly indicate that ANXA2 down-modulation significantly reduces the expression of genes involved in DNA replication and chromosome segregation (Figure 9C, 9F, 9G), thus impairing GBM cell proliferation at the S-G2/M transition (Figure 16E-16H). This potential mechanism is added to different previous studies showing that ANXA2-mediated cell cycle effects could be attributed to p53 over-expression [119], Stat3 inhibition [120] or c-Myc-dependent cyclin D1 transcription [121].

Interestingly, ANXA2 over-expression did not alter GBM cell proliferation in our setting, suggesting that an intact ANXA2 function is necessary to sustain the complete oncogenic program engaged by GBM, but its up-regulation is not sufficient to trigger proliferation or

activate a de-differentiation program by itself. In a previous study, Rescher et al. demonstrated that insulin stimulation of normal BHK cells induced a massive rearrangement of actin fibers accompanied by cell spreading and detachment, and promoted a strong accumulation of F-actin and ANXA2 into FA-like structures at the cell periphery [122]. Authors proposed an ANXA2-mediated Rho/ROCK pathway control as the major responsible for the observed cytoskeletal remodeling. Our results are in line with these previous findings, showing that ANXA2<sup>hi</sup> cells organize actin fibers into FA-like structures at the cell periphery; conversely, ANXA2 inhibited/silenced GBM cells acquire a less “contracting” and more flattened cell shape (Figure 13A-13D). Moreover, it has recently been reported that ANXA2 should control the invasive properties of glioma cells by a double mechanism consisting of: i) augmented cancer cell binding to endothelial cells that eases the process of vascular co-option; ii) increase of VEGF and PDGF production which induce angiogenesis [123]. These data add further evidence to the multiple invasion mechanisms reported for ANXA2. Finally, based on gene expression data of ANXA2 neutralized cells, we were able to test the prognostic potential of an ANXA2<sup>down</sup> signature in multiple cancer datasets, demonstrating that expression of genes regulated (most likely indirectly) by ANXA2 fluctuations predict cancer patients outcome by themselves (Figure 18A-18F). These results are particularly relevant since they allow to generalize the prognostic potential of ANXA2 and/or ANXA2-modulated transcripts to multiple solid tumors, thus highlighting its relevance as a master controller of cancer cell dissemination and metastasis. In this context, increasing evidence suggests the participation of ANXA2 in regulating the localization as well as translation of specific transcripts. Indeed, specific ANXA2 domains are reported to bind to the 3'-UTRs of c-myc [89], collagen prolyl 4-hydroxylase- $\alpha$ (I) (C-P4H) [88] and N-methyl- D-aspartate R1 (NMDA-R1) [124] mRNAs, contributing to the post-transcriptional regulation of particular genes [125]. Therefore, a better comprehension of the direct or indirect effects mediated by ANXA2 on ECM degradation, cytoskeletal remodeling and gene transcription, will inevitably lead ANXA2 as future marker to be assessed for GBM management or to be targeted to inhibit dissemination.

Finally this project aimed to validate different bioinformatics tools for drug repurposing in GBM. To this purpose, we used the ANXA2 dependent transcriptional signatures derived from the comparison between ANXA2<sup>hi</sup> versus ANXA2<sup>lo</sup> expressing GBM patients in the TCGA and GSE13041 datasets by querying the Connectivity Map software [37]. The

software identified nine approved compounds able to revert the ANXA2-dependent signature of GBM aggressiveness, three of which have been functionally validated for their ability to inhibit cell proliferation, motility and invasion in primary GBM cultures *in vitro*, as ANXA2 modulation did. Thus, the Connectivity Map has proven to be a powerful and efficient tool to predict perturbagens and drugs able to reproduce the transcriptional effects mediated by ANXA2 activity down-modulation. Therefore, it can be considered a good gene-expression-based screening approach for poly-pharmacology drug discovery, in order to identify potential small molecule compounds, which may be further investigated as candidates for repurposing to cancer treatment.

More recently, the development of the QUADrATiC tool provided an improvement over existing connectivity map software, offering potential to biological researchers to analyze transcriptional data and generate potential therapeutics for focused study [39]. Indeed, QUADrATiC represents a step change in the process of investigating gene expression connectivity and provides more biologically and clinically relevant results than previous alternative solutions. For this reason, we decided to submit to the QUADrATiC software the ANXA2 dependent transcriptional signatures that we previously generated from primary GBM cell cultures after ANXA2 inhibition/silencing. Thus, we retrieved a list of seven FDA approved drugs in common between the two ANXA2-specific transcriptional profiles (Figure 24C, 24D). In particular, we found the therapeutic Bortezomib and the cardiac glycoside Oubain as the most significant drugs. Indeed, the effects of the bortezomib have been already evaluated in patients with recurrent malignant gliomas during a phase II trial [126] and a recent study revealed ouabain, as a sustainer of glioma cell apoptosis partly via ROS accumulation in glioblastoma cells [127]. These evidences highlight the relevance of QUADrATiC software for the identification of perturbagens and FDA approved drugs able to revert the gene signature of a specific cancer to a less aggressive or drug-sensitive transcriptional profile, with reported applications in brain tumors.

## 8. FUTURE PROSPECTIVES

This project allowed us to identify a new target protein (ANXA2) strictly involved in GBM aggressiveness and, as a further confirmation, we demonstrated that ANXA2 inhibition is an important step forward towards GBM therapy. In particular, we uncovered seven new FDA approved drugs able to revert the effects mediated by the high levels of ANXA2 in GBM by the QUADrATiC software. In the future, we aim to test these compounds in a series of established primary GBM cell lines for their ability to impair cell proliferation, motility and invasion both in “plastic-based” cell cultures and in organoid-culture models, a new three-dimensional *in vitro* culture system able to recapitulate the original tumor architecture. Moreover, given the results obtained by GSEA analysis we aim also to investigate drug effects on GBM cells phenotype and differentiation status.

Finally, in order to investigate the molecular mechanisms by which ANXA2 controls gene transcription and the relative intracellular functions, we propose to identify specific mRNAs, directly bound by intracellular cytoskeleton-associated ANXA2, to be considered as new potential GBM targets by exploiting the cross-linking immunoprecipitation (CLIP) technique. CLIP could be applied to at least three primary GBM cultures in order to map the binding of ANXA2 to specific transcripts on a genome-wide scale through RNA-sequencing. These new ANXA2-dependent targets, could be the starting point for the future set up of novel GBM targeting approaches.

## 9. MATERIALS AND METHODS

### **Neurosurgical sample collection, isolation and gas-controlled expansion of GBM cells.**

Written informed consent for the donation of adult tumor brain tissues was obtained from patients before tissue collection under the auspices of the protocol for the acquisition of human brain tissues obtained from the Ethical Committee of the Padova University-Hospital. All tissues were acquired following the tenets of the Declaration of Helsinki. For this study we used GBM specimens isolated from 89 tumors taken at surgery and then formalin-fixed and paraffin embedded (FFPE) for subsequent IHC analysis. Moreover, 8 primary GBM cultures have been used for in vitro experiments. General characteristics of patients from which we derived GBM primary cells are listed in Suppl. Table S4. Primary GBM cells were isolated and maintained in culture as described previously [128]. Briefly, tumor biopsies were subjected to mechanical dissociation and the resulting cell suspension was cultured on fibronectin-coated dishes in DMEM/F12 medium supplemented with BIT9500 (Stemcell Technologies Inc., Vancouver, Canada), 20ng/ml basic Fibroblast Growth Factor (bFGF; Sigma-Aldrich S.r.l., Milan, Italy) and 20ng/ml Epidermal Growth Factor (EGF; R&D Systems, Minneapolis, MN). GBM cells were maintained in an atmosphere of 2% oxygen, 5% carbon dioxide and balanced nitrogen in a Ruskinn C300 system for a proper cell expansion in hypoxic conditions (Ruskinn Technology Ltd, Bridgend, UK). Cells were not cultured for more than 8 passages in vitro in order to avoid long term culture related effects. In some experiments, GBM cells were treated with an anti-ANXA2 monoclonal antibody (clone C-10; Santa Cruz Biotechnology, Santa Cruz, CA; Suppl. Table S8) at a final concentration of 5 or 20µg/ml [96, 97] and then cultured for 24-96h.

### **Immunohistochemistry**

ANXA2 immunohistochemistry was conducted on 5µm sections from 89 FFPE GBM specimens with standard procedures. Briefly, sections were re-hydrated and then antigen retrieval was performed by incubation with citrate buffer 0.01M pH6 at 95°C. After saturation with the appropriate normal serum, slides were incubated with an anti-ANXA2 antibody (clone 5/Annexin II; BD Bioscience, San Jose, CA; Supplementary Table S8). After incubation, sections were washed and incubated with species-specific biotin-conjugated secondary antibodies (Vector Laboratories Inc. Burlingame, CA; Supplementary Table S8).



ANXA2 expression was revealed by using the Dako Liquid DAB<sup>+</sup> Substrate Chromogen System (Dako, Glostrup, Denmark) according to manufacturer's guidelines. Tissues were counterstained with Meyer's Hematoxylin and images acquired with a Zeiss Imager M1 microscope (Carl Zeiss, Oberkochen, Germany). The specificity of each staining procedure was confirmed by replacing the primary antibodies with an Isotype control. The expression level of ANXA2 was scored using a combined method accounting for both the staining intensity and the percentage of positive stained cells. The resulting combined score was calculated as the multiplication of the score accounting for the percentage of ANXA2<sup>+</sup> cells (0-6) and the intensity score (0-3). ANXA2 stained slides were independently evaluated by two different pathologists.

### **Transfection of primary GBM cells.**

To achieve a suitable gene silencing, GBM cells were transfected with 200pmol of two different small interfering RNAs (siRNAs) against ANXA2 as well as with a non targeting siRNA (siNEG) using the Lipofectamine RNAiMAX reagent (Thermo Fisher Scientific, Waltham, MA) according to manufacturer's instructions. siANXA2#1 siRNA sequence: (RNA)-5'-GCG ACU ACC AGA AAG CGC UGC UGU A-3'; siANXA2#2 siRNA sequence: (RNA)-5'-GAC UGA UCU GGA GAA GGA CAU UAU U-3' (Stealth RNAi™; siANXA2#1 cat.# 10620318, siANXA2#2 cat.# 10620319). For ANXA2-overexpression experiments, the ANXA2 complete cDNA sequence was cloned into a pcDNA3.1 empty vector in order to generate an expression vector named pcDNA3.1-ANXA2. Primers used for ANXA2 coding sequence amplification are listed in Supplementary Table S9. In over-expression experiments, GBM cells were transfected with an opportune quantity of pcDNA3.1-ANXA2 or pcDNA3.1 empty vector using the TransIT®-LT1 Transfection Reagent (Mirus Bio LLC, Madison, WI) according to manufacturer's instructions. Transfected cells were then cultured for 24-96h depending on the experimental endpoints. The analysis of silencing or overexpression specificity was achieved by WB and qRT-PCR.

### **Western blot.**

Equal amounts of proteins (10µg) extracted from primary GBM cells were resolved using a SDS-PAGE gels and transferred to polyvinylidene difluoride (PVDF) Immobilon-p membrane (Merk-Millipore, Darmstadt, Germany). Membranes were blocked with I-block™

(Thermo Fisher Scientific, Waltham, MA) for at least 1 hour at room temperature and then were incubated overnight at 4°C under constant shaking with the primary antibody against Membranes were next incubated with HRP-labeled goat anti-mouse IgG (1:50000; Sigma-Aldrich, Milan, Italy; Supplementary Table S8) for 60 minutes. All membranes were visualized using ECL Select (GE Healthcare, Catania, Italy) and exposed to Amersham Hyperfilm ECL (GE Healthcare).  $\beta$ -actin staining (Sigma-Aldrich S.r.l., Milan, Italy; Supplementary Table S8) was used as loading control.

### **Gene expression profiling of ANXA2 antibody-treated and silenced GBM cells and data analysis.**

For microarray experiments, in vitro transcription, hybridization and biotin labeling of RNA from GBM cells treated with anti-ANXA2 neutralizing antibody and siRNA against ANXA2 were performed according to Affymetrix 3'IVT Express Plus protocol, after 48h of treatment with ANXA2 antibody or a matched isotype control and 48h of silencing with siANXA2 as well as with a siNEG. GeneChip Human Genome U133 Plus 2.0 (Affymetrix, Santa Clara, CA) was used. Microarray data (CEL files) were generated using default Affymetrix microarray analysis parameters (Command Console suite software, Affymetrix). CEL files were normalized using the robust multiarray averaging expression measure of Affy-R package ([www.bioconductor.org](http://www.bioconductor.org)). Shrinkage t-test [129] was applied to identify genes that were differently expressed along ANXA2 antibody and isotype control-treated GBM cells in four independent experiments and along siANXA2 and siNEG-silenced GBM cells in three independent experiments. Local False Discovery Rate (IFDR) $<0.05$  was used as multiplicity correction of p-value to identify gene differently expressed. A heat map was generated by R software ([www.R-project.org](http://www.R-project.org)) using Euclidean distance as a distance measure between genes and Ward method for clustering probe sets. Expression data have been deposited into the Gene Expression Omnibus (GEO) database under Series Accession Number GSE76786 and are accessible without restrictions. Gene Set Enrichment Analysis (GSEA) was performed using GSEAv2.0 with probe sets ranked by signal-to-noise ratio and statistical significance determined by 1000 permutations [130]. Gene sets permutations ( $<7$  replicates in each class) were used to enable direct comparisons between ANXA2 antibody and isotype control-treated GBM cells and siANXA2 and siNEG-silenced GBM cells. Minimum gene set size was set to 15; maximum of probe sets was used to collapse multiple probe sets into gene. For GSEA an

FDR cutoff <0.05 was used. MgSigDataBase derived from c2 curated dataset and c5 Gene Ontology dataset were selected to obtain the enrichment gene sets. Enrichment map was generated using Enrichment Map Cytoscape v3.2.1 plug-in [131]. Only Gene sets with FDR q value  $\leq 0.05$ , derived from c5 Gene Ontology MSigDB GSEA were used to build the network. Node represents the functional gene sets and the size is proportional to size of gene set. Edge represents the degree of gene overlap that exist between two gene sets and the thickness is proportional to the overlap between the gene sets. To generate the gene sets relationship we used Overlap Coefficient parameters (Overlap Coefficient = [size of (A intersect B)] / [size of (minimum(A , B))], where A and B are two gene sets). Redundant gene sets with common biological function were grouped in cluster and manually labeled with Gene Ontology terms. Blue indicate enrichment in ANXA2 antibody-treated GBM cells.

### **Reverse transcription and real-time PCR.**

RNA was extracted from GBM cells using TRIzol reagent (Thermo Fisher Scientific, Waltham, MA) according to manufacturer's instructions and 1–2 $\mu$ g of total RNA reverse-transcribed using SuperScript RNase II Reverse Transcriptase (Thermo Fisher Scientific, Waltham, MA). Quantitative RT-PCR reactions were run in triplicate using Platinum SYBR Green Q-PCR Super Mix (Thermo Fisher Scientific, Waltham, MA). Fluorescent emission was recorded in real-time (Sequence Detection System 7900HT, Applied Biosystems, Foster City, CA). The specificity of primers was confirmed for every PCR run by dissociation curve analysis. Primers used are listed in Supplementary Table S9 and their specificity was confirmed by the software Human BLAT Search (<http://genome.ucsc.edu>). Relative RNA quantities were normalized to GUSB according to the  $\Delta\Delta$ Ct Method.

### **Scratch-migration and invasion assays.**

To evaluate the effects of ANXA2 modulation on the migratory properties of GBM cells, they were cultured on 35-mm culture dishes until they reached at least 80% confluence. 24h after antibody treatment or 48h after ANXA2 silencing/over-expression, GBM cell monolayer has been gently scratched horizontally and vertically. After being scratched, GBM cells were washed twice with culture medium to remove cell debris and incubated until pre-determined endpoints. Migrated cells were defined as cells that moved into the scratch and detached away from the cell monolayer. Cell migration was evaluated by measuring the distance between the

two edges of the scratch in at least 8 random fields by using Adobe Photoshop CS6 (Adobe Systems Incorporated, La Jolla, CA; [www.adobe.com](http://www.adobe.com)). Images were acquired by using with a Nikon TS100 inverted microscope (Nikon, Melville, NY).

To assess the invasive capacity of GBM cells depending on ANXA2 levels, soluble extracellular matrix Matrigel was dispensed in 24-well plates and allowed to gel for about 45 min at 37°C. GBM cells were then added onto Matrigel layer in a volume of 0.5ml, treated with anti-ANXA2 antibody for 72h or 7 days at 5 or 20µg/ml. Images were captured with a Nikon TS100 inverted microscope (Nikon, Melville, NY). Calculation of number and length of branches and invading cells was performed with Angiogenesis plugin from ImageJ software (<https://imagej.nih.gov>). Moreover, GBM invasion was also evaluated using the CultreCoat® 24-Well BME Cell Invasion Assay (Trevigen, Gaithersburg, MD) according to the manufacturer's instructions. Invasion was measured 48h after plating, at 485-520nm using a VICTOR spectrophotometer (Perkin Elmer, Milan, Italy).

#### **Chick embryo chorioallantoic membrane invasion assay.**

Plastic rings were placed on the chorioallantoic membrane (CAM) of fertilized White Leghorn chicken eggs at day 8 (8-10 CAMs/experimental group). Then, 6µl of a cell suspension containing  $1.5 \times 10^5$  EGFP-GBM cells (HuTuP13) were injected inside the ring. CAMs were treated with a solution containing 2µg of isotype or anti-ANXA2 antibodies every day for 3 consecutive days. On day 11, CAMs were fixed with PFA 3%, washed and mounted with Vectashield Antifade Mounting Medium (Vector Laboratories Inc. Burlingame, CA). Samples were acquired under an Axiovert 200 fluorescence microscope equipped with a EC Plan Neofluar 20x/0.5 NA objective and ApoTome system (Carl Zeiss, Oberkochen, Germany). EGFP-positive areas were quantified using Image-Pro Plus software (Media Cybernetics, Inc., Rockville, MD).

#### **Immunofluorescence.**

GBM cells were cultured on 4-well chamber slides (BD Bioscience, San Jose, CA), treated depending on the experimental plan. After treatment, cells were fixed in cold 4% formaldehyde and stored at +4°C prior to analysis. Primary antibody staining was performed for Nestin (Merk-Millipore, Darmstadt, Germany), Ki67, GFAP, S100 (all from Dako, Glostrup, Denmark), MAP2 (Sigma-Aldrich, Milan, Italy), OSP (Abcam, Cambridge, UK),

ANXA2 (clone C-10; Santa Cruz Biotechnology, Santa Cruz, CA), FITC-conjugated Phalloidin (1:1000; Sigma-Aldrich, Milan, Italy) and Sox2 (Cell Signaling Technology). For additional details on antibodies used for immunofluorescence, please see Supplementary Table S7. After incubation, cells were washed and incubated with species-specific secondary antibodies conjugated to Alexa dyes (Thermo Fisher Scientific, Waltham, MA; Supplementary Table S8). Cells were counterstained with DAPI (1:10000; Sigma-Aldrich, Milan, Italy) to measure total cell number. Staining was visualized by epifluorescence with a ViCo microscope (Vico, Nikon, Melville, NY).

### **Cytofluorimetric analyses.**

CD133 were incubated with anti-human CD133 (clone CD133/1-PE; Miltenyi Biotec, Bergisch Gladbach, Germany) as previously described (Supplementary Table S8). Relative percentages of different subpopulations were calculated based on live gated cells (as indicated by physical parameters, side scatter and forward scatter). Unlabeled cells and cells incubated with appropriate isotype control antibodies were first acquired to ensure labelling specificity. To perform cell cycle analysis, GBM cells were collected after 72h of treatment (anti-ANXA2 antibody, ANXA2 silencing or over-expression), centrifuged and fixed with ice-cold ethanol (70%). Cells were then treated with permeabilization buffer containing RNase A, 0.1% Triton X-100 and propidium iodide (PI) at room temperature for 30 minutes prior to analysis. DNA histograms were analyzed using Multi-Cycle® for Windows (Phoenix Flow Systems, San Diego, CA). Analysis of BrdU incorporation was performed with a BrdU Staining Kit for Flow Cytometry FITC (eBioscience, Hatfield, UK) according to the manufacturer's instructions. BrdU was incubated with cells for 72h. For all stainings, samples were acquired on a Cytomic FC500 flow cytometer (Beckman Coulter, Brea, CA).

### **Correlation of ANXA2<sup>down</sup> signature to clinical outcome.**

The ANXA2<sup>down</sup> gene signature was generated by using the most significant down-regulated genes after treatment of GBM cells with the monoclonal antibody against ANXA2 (fold change  $\leq 0.8$ ; Suppl. Table S5). Then, we evaluated the prognostic potential of this signature in TCGA [92], GSE13041 [94], GSE17536 [100], E-MTAB-365 [101] and GSE31210 [102] datasets. The log<sub>2</sub> expression values for each sample in each dataset were centered to zero mean. The sum of the mean-centered log<sub>2</sub> expression values of the ANXA2<sup>down</sup> probe sets

was used as the Risk Score for each subject and the 519 subjects from TCGA, 191 from GSE13041, 177 from GSE17536, 409 from E-MTAB-365 and 217 from GSE31210 were split into high- and low-risk groups greater and less than the median risk score respectively [132]. These risk groups were assessed for prognostication of OS and PFS in univariate Cox analysis (log-rank test).

### **Drug screening.**

Selected drugs were analyzed in vitro for their ability to inhibit GBM cell proliferation, motility and invasion. MTT assay was performed in order to determine the potential anti-proliferative effects of compounds and the optimal concentration to be used in subsequent experiments. GBM cells were treated at different concentrations and 10 $\mu$ l of 3-(4,5-dimethylthiazol-2-yl)-2,5-diphenyltetrazolium bromide (MTT) was added into 96-well, after 96h from treatment; cells were incubated for 3-4 hours and 100 $\mu$ l of isopropanol solution was then added to each well to dissolve crystals formed. Cell proliferation was subsequently evaluated by VICTOR spectrophotometer. Cell motility was investigated by scratching a monolayer of GBM cells and monitoring the ability to close the wound during time of 72h. Cell migration was evaluated by measuring the distance between the two edges of the scratch in at least 8 random fields by using Adobe Photoshop CS6 (Adobe Systems Incorporated, La Jolla, CA; [www.adobe.com](http://www.adobe.com)). Images were acquired by using with a Nikon TS100 inverted microscope (Nikon, Melville, NY). Moreover, invasion was assessed by measuring cell spreading onto Matrigel coated dishes after 72h or 7 days. Images were captured with a Nikon TS100 inverted microscope (Nikon, Melville, NY). Compounds able to significantly reduce disseminating properties of GBM cells were tested for their potential effect in reorganizing cytoskeletal fibers. To this end, treated cells were stained with FITC-coniugated Phalloidin (1:1000; Sigma-Aldrich, Milan, Italy) and staining was visualized by epifluorescence with a ViCo microscope (Vico, Nikon, Melville, NY).

### **Statistics.**

Graphs and associated statistical analyses were generated using Graph Pad Prism 6.07 (GraphPad, La Jolla, CA). All data in bar graphs are presented as mean  $\pm$  standard error of the mean (S.E.M.). Statistical significance was measured by one-way ANOVA with Newman–Keuls multiple comparison post test (for more than two comparisons) and paired t-test

(comparison of two groups); \* $p < 0.05$ , \*\* $p < 0.01$ , \*\*\* $p < 0.001$ , \*\*\*\* $p < 0.0001$ . For all graphs, asterisks over brackets indicate a significant difference with another variable as indicated and asterisks over bars indicate a significant difference with the control group.

Survival analyses were performed by generating Kaplan Meier survival curves and significance calculated by log-rank (Mantel-Cox) test. In all comparisons of survival, Hazard Ratio have been calculated as ANXA2 High risk/ANXA2 Very Low risk. Independent prognostic value of GBM patient subgroups generated on the basis of ANXA2 expression was calculated by applying a multivariate Cox analysis (Wald test) with SPSS 13 software (SPSS Inc., Chicago, IL).

## 10. REFERENCES

1. Ferluga S and Debinski W. Ephs and Ephrins in malignant gliomas. Growth factors (Chur, Switzerland). 2014; 32(6):190-201.
2. Louis DN, Ohgaki H, Wiestler OD, Cavenee WK, Burger PC, Jouvet A, Scheithauer BW and Kleihues P. The 2007 WHO classification of tumours of the central nervous system. Acta neuropathologica. 2007; 114(2):97-109.
3. Ohgaki H and Kleihues P. Epidemiology and etiology of gliomas. Acta neuropathologica. 2005; 109(1):93-108.
4. Villano JL, Seery TE and Bressler LR. Temozolomide in malignant gliomas: current use and future targets. Cancer Chemother Pharmacol. 2009; 64(4):647-655.
5. ABTA. Brain Tumors – A Handbook for the Newly Diagnosed. American Brain Tumors Association).
6. Westphal M and Lamszus K. The neurobiology of gliomas: from cell biology to the development of therapeutic approaches. Nature reviews Neuroscience. 2011; 12(9):495-508.
7. Dixit S, Hingorani M, Achawal S and Scott I. The sequential use of carmustine wafers (Gliadel(R)) and post-operative radiotherapy with concomitant temozolomide followed by adjuvant temozolomide: a clinical review. Br J Neurosurg. 2011; 25(4):459-469.
8. Stupp R, Mason WP, van den Bent MJ, Weller M, Fisher B, Taphoorn MJ, Belanger K, Brandes AA, Marosi C, Bogdahn U, Curschmann J, Janzer RC, Ludwin SK, Gorlia T, Allgeier A, Lacombe D, et al. Radiotherapy plus concomitant and adjuvant temozolomide for glioblastoma. N Engl J Med. 2005; 352(10):987-996.
9. Sanai N and Berger MS. Glioma extent of resection and its impact on patient outcome. Neurosurgery. 2008; 62(4):753-764; discussion 264-756.
10. Uchida N, Buck DW, He D, Reitsma MJ, Masek M, Phan TV, Tsukamoto AS, Gage FH and Weissman IL. Direct isolation of human central nervous system stem cells. Proc Natl Acad Sci U S A. 2000; 97(26):14720-14725.
11. Thomas AA, Brennan CW, DeAngelis LM and Omuro AM. Emerging therapies for glioblastoma. JAMA neurology. 2014; 71(11):1437-1444.
12. Della Puppa A, Ciccarino P, Lombardi G, Rolma G, Cecchin D and Rossetto M. 5-Aminolevulinic acid fluorescence in high grade glioma surgery: surgical outcome, intraoperative findings, and fluorescence patterns. BioMed research international. 2014; 2014:232561.
13. Pistollato F, Abbadì S, Rampazzo E, Persano L, Della Puppa A, Frasson C, Sarto E, Scienza R, D'Avella D and Basso G. Intratumoral hypoxic gradient drives stem cells distribution and MGMT expression in glioblastoma. Stem Cells. 2010; 28(5):851-862.



14. Della Puppa A, Persano L, Masi G, Rampazzo E, Sinigaglia A, Pistollato F, Denaro L, Barzon L, Palu G, Basso G, Scienza R and d'Avella D. MGMT expression and promoter methylation status may depend on the site of surgical sample collection within glioblastoma: a possible pitfall in stratification of patients? *Journal of neuro-oncology*. 2012; 106(1):33-41.
15. Stummer W, van den Bent MJ and Westphal M. Cytoreductive surgery of glioblastoma as the key to successful adjuvant therapies: new arguments in an old discussion. *Acta Neurochir (Wien)*. 2011; 153(6):1211-1218.
16. Idoate MA, Diez Valle R, Echeveste J and Tejada S. Pathological characterization of the glioblastoma border as shown during surgery using 5-aminolevulinic acid-induced fluorescence. *Neuropathology*. 2011; 31(6):575-582.
17. Lacroix M, Abi-Said D, Fourney DR, Gokaslan ZL, Shi W, DeMonte F, Lang FF, McCutcheon IE, Hassenbusch SJ, Holland E, Hess K, Michael C, Miller D and Sawaya R. A multivariate analysis of 416 patients with glioblastoma multiforme: prognosis, extent of resection, and survival. *J Neurosurg*. 2001; 95(2):190-198.
18. Gaspar LE, Fisher BJ, Macdonald DR, LeBer DV, Halperin EC, Schold SC, Jr. and Cairncross JG. Supratentorial malignant glioma: patterns of recurrence and implications for external beam local treatment. *Int J Radiat Oncol Biol Phys*. 1992; 24(1):55-57.
19. Giese A, Bjerkvig R, Berens ME and Westphal M. Cost of migration: invasion of malignant gliomas and implications for treatment. *J Clin Oncol*. 2003; 21(8):1624-1636.
20. Stummer W, Stocker S, Wagner S, Stepp H, Fritsch C, Goetz C, Goetz AE, Kieffmann R and Reulen HJ. Intraoperative detection of malignant gliomas by 5-aminolevulinic acid-induced porphyrin fluorescence. *Neurosurgery*. 1998; 42(3):518-525; discussion 525-516.
21. Theeler BJ and Groves MD. High-grade gliomas. *Curr Treat Options Neurol*. 2011; 13(4):386-399.
22. Aldave G, Tejada S, Pay E, Marigil M, Bejarano B, Idoate MA and Diez-Valle R. Prognostic value of residual fluorescent tissue in glioblastoma patients after gross total resection in 5-aminolevulinic Acid-guided surgery. *Neurosurgery*. 2013; 72(6):915-920; discussion 920-911.
23. Stummer W, Novotny A, Stepp H, Goetz C, Bise K and Reulen HJ. Fluorescence-guided resection of glioblastoma multiforme by using 5-aminolevulinic acid-induced porphyrins: a prospective study in 52 consecutive patients. *J Neurosurg*. 2000; 93(6):1003-1013.
24. Chinot OL, Barrie M, Fuentes S, Eudes N, Lancelot S, Metellus P, Muracciole X, Braguer D, Ouafik L, Martin PM, Dufour H and Figarella-Branger D. Correlation between O6-methylguanine-DNA methyltransferase and survival in inoperable newly diagnosed glioblastoma patients treated with neoadjuvant temozolomide. *J Clin Oncol*. 2007; 25(12):1470-1475.
25. Hegi ME, Liu L, Herman JG, Stupp R, Wick W, Weller M, Mehta MP and Gilbert MR. Correlation of O6-methylguanine methyltransferase (MGMT) promoter methylation

with clinical outcomes in glioblastoma and clinical strategies to modulate MGMT activity. *J Clin Oncol*. 2008; 26(25):4189-4199.

26. Bates DO. Vascular endothelial growth factors and vascular permeability. *Cardiovascular research*. 2010; 87(2):262-271.

27. Gerstner ER, Duda DG, di Tomaso E, Ryg PA, Loeffler JS, Sorensen AG, Ivy P, Jain RK and Batchelor TT. VEGF inhibitors in the treatment of cerebral edema in patients with brain cancer. *Nature reviews Clinical oncology*. 2009; 6(4):229-236.

28. Cohen MH, Shen YL, Keegan P and Pazdur R. FDA drug approval summary: bevacizumab (Avastin) as treatment of recurrent glioblastoma multiforme. *The oncologist*. 2009; 14(11):1131-1138.

29. Takano S, Kimu H, Tsuda K, Osuka S, Nakai K, Yamamoto T, Ishikawa E, Akutsu H, Matsuda M and Matsumura A. Decrease in the apparent diffusion coefficient in peritumoral edema for the assessment of recurrent glioblastoma treated by bevacizumab. *Acta neurochirurgica Supplement*. 2013; 118:185-189.

30. Bota DA, Desjardins A, Quinn JA, Affronti ML and Friedman HS. Interstitial chemotherapy with biodegradable BCNU (Gliadel) wafers in the treatment of malignant gliomas. *Therapeutics and clinical risk management*. 2007; 3(5):707-715.

31. Westphal M, Hilt DC, Bortey E, Delavault P, Olivares R, Warnke PC, Whittle IR, Jaaskelainen J and Ram Z. A phase 3 trial of local chemotherapy with biodegradable carmustine (BCNU) wafers (Gliadel wafers) in patients with primary malignant glioma. *Neuro-oncology*. 2003; 5(2):79-88.

32. Affronti ML, Heery CR, Herndon JE, 2nd, Rich JN, Reardon DA, Desjardins A, Vredenburgh JJ, Friedman AH, Bigner DD and Friedman HS. Overall survival of newly diagnosed glioblastoma patients receiving carmustine wafers followed by radiation and concurrent temozolomide plus rotational multiagent chemotherapy. *Cancer*. 2009; 115(15):3501-3511.

33. De Bonis P, Anile C, Pompucci A, Fiorentino A, Balducci M, Chiesa S, Maira G and Mangiola A. Safety and efficacy of Gliadel wafers for newly diagnosed and recurrent glioblastoma. *Acta Neurochir (Wien)*. 2012; 154(8):1371-1378.

34. Kleinberg L. Polifeprosan 20, 3.85% carmustine slow-release wafer in malignant glioma: evidence for role in era of standard adjuvant temozolomide. *Core evidence*. 2012; 7:115-130.

35. Nabors LB, Ammirati M, Bierman PJ, Brem H, Butowski N, Chamberlain MC, DeAngelis LM, Fenstermaker RA, Friedman A, Gilbert MR, Hesser D, Holdhoff M, Junck L, Lawson R, Loeffler JS, Maor MH, et al. Central nervous system cancers. *Journal of the National Comprehensive Cancer Network : JNCCN*. 2013; 11(9):1114-1151.

36. Cheng HW, Liang YH, Kuo YL, Chuu CP, Lin CY, Lee MH, Wu AT, Yeh CT, Chen EI, Whang-Peng J, Su CL and Huang CY. Identification of thioridazine, an antipsychotic

drug, as an antiglioblastoma and anticancer stem cell agent using public gene expression data. *Cell Death Dis.* 2015; 6:e1753.

37. Lamb J, Crawford ED, Peck D, Modell JW, Blat IC, Wrobel MJ, Lerner J, Brunet JP, Subramanian A, Ross KN, Reich M, Hieronymus H, Wei G, Armstrong SA, Haggarty SJ, Clemons PA, et al. The Connectivity Map: using gene-expression signatures to connect small molecules, genes, and disease. *Science (New York, NY)*. 2006; 313(5795):1929-1935.

38. Faria CC, Agnihotri S, Mack SC, Golbourn BJ, Diaz RJ, Olsen S, Bryant M, Bebenek M, Wang X, Bertrand KC, Kushida M, Head R, Clark I, Dirks P, Smith CA, Taylor MD, et al. Identification of alsterpaullone as a novel small molecule inhibitor to target group 3 medulloblastoma. *Oncotarget*. 2015; 6(25):21718-21729.

39. O'Reilly PG, Wen Q, Bankhead P, Dunne PD, McArt DG, McPherson S, Hamilton PW, Mills KI and Zhang SD. QUADrATiC: scalable gene expression connectivity mapping for repurposing FDA-approved therapeutics. *BMC bioinformatics*. 2016; 17(1):198.

40. Chicoine MR and Silbergeld DL. Mitogens as motogens. *Journal of neuro-oncology*. 1997; 35(3):249-257.

41. Cuddapah VA, Robel S, Watkins S and Sontheimer H. A neurocentric perspective on glioma invasion. *Nature reviews Neuroscience*. 2014; 15(7):455-465.

42. Friedl P and Alexander S. Cancer invasion and the microenvironment: plasticity and reciprocity. *Cell*. 2011; 147(5):992-1009.

43. Xu R, Boudreau A and Bissell MJ. Tissue architecture and function: dynamic reciprocity via extra- and intra-cellular matrices. *Cancer metastasis reviews*. 2009; 28(1-2):167-176.

44. Midwood KS, Williams LV and Schwarzbauer JE. Tissue repair and the dynamics of the extracellular matrix. *The international journal of biochemistry & cell biology*. 2004; 36(6):1031-1037.

45. Bissell MJ, Kenny PA and Radisky DC. Microenvironmental regulators of tissue structure and function also regulate tumor induction and progression: the role of extracellular matrix and its degrading enzymes. *Cold Spring Harbor symposia on quantitative biology*. 2005; 70:343-356.

46. Bissell MJ, Hall HG and Parry G. How does the extracellular matrix direct gene expression? *Journal of theoretical biology*. 1982; 99(1):31-68.

47. Demuth T and Berens ME. Molecular mechanisms of glioma cell migration and invasion. *Journal of neuro-oncology*. 2004; 70(2):217-228.

48. Goldbrunner RH, Bernstein JJ and Tonn JC. Cell-extracellular matrix interaction in glioma invasion. *Acta Neurochir (Wien)*. 1999; 141(3):295-305; discussion 304-295.

49. Cocucci E, Racchetti G and Meldolesi J. Shedding microvesicles: artefacts no more. *Trends in cell biology*. 2009; 19(2):43-51.

50. Skog J, Wurdinger T, van Rijn S, Meijer DH, Gainche L, Sena-Esteves M, Curry WT, Jr., Carter BS, Krichevsky AM and Breakefield XO. Glioblastoma microvesicles transport RNA and proteins that promote tumour growth and provide diagnostic biomarkers. *Nature cell biology*. 2008; 10(12):1470-1476.
51. Valadi H, Ekstrom K, Bossios A, Sjostrand M, Lee JJ and Lotvall JO. Exosome-mediated transfer of mRNAs and microRNAs is a novel mechanism of genetic exchange between cells. *Nature cell biology*. 2007; 9(6):654-659.
52. Naus CC and Laird DW. Implications and challenges of connexin connections to cancer. *Nature reviews Cancer*. 2010; 10(6):435-441.
53. Hajjar KA and Krishnan S. Annexin II: a mediator of the plasmin/plasminogen activator system. *Trends Cardiovasc Med*. 1999; 9(5):128-138.
54. Huebner K, Cannizzaro LA, Frey AZ, Hecht BK, Hecht F, Croce CM and Wallner BP. Chromosomal localization of the human genes for lipocortin I and lipocortin II. *Oncogene research*. 1988; 2(4):299-310.
55. Hajjar KA, Mauri L, Jacovina AT, Zhong F, Mirza UA, Padovan JC and Chait BT. Tissue plasminogen activator binding to the annexin II tail domain. Direct modulation by homocysteine. *J Biol Chem*. 1998; 273(16):9987-9993.
56. Johnsson N, Marriott G and Weber K. p36, the major cytoplasmic substrate of src tyrosine protein kinase, binds to its p11 regulatory subunit via a short amino-terminal amphiphatic helix. *Embo j*. 1988; 7(8):2435-2442.
57. Filipenko NR and Waisman DM. The C terminus of annexin II mediates binding to F-actin. *J Biol Chem*. 2001; 276(7):5310-5315.
58. Kassam G, Manro A, Braat CE, Louie P, Fitzpatrick SL and Waisman DM. Characterization of the heparin binding properties of annexin II tetramer. *J Biol Chem*. 1997; 272(24):15093-15100.
59. Hajjar KA, Jacovina AT and Chacko J. An endothelial cell receptor for plasminogen/tissue plasminogen activator. I. Identity with annexin II. *J Biol Chem*. 1994; 269(33):21191-21197.
60. Moss SE and Morgan RO. The annexins. *Genome biology*. 2004; 5(4):219.
61. Thiel C, Osborn M and Gerke V. The tight association of the tyrosine kinase substrate annexin II with the submembranous cytoskeleton depends on intact p11- and Ca(2+)-binding sites. *J Cell Sci*. 1992; 103 ( Pt 3):733-742.
62. Waisman DM. Annexin II tetramer: structure and function. *Molecular and cellular biochemistry*. 1995; 149-150:301-322.
63. Sharma MR, Koltowski L, Ownbey RT, Tuszynski GP and Sharma MC. Angiogenesis-associated protein annexin II in breast cancer: selective expression in invasive

breast cancer and contribution to tumor invasion and progression. *Exp Mol Pathol.* 2006; 81(2):146-156.

64. Vishwanatha JK, Chiang Y, Kumble KD, Hollingsworth MA and Pour PM. Enhanced expression of annexin II in human pancreatic carcinoma cells and primary pancreatic cancers. *Carcinogenesis.* 1993; 14(12):2575-2579.

65. Domoto T, Miyama Y, Suzuki H, Teratani T, Arai K, Sugiyama T, Takayama T, Mugiya S, Ozono S and Nozawa R. Evaluation of S100A10, annexin II and B-FABP expression as markers for renal cell carcinoma. *Cancer Sci.* 2007; 98(1):77-82.

66. Reeves SA, Chavez-Kappel C, Davis R, Rosenblum M and Israel MA. Developmental regulation of annexin II (Lipocortin 2) in human brain and expression in high grade glioma. *Cancer Res.* 1992; 52(24):6871-6876.

67. Yeatman TJ, Updyke TV, Kaetzel MA, Dedman JR and Nicolson GL. Expression of annexins on the surfaces of non-metastatic and metastatic human and rodent tumor cells. *Clinical & experimental metastasis.* 1993; 11(1):37-44.

68. Inokuchi J, Narula N, Yee DS, Skarecky DW, Lau A, Ornstein DK and Tyson DR. Annexin A2 positively contributes to the malignant phenotype and secretion of IL-6 in DU145 prostate cancer cells. *International journal of cancer.* 2009; 124(1):68-74.

69. Bao H, Jiang M, Zhu M, Sheng F, Ruan J and Ruan C. Overexpression of Annexin II affects the proliferation, apoptosis, invasion and production of proangiogenic factors in multiple myeloma. *Int J Hematol.* 2009; 90(2):177-185.

70. Diaz VM, Hurtado M, Thomson TM, Reventos J and Paciucci R. Specific interaction of tissue-type plasminogen activator (t-PA) with annexin II on the membrane of pancreatic cancer cells activates plasminogen and promotes invasion in vitro. *Gut.* 2004; 53(7):993-1000.

71. Liu JW, Shen JJ, Tanzillo-Swartz A, Bhatia B, Maldonado CM, Person MD, Lau SS and Tang DG. Annexin II expression is reduced or lost in prostate cancer cells and its re-expression inhibits prostate cancer cell migration. *Oncogene.* 2003; 22(10):1475-1485.

72. Sharma M, Ownbey RT and Sharma MC. Breast cancer cell surface annexin II induces cell migration and neoangiogenesis via tPA dependent plasmin generation. *Exp Mol Pathol.* 2010; 88(2):278-286.

73. Hayes MJ, Shao D, Bailly M and Moss SE. Regulation of actin dynamics by annexin 2. *EMBO J.* 2006; 25(9):1816-1826.

74. Dassah M, Deora AB, He K and Hajjar KA. The endothelial cell annexin A2 system and vascular fibrinolysis. *General physiology and biophysics.* 2009; 28 Spec No Focus:F20-28.

75. Kwon M, Caplan JF, Filipenko NR, Choi KS, Fitzpatrick SL, Zhang L and Waisman DM. Identification of annexin II heterotetramer as a plasmin reductase. *J Biol Chem.* 2002; 277(13):10903-10911.

76. Mai J, Waisman DM and Sloane BF. Cell surface complex of cathepsin B/annexin II tetramer in malignant progression. *Biochim Biophys Acta*. 2000; 1477(1-2):215-230.
77. Roda O, Valero ML, Peiro S, Andreu D, Real FX and Navarro P. New insights into the tPA-annexin A2 interaction. Is annexin A2 CYS8 the sole requirement for this association? *J Biol Chem*. 2003; 278(8):5702-5709.
78. Tressler RJ, Updyke TV, Yeatman T and Nicolson GL. Extracellular annexin II is associated with divalent cation-dependent tumor cell-endothelial cell adhesion of metastatic RAW117 large-cell lymphoma cells. *Journal of cellular biochemistry*. 1993; 53(3):265-276.
79. Myrvang HK, Guo X, Li C and Dekker LV. Protein interactions between surface annexin A2 and S100A10 mediate adhesion of breast cancer cells to microvascular endothelial cells. *FEBS letters*. 2013; 587(19):3210-3215.
80. Zhang F, Zhang L, Zhang B, Wei X, Yang Y, Qi RZ, Ying G, Zhang N and Niu R. Anxa2 plays a critical role in enhanced invasiveness of the multidrug resistant human breast cancer cells. *Journal of proteome research*. 2009; 8(11):5041-5047.
81. Shiozawa Y, Havens AM, Jung Y, Ziegler AM, Pedersen EA, Wang J, Wang J, Lu G, Roodman GD, Loberg RD, Pienta KJ and Taichman RS. Annexin II/annexin II receptor axis regulates adhesion, migration, homing, and growth of prostate cancer. *Journal of cellular biochemistry*. 2008; 105(2):370-380.
82. Lokman NA, Elder AS, Ween MP, Pyragius CE, Hoffmann P, Oehler MK and Ricciardelli C. Annexin A2 is regulated by ovarian cancer-peritoneal cell interactions and promotes metastasis. *Oncotarget*. 2013; 4(8):1199-1211.
83. Zhao P, Zhang W, Tang J, Ma XK, Dai JY, Li Y, Jiang JL, Zhang SH and Chen ZN. Annexin II promotes invasion and migration of human hepatocellular carcinoma cells in vitro via its interaction with HAb18G/CD147. *Cancer Sci*. 2010; 101(2):387-395.
84. Cesarman GM, Guevara CA and Hajjar KA. An endothelial cell receptor for plasminogen/tissue plasminogen activator (t-PA). II. Annexin II-mediated enhancement of t-PA-dependent plasminogen activation. *J Biol Chem*. 1994; 269(33):21198-21203.
85. Ranson M and Andronicos NM. Plasminogen binding and cancer: promises and pitfalls. *Frontiers in bioscience : a journal and virtual library*. 2003; 8:s294-304.
86. Liu J and Vishwanatha JK. Regulation of nucleo-cytoplasmic shuttling of human annexin A2: a proposed mechanism. *Molecular and cellular biochemistry*. 2007; 303(1-2):211-220.
87. Eberhard DA, Karns LR, VandenBerg SR and Creutz CE. Control of the nuclear-cytoplasmic partitioning of annexin II by a nuclear export signal and by p11 binding. *J Cell Sci*. 2001; 114(Pt 17):3155-3166.
88. Fahling M, Mrowka R, Steege A, Nebrich G, Perlewitz A, Persson PB and Thiele BJ. Translational control of collagen prolyl 4-hydroxylase-alpha(I) gene expression under hypoxia. *J Biol Chem*. 2006; 281(36):26089-26101.

89. Mickleburgh I, Burtle B, Hollas H, Campbell G, Chrzanowska-Lightowlers Z, Vedeler A and Hesketh J. Annexin A2 binds to the localization signal in the 3' untranslated region of c-myc mRNA. *FEBS J.* 2005; 272(2):413-421.
90. Sun L, Hui AM, Su Q, Vortmeyer A, Kotliarov Y, Pastorino S, Passaniti A, Menon J, Walling J, Bailey R, Rosenblum M, Mikkelsen T and Fine HA. Neuronal and glioma-derived stem cell factor induces angiogenesis within the brain. *Cancer Cell.* 2006; 9(4):287-300.
91. Murat A, Migliavacca E, Gorlia T, Lambiv WL, Shay T, Hamou MF, de Tribolet N, Regli L, Wick W, Kouwenhoven MC, Hainfellner JA, Heppner FL, Dietrich PY, Zimmer Y, Cairncross JG, Janzer RC, et al. Stem cell-related "self-renewal" signature and high epidermal growth factor receptor expression associated with resistance to concomitant chemoradiotherapy in glioblastoma. *J Clin Oncol.* 2008; 26(18):3015-3024.
92. Cancer Genome Atlas Research N. Comprehensive genomic characterization defines human glioblastoma genes and core pathways. *Nature.* 2008; 455(7216):1061-1068.
93. Cancer Genome Atlas Research N, Weinstein JN, Collisson EA, Mills GB, Shaw KR, Ozenberger BA, Ellrott K, Shmulevich I, Sander C and Stuart JM. The Cancer Genome Atlas Pan-Cancer analysis project. *Nat Genet.* 2013; 45(10):1113-1120.
94. Lee Y, Scheck AC, Cloughesy TF, Lai A, Dong J, Farooqi HK, Liao LM, Horvath S, Mischel PS and Nelson SF. Gene expression analysis of glioblastomas identifies the major molecular basis for the prognostic benefit of younger age. *BMC Med Genomics.* 2008; 1:52.
95. Verhaak RG, Hoadley KA, Purdom E, Wang V, Qi Y, Wilkerson MD, Miller CR, Ding L, Golub T, Mesirov JP, Alexe G, Lawrence M, O'Kelly M, Tamayo P, Weir BA, Gabriel S, et al. Integrated genomic analysis identifies clinically relevant subtypes of glioblastoma characterized by abnormalities in PDGFRA, IDH1, EGFR, and NF1. *Cancer Cell.* 2010; 17(1):98-110.
96. Chen CY, Lin YS, Chen CL, Chao PZ, Chiou JF, Kuo CC, Lee FP, Lin YF, Sung YH, Lin YT, Li CF, Chen YJ and Chen CH. Targeting annexin A2 reduces tumorigenesis and therapeutic resistance of nasopharyngeal carcinoma. *Oncotarget.* 2015; 6(29):26946-26959.
97. Zhai H, Acharya S, Gravanis I, Mehmood S, Seidman RJ, Shroyer KR, Hajjar KA and Tsirka SE. Annexin A2 promotes glioma cell invasion and tumor progression. *J Neurosci.* 2011; 31(40):14346-14360.
98. Critchley DR, Holt MR, Barry ST, Priddle H, Hemmings L and Norman J. Integrin-mediated cell adhesion: the cytoskeletal connection. *Biochem Soc Symp.* 1999; 65:79-99.
99. Wozniak MA, Modzelewska K, Kwong L and Keely PJ. Focal adhesion regulation of cell behavior. *Biochim Biophys Acta.* 2004; 1692(2-3):103-119.
100. Smith JJ, Deane NG, Wu F, Merchant NB, Zhang B, Jiang A, Lu P, Johnson JC, Schmidt C, Bailey CE, Eschrich S, Kis C, Levy S, Washington MK, Heslin MJ, Coffey RJ, et al. Experimentally derived metastasis gene expression profile predicts recurrence and death in patients with colon cancer. *Gastroenterology.* 2010; 138(3):958-968.

101. Guedj M, Marisa L, de Reynies A, Orsetti B, Schiappa R, Bibeau F, MacGrogan G, Lerebours F, Finetti P, Longy M, Bertheau P, Bertrand F, Bonnet F, Martin AL, Feugeas JP, Bieche I, et al. A refined molecular taxonomy of breast cancer. *Oncogene*. 2012; 31(9):1196-1206.
102. Okayama H, Kohno T, Ishii Y, Shimada Y, Shiraishi K, Iwakawa R, Furuta K, Tsuta K, Shibata T, Yamamoto S, Watanabe S, Sakamoto H, Kumamoto K, Takenoshita S, Gotoh N, Mizuno H, et al. Identification of genes upregulated in ALK-positive and EGFR/KRAS/ALK-negative lung adenocarcinomas. *Cancer Res*. 2012; 72(1):100-111.
103. Hou LC, Veeravagu A, Hsu AR and Tse VC. Recurrent glioblastoma multiforme: a review of natural history and management options. *Neurosurg Focus*. 2006; 20(4):E5.
104. Piccirillo SG, Dietz S, Madhu B, Griffiths J, Price SJ, Collins VP and Watts C. Fluorescence-guided surgical sampling of glioblastoma identifies phenotypically distinct tumour-initiating cell populations in the tumour mass and margin. *Br J Cancer*. 2012; 107(3):462-468.
105. Rampazzo E, Della Puppa A, Frasson C, Battilana G, Bianco S, Scienza R, Basso G and Persano L. Phenotypic and functional characterization of Glioblastoma cancer stem cells identified through 5-aminolevulinic acid-assisted surgery [corrected]. *Journal of neuro-oncology*. 2014; 116(3):505-513.
106. Zheng L, Foley K, Huang L, Leubner A, Mo G, Olin K, Edil BH, Mizuma M, Sharma R, Le DT, Anders RA, Illei PB, Van Eyk JE, Maitra A, Laheru D and Jaffee EM. Tyrosine 23 phosphorylation-dependent cell-surface localization of annexin A2 is required for invasion and metastases of pancreatic cancer. *PLoS One*. 2011; 6(4):e19390.
107. Emoto K, Yamada Y, Sawada H, Fujimoto H, Ueno M, Takayama T, Kamada K, Naito A, Hirao S and Nakajima Y. Annexin II overexpression correlates with stromal tenascin-C overexpression: a prognostic marker in colorectal carcinoma. *Cancer*. 2001; 92(6):1419-1426.
108. Ohno Y, Izumi M, Kawamura T, Nishimura T, Mukai K and Tachibana M. Annexin II represents metastatic potential in clear-cell renal cell carcinoma. *Br J Cancer*. 2009; 101(2):287-294.
109. Liu Y, Wang Z, Jiang M, Dai L, Zhang W, Wu D and Ruan C. The expression of annexin II and its role in the fibrinolytic activity in acute promyelocytic leukemia. *Leuk Res*. 2011; 35(7):879-884.
110. Gao H, Yu B, Yan Y, Shen J, Zhao S, Zhu J, Qin W and Gao Y. Correlation of expression levels of ANXA2, PGAM1, and CALR with glioma grade and prognosis. *J Neurosurg*. 2013; 118(4):846-853.
111. Iwadate Y, Sakaida T, Hiwasa T, Nagai Y, Ishikura H, Takiguchi M and Yamaura A. Molecular classification and survival prediction in human gliomas based on proteome analysis. *Cancer Res*. 2004; 64(7):2496-2501.



112. Nygaard SJ, Haugland HK, Kristoffersen EK, Lund-Johansen M, Laerum OD and Tysnes OB. Expression of annexin II in glioma cell lines and in brain tumor biopsies. *Journal of neuro-oncology*. 1998; 38(1):11-18.
113. Mussunoor S and Murray GI. The role of annexins in tumour development and progression. *J Pathol*. 2008; 216(2):131-140.
114. Arjona D, Rey JA and Taylor SM. Early genetic changes involved in low-grade astrocytic tumor development. *Curr Mol Med*. 2006; 6(6):645-650.
115. Phillips HS, Kharbanda S, Chen R, Forrest WF, Soriano RH, Wu TD, Misra A, Nigro JM, Colman H, Soroceanu L, Williams PM, Modrusan Z, Feuerstein BG and Aldape K. Molecular subclasses of high-grade glioma predict prognosis, delineate a pattern of disease progression, and resemble stages in neurogenesis. *Cancer Cell*. 2006; 9(3):157-173.
116. Watanabe K, Tachibana O, Sata K, Yonekawa Y, Kleihues P and Ohgaki H. Overexpression of the EGF receptor and p53 mutations are mutually exclusive in the evolution of primary and secondary glioblastomas. *Brain Pathol*. 1996; 6(3):217-223; discussion 223-214.
117. Yan H, Parsons DW, Jin G, McLendon R, Rasheed BA, Yuan W, Kos I, Batinic-Haberle I, Jones S, Riggins GJ, Friedman H, Friedman A, Reardon D, Herndon J, Kinzler KW, Velculescu VE, et al. IDH1 and IDH2 mutations in gliomas. *N Engl J Med*. 2009; 360(8):765-773.
118. Tatenhorst L, Rescher U, Gerke V and Paulus W. Knockdown of annexin 2 decreases migration of human glioma cells in vitro. *Neuropathol Appl Neurobiol*. 2006; 32(3):271-277.
119. Wang CY, Chen CL, Tseng YL, Fang YT, Lin YS, Su WC, Chen CC, Chang KC, Wang YC and Lin CF. Annexin A2 silencing induces G2 arrest of non-small cell lung cancer cells through p53-dependent and -independent mechanisms. *J Biol Chem*. 2012; 287(39):32512-32524.
120. Wang YQ, Zhang F, Tian R, Ji W, Zhou Y, Sun XM, Liu Y, Wang ZY and Niu RF. Tyrosine 23 Phosphorylation of Annexin A2 Promotes Proliferation, Invasion, and Stat3 Phosphorylation in the Nucleus of Human Breast Cancer SK-BR-3 Cells. *Cancer Biol Med*. 2012; 9(4):248-253.
121. Wu B, Zhang F, Yu M, Zhao P, Ji W, Zhang H, Han J and Niu R. Up-regulation of Anxa2 gene promotes proliferation and invasion of breast cancer MCF-7 cells. *Cell Prolif*. 2012; 45(3):189-198.
122. Rescher U, Ludwig C, Konietzko V, Kharitononkov A and Gerke V. Tyrosine phosphorylation of annexin A2 regulates Rho-mediated actin rearrangement and cell adhesion. *J Cell Sci*. 2008; 121(Pt 13):2177-2185.
123. Onishi M, Ichikawa T, Kurozumi K, Inoue S, Maruo T, Otani Y, Fujii K, Ishida J, Shimazu Y, Yoshida K, Michiue H, Antonio Chiocca E and Date I. Annexin A2 regulates angiogenesis and invasion phenotypes of malignant glioma. *Brain Tumor Pathol*. 2015; 32(3):184-194.

124. Anji A and Kumari M. A cis-acting region in the N-methyl-d-aspartate R1 3'-untranslated region interacts with the novel RNA-binding proteins beta subunit of alpha glucosidase II and annexin A2--effect of chronic ethanol exposure in vivo. *Eur J Neurosci*. 2011; 34(8):1200-1211.
125. Vedeler A, Hollas H, Grindheim AK and Raddum AM. Multiple roles of annexin A2 in post-transcriptional regulation of gene expression. *Curr Protein Pept Sci*. 2012; 13(4):401-412.
126. Raizer JJ, Chandler JP, Ferrarese R, Grimm SA, Levy RM, Muro K, Rosenow J, Helenowski I, Rademaker A, Paton M and Bredel M. A phase II trial evaluating the effects and intra-tumoral penetration of bortezomib in patients with recurrent malignant gliomas. *Journal of neuro-oncology*. 2016; 129(1):139-146.
127. Yan X, Liang F, Li D and Zheng J. Ouabain elicits human glioblastoma cells apoptosis by generating reactive oxygen species in ERK-p66SHC-dependent pathway. *Molecular and cellular biochemistry*. 2015; 398(1-2):95-104.
128. Rampazzo E, Persano L, Pistollato F, Moro E, Frasson C, Porazzi P, Della Puppa A, Bresolin S, Battilana G, Indraccolo S, Te Kronnie G, Argenton F, Tiso N and Basso G. Wnt activation promotes neuronal differentiation of glioblastoma. *Cell Death Dis*. 2013; 4:e500.
129. Opgen-Rhein R and Strimmer K. Accurate ranking of differentially expressed genes by a distribution-free shrinkage approach. *Stat Appl Genet Mol Biol*. 2007; 6:Article9.
130. Subramanian A, Tamayo P, Mootha VK, Mukherjee S, Ebert BL, Gillette MA, Paulovich A, Pomeroy SL, Golub TR, Lander ES and Mesirov JP. Gene set enrichment analysis: a knowledge-based approach for interpreting genome-wide expression profiles. *Proc Natl Acad Sci U S A*. 2005; 102(43):15545-15550.
131. Merico D, Isserlin R, Stueker O, Emili A and Bader GD. Enrichment map: a network-based method for gene-set enrichment visualization and interpretation. *PLoS One*. 2010; 5(11):e13984.
132. Eppert K, Takenaka K, Lechman ER, Waldron L, Nilsson B, van Galen P, Metzeler KH, Poepl A, Ling V, Beyene J, Canty AJ, Danska JS, Bohlander SK, Buske C, Minden MD, Golub TR, et al. Stem cell gene expression programs influence clinical outcome in human leukemia. *Nat Med*. 2011; 17(9):1086-1093.

## 11. SUPPLEMENTARY TABLES

### 11.1 Newman-Keuls multiple comparisons test from GSE4290.

Comparison	p value
Normal Brain vs. Glioma II	p<0.05
Normal Brain vs. Glioma III	p<0.001
Normal Brain vs. GBM	p<0.0001
Glioma II vs. Glioma III	p<0.05
Glioma II vs. GBM	p<0.0001
Glioma III vs. GBM	p<0.001

### 11.2 Clinical characteristics of glioma patients included in survival and multivariate analyses.

<i>Sample ID</i>	<i>Age (y)</i>	<i>Gender</i>	<i>Grade</i>	<i>Occurrence</i>	<i>Site of Lesion</i>	<i>Performance Score</i>	<i>Methylation of MGMT promoter</i>	<i>IDH mutation</i>	<i>Surge ry</i>
HuTuP07	66	m	4	primary	frontal	1	u	wt	GTR
HuTuP10	75	f	4	primary	temporal	n/a	n/a	n/a	GTR
HuTuP14	39	f	4	primary	temporal	0	u	wt	GTR
HuTuP16	66	m	4	primary	parietal	n/a	n/a	n/a	GTR
HuTuP17	65	f	3	primary	parietal	1	m	mut	GTR
HuTuP20	60	m	4	primary	frontal	1	m	wt	GTR
HuTuP26	62	m	4	primary	temporal	n/a	n/a	n/a	GTR
HuTuP31	53	m	4	primary	frontal	0	m	mut	GTR
HuTuP34	57	f	4	primary	occipital	1	u	wt	GTR
HuTuP36	49	f	4	primary	temporal	n/a	n/a	n/a	GTR
HuTuP37	79	f	4	primary	temporal	0	m	wt	GTR
HuTuP40	68	f	4	primary	parietal	n/a	n/a	n/a	STR
HuTuP47	81	f	4	primary	frontal	n/a	n/a	n/a	GTR
HuTuP53	70	m	4	primary	parietal	n/a	n/a	n/a	GTR
HuTuP55	62	m	4	primary	frontal	1	m	wt	GTR
HuTuP56	50	m	4	primary	frontal	1	u	wt	GTR
HuTuP58	63	f	4	primary	temporal	3	u	wt	GTR
HuTuP60	62	m	4	primary	parietal	2	m	wt	STR
HuTuP63	40	f	4	secondary	parietal	0	u	mut	GTR
HuTuP65	56	f	4	secondary	temporal	0	m	mut	GTR
HuTuP67	52	m	4	primary	occipital	1	u	wt	GTR
HuTuP69	47	m	4	secondary	frontal	1	u	wt	GTR
HuTuP70	43	m	4	primary	frontal	2	u	wt	GTR
HuTuP77	62	m	2	primary	occipital	1	m	mut	GTR
HuTuP82	53	m	4	primary	frontal	0	m	wt	GTR

<b>HuTuP83</b>	57	m	4	primary	frontal	2	u	wt	GTR
<b>HuTuP88</b>	71	m	4	primary	frontal	2	u	wt	GTR
<b>HuTuP89</b>	47	f	3	primary	parietal	0	m	mut	GTR
<b>HuTuP91</b>	38	f	2	primary	parietal	2	m	wt	GTR
<b>HuTuP95</b>	68	m	4	primary	frontal	1	m	wt	GTR
<b>HuTuP97</b>	52	m	2	primary	frontal	1	u	wt	GTR
<b>HuTuP99</b>	42	m	4	primary	temporal	3	n/a	n/a	GTR
<b>HutuP100</b>	59	m	4	primary	temporal	0	n/a	n/a	STR
<b>HuTuP102</b>	42	f	2	primary	temporal	0	m	mut	GTR
<b>HuTuP102</b>	42	f	4	primary	temporal	0	m	mut	GTR
<b>HuTuP106</b>	74	m	4	primary	occipital	0	m	mut	GTR
<b>HuTuP107</b>	67	m	4	primary	parietal	2	u	wt	GTR
<b>HuTuP108</b>	64	m	4	primary	frontal	0	u	wt	GTR
<b>HuTuP109</b>	60	m	4	primary	frontal	1	u	wt	GTR
<b>HuTuP113</b>	50	m	4	secondary	parietal	1	u	wt	GTR
<b>HuTuP116</b>	65	m	4	primary	occipital	1	u	wt	STR
<b>HuTuP117</b>	40	m	4	secondary	frontal	n/a	n/a	n/a	GTR
<b>HuTuP119</b>	56	m	4	primary	frontal	3	u	wt	GTR
<b>HuTuP120</b>	56	m	4	primary	temporal	2	u	wt	GTR
<b>HuTuP121</b>	53	f	4	primary	occipital	0	m	wt	GTR
<b>HuTuP122</b>	44	f	4	primary	frontal	0	m	mut	GTR
<b>HuTuP127</b>	75	m	4	secondary	occipital	2	m	wt	GTR
<b>HuTuP129</b>	68	m	4	primary	parietal	0	m	wt	STR
<b>HuTuP135</b>	50	f	4	primary	parietal	0	u	wt	GTR
<b>HuTuP136</b>	70	f	4	primary	parietal	3	u	wt	GTR
<b>HuTuP138</b>	71	m	4	primary	temporal	1	m	wt	GTR
<b>HuTuP142</b>	65	m	4	primary	temporal	3	u	wt	GTR
<b>HuTuP145</b>	51	m	4	primary	parietal	0	u	wt	GTR
<b>HuTuP147</b>	65	m	4	primary	parietal	2	u	wt	GTR
<b>HuTuP151</b>	52	f	4	primary	frontal	n/a	n/a	n/a	GTR
<b>HuTuP152</b>	67	m	4	primary	frontal	1	u	wt	GTR
<b>HuTuP153</b>	79	f	4	primary	temporal	2	n/a	n/a	GTR
<b>HuTuP154</b>	68	f	4	primary	temporal	1	u	wt	GTR
<b>HuTuP155</b>	49	f	4	primary	temporal	1	u	wt	GTR

(y): years; m: male, f: female; u: unmethylated, m: methylated; wt: wild type, mut: mutated, GTR: gross total removal (>90%), STR: sub-total removal (<90%). All patients underwent standard Stupp protocol of treatment.

**11.3 Differentially expressed genes in common between TGCA and GSE13041 datasets derived from comparison between ANXA2 Very Low and ANXA2 High patients.**

Genes	Regulation	Genes	Regulation	Genes	Regulation
ABCA1	Up	CA3	Up	COL4A1	Up
ABCC3	Up	CA9	Up	COL4A2	Up
ACSL1	Up	CALD1	Up	COL5A1	Up
ACTA2	Up	CAPG	Up	COL5A2	Up
ACTN1	Up	CASP1	Up	COL6A1	Up
ADAM12	Up	CAV1	Up	COL6A2	Up
ADAM28	Up	CAV2	Up	COL6A3	Up
ADAMTS1	Up	CBR1	Up	COL8A2	Up
ADM	Up	CCDC109B	Up	COLEC12	Up
AEBP1	Up	CCL18	Up	CP	Up
AHNAK2	Up	CCL2	Up	CPVL	Up
AHR	Up	CCL20	Up	CRIP1	Up
AIM1	Up	CCR1	Up	CRISPLD2	Up
AKAP12	Up	CD14	Up	CSRP2	Up
ALOX5	Up	CD163	Up	CSTA	Up
ALOX5AP	Up	CD44	Up	CTGF	Up
AMIGO2	Up	CD53	Up	CTSC	Up
ANGPT2	Up	CD58	Up	CTSH	Up
ANGPTL4	Up	CD74	Up	CTSK	Up
ANXA1	Up	CD86	Up	CTSS	Up
ANXA2	Up	CD93	Up	CTSZ	Up
ANXA4	Up	CD99	Up	CXCL10	Up
APOC1	Up	CDH11	Up	CXCL11	Up
AQP9	Up	CDH6	Up	CXCL14	Up
ARL4C	Up	CDKN1A	Up	CXCL2	Up
ASPN	Up	CEBPD	Up	CXCL3	Up
ATF3	Up	CECR1	Up	CXCL5	Up
BCAT1	Up	CFB	Up	CXCR4	Up
BCL2A1	Up	CFI	Up	CYBB	Up
BHLHE40	Up	CH25H	Up	CYP1B1	Up
BIRC3	Up	CHI3L1	Up	CYR61	Up
BST2	Up	CHI3L2	Up	DAB2	Up
C10orf10	Up	CHRNA9	Up	DCN	Up
C1QA	Up	CHST2	Up	DIRAS3	Up
C1QB	Up	CHST7	Up	DOK5	Up
C1R	Up	CLEC2B	Up	DPYD	Up
C1RL	Up	CLEC5A	Up	DPYSL3	Up
C1S	Up	CLIC4	Up	DSE	Up
C21orf62	Up	CLU	Up	DUSP1	Up
C3	Up	CNGA3	Up	DUSP4	Up
C5AR1	Up	COL15A1	Up	DUSP5	Up
C8orf4	Up	COL1A1	Up	DUSP6	Up
CA12	Up	COL1A2	Up	ECHDC2	Up
CA2	Up	COL3A1	Up	ECM2	Up

<i>EFEMP1</i>	Up
<i>EFEMP2</i>	Up
<i>EFHC2</i>	Up
<i>EFNB2</i>	Up
<i>EGR1</i>	Up
<i>ELOVL2</i>	Up
<i>EMP1</i>	Up
<i>EMP3</i>	Up
<i>ENO1</i>	Up
<i>ERAP2</i>	Up
<i>ETV5</i>	Up
<i>F13A1</i>	Up
<i>F2RL1</i>	Up
<i>F3</i>	Up
<i>FABP5</i>	Up
<i>FABP7</i>	Up
<i>FAM129A</i>	Up
<i>FAS</i>	Up
<i>FBLN1</i>	Up
<i>FBLN5</i>	Up
<i>FBN1</i>	Up
<i>FCER1G</i>	Up
<i>FCGBP</i>	Up
<i>FCGR1B</i>	Up
<i>FCGR2A</i>	Up
<i>FCGR2B</i>	Up
<i>FCGR2C</i>	Up
<i>FERMT2</i>	Up
<i>FJX1</i>	Up
<i>FKBP5</i>	Up
<i>FLNC</i>	Up
<i>FMOD</i>	Up
<i>FN1</i>	Up
<i>FOS</i>	Up
<i>FPR1</i>	Up
<i>FXYD5</i>	Up
<i>FZD7</i>	Up
<i>G0S2</i>	Up
<i>GADD45B</i>	Up
<i>GAP43</i>	Up
<i>GBP1</i>	Up
<i>GBP2</i>	Up
<i>GCH1</i>	Up
<i>GDF15</i>	Up
<i>GEM</i>	Up
<i>GFPT2</i>	Up
<i>GLIPR1</i>	Up
<i>GPNMB</i>	Up
<i>NDRG1</i>	Up
<i>NES</i>	Up

<i>GRB10</i>	Up
<i>GSAP</i>	Up
<i>HAMP</i>	Up
<i>HAS2</i>	Up
<i>HCK</i>	Up
<i>HCLS1</i>	Up
<i>HILPDA</i>	Up
<i>HK2</i>	Up
<i>HLA-DMA</i>	Up
<i>HLA-DMB</i>	Up
<i>HLA-DPA1</i>	Up
<i>HLA-DPB1</i>	Up
<i>HLA-DQB1</i>	Up
<i>HLA-DRA</i>	Up
<i>HMOX1</i>	Up
<i>HP</i>	Up
<i>HRH1</i>	Up
<i>HSPA6</i>	Up
<i>ICAM1</i>	Up
<i>IER3</i>	Up
<i>IFI16</i>	Up
<i>IFI30</i>	Up
<i>IFI35</i>	Up
<i>IFI44</i>	Up
<i>IFITM1</i>	Up
<i>IGF2BP2</i>	Up
<i>IGFBP2</i>	Up
<i>IGFBP3</i>	Up
<i>IGFBP4</i>	Up
<i>IGFBP5</i>	Up
<i>IL13RA1</i>	Up
<i>IL1R1</i>	Up
<i>IL1R2</i>	Up
<i>IL1RAP</i>	Up
<i>IL6</i>	Up
<i>IL8</i>	Up
<i>IQCG</i>	Up
<i>IQGAP1</i>	Up
<i>ITGA7</i>	Up
<i>ITGAM</i>	Up
<i>ITGB2</i>	Up
<i>ITGB4</i>	Up
<i>KCNE4</i>	Up
<i>KCTD12</i>	Up
<i>KIAA0226L</i>	Up
<i>KYNU</i>	Up
<i>LAMA2</i>	Up
<i>LAMA4</i>	Up
<i>RARRES1</i>	Up
<i>RARRES2</i>	Up

<i>LAMB1</i>	Up
<i>LAPTM5</i>	Up
<i>LDLR</i>	Up
<i>LEF1</i>	Up
<i>LGALS3</i>	Up
<i>LIF</i>	Up
<i>LMO2</i>	Up
<i>LOX</i>	Up
<i>LOXL1</i>	Up
<i>LOXL2</i>	Up
<i>LPHN2</i>	Up
<i>LRRFIP1</i>	Up
<i>LTF</i>	Up
<i>LUM</i>	Up
<i>LY96</i>	Up
<i>LYPD1</i>	Up
<i>LYVE1</i>	Up
<i>LYZ</i>	Up
<i>LZTS1</i>	Up
<i>MAFB</i>	Up
<i>MAFF</i>	Up
<i>MAN1A1</i>	Up
<i>MAN1C1</i>	Up
<i>MAOB</i>	Up
<i>MDFIC</i>	Up
<i>MDK</i>	Up
<i>MEOX2</i>	Up
<i>MEST</i>	Up
<i>MFAP2</i>	Up
<i>MFAP4</i>	Up
<i>MGP</i>	Up
<i>MMP7</i>	Up
<i>MMP9</i>	Up
<i>MNDA</i>	Up
<i>MOXD1</i>	Up
<i>MRC1</i>	Up
<i>MREG</i>	Up
<i>MRPS17</i>	Up
<i>MS4A4A</i>	Up
<i>MS4A6A</i>	Up
<i>MSR1</i>	Up
<i>MT1E</i>	Up
<i>MX1</i>	Up
<i>MXRA5</i>	Up
<i>MYL9</i>	Up
<i>MYOF</i>	Up
<i>NAMPT</i>	Up
<i>NCF2</i>	Up
<i>STC1</i>	Up
<i>STEAP1</i>	Up

<i>NID2</i>	Up
<i>NNMT</i>	Up
<i>NPL</i>	Up
<i>NR2E1</i>	Up
<i>NRP1</i>	Up
<i>NUPR1</i>	Up
<i>OLFML2B</i>	Up
<i>OLFML3</i>	Up
<i>OSBPL3</i>	Up
<i>OXTR</i>	Up
<i>P4HA2</i>	Up
<i>PCOLCE</i>	Up
<i>PCOLCE2</i>	Up
<i>PCSK5</i>	Up
<i>PDGFA</i>	Up
<i>PDGFD</i>	Up
<i>PDLIM1</i>	Up
<i>PDLIM3</i>	Up
<i>PDLIM4</i>	Up
<i>PDPN</i>	Up
<i>PHLDA2</i>	Up
<i>PI3</i>	Up
<i>PLA2G2A</i>	Up
<i>PLA2G5</i>	Up
<i>PLAGL1</i>	Up
<i>PLAT</i>	Up
<i>PLAU</i>	Up
<i>PLAUR</i>	Up
<i>PLIN2</i>	Up
<i>PLP2</i>	Up
<i>PLTP</i>	Up
<i>PMP22</i>	Up
<i>POSTN</i>	Up
<i>PPIC</i>	Up
<i>PROS1</i>	Up
<i>PRRX1</i>	Up
<i>PRSS23</i>	Up
<i>PSRC1</i>	Up
<i>PTGER4</i>	Up
<i>PTGS1</i>	Up
<i>PTGS2</i>	Up
<i>PTPRC</i>	Up
<i>PTRF</i>	Up
<i>PTX3</i>	Up
<i>PXDN</i>	Up
<i>PYGL</i>	Up
<i>ZYX</i>	Up

Genes	Regulation
<i>ABAT</i>	Down

<i>RARRES3</i>	Up
<i>RBM47</i>	Up
<i>RBP1</i>	Up
<i>RBPM5</i>	Up
<i>RCAN1</i>	Up
<i>RFTN1</i>	Up
<i>RGS1</i>	Up
<i>RGS2</i>	Up
<i>RNASE6</i>	Up
<i>S100A10</i>	Up
<i>S100A11</i>	Up
<i>S100A13</i>	Up
<i>S100A4</i>	Up
<i>S100A8</i>	Up
<i>S100A9</i>	Up
<i>SAMSN1</i>	Up
<i>SDC2</i>	Up
<i>SDC4</i>	Up
<i>SEC61G</i>	Up
<i>SEL1L3</i>	Up
<i>SERPINA1</i>	Up
<i>SERPINA3</i>	Up
<i>SERPINB1</i>	Up
<i>SERPINE1</i>	Up
<i>SERPING1</i>	Up
<i>SFRP4</i>	Up
<i>SKAP2</i>	Up
<i>SLAMF8</i>	Up
<i>SLC16A3</i>	Up
<i>SLC2A10</i>	Up
<i>SLC2A3</i>	Up
<i>SLC2A5</i>	Up
<i>SLC39A8</i>	Up
<i>SLN</i>	Up
<i>SLPI</i>	Up
<i>SNAI2</i>	Up
<i>SOCS2</i>	Up
<i>SPP1</i>	Up
<i>SPRY1</i>	Up
<i>SPRY2</i>	Up
<i>SPRY4</i>	Up
<i>SQRDL</i>	Up
<i>SRGN</i>	Up
<i>SRPX</i>	Up
<i>SRPX2</i>	Up
<i>STAB1</i>	Up
<b>Genes</b>	<b>Regulation</b>
<i>CDKN1C</i>	Down
<i>CHD7</i>	Down
<i>CHGA</i>	Down

<i>STEAP3</i>	Up
<i>SVIL</i>	Up
<i>SYNC</i>	Up
<i>SYNM</i>	Up
<i>SYNPO</i>	Up
<i>SYPL1</i>	Up
<i>TAGLN</i>	Up
<i>TDO2</i>	Up
<i>TFPI2</i>	Up
<i>TGFB2</i>	Up
<i>TGFBI</i>	Up
<i>TGFBR2</i>	Up
<i>THBD</i>	Up
<i>THBS1</i>	Up
<i>THBS2</i>	Up
<i>THEMIS2</i>	Up
<i>TIMP1</i>	Up
<i>TM4SF1</i>	Up
<i>TMEM158</i>	Up
<i>TMEM176B</i>	Up
<i>TMEM45A</i>	Up
<i>TNC</i>	Up
<i>TNFAIP2</i>	Up
<i>TNFAIP3</i>	Up
<i>TNFAIP6</i>	Up
<i>TNFAIP8</i>	Up
<i>TNFSF10</i>	Up
<i>TNFSF13</i>	Up
<i>TOM1L1</i>	Up
<i>TPM2</i>	Up
<i>TREM1</i>	Up
<i>TREM2</i>	Up
<i>TRIM22</i>	Up
<i>TUBB6</i>	Up
<i>TYROBP</i>	Up
<i>UPP1</i>	Up
<i>VAMP3</i>	Up
<i>VAMP5</i>	Up
<i>VAMP8</i>	Up
<i>VCAM1</i>	Up
<i>VEGFA</i>	Up
<i>VOPP1</i>	Up
<i>VSIG4</i>	Up
<i>WWTR1</i>	Up
<i>YME1L1</i>	Up
<i>ZFP36</i>	Up
<b>Genes</b>	<b>Regulation</b>
<i>FXYD6</i>	Down
<i>FXYD7</i>	Down
<i>GABBR1</i>	Down

<i>ABCG2</i>	Down
<i>ACTL6B</i>	Down
<i>ADAM22</i>	Down
<i>ADCY1</i>	Down
<i>ADCY2</i>	Down
<i>AK5</i>	Down
<i>AKAP7</i>	Down
<i>ALCAM</i>	Down
<i>ALDH5A1</i>	Down
<i>ALDOC</i>	Down
<i>AMOTL2</i>	Down
<i>AMPH</i>	Down
<i>ANK3</i>	Down
<i>APBA2</i>	Down
<i>ARHGEF4</i>	Down
<i>ARPP21</i>	Down
<i>ASCL1</i>	Down
<i>ASTN1</i>	Down
<i>ASTN2</i>	Down
<i>ATP1A2</i>	Down
<i>ATP2B2</i>	Down
<i>ATP6V1G2</i>	Down
<i>ATP8A1</i>	Down
<i>ATRNL1</i>	Down
<i>BAALC</i>	Down
<i>BAI3</i>	Down
<i>BASP1</i>	Down
<i>BCAN</i>	Down
<i>BCAS1</i>	Down
<i>BEX1</i>	Down
<i>BRINP1</i>	Down
<i>BRINP2</i>	Down
<i>C14orf132</i>	Down
<i>C1QL1</i>	Down
<i>C1orf61</i>	Down
<i>CA10</i>	Down
<i>CACNA1A</i>	Down
<i>CADM3</i>	Down
<i>CAMTA1</i>	Down
<i>CAPN3</i>	Down
<i>CCK</i>	Down
<i>CDH10</i>	Down
<i>CDK5R</i>	Down
<i>LAMP5</i>	Down
<i>LDB2</i>	Down
<i>LDOC1</i>	Down
<i>LPHN3</i>	Down
<i>LPPR1</i>	Down

<i>CHGB</i>	Down
<i>CHRDL1</i>	Down
<i>CLASP2</i>	Down
<i>CLGN</i>	Down
<i>CNTN1</i>	Down
<i>CNTNAP2</i>	Down
<i>CSGALNACT1</i>	Down
<i>CSPG5</i>	Down
<i>CTNNA2</i>	Down
<i>CTNND2</i>	Down
<i>CXorf57</i>	Down
<i>DAAM2</i>	Down
<i>DCX</i>	Down
<i>DIRAS2</i>	Down
<i>DLL3</i>	Down
<i>DNAJC6</i>	Down
<i>DNM1</i>	Down
<i>DNM3</i>	Down
<i>DPP6</i>	Down
<i>DPY19L2P2</i>	Down
<i>DPYSL4</i>	Down
<i>DYNC1I1</i>	Down
<i>EEF1A2</i>	Down
<i>EFHD1</i>	Down
<i>ELAVL4</i>	Down
<i>ELMO1</i>	Down
<i>EPHB1</i>	Down
<i>ERBB3</i>	Down
<i>ERBB4</i>	Down
<i>ERC2</i>	Down
<i>ETNPPL</i>	Down
<i>EYA1</i>	Down
<i>FA2H</i>	Down
<i>FAIM2</i>	Down
<i>FAM107A</i>	Down
<i>FAM171A1</i>	Down
<i>FAM5C</i>	Down
<i>FERMT1</i>	Down
<i>FGF13</i>	Down
<i>FGF14</i>	Down
<i>FGF9</i>	Down
<i>FGFR2</i>	Down
<i>FUT9</i>	Down
<i>NTSR2</i>	Down
<i>OLFM1</i>	Down
<i>OLIG2</i>	Down
<i>OMG</i>	Down
<i>OPCML</i>	Down

<i>GABBR2</i>	Down
<i>GABRA2</i>	Down
<i>GABRB1</i>	Down
<i>GAD1</i>	Down
<i>GAD2</i>	Down
<i>GNAI1</i>	Down
<i>GNAL</i>	Down
<i>GNAO1</i>	Down
<i>GNAS</i>	Down
<i>GNG3</i>	Down
<i>GNG4</i>	Down
<i>GOLGA8A</i>	Down
<i>GPM6A</i>	Down
<i>GPR17</i>	Down
<i>GPRASP1</i>	Down
<i>GPRC5B</i>	Down
<i>GRIA2</i>	Down
<i>GRIA3</i>	Down
<i>GRIK2</i>	Down
<i>GRM3</i>	Down
<i>HLF</i>	Down
<i>HMP19</i>	Down
<i>HPCA</i>	Down
<i>HPCAL4</i>	Down
<i>HRASLS</i>	Down
<i>HSPA12A</i>	Down
<i>INA</i>	Down
<i>ITM2A</i>	Down
<i>KAT2B</i>	Down
<i>KBTBD11</i>	Down
<i>KCNB1</i>	Down
<i>KCND2</i>	Down
<i>KCND3</i>	Down
<i>KCNK1</i>	Down
<i>KCNN2</i>	Down
<i>KCNN3</i>	Down
<i>KCNQ2</i>	Down
<i>KIAA1107</i>	Down
<i>KIF1A</i>	Down
<i>KIF5C</i>	Down
<i>KIT</i>	Down
<i>KLRC3</i>	Down
<i>L1CAM</i>	Down
<i>RTN1</i>	Down
<i>RUFY3</i>	Down
<i>RUNDC3A</i>	Down
<i>RUNX1T1</i>	Down
<i>S100A1</i>	Down



<i>LRP4</i>	Down
<i>LRRTM2</i>	Down
<i>LY6H</i>	Down
<i>MAG</i>	Down
<i>MAP1A</i>	Down
<i>MAP2</i>	Down
<i>MAPT</i>	Down
<i>MBP</i>	Down
<i>MEG3</i>	Down
<i>MLLT11</i>	Down
<i>MMP16</i>	Down
<i>MOBP</i>	Down
<i>MOG</i>	Down
<i>MPPED2</i>	Down
<i>MYCN</i>	Down
<i>MYO10</i>	Down
<i>MYRF</i>	Down
<i>MYT1L</i>	Down
<i>NAP1L2</i>	Down
<i>NAP1L3</i>	Down
<i>NAV3</i>	Down
<i>NBEA</i>	Down
<i>NCALD</i>	Down
<i>NCAM1</i>	Down
<i>NCAN</i>	Down
<i>NDN</i>	Down
<i>NDRG2</i>	Down
<i>NDRG4</i>	Down
<i>NEFL</i>	Down
<i>NEFM</i>	Down
<i>NET1</i>	Down
<i>NEUROD1</i>	Down
<i>NKX2-2</i>	Down
<i>NMNAT2</i>	Down
<i>NPY</i>	Down
<i>NRGN</i>	Down
<i>NRXN1</i>	Down
<i>NRXN2</i>	Down
<i>NRXN3</i>	Down
<i>NTM</i>	Down
<i>NTRK2</i>	Down
<i>NTRK3</i>	Down
<i>LAMP5</i>	Down
<i>TF</i>	Down
<i>THSD7A</i>	Down
<i>TMEM100</i>	Down
<i>TMEM246</i>	Down
<i>TMEM35</i>	Down
<i>TOX</i>	Down
<i>TOX3</i>	Down

<i>PAIP1</i>	Down
<i>PAK3</i>	Down
<i>PAQR6</i>	Down
<i>PCDH17</i>	Down
<i>PCLO</i>	Down
<i>PCSK1N</i>	Down
<i>PCSK2</i>	Down
<i>PDE4DIP</i>	Down
<i>PDE8B</i>	Down
<i>PDGFRA</i>	Down
<i>PDYN</i>	Down
<i>PEG10</i>	Down
<i>PEG3</i>	Down
<i>PHLPP1</i>	Down
<i>PID1</i>	Down
<i>PKIA</i>	Down
<i>PKP4</i>	Down
<i>PLCB1</i>	Down
<i>PLEKHB1</i>	Down
<i>PLLP</i>	Down
<i>PLP1</i>	Down
<i>PNMAL1</i>	Down
<i>PPP1R16B</i>	Down
<i>PPP1R1A</i>	Down
<i>PRKCB</i>	Down
<i>PRKCZ</i>	Down
<i>PSAT1</i>	Down
<i>PSD3</i>	Down
<i>PTCH1</i>	Down
<i>PTPRD</i>	Down
<i>RAB33A</i>	Down
<i>RAB6B</i>	Down
<i>RALYL</i>	Down
<i>RAP1GAP</i>	Down
<i>RAPGEF2</i>	Down
<i>RAPGEF4</i>	Down
<i>RAPGEF5</i>	Down
<i>REEP1</i>	Down
<i>RGCC</i>	Down
<i>RGS5</i>	Down
<i>RGS7</i>	Down
<i>RIMS3</i>	Down
<i>NTSR2</i>	Down
<i>TRIL</i>	Down
<i>TSFM</i>	Down
<i>TSPAN7</i>	Down
<i>TTYH1</i>	Down
<i>TUBB4A</i>	Down
<i>TUSC3</i>	Down
<i>UGT8</i>	Down

<i>SATB1</i>	Down
<i>SCG3</i>	Down
<i>SCN1A</i>	Down
<i>SCN3A</i>	Down
<i>SCN3B</i>	Down
<i>SEMA6A</i>	Down
<i>SERPINE2</i>	Down
<i>SERPINI1</i>	Down
<i>SEZ6L</i>	Down
<i>SH3GL2</i>	Down
<i>SH3GL3</i>	Down
<i>SLC12A5</i>	Down
<i>SLC14A1</i>	Down
<i>SLC15A2</i>	Down
<i>SLC16A7</i>	Down
<i>SLC17A6</i>	Down
<i>SLC1A1</i>	Down
<i>SLC24A3</i>	Down
<i>SLC38A1</i>	Down
<i>SLC6A1</i>	Down
<i>SLITRK3</i>	Down
<i>SLITRK5</i>	Down
<i>SNAP25</i>	Down
<i>SNAP91</i>	Down
<i>SOBP</i>	Down
<i>SOX10</i>	Down
<i>SOX4</i>	Down
<i>SPEN</i>	Down
<i>SPOCK1</i>	Down
<i>SPON1</i>	Down
<i>SST</i>	Down
<i>ST18</i>	Down
<i>STMN2</i>	Down
<i>STMN4</i>	Down
<i>STXBP1</i>	Down
<i>SUSD5</i>	Down
<i>SYBU</i>	Down
<i>SYN1</i>	Down
<i>SYNGR3</i>	Down
<i>SYT1</i>	Down
<i>TAGLN3</i>	Down
<i>TCEAL2</i>	Down
<i>RTN1</i>	Down
<i>WASF1</i>	Down
<i>WASF3</i>	Down
<i>XYLT1</i>	Down
<i>ZDHHC11</i>	Down
<i>ZFPM2</i>	Down
<i>ZNF365</i>	Down
<i>ZNF423</i>	Down

#### 11.4 Primary GBM cells used in the study.

<i>Code</i>	<i>Diagnosis</i>	<i>Age (y)</i>	<i>Sex</i>
HuTuP13	GBM	67	male
HuTuP53	GBM	70	male
HuTuP82	GBM	50	male
HuTuP83	GBM	55	male
HuTuP107	GBM	65	male
HuTuP174	GBM	69	male
HuTuP175	GBM	54	female
HuTuP176	GBM	59	male

#### 11.5 Differentially expressed genes between Isotype and anti-ANXA2 antibody treated GBM cells.

Probe set	Gene symbol	Lfdr	log2 means_Group Isotype	log2 means_Group anti-ANXA2
1555347_at	<i>PDXDC1</i>	4,00E-13	5,514516676	7,363199447
211214_s_at	<i>DAPK1</i>	4,00E-13	5,879259494	7,47110523
1554332_a_at	<i>LOC100127888</i>	4,00E-13	8,045837747	9,883646295
239802_at	<i>SAP30L</i>	4,00E-13	5,207306733	6,287556134
222293_at	<i>CADM4</i>	4,00E-13	6,828035875	8,049482022
222026_at	<i>RBM3</i>	4,00E-13	8,118242	9,124756523
202813_at	<i>TARBP1</i>	4,00E-13	9,111752136	8,373073718
39817_s_at	<i>DNPH1</i>	4,00E-13	8,075397829	7,231631191
203227_s_at	<i>TSPAN31</i>	4,00E-13	9,919584351	8,737609922
213244_at	<i>SCAMP4</i>	4,00E-13	8,244489664	7,247913843
206397_x_at	NA	4,00E-13	10,75188841	9,451924427
209759_s_at	<i>ECI1</i>	4,00E-13	8,991284665	7,867415131
218400_at	<i>OAS3</i>	4,00E-13	8,504700069	7,354669487
228791_at	NA	4,00E-13	8,454710102	7,298677071
238440_at	<i>CLYBL</i>	4,00E-13	7,236900712	6,11548114
226722_at	<i>FAM20C</i>	4,00E-13	10,61036612	8,959940703
213245_at	<i>ADCY1</i>	4,00E-13	7,889058412	6,551059084
209502_s_at	<i>BAIAP2</i>	4,00E-13	7,684178499	6,198075267
203006_at	<i>INPP5A</i>	4,00E-13	8,66694804	6,966453732
1556216_s_at	NA	4,00E-13	7,606679076	5,951444222
226325_at	<i>ADSSL1</i>	4,00E-13	6,673487897	5,201096182
203570_at	<i>LOXL1</i>	4,00E-13	12,12706334	9,31239658
235275_at	<i>BMP8B</i>	4,00E-13	8,667808242	6,573537974
225060_at	<i>LRP11</i>	4,00E-13	10,16131565	7,70361025
224478_s_at	<i>C7orf50</i>	4,00E-13	9,714294266	7,176805864
221973_at	NA	4,00E-13	6,187823966	4,159297846

46142_at	<i>LMF1</i>	4,00E-13	7,568654472	4,455740893
237094_at	<i>FAM19A5</i>	4,00E-13	7,625734943	4,351092194
229459_at	<i>FAM19A5</i>	4,00E-13	8,701234021	4,903387036
242281_at	<i>GLUL</i>	1,62E-11	6,518014998	7,547374567
213110_s_at	<i>COL4A5</i>	1,62E-11	11,1246341	10,07232139
210006_at	<i>ABHD14A</i>	1,62E-11	7,410678278	5,977322812
229656_s_at	<i>EML6</i>	1,62E-11	9,39690791	7,400688445
41660_at	<i>CELSR1</i>	5,79E-11	9,288742944	7,46769201
229655_at	<i>FAM19A5</i>	5,79E-11	8,135754405	5,896075968
225918_at	<i>GLG1</i>	7,72E-11	9,299843409	8,281618871
210410_s_at	<i>NA</i>	7,72E-11	8,636934397	7,112332821
233893_s_at	<i>UVSSA</i>	7,72E-11	8,691053741	6,984356762
235776_x_at	<i>LINC00475</i>	9,46E-11	6,0863453	6,885207331
226446_at	<i>HES6</i>	9,46E-11	9,367021212	10,37206735
227420_at	<i>TNFAIP8L1</i>	9,46E-11	8,197355479	7,074368292
205248_at	<i>DOPEY2</i>	9,46E-11	5,611972177	4,376208125
219543_at	<i>PBLD</i>	9,46E-11	5,870401367	4,428868859
219135_s_at	<i>LMF1</i>	9,46E-11	7,51175052	5,226885107
231219_at	<i>CMTM1</i>	2,67E-10	6,07723334	7,077246829
208691_at	<i>TFRC</i>	2,67E-10	12,25581851	13,09477444
218387_s_at	<i>PGLS</i>	2,67E-10	10,21466295	9,227874412
214140_at	<i>SLC25A16</i>	2,67E-10	6,306315465	5,131966917
1564083_at	<i>NA</i>	2,67E-10	5,940790241	4,654325825
219828_at	<i>RABL6</i>	3,92E-10	7,642411513	9,616256767
205262_at	<i>KCNH2</i>	3,92E-10	8,401967913	7,536167185
212811_x_at	<i>SLC1A4</i>	3,92E-10	8,058318434	7,096887917
1556097_at	<i>HOMER2</i>	3,92E-10	8,626040155	7,473386727
51200_at	<i>C19orf60</i>	3,92E-10	9,228341122	7,743440461
37590_g_at	<i>NA</i>	3,92E-10	8,777813839	7,271173062
212890_at	<i>SLC38A10</i>	3,92E-10	7,773566382	6,093442334
203115_at	<i>FECH</i>	4,98E-10	8,412548924	7,479072624
225008_at	<i>ASPH</i>	5,68E-10	8,603556904	7,755888652
204078_at	<i>LEPREL4</i>	5,68E-10	9,303773183	8,250107722
1560371_at	<i>LINC00997</i>	5,68E-10	6,139893442	5,186208209
244435_at	<i>FAM196A</i>	2,00E-09	7,852492356	5,68134306
219136_s_at	<i>LMF1</i>	2,00E-09	8,53330488	6,114393491
213703_at	<i>LINC00342</i>	2,00E-09	6,37655699	4,527883563
203449_s_at	<i>TERF1</i>	5,83E-09	8,11582943	7,417359288
226891_at	<i>XXYL1</i>	5,83E-09	8,712109226	6,582942821
229050_s_at	<i>NA</i>	1,37E-08	9,58212427	10,74128325
207332_s_at	<i>TFRC</i>	1,37E-08	11,63653707	12,63646667
205961_s_at	<i>PSIP1</i>	1,37E-08	11,56152312	10,63628831
220227_at	<i>CDH4</i>	1,37E-08	11,2251775	10,00869333
230763_at	<i>SPATA17</i>	1,37E-08	5,211454598	4,440231029
203758_at	<i>CTSO</i>	1,37E-08	8,229748682	6,350409224
203116_s_at	<i>FECH</i>	1,53E-08	9,974853884	9,354482743
224996_at	<i>ASPH</i>	1,53E-08	9,718808272	9,06677036
219479_at	<i>KDELC1</i>	1,53E-08	9,56443422	8,736243919
227778_at	<i>NA</i>	1,53E-08	7,748408321	6,825974676
201900_s_at	<i>AKR1A1</i>	1,53E-08	8,847394231	7,674468989

229883_at	<i>GRIN2D</i>	1,53E-08	7,916844727	6,811708236
204337_at	<i>RGS4</i>	1,53E-08	11,16751461	9,408823972
201911_s_at	<i>FARP1</i>	5,08E-08	9,176320691	8,217474207
1557137_at	<i>TMEM17</i>	5,08E-08	8,435410644	7,368231609
210130_s_at	<i>TM7SF2</i>	5,08E-08	8,873196648	7,292724465
1558430_at	<i>PDXDC1</i>	5,08E-08	5,898300725	4,640008733
1553978_at	<i>MEF2BNB</i>	5,08E-08	6,115577863	4,807055685
203197_s_at	<i>C1orf123</i>	9,02E-08	9,51456283	8,485692718
218918_at	<i>MAN1C1</i>	9,02E-08	7,645431238	6,076203122
203608_at	<i>ALDH5A1</i>	1,57E-07	9,045013354	8,348058543
213657_s_at	<i>NA</i>	1,57E-07	9,280611775	7,729752966
205405_at	<i>SEMA5A</i>	1,61E-07	10,93705824	9,722102202
213992_at	<i>COL4A6</i>	1,61E-07	8,204305321	6,444585693
210896_s_at	<i>ASPH</i>	1,95E-07	10,74775663	9,96357459
226145_s_at	<i>FRAS1</i>	1,95E-07	12,20063032	10,46784887
229354_at	<i>AHRR</i>	1,95E-07	9,859870814	8,353125327
231867_at	<i>TENM2</i>	1,95E-07	6,176301733	5,115256068
234193_at	<i>NA</i>	2,44E-07	4,955558734	5,518985113
211779_x_at	<i>AP2A2</i>	2,44E-07	9,823511278	9,071371996
209337_at	<i>PSIP1</i>	2,44E-07	12,17528791	11,21135632
218388_at	<i>PGLS</i>	2,44E-07	10,76159531	9,858845159
219048_at	<i>PIGN</i>	2,44E-07	8,658162225	7,888010096
207980_s_at	<i>CITED2</i>	2,44E-07	8,012126139	7,148603956
1552291_at	<i>PIGX</i>	2,44E-07	8,391548353	7,386128633
238692_at	<i>BTBD11</i>	2,44E-07	6,539676611	5,668501124
227903_x_at	<i>TPGS1</i>	2,44E-07	7,657309024	6,521247011
213995_at	<i>ATP5S</i>	2,44E-07	7,493791179	6,128169283
238957_at	<i>NA</i>	2,44E-07	5,545043354	4,229772075
236660_at	<i>NA</i>	6,76E-07	8,104201364	8,903127205
230131_x_at	<i>ARSD</i>	6,76E-07	7,092267013	6,08963049
226923_at	<i>SCFD2</i>	7,48E-07	12,48901837	11,52174562
214647_s_at	<i>HFE</i>	7,48E-07	5,937404454	4,75214035
1554646_at	<i>OSBPL1A</i>	8,79E-07	6,634366716	7,24541223
204285_s_at	<i>PMAIP1</i>	8,79E-07	12,0700976	11,43343063
223148_at	<i>PIGS</i>	8,79E-07	9,30107596	8,718914766
212692_s_at	<i>LRBA</i>	8,79E-07	10,34195084	9,33791864
233375_at	<i>EFCAB2</i>	8,79E-07	6,73894247	5,992980979
202952_s_at	<i>ADAM12</i>	8,79E-07	10,04687923	8,750362608
206087_x_at	<i>HFE</i>	8,79E-07	8,127752062	7,014170138
212364_at	<i>MYO1B</i>	8,79E-07	5,351551112	4,314737309
228388_at	<i>NFKBIB</i>	1,08E-06	6,481655219	7,397892811
226206_at	<i>MAFK</i>	1,08E-06	7,622065487	8,481331613
209726_at	<i>CA11</i>	1,08E-06	7,235605741	6,647382918
235502_at	<i>NA</i>	1,08E-06	6,103471523	5,38376106
227094_at	<i>DHTKD1</i>	1,08E-06	8,414800172	7,336592705
226612_at	<i>UBE2QL1</i>	1,08E-06	6,305490822	4,6719334
215259_s_at	<i>CADM4</i>	1,62E-06	7,351026925	8,620417945
225617_at	<i>ODF2</i>	1,62E-06	9,057765706	8,210767079
240402_at	<i>KIRREL3</i>	1,62E-06	6,042143976	5,175929728
218844_at	<i>ACSF2</i>	1,63E-06	8,339882381	7,280744995

213321_at	<i>BCKDHB</i>	2,49E-06	7,917546028	7,357037757
212159_x_at	<i>AP2A2</i>	2,49E-06	9,892970817	9,175450465
218046_s_at	<i>MRPS16</i>	2,49E-06	8,455320039	7,626850347
202729_s_at	<i>LTBP1</i>	2,49E-06	9,052154311	8,042935756
225868_at	<i>TRIM47</i>	4,08E-06	8,718976816	9,391274889
219077_s_at	<i>WVOX</i>	4,08E-06	8,231254942	7,407996849
223411_at	<i>MIF4GD</i>	4,08E-06	8,276764022	7,35572144
204800_s_at	<i>DHRS12</i>	4,08E-06	7,370652119	6,305670838
221586_s_at	<i>E2F5</i>	4,08E-06	9,122434991	7,611404605
217904_s_at	<i>BACE1</i>	4,08E-06	8,656560513	6,968282344
218755_at	<i>KIF20A</i>	4,08E-06	9,231658787	6,437711513
240084_at	<i>CBX2</i>	4,53E-06	7,124987676	8,490441663
228796_at	<i>CPNE4</i>	4,53E-06	7,932482638	6,963998455
225182_at	<i>TMEM50B</i>	4,53E-06	10,09682554	8,791752667
238183_at	<i>NA</i>	5,12E-06	7,154283329	8,698171382
219905_at	<i>ERMAP</i>	5,12E-06	7,53688713	6,815768834
230547_at	<i>KCNC1</i>	5,12E-06	8,40583103	7,059735006
205652_s_at	<i>TTLL1</i>	6,70E-06	8,551432533	7,570385246
212810_s_at	<i>SLC1A4</i>	6,70E-06	7,348956934	6,215922703
213591_at	<i>ALDH7A1</i>	7,66E-06	6,439556759	5,634119961
213223_at	<i>RPL28</i>	1,12E-05	8,926299621	9,785266326
218552_at	<i>ECHDC2</i>	1,12E-05	8,921085225	8,240909258
213195_at	<i>LYRM9</i>	1,12E-05	7,147310024	6,501842298
243594_x_at	<i>SPIRE2</i>	1,12E-05	7,002397505	6,179957748
229647_at	<i>NDUFS1</i>	1,12E-05	7,613047242	6,525522777
235311_at	<i>FKBP14</i>	1,12E-05	6,951819245	5,893552652
223636_at	<i>ZMYND12</i>	1,12E-05	5,904782745	4,967696049
223464_at	<i>OSBPL5</i>	1,12E-05	6,825681628	5,176814927
205150_s_at	<i>TRIL</i>	1,12E-05	7,449592253	5,370382639
205367_at	<i>SH2B2</i>	1,22E-05	7,804542254	8,894136204
217995_at	<i>SQRDL</i>	1,22E-05	7,318784346	8,209846775
226079_at	<i>FLYWCH2</i>	1,22E-05	7,508189748	6,668701684
209871_s_at	<i>APBA2</i>	1,22E-05	9,297151045	8,077333669
213947_s_at	<i>NUP210</i>	1,22E-05	8,757115413	7,423820856
220325_at	<i>TAF7L</i>	1,23E-05	3,982299226	4,699932331
235422_at	<i>NA</i>	1,23E-05	7,823823802	9,086848076
1559893_at	<i>GPATCH11</i>	1,23E-05	4,399677756	4,890458476
205412_at	<i>ACAT1</i>	1,23E-05	10,82888382	10,17559159
204295_at	<i>SURF1</i>	1,23E-05	10,08731757	9,397452814
225366_at	<i>PGM2</i>	1,23E-05	8,421597299	7,782728979
225302_at	<i>TMX3</i>	1,23E-05	11,22170533	10,32232401
232297_at	<i>KLHL5</i>	1,23E-05	8,12434185	7,385130636
223917_s_at	<i>SLC39A3</i>	1,23E-05	8,608738602	7,726332246
202944_at	<i>NAGA</i>	1,23E-05	8,01908337	7,033818387
218958_at	<i>C19orf60</i>	1,23E-05	7,45625678	6,422062165
224821_at	<i>ABHD14B</i>	1,23E-05	5,961008256	5,091423082
242064_at	<i>SDK2</i>	1,23E-05	8,956648071	7,10376132
228943_at	<i>MAP6</i>	4,06E-05	8,730117192	8,095417366
230129_at	<i>PSTK</i>	4,06E-05	7,076219167	6,456258571

209610_s_at	<i>SLC1A4</i>	4,06E-05	7,855462366	6,713977347
206083_at	<i>BAI1</i>	4,06E-05	7,535985186	6,414691028
204792_s_at	<i>IFT140</i>	4,06E-05	5,945686744	5,020588797
225704_at	<i>FBRSL1</i>	4,06E-05	8,08785236	6,266893281
230954_at	<i>C20orf112</i>	4,34E-05	6,593948318	7,854651215
241478_at	<i>MICALL2</i>	4,34E-05	6,755975184	7,639986652
1556127_at	<i>DIP2A</i>	4,34E-05	6,781224606	7,613163999
208833_s_at	<i>ATXN10</i>	4,34E-05	12,58405581	11,93010099
226935_s_at	<i>CLPTM1L</i>	4,34E-05	10,14522875	9,270766058
203859_s_at	<i>PALM</i>	4,34E-05	7,844873391	6,868555488
207548_at	<i>GRM7</i>	4,34E-05	6,502495408	5,121186373
225503_at	<i>DHRX</i>	4,73E-05	9,580189257	8,973020812
218317_x_at	<i>NA</i>	4,73E-05	8,116564137	7,500663147
64942_at	<i>GPR153</i>	4,73E-05	9,958177679	9,120318074
1554701_a_at	<i>TBC1D16</i>	4,73E-05	7,546354384	6,866617857
228570_at	<i>BTBD11</i>	4,73E-05	8,517238596	7,631876083
219419_at	<i>RBFA</i>	4,73E-05	8,338499075	7,43976327
208291_s_at	<i>TH</i>	4,73E-05	6,263316742	4,878698965
224870_at	<i>DANCR</i>	7,37E-05	9,710102257	10,82939525
211475_s_at	<i>BAG1</i>	7,37E-05	8,427985546	9,267912464
202814_s_at	<i>HEXIM1</i>	7,37E-05	8,5443679	9,367933878
229480_at	<i>MAGI2-AS3</i>	7,37E-05	7,163240165	7,671012211
203919_at	<i>TCEA2</i>	7,37E-05	10,50917655	9,62100583
229588_at	<i>DNAJC10</i>	7,37E-05	7,876508664	7,044540915
239221_at	<i>GPR123</i>	7,37E-05	7,905787019	6,970009897
213169_at	<i>SEMA5A</i>	7,37E-05	11,60570695	10,1859005
233543_s_at	<i>FAM175A</i>	7,37E-05	6,016180826	5,128452158
204238_s_at	<i>DNPH1</i>	7,37E-05	7,276618508	5,861388777
213658_at	<i>NA</i>	7,37E-05	6,987989035	5,580792732
1556496_a_at	<i>NA</i>	7,77E-05	5,427249256	6,288970476
244360_at	<i>FBXL17</i>	7,77E-05	6,899544302	7,982231988
205028_at	<i>TRO</i>	7,77E-05	6,978629651	7,498323304
202108_at	<i>PEPD</i>	7,77E-05	9,442296198	8,654164558
203741_s_at	<i>ADCY7</i>	7,77E-05	5,787761355	5,058293061
224674_at	<i>TTYH3</i>	7,77E-05	10,15266514	8,726866688
203764_at	<i>DLGAP5</i>	7,77E-05	10,10503033	7,956775429
1560069_at	<i>PLEKHM3</i>	8,81E-05	6,128683198	6,855211377
228318_s_at	<i>CRIPAK</i>	8,81E-05	8,470959194	6,822804297
236273_at	<i>NBPF1</i>	8,90E-05	8,817468249	9,772676868
235174_s_at	<i>LINC01003</i>	8,90E-05	10,60121036	11,41629089
225174_at	<i>DNAJC10</i>	8,90E-05	10,90989961	10,05163667
225280_x_at	<i>ARSD</i>	8,90E-05	7,394906183	6,39117306
211330_s_at	<i>HFE</i>	8,90E-05	6,315576295	4,985336667
227211_at	<i>PHF19</i>	8,90E-05	8,792007273	10,09513448
242794_at	<i>MAML3</i>	8,90E-05	6,616161929	5,549146434
223194_s_at	<i>SLC22A23</i>	8,90E-05	9,599400831	7,731575837
231202_at	<i>ALDH1L2</i>	8,90E-05	6,245268124	4,213404065
230622_at	<i>MLLT4</i>	9,43E-05	6,461982638	7,188828818
200962_at	<i>RPL31</i>	9,43E-05	8,635909979	9,285834624

209238_at	STX3	9,43E-05	8,916363024	9,585679584
227966_s_at	NA	9,43E-05	9,318924684	8,807834519
225198_at	VAPA	9,43E-05	10,37411621	9,680700206
210046_s_at	IDH2	9,43E-05	10,56011105	9,686216055
221883_at	PKNOX1	9,43E-05	8,016410326	7,279435337
230036_at	SAMD9L	9,43E-05	6,701727309	6,084467982
213116_at	NEK3	9,43E-05	7,714989553	6,898164623
226932_at	SSPN	9,43E-05	9,474883087	8,101979348
223696_at	ARSD	9,43E-05	8,260833185	6,963596202
226519_s_at	PHYKPL	0,00016474	7,915359766	7,138537219
1553285_s_at	RAD9B	0,00016474	3,926682273	3,364125086
1563345_at	NA	0,000192793	6,594551152	7,290222598
230508_at	DKK3	0,000192793	10,99714162	11,95469791
204058_at	ME1	0,000192793	8,554847359	9,139797372
225042_s_at	CSRNP2	0,000192793	7,719052582	8,244961114
219520_s_at	WWC3	0,000192793	9,957053936	9,455912398
225708_at	MED29	0,000192793	9,010155	8,539661113
213980_s_at	CTBP1	0,000192793	11,25801494	10,64515152
213041_s_at	ATP5D	0,000192793	10,79795519	10,15895665
213904_at	NA	0,000192793	9,00215264	8,431937103
202916_s_at	FAM20B	0,000192793	9,159756833	8,549971028
214198_s_at	DGCR2	0,000192793	9,487045803	8,850767448
202867_s_at	DNAJB12	0,000192793	6,344235187	5,720615319
241411_at	NA	0,000192793	7,666692105	6,888407238
1555824_a_at	PACS2	0,000192793	7,368801338	6,619314801
205500_at	C5	0,000192793	7,66437496	6,828095278
214109_at	LRBA	0,000192793	8,75140646	7,70052828
214068_at	BEAN1	0,000192793	5,07809801	4,423284558
210380_s_at	CACNA1G	0,000192793	7,054661858	6,004808051
205229_s_at	COCH	0,000192793	6,765093409	5,504955206
203418_at	CCNA2	0,000192793	8,484416485	6,731593298
211105_s_at	NFATC1	0,000192793	7,351608278	5,548495324
244452_at	ERLEC1	0,000320843	5,790301309	7,016037179
206777_s_at	NA	0,000320843	8,326212983	9,252445848
221640_s_at	PIDD	0,000320843	8,311894238	9,109477524
219129_s_at	SAP30L	0,000320843	8,623020637	9,159279785
214789_x_at	SRSF8	0,000320843	10,71535223	11,30712577
226344_at	ZMAT1	0,000320843	7,836238442	7,082360836
213259_s_at	NA	0,000320843	7,365937206	6,567548722
224150_s_at	CEP70	0,000320843	7,415312669	6,610498755
218928_s_at	SLC37A1	0,000320843	7,258685648	6,388802689
202177_at	GAS6	0,000320843	6,769380741	5,810624993
1554597_at	NA	0,000320843	7,262379398	6,167482479
205151_s_at	TRIL	0,000320843	7,799464914	6,606267323
225834_at	NA	0,000320843	10,88777145	8,963406067
220940_at	ANKRD36B	0,000320843	7,143233742	5,015494719
230612_at	WDR73	0,00047641	6,233391838	6,93527546
237954_x_at	ARHGEF40	0,00047641	5,869565687	6,474305398
208820_at	PTK2	0,00047641	11,58808584	11,0054537
1568629_s_at	PIK3R2	0,00047641	11,36032941	10,78356243

236359_at	SCN4B	0,00047641	8,77674388	8,035925821
36553_at	ASMTL	0,00047641	9,295755292	8,407024102
241049_at	GRM7	0,00047641	5,401748264	4,630692787
218983_at	C1RL	0,00047641	7,990625633	5,358454154
1554018_at	GPNMB	0,000744147	4,668434268	6,585210522
1553448_at	FLJ34503	0,000744147	3,910641191	5,190366506
1558706_a_at	ATOH8	0,000744147	7,460848188	9,050685637
242786_at	SBF2-AS1	0,000744147	6,612267544	7,408985318
237033_at	FAM159A	0,000744147	6,252433425	6,878237543
220685_at	FAM120C	0,000744147	6,371301764	6,99339194
238525_at	DDX56	0,000744147	7,816662784	8,573441148
228378_at	C12orf29	0,000744147	7,97947433	8,689769694
202387_at	BAG1	0,000744147	8,68965289	9,425512501
219019_at	PIDD	0,000744147	9,111610755	9,842642482
225466_at	PATL1	0,000744147	9,834317196	10,49715509
225098_at	ABI2	0,000744147	11,49139321	10,97957177
208964_s_at	NA	0,000744147	10,37631269	9,892475461
209273_s_at	ISCA1	0,000744147	9,585346922	9,094772851
217809_at	BZW2	0,000744147	10,92734017	10,29482016
201620_at	MBTPS1	0,000744147	9,565633462	8,905463418
204591_at	CHL1	0,000744147	12,55839648	11,6579601
1554314_at	C6orf141	0,000744147	10,18864393	9,412767024
231017_at	STK11	0,000744147	8,076896811	7,391780991
222062_at	IL27RA	0,000744147	8,035334043	7,257510129
212912_at	RPS6KA2	0,000744147	9,637273335	8,575981623
213155_at	NA	0,000744147	11,46140392	10,18417278
223695_s_at	ARSD	0,000744147	6,898065141	6,087065286
212314_at	SEL1L3	0,000744147	11,5544666	10,17579092
1552439_s_at	MEGF11	0,000744147	7,447732322	6,551575812
243512_x_at	NA	0,000744147	7,223121612	6,247512485
221892_at	H6PD	0,000744147	7,492304056	6,367056633
1552701_a_at	CARD16	0,000744147	5,311625867	4,494296344
234994_at	TMEM200A	0,000744147	6,591829253	5,549763426
228199_at	NA	0,000744147	6,550109732	5,441407301
212488_at	COL5A1	0,000744147	8,437678746	6,937911421
1556308_at	PRRT3	0,000744147	7,347666894	5,838680709
204962_s_at	NA	0,000744147	9,569490588	7,562435804
209010_s_at	TRIO	0,00084956	4,980760694	5,590694342
208033_s_at	ZFH3	0,00084956	6,188689503	6,623415321
212461_at	AZIN1	0,00084956	11,00199044	10,24841303
238569_at	GABBR1	0,00084956	7,976959796	7,354644053
225973_at	TAP2	0,00084956	8,917658687	8,111098068
230454_at	ICA1L	0,00084956	8,346889612	7,503884177
212316_at	NUP210	0,00084956	8,080393103	7,193577799
212315_s_at	NUP210	0,00084956	6,991292924	5,909852011
228488_at	TBC1D16	0,00084956	7,355411994	6,172994334
212022_s_at	MKI67	0,00084956	8,450220923	6,878180641
217584_at	NPC1	0,001016322	6,452908506	7,173644053
223625_at	FAM126A	0,001016322	8,435982461	9,090558285
206364_at	KIF14	0,001016322	8,62432718	6,915338752



209709_s_at	HMMR	0,001016322	8,23412549	6,36916367
1552257_a_at	TLL12	0,001903541	7,799735433	6,852612604
205380_at	PDZK1	0,001918907	4,858231923	6,150935314
1555323_at	ABC9	0,001918907	5,147938783	6,188706229

**11.6 Summary of Log-rank analysis for ANXA2-dependent Risk Score on TCGA, GSE13041, GSE17536, E-MTAB-365 and GSE31210 cohorts of cancer patients.**

<i>Tumour type (origin of data)</i>	<i>Survival</i>	<i>ANXA2 status</i>	<i>Median Survival (months)</i>	<i>Log-rank (Mantel-Cox) p value</i>	<i>Hazard Ratio (logrank) Risk score low/Risk score high</i>
<i>GBM from TCGA</i>	PFS	Risk Score High Risk Score Low	7.83 8.72	0.019	1.288
	OS	Risk Score High Risk Score Low	12.93 14.41	0.0261	1.242
<i>GBM from GSE13041</i>	OS	Risk Score High Risk Score Low	11.7 13.55	0.0486	1.353
<i>Colon cancer from GSE17536</i>	DSS	Risk Score High Risk Score Low	77.6 N.D.	0.006	2.149
<i>Breast cancer from E-MTAB- 365</i>	RFS	Risk Score High Risk Score Low	N.D. N.D.	0.002	1.739
<i>Lung adenocarcinoma from GSE31210</i>	RFS	Risk Score High Risk Score Low	N.D. N.D.	0.0605	1.61

N.D. Not Determined

**11.7 Differentially expressed genes between SiNEG and SiANXA2 transfected GBM cells.**

Probe set	Gene symbol	log2 means_Group SiNEG	log2 means_Group SiANXA2
229947_at	PII5	3,775176372	7,332248918
204298_s_at	LOX	4,950343226	9,322598731
220415_at	NA	3,206882819	5,830594434
215442_s_at	TSHR	2,835625138	5,152342142
224275_at	ADGRV1	3,163232954	5,725282716
219949_at	LRRC2	3,231599698	5,788707525
231930_at	NA	5,588319618	9,873290444
214822_at	BRINP2	5,262941358	9,132007604
209990_s_at	GABBR2	4,027621796	6,988252245
229407_at	SDK1	4,698773003	8,072064245
210055_at	TSHR	3,432514142	5,850187566
228235_at	NA	5,017397219	8,470908386
220148_at	ALDH8A1	3,46596668	5,828624744
223582_at	ADGRV1	5,155129473	8,649960941
221019_s_at	COLEC12	5,424897421	9,073726606
215446_s_at	LOX	6,711539644	11,14749781
205943_at	TDO2	3,107986793	5,142119023
207242_s_at	GRIK1	6,274758277	10,3509047
214611_at	GRIK1	5,220012916	8,59283502
216191_s_at	NA	5,11981276	8,413321656
205609_at	ANGPT1	4,323696643	7,070394633
208096_s_at	COL21A1	3,906225532	6,369709408
243183_at	NA	4,243725008	6,899411434
206529_x_at	SLC26A4	4,624893808	7,514592426
229912_at	SDK1	5,880817024	9,522035809
238262_at	SPDYA	3,160894638	5,10150804
242005_at	LINC00973	3,119822127	5,030633491
237302_at	CNKSR3	3,439279279	5,545686376
227752_at	SPTLC3	4,185523441	6,744594677
1570445_a_at	LOC643201	4,107585429	6,538621847
237973_at	NA	4,490303447	7,143246153
209301_at	CA2	4,843694085	7,687186819
230250_at	PTPRB	3,059417138	4,855330803
225016_at	APCDD1	5,419458347	8,583285197
203789_s_at	SEMA3C	3,926285927	6,216006514
217280_x_at	GABRA5	3,678954069	5,805434743
201110_s_at	THBS1	4,336123853	6,840016022
239148_at	MARVELD3	3,694447061	5,801285137
205466_s_at	HS3ST1	5,385619666	8,448949216
208498_s_at	NA	4,328129209	6,783827677
205100_at	GFPT2	4,635884469	7,260874183
243541_at	IL31RA	4,849726664	7,590179524
215443_at	TSHR	3,602759596	5,608757557
241986_at	BMPER	3,444826315	5,362049284
1553614_a_at	LINC01198	3,489094634	5,425478687
239006_at	SLC26A7	5,146218155	7,998286054
226228_at	AQP4	4,802139472	7,414965132
206698_at	XK	3,91223922	6,033936678
239761_at	GCNT1	4,914309274	7,573525627
229927_at	LEMD1	5,826995696	8,964923555

1558404_at	LINC00622	2,902176131	4,458227886
215531_s_at	GABRA5	4,39628119	6,735581843
206185_at	CRYBB1	4,802609652	7,348796048
243163_at	HECW1	2,786111284	4,259800738
1552880_at	SEC16B	3,696583871	5,631907226
231438_x_at	CDH8	5,648661806	8,594898568
227654_at	FAM65C	4,823010972	7,317174166
205505_at	GCNT1	4,468090621	6,75998922
236201_at	SPTLC3	4,762832227	7,196117641
229580_at	CLSTN2	4,297919317	6,489073823
201109_s_at	THBS1	3,944433956	5,932710241
213830_at	YMEIL1	5,825266338	8,73849588
1570444_at	LOC643201	2,693618855	4,037802796
204114_at	NID2	4,051162693	6,072764395
1563488_at	TMEM132B	4,334079685	6,49602947
225328_at	FBXO32	4,663145974	6,946908328
1559256_at	MAGI1	3,839636403	5,697618226
206456_at	GABRA5	5,731679663	8,484875506
239556_at	LOC645513	3,653973105	5,405008592
213075_at	OLFML2A	5,972605032	8,826458074
1565638_at	PMP22	3,404849246	5,009551941
213241_at	PLXNC1	4,10805884	6,041720915
217143_s_at	YMEIL1	6,283370971	9,230240068
1569512_at	NA	3,51111017	5,140260368
206300_s_at	PTHLH	4,774467206	6,967371916
239519_at	NA	3,111001171	4,53548375
211756_at	PTHLH	5,266878905	7,665360976
220266_s_at	KLF4	4,350207653	6,330127529
231234_at	CTSC	5,360049107	7,792780192
220679_s_at	CDH7	3,745041822	5,443627306
230865_at	LIX1	2,815856847	4,075129134
232060_at	ROR1	3,855433721	5,574304049
233871_at	NA	5,871124469	8,456656311
215578_at	NA	3,936201863	5,666633143
209955_s_at	FAP	5,058481542	7,25186599
228469_at	PPID	5,520385187	7,911318323
1555431_a_at	IL31RA	3,013556198	4,311995645
201438_at	COL6A3	4,019152286	5,740211515
225646_at	CTSC	6,952460553	9,8882529
236089_at	HECW2	3,978402213	5,610964582
219450_at	C4orf19	5,138674253	7,238834405
241762_at	FBXO32	2,82254773	3,972663056
221900_at	COL8A2	6,260091972	8,794919498
1569052_at	NA	3,960450953	5,545364994
240898_at	SPAG16	4,365208878	6,108317256
1559923_at	GRIK1	3,25226404	4,549648714
230220_at	UNC80	5,075047491	7,097849953
221841_s_at	KLF4	6,43948032	8,98966781
223634_at	RASD2	6,245356325	8,702656902
215081_at	KIAA1024	4,260330318	5,92915294
222725_s_at	PALMD	3,040552119	4,226956556
213125_at	OLFML2B	4,65982295	6,475676995
1553219_a_at	AMMECR1	4,352897359	6,048916644
213217_at	ADCY2	6,121417197	8,501942125
1569167_at	NA	4,492356312	6,237582868
208025_s_at	HMGA2	4,081098488	5,66480795

230962_at	DCLK1	5,754749094	7,978134377	223529_at	SYT4	5,250601574	6,8992595
210305_at	PDE4DIP	4,946258269	6,824043564	207789_s_at	DPP6	6,179484037	8,118737472
226273_at	CLCN5	4,582352762	6,317906661	202283_at	SERPINF1	4,929226723	6,475743978
205338_s_at	DCT	3,755638963	5,171966944	241500_at	CDH8	5,482869609	7,195833131
1556499_s_at	COL1A1	4,792002705	6,588139794	229256_at	PGM2L1	7,295157873	9,568423097
230179_at	LOC285812	4,148639553	5,690640051	225345_s_at	FBXO32	3,987320115	5,227155049
206466_at	ACSBG1	3,395018696	4,653698633	225207_at	PDK4	6,197357431	8,115175835
227240_at	NGEF	5,423624706	7,388743936	227361_at	HS3ST3B1	6,60507123	8,647283442
215076_s_at	COL3A1	3,535270536	4,814475084	203066_at	CHST15	6,584296558	8,600665661
230303_at	SYNPR	3,33181995	4,537298202	242639_at	ICE2	5,104039933	6,666309555
225647_s_at	CTSC	7,536000456	10,25560666	223605_at	SLC25A18	6,48449894	8,464073533
214963_at	NUP160	4,953292348	6,739467582	1559257_a_at	MAGI1	4,839738516	6,313795371
226912_at	ZDHHC23	5,048875597	6,86494677	230493_at	SHISA2	2,634366448	3,435175179
236994_at	FBXL4	5,377995998	7,309074968	1554789_a_at	PDE8B	5,49791292	7,15903682
242587_at	SLC9A9	4,702009133	6,375118695	205651_x_at	RAPGEF4	5,624968656	7,318524331
203304_at	BAMBI	5,594891492	7,583849136	232181_at	PPARGC1B	3,891298365	5,062360346
235350_at	C4orf19	4,476480555	6,060869042	1554378_a_at	PDE1C	5,219213672	6,789623909
228546_at	DPP6	5,942051788	8,043307184	209906_at	C3AR1	6,239222126	8,111650988
204513_s_at	ELMO1	7,075778217	9,561778182	223644_s_at	CRYGS	5,649933598	7,340747835
236796_at	NA	4,649631958	6,276154755	204051_s_at	SFRP4	5,204398834	6,758394671
227911_at	ARHGAP28	3,366407221	4,540522609	210518_at	CDH8	5,754208167	7,470436362
238533_at	EPHA7	6,972090626	9,401683697	228150_at	SEC16B	6,04709604	7,840259601
231384_at	GRIN2A	3,6916463	4,969596941	210732_s_at	LGALS8	3,672305824	4,760164561
209700_x_at	PDE4DIP	5,002603585	6,733907312	1559521_at	NA	5,358609727	6,943713174
202436_s_at	CYP1B1	5,799849473	7,799033753	229951_x_at	NA	4,74297164	6,145903923
228740_at	NA	5,855492704	7,868532521	233081_at	NA	4,271938807	5,527558963
240455_at	NA	3,724694014	5,001034042	203881_s_at	DMD	4,344819215	5,619061213
201852_x_at	COL3A1	3,233603347	4,339933183	219414_at	CLSTN2	3,860817059	4,990347668
214797_s_at	CDK18	5,002312731	6,713301099	1560556_a_at	PLEKHA8	4,197614191	5,424434791
218858_at	DEPTOR	4,532357284	6,081122646	208063_s_at	CAPN9	4,837520231	6,249398012
221234_s_at	BACH2	6,56057668	8,79288694	52255_s_at	COL5A3	6,139352709	7,928545509
221107_at	CHRNA9	7,631340126	10,22690321	201141_at	GPNMB	4,089642872	5,275426326
214321_at	NOV	5,13506307	6,874537207	206167_s_at	ARHGAP6	5,936053129	7,642449365
213496_at	LPPR4	5,284554884	7,05850455	214475_x_at	CAPN3	4,54054041	5,845684578
229441_at	PRSS23	5,347259143	7,123184042	224480_s_at	GPAT3	7,292151028	9,387693665
223395_at	ABI3BP	3,177590895	4,232696564	238688_at	TPM1	6,237897641	8,029853497
239650_at	NCKAP5	4,055970341	5,400411648	1562904_s_at	FAM86B3P	4,206096759	5,414152037
218063_s_at	CDC42EP4	5,136450854	6,837323954	211668_s_at	PLAU	5,639517867	7,258477819
226333_at	IL6R	4,674295049	6,218180646	219938_s_at	PSTPIP2	5,306007765	6,828589515
231358_at	MRO	3,980625851	5,289072488	201739_at	SGK1	6,035612182	7,764451741
232049_at	SNX2	4,189234908	5,566112111	228111_s_at	DNAH1	4,258054441	5,46978186
1558387_at	UG0898H09	5,170697917	6,869371643	1557177_at	LOC10050625 8	3,787298708	4,864260278
202458_at	PRSS23	7,685050085	10,20931087	226811_at	FAM46C	4,168277882	5,351072519
52651_at	COL8A2	6,285394863	8,345759033	232994_s_at	ARHGFEF28	6,20730963	7,96723372
226279_at	PRSS23	6,954790368	9,22064911	240709_at	SEZ6L	4,052720272	5,200696361
1558668_s_at	SPATA22	3,026227385	4,011799294	1558522_at	MPP6	5,980103154	7,667595913
215303_at	DCLK1	6,44780521	8,540483499	1556200_a_at	C10orf90	4,652682405	5,963634517
239230_at	HES5	5,907036888	7,823948716	235004_at	RBM24	5,273460636	6,755046119
240472_at	NA	4,12453929	5,462685026	215435_at	NA	4,696101934	6,01503294
225803_at	FBXO32	5,219872055	6,904359183	229784_at	NA	4,969588828	6,363005339
217574_at	CDH8	6,491280573	8,578607422	232429_at	DTWD1	4,11727922	5,266619841
202435_s_at	CYP1B1	5,808621458	7,669358513	241497_at	NA	4,094690043	5,236747112
229437_at	NA	6,087122161	8,032214	231214_at	NA	6,006489553	7,67580026
206852_at	EPHA7	5,70497306	7,526685972	231364_at	NFIA-AS2	3,717970824	4,751073479
212713_at	MFAP4	6,189161312	8,158633647	209189_at	FOS	6,021014848	7,691190967
242540_at	DNHD1	3,304142289	4,347084171	1557260_a_at	ZNF382	3,999651129	5,108657797

223772_s at	TMEM87A	5,132576753	6,551697249
206465_at	ACSBG1	6,656856077	8,487151277
238462_at	UBASH3B	6,650984771	8,478897258
1563621_at	NA	5,024878498	6,403592161
205528_s at	RUNX1T1	5,764064076	7,339138848
227532_at	LRRC39	3,91810436	4,986463994
225630_at	EEPD1	5,912922962	7,52413635
204984_at	GPC4	8,248409643	10,48914969
238752_at	GPLD1	4,497969789	5,717372771
212187_x at	PTGDS	7,792243802	9,903958817
226218_at	IL7R	5,099346583	6,472306422
213415_at	CLIC2	4,046081614	5,133835714
204983_s at	GPC4	7,63950238	9,689580568
223827_at	TNFRSF19	5,880320083	7,45754057
1559062_at	NA	4,009357577	5,084605488
227791_at	SLC9A9	6,870239594	8,709639908
220021_at	TMC7	4,802961594	6,087815558
230534_at	ZNF678	5,231535672	6,630334207
205668_at	LY75	6,018332712	7,624016214
226274_at	CLCN5	6,354333947	8,047514841
238417_at	PGM2L1	6,439797918	8,150665776
210121_at	B3GALT2	5,585728827	7,060807711
234051_at	NA	4,011112145	5,069375272
206144_at	MAG11	6,276124489	7,930149048
226997_at	ADAMTS12	7,249155365	9,156273473
236197_at	NA	3,502696529	4,423369946
228461_at	SH3RF3	5,55482167	7,013500694
228827_at	RUNX1T1	6,665822177	8,409906077
1562926_at	NA	4,412844012	5,562683002
207303_at	PDE1C	6,321485024	7,962733997
209627_s at	OSBPL3	7,139114403	8,985722155
229725_at	ACSL6	5,5600462	6,994923247
230451_at	NA	4,913739053	6,181027829
1554910_at	PRKD3	4,756707048	5,982658004
211748_x at	PTGDS	8,068244031	10,14518399
204184_s at	ADRBK2	6,233021451	7,83272267
235761_at	NA	4,971365183	6,242779692
229288_at	EPHA7	8,883974433	11,1519055
213228_at	PDE8B	6,492641142	8,149552839
235020_at	TAF4B	5,525999571	6,93615339
238890_at	BRWD1	6,021432795	7,548738481
230248_x at	NA	4,007975949	5,022333725
205805_s at	ROR1	4,094071888	5,128709872
236179_at	CDH11	6,599036678	8,261382294
1557345_at	LOC283516	3,088364428	3,866053416
204796_at	EML1	6,778967121	8,482692719
212594_at	NA	4,939014713	6,178761748
206117_at	TPM1	5,835428846	7,297451151
236795_at	NA	4,765279632	5,958756186
232803_at	NA	2,611763193	3,263919884
218002_s at	CXCL14	7,377458312	9,208346847
242593_at	NA	4,534096934	5,658218659
1559966_a at	ZFH4-AS1	6,590472298	8,221717605
202834_at	AGT	8,52652754	10,63208675
218850_s at	LIMD1	6,96422458	8,683782486
219714_s at	CACNA2D3	3,679420911	4,587144708

226982_at	ELL2	4,629900147	5,771236666
1564150_a at	LINC01619	3,077252276	3,835501864
239218_at	PDE1C	8,207993649	10,23008251
239476_at	NA	5,33281137	6,646153503
205960_at	PDK4	3,845057025	4,791833236
232538_at	NA	5,432900164	6,769570532
230908_at	TACR1	4,201435194	5,233827665
217452_s at	B3GALT2	5,849857103	7,278826917
223601_at	OLFM2	5,854766829	7,282810488
210954_s at	TSC22D2	3,38807614	4,213048265
239835_at	KBTD8	5,599002837	6,959246258
207414_s at	NA	4,518483025	5,615523583
1557685_at	ASAP1-IT2	5,668520841	7,043427121
226418_at	ERGIC2	5,193786992	6,445643832
205560_at	PCSK5	6,081182651	7,54350414
1556773_at	NA	3,703587112	4,588474669
227828_s at	EVA1A	5,099394608	6,316101745
214967_at	NA	4,594745504	5,689907223
224489_at	NA	4,930033355	6,104717541
238658_at	NA	5,638063348	6,980136673
219610_at	ARHGFEF28	6,482382286	8,02458788
206591_at	RAG1	2,86791038	3,548904726
230495_at	LINC01102	7,062498257	8,736017269
212473_s at	MICAL2	6,211923454	7,68146446
242443_at	NA	5,401105585	6,671004265
227038_at	SGMS2	5,520228798	6,817235648
240061_at	NA	5,134506633	6,336997129
221935_s at	EOGT	6,710999683	8,279679324
215318_at	MINOS1P1	4,543329239	5,605113657
238587_at	UBASH3B	6,546934794	8,074007086
1554824_at	ZNF585A	5,420120162	6,683769897
212298_at	NRP1	7,599073756	9,367208556
1559965_at	ZFH4-AS1	7,606223036	9,374430738
214930_at	SLITRK5	4,388944197	5,409135562
231807_at	KIAA1217	5,130833578	6,323458039
227173_s at	BACH2	7,080810217	8,726206304
1554741_s at	NA	3,994356142	4,922434002
205479_s at	PLAU	6,907444918	8,51169299
239350_at	MARVELD3	5,286150419	6,513771204
218062_x at	CDC42EP4	9,167015166	11,29316081
225631_at	EEPD1	5,061968233	6,235881796
235209_at	SBSPON	4,577057973	5,638068016
213652_at	PCSK5	6,685407072	8,234265032
205932_s at	MSX1	8,620106885	10,61623351
220456_at	SPTLC3	3,348562539	4,123533603
1565639_a at	PMP22	6,038490763	7,435900945
1558250_s at	NA	6,278190221	7,730609226
203498_at	RCAN2	9,855949499	12,12735569
222484_s at	CXCL14	7,423587917	9,133180015
202431_s at	MYC	7,076835037	8,703109141
230278_at	NA	5,731180619	7,046860652
212489_at	COL5A1	6,631184774	8,152080819
244663_at	ZNF431	6,002932859	7,378159424
235970_at	LCORL	5,789315873	7,114964442
229521_at	CCDC71L	6,374675309	7,832860033
238623_at	NA	6,842531951	8,406505772

211679_x_at	GABBR2	4,426436257	5,437184518	210987_x_at	TPM1	9,348753923	11,31719524
229178_at	PRTG	5,495341837	6,749865747	221796_at	NTRK2	3,421542123	4,140704188
219523_s_at	TENM3	5,655773093	6,946194976	218975_at	COL5A3	6,09121358	7,369103693
1560814_a_at	C15orf57	5,721444288	7,026153807	229132_at	MINA	5,546961263	6,707020899
222520_s_at	IFT57	3,910421781	4,801747407	230763_at	SPATA17	4,570801865	5,525371061
215209_at	SEC24D	3,871854359	4,753503536	228188_at	FOSL2	7,934539748	9,590127169
220454_s_at	SEMA6A	6,020055053	7,390103794	229553_at	PGM2L1	7,852666711	9,489593335
232000_at	TTC39B	5,015336976	6,15604101	232355_at	SNORD114-3	6,423080631	7,761092138
209829_at	FAM65B	7,339530218	9,007042643	229073_at	PRTG	5,687131884	6,870177619
1569029_at	METAP1D	4,555949954	5,590476893	229091_s_at	CCNJ	5,599858348	6,760242107
212240_s_at	PIK3R1	8,129315447	9,97354029	235416_at	LOC643201	5,779346713	6,974959303
211925_s_at	PLCB1	5,191612408	6,368734442	231468_at	SH3BP4	4,066106152	4,904642556
236824_at	TMEM132B	9,659140073	11,84843436	204183_s_at	ADRBK2	5,849383936	7,049330737
227755_at	ERN1	5,894586215	7,227908476	217565_at	GRIA3	5,884747009	7,091730671
235683_at	SESN3	6,437534308	7,884065629	210944_s_at	CAPN3	6,175895307	7,442538991
235658_at	NA	5,416388057	6,62815307	1562059_at	NA	4,628695485	5,576542938
213601_at	SLIT1	6,896628123	8,436281228	227775_at	CELF6	3,751152033	4,516488847
235497_at	LINC01128	5,973970577	7,30616972	203325_s_at	COL5A1	7,225084601	8,694553919
1558388_a_at	UG0898H09	8,15075178	9,968221439	219279_at	DOCK10	6,258261887	7,530204539
219313_at	GRAMD1C	7,181385313	8,779566827	221583_s_at	KCNMA1	5,555208112	6,6841236
233801_s_at	SEMA6D	7,696864334	9,408160591	233055_at	NA	5,679507791	6,831969782
243042_at	FAM73A	6,049293409	7,389220094	240172_at	ERGIC2	6,682543394	8,035302848
206116_s_at	TPM1	9,112596998	11,1298247	1560407_at	MARK1	5,128822998	6,162123015
204976_s_at	AMMECR1	7,539886331	9,208756068	214962_s_at	NUP160	5,470994473	6,572691839
238495_at	LRRC57	5,479276849	6,690171333	215523_at	ZNF391	4,060343218	4,876687854
233555_s_at	SULF2	8,392222035	10,24224499	212256_at	GALNT10	7,912638765	9,499394728
204149_s_at	GSTM4	6,282081022	7,664554319	213139_at	SNAI2	8,177154651	9,815757724
242979_at	IRS1	5,068203936	6,180142668	230650_at	SLCO5A1	7,633512683	9,162557788
214721_x_at	CDC42EP4	9,486837348	11,56548592	241156_at	NA	5,050595522	6,060783235
239698_at	NA	4,804129228	5,854494277	233882_s_at	SEMA6D	8,984561965	10,780373392
238484_s_at	SSBP2	6,048345646	7,3669754	235111_at	LSAMP	8,109040912	9,729667721
232384_s_at	LOC10192727 2	3,440942596	4,189802538	216724_at	DCLK2	6,303903743	7,562018236
242342_at	GUCY1A2	4,500304174	5,477590657	226886_at	GFPT1	7,664959763	9,193882756
208944_at	TGFBR2	6,301817323	7,668975905	203865_s_at	ADARB1	5,465368629	6,554957595
207426_s_at	TNFSF4	5,44760455	6,623468245	1558945_s_at	CACNA1A	5,219611298	6,258380128
240557_at	TSC22D2	7,184612834	8,73539514	235348_at	ABHD13	6,173931258	7,400957138
232313_at	TMEM132C	4,528266215	5,50552576	204345_at	COL16A1	8,792022736	10,5377617
210068_s_at	AQP4	3,815350229	4,637982864	221103_s_at	CFAP44	6,099205834	7,310190231
220467_at	NA	3,657607248	4,442709596	227213_at	ADAT2	5,889427731	7,058622324
235545_at	DEPDC1	7,681781429	9,326628787	233297_s_at	NA	4,477386186	5,363943479
233609_at	PTPRK	5,197835206	6,310000407	203884_s_at	RAB11FIP2	7,331531553	8,781038337
1557506_a_at	NA	5,070890149	6,154153392	227568_at	HECTD2	8,704572442	10,42246827
243851_at	NA	4,35639051	5,287003029	216452_at	TRPM3	4,572551246	5,474191541
220141_at	C11orf63	6,014297507	7,2989165	212249_at	PIK3R1	7,107001494	8,506507237
215386_at	NA	4,938576309	5,992485427	214748_at	N4BP2L2	7,910118292	9,466847262
1569685_at	COX10	4,995730154	6,060716347	207434_s_at	NA	4,794361268	5,737253933
226076_s_at	NA	5,070794469	6,148167809	204501_at	NOV	4,771803474	5,708324482
242088_at	KLHL24	4,55974732	5,526302924	210986_s_at	TPM1	9,996449774	11,95485333
239999_at	MIR99AHG	6,805599964	8,246220282	215715_at	SLC6A2	5,535058753	6,618905594
241370_at	LOC286052	5,838743056	7,074464697	222735_at	TMEM38B	8,018726776	9,588098221
227046_at	SLC39A11	6,981966564	8,459275006	236163_at	LIX1	3,977760802	4,755424016
235888_at	NA	5,077216748	6,150780917	205429_s_at	MPP6	7,822898756	9,349574076
213609_s_at	SEZ6L	8,749909555	10,59824434	235382_at	LVRN	3,174763879	3,79423591
205442_at	MFAP3L	4,978923447	6,030337068	236769_at	LOC158402	5,739930592	6,855754785
1557433_at	NA	6,597713838	7,990576133	201811_x_at	SH3BP5	8,273456082	9,879755718
236717_at	FAM179A	5,194908491	6,291458332	1554640_at	PALM2	4,339073408	5,181062634

202883_s at	PPP2R1B	8,632801363	10,30181686
201487_at	CTSC	7,899179374	9,423596055
214193_s at	DIEXF	6,372294171	7,597206441
226018_at	MTURN	7,321455233	8,725590942
238537_at	CA8	4,688066182	5,586296368
234258_at	NA	3,965597765	4,725173858
222315_at	LOC10099675 6	6,254448021	7,449709183
1569940_at	SLC6A16	4,418516916	5,262917911
228481_at	NA	6,407788495	7,631251441
223044_at	SLC40A1	8,09088897	9,63411402
236097_at	NA	5,946833447	7,080432721
215028_at	SEMA6A	8,107144125	9,651446334
210641_at	CAPN9	4,204734879	5,004520716
242923_at	ZNF678	7,047837018	8,387590951
1554462_a at	DNAJB9	8,093754379	9,632010011
222820_at	TNRC6C	6,642601149	7,902084857
233020_at	NA	5,567249888	6,620712755
231249_at	SZT2	4,741204851	5,637405728
230655_at	NA	7,202442391	8,562702221
64408_s at	CALML4	5,236269066	6,225094666
236335_at	GUCY1A2	6,203075249	7,373995898
228375_at	IGSF11	7,290872363	8,667056088
202008_s at	NID1	7,838788228	9,317914774
202481_at	DHRS3	5,012965252	5,957482024
223694_at	TRIM7	6,051415752	7,191273504
213413_at	STON1	5,966625705	7,089433609
228949_at	WLS	8,264075686	9,818326043
233528_s at	GATSL3	6,799206802	8,077769144
1552486_s at	LACTB	5,889525423	6,996878567
240277_at	NA	6,501022414	7,722434737
204194_at	BACH1	8,374463146	9,943933842
227314_at	ITGA2	5,40263743	6,415011941
207873_x at	SEZ6L	6,59926755	7,83502141
207172_s at	CDH11	7,682362087	9,120923853
204797_s at	EML1	7,983851788	9,47802683
207173_x at	CDH11	8,673912975	10,29703088
203504_s at	ABCA1	7,854171118	9,323089721
230861_at	DKFZP434L1 87	6,29188664	7,467487442
1559005_s at	CNTLN	4,32329913	5,130702648
204854_at	P3H3	6,629411125	7,867314832
203196_at	ABCC4	6,104328647	7,243664009
215501_s at	DUSP10	5,324182187	6,316110869
227614_at	HKDC1	6,866453929	8,141913954
228473_at	MSX1	5,439908634	6,450380136
244030_at	STYX	6,50248071	7,709016488
214896_at	LINC01314	7,361013602	8,725543729
1553208_s at	ARL10	3,869268181	4,586197283
224728_at	ATPAF1	7,807734314	9,249889659
232589_at	LOC10260646 5	6,66974235	7,897354377
1568619_s at	ITPRIPL2	8,816653666	10,4389553
210912_x at	GSTM4	6,513615443	7,711718655
224724_at	SULF2	9,801607937	11,60363288
205872_x at	PDE4DIP	6,050808159	7,162186703
213222_at	PLCB1	9,072184545	10,73632883
204949_at	ICAM3	6,373447488	7,54140892
239360_at	LOC10272388 6	4,249459844	5,027976287
226158_at	KLHL24	8,435356292	9,980389287
226613_at	GATSL3	6,754667429	7,990986863
222360_at	DPH5	6,843899777	8,095288616
201810_s at	SH3BP5	7,915240758	9,360376064
226601_at	SLC30A7	8,119219081	9,601258269
220574_at	SEMA6D	7,301337451	8,632694951
227488_at	NA	6,662006371	7,874146738
1554004_a at	ARHGEF28	6,094702617	7,203118616
203549_s at	LPL	7,505860097	8,870421037
227095_at	LEPROT	8,274285038	9,77664756
244761_at	C5orf63	5,181356987	6,122070691
222670_s at	MAFB	9,571991118	11,3097582
213103_at	STARD13	7,176183577	8,477511051
231919_at	DBT	6,513567954	7,69402232
205525_at	CALD1	7,726402069	9,125983952
213372_at	PAQR3	9,051251121	10,68988368
211894_x at	SEZ6L	6,675826095	7,883645684
213943_at	TWIST1	6,822028646	8,054609456
228256_s at	EPB41L4A	6,088137813	7,187564224
1570360_s at	DDX3Y	7,157940399	8,450536019
240083_at	NA	5,288873216	6,24231962
209966_x at	ESRRG	4,901499423	5,784872001
243491_at	ZNF431	5,771242056	6,809228992
1558754_at	ZNF763	3,321465752	3,918747162
223449_at	SEMA6A	9,49170935	11,19787757
1559397_s at	PRR14	5,991830009	7,066973023
232791_at	NA	4,013060881	4,732314005
1553613_s at	FOXC1	6,948536261	8,193682691
240592_at	LCORL	8,188483441	9,654647057
204079_at	TPST2	7,412072055	8,73735773
232028_at	ZNF678	6,420255393	7,568078254
238178_at	NA	5,544296764	6,53527421
229498_at	MBNL3	7,211511958	8,500231436
200670_at	XBP1	7,731871507	9,112601426
226321_at	LYSMD3	8,172772556	9,62942106
216047_x at	SEZ6L	6,753844953	7,954353656
235125_x at	FAM73A	7,373731482	8,68297462
211663_x at	PTGDS	6,96736217	8,203002829
227782_at	ZBTB7C	5,818036036	6,849723209
229480_at	MAGI2-AS3	6,711282799	7,899218116
1559094_at	FBXO9	6,720154472	7,904829798
242100_at	CHSY3	7,548488997	8,877966653
218772_x at	TMEM38B	8,145568889	9,579163689
215351_at	RTCA	4,269380793	5,019755283
226671_at	LAMP2	8,684713226	10,20977703
233728_at	NA	4,948130166	5,816340224
227954_at	ITPRIPL2	7,990974261	9,392578182
213672_at	NA	5,756488168	6,765615271
218559_s at	MAFB	10,44392496	12,27346719
1556654_at	CDK12	3,358596439	3,945999732
209081_s at	COL18A1	4,867330075	5,718236646
205559_s at	PCSK5	7,677900165	9,016761034
222564_at	POGK	4,628514367	5,435420404
1558739_at	BORCS5	5,117070731	6,008305767

238879_at	DCUN1D1	6,795664605	7,978246726
203883_s_at	RAB11FIP2	7,522936749	8,831743321
203201_at	PMM2	6,65854276	7,816869806
224090_s_at	TNFRSF19	6,016182446	7,061101381
226709_at	ROBO2	6,189187333	7,26336366
212510_at	GPD1L	8,553346935	10,0370304
232696_at	NA	3,812030875	4,472700151
204121_at	GADD45G	6,629494709	7,769571416
243050_at	NA	5,810036717	6,804383786
1557430_at	SMIM17	5,786119255	6,77605762
210794_s_at	MEG3	8,228081724	9,634877428
218638_s_at	NA	8,479885248	9,928792811
222762_x_at	LIMD1	8,724575472	10,21186142
228575_at	IL20RB	4,261119833	4,987465118
214460_at	LSAMP	8,464901418	9,906738424
235149_at	PGM2L1	5,853136607	6,847409751
226884_at	LRRN1	9,874973745	11,55184339
212841_s_at	PPFIBP2	7,515488862	8,791618304
222663_at	RIOK2	6,790302609	7,94291124
203548_s_at	LPL	7,595947223	8,88500094
230174_at	LYPLAL1	7,705605569	9,012861599
227763_at	LYPD6	5,168227128	6,044600285
206775_at	CUBN	5,023416525	5,874113918
1556656_at	NA	4,541306797	5,309422587
206204_at	GRB14	6,640583257	7,761879453
222877_at	NRP2	7,404494702	8,653909893
238761_at	ELK4	7,501800809	8,767310457
203143_s_at	KIAA0040	4,725632146	5,522530051
202566_s_at	SVIL	8,47700201	9,903019025
228043_at	UTP15	5,120172015	5,980186672
207060_at	EN2	6,410699647	7,487027632
227149_at	TNRC6C	4,993040178	5,829638008
227390_at	MEG3	6,441852528	7,52085147
230444_at	PDE7A	6,058109082	7,072133303
228141_at	GPX8	7,558528983	8,819443387
228732_at	GUCY1A2	5,643014615	6,583583612
242671_at	NA	7,691611492	8,972373335
215126_at	LINC01314	7,625513885	8,895063535
211064_at	ZNF493	4,574343962	5,335764503
202828_s_at	MMP14	7,818609995	9,119335508
222316_at	NA	6,150006689	7,172993439
227666_at	DCLK2	8,781307222	10,23958044
235061_at	PPM1K	5,649348973	6,587095527
242986_at	NAV1	4,649308214	5,42060598
218839_at	HEY1	9,914892348	11,55953679
232405_at	NA	5,163555769	6,019564942
207401_at	PROX1	7,320912563	8,533569515
219750_at	TMEM144	4,195363687	4,890134182
208442_s_at	ATM	6,006247439	6,999323447
220773_s_at	GPHN	7,73363811	9,010623678
232080_at	HECW2	6,456099778	7,519996906
212472_at	MICAL2	5,403412238	6,293771414
202842_s_at	DNAJB9	9,534887014	11,10564256
242982_x_at	ITGB8	5,900434035	6,872392088
205701_at	IPO8	6,263481301	7,294134442
1554449_at	MIER3	5,441945153	6,336081606

218806_s_at	VAV3	6,674960659	7,768192665
238441_at	PRKAA2	6,142085083	7,146812842
205139_s_at	UST	8,020870222	9,330637416
231205_at	NA	6,469873099	7,526095896
227514_at	ITPRIPL2	8,360927348	9,724669806
240642_at	ZMYM2	4,143264931	4,818867389
218880_at	FOSL2	6,392947712	7,433826677
231383_at	NA	4,053336515	4,712008814
209626_s_at	OSBPL3	7,89282148	9,174625568
226217_at	SLC30A7	8,617531123	10,01547823
236166_at	LOC285147	5,573310659	6,476262905
225868_at	TRIM47	7,2191991	8,388293357
205057_s_at	IDUA	4,330947719	5,032117935
227440_at	ANKS1B	5,138432875	5,969738152
235494_at	LSAMP	9,477331282	11,00908783
214874_at	PKP4	4,822308342	5,599732815
225354_s_at	SH3BGR2	6,773729372	7,865302486
37547_at	BBS9	6,055237106	7,030582924
1563941_at	NA	3,605851763	4,186203191
236153_at	NA	6,701110355	7,77869942
235989_at	NA	6,790971338	7,880930275
212239_at	PIK3R1	8,646753344	10,02656724
204964_s_at	SSPN	7,253827979	8,408295901
239995_at	NA	6,582831837	7,630097503
218940_at	VCPKMT	8,179167208	9,478826093
212122_at	RHOQ	6,826253799	7,910741045
205059_s_at	IDUA	6,506722696	7,54036966
216869_at	PDE1C	6,403866372	7,420859517
227812_at	TNFRSF19	9,590874825	11,11205991
219195_at	PPARGC1A	7,201923814	8,343219953
229685_at	LOC10013493 7	5,295779935	6,134564361
205574_x_at	BMP1	6,228459507	7,213129237
1562848_at	IST1	5,515058074	6,384219701
202687_s_at	TNFSF10	4,233722287	4,900235632
202363_at	SPOCK1	9,984997288	11,55640319
1559096_x_at	FBXO9	7,470528317	8,646210393
218816_at	LRRC1	7,02860414	8,134727505
1558944_at	CACNA1A	5,808480635	6,721177216
236016_at	SMARCE1	6,097830466	7,055346743
223568_s_at	PPAPDC1B	7,590155759	8,780844947
210611_s_at	DTNA	6,48240075	7,499288842
1553221_at	ZNF583	6,559870889	7,587177066
222736_s_at	TMEM38B	7,879721626	9,111914685
219923_at	TRIM45	6,417562681	7,420485308
213683_at	ACSL6	4,523675957	5,230208529
227792_at	ITPRIPL2	10,0301523	11,59399688
229435_at	GLIS3	9,082109914	10,49546943
236344_at	PDE1C	7,627195177	8,813020678
238519_at	NA	6,996402464	8,083845016
229796_at	SIX4	6,615781897	7,64251457
160020_at	MMP14	8,624476114	9,962608182
219511_s_at	SNCAIP	7,787471216	8,994525733
215921_at	NA	5,75941814	6,651995911
232231_at	RUNX2	6,493492069	7,499067154
226641_at	ANKRD44	6,932923217	8,005941391
227282_at	PCDH19	9,023328245	10,41831483

228359_at	UBASH3B	5,71624819	6,596624368
227892_at	PRKAA2	6,163759358	7,112643054
234111_at	ZNF81	7,367781409	8,501567399
213938_at	ERC2	3,776083014	4,355732318
204963_at	SSPN	8,208174277	9,466559395
226931_at	TMTC1	6,777811766	7,815986205
241731_x_at	ZNF440	6,413654148	7,394951937
205138_s_at	UST	4,778675779	5,508695573
228454_at	LCOR	7,758171472	8,942498255
222687_s_at	ACER3	6,958680005	8,019757664
228879_at	NA	6,874096061	7,92183276
226238_at	MCEE	6,732544701	7,758505888
1555967_at	NA	6,692323347	7,711261119
222552_at	GOLT1B	9,024672591	10,39645024
242852_at	LOC285147	4,896560176	5,640539532
219617_at	CAMKMT	7,487356655	8,62461614
228608_at	NALCN	4,568227299	5,261800633
235756_at	NA	6,552906563	7,547702464
237320_at	FAM71F2	4,598417362	5,296032331
203505_at	ABCA1	8,828891124	10,16826755
1555968_a_at	NA	6,863819352	7,905071601
213273_at	TENM4	7,581713906	8,729079043
223319_at	GPHN	8,889606479	10,23230232
228853_at	STYX	7,704947969	8,868519144
226534_at	KITLG	6,90289649	7,943706003
239951_at	NA	6,905957991	7,944573603
227449_at	EPHA4	7,043047498	8,100381768
206073_at	COLQ	4,80833574	5,529965503
207563_s_at	OGT	7,395320105	8,5009134
226150_at	PPAPDC1B	8,643048997	9,935016309
239161_at	FDX1	5,762252403	6,623119324
222656_at	UBE2W	8,511219848	9,782166568
226802_s_at	BMS1P20	7,907006015	9,085859481
232612_s_at	ATG16L1	6,594471704	7,577613228
235610_at	ALKBH8	6,643402039	7,633136267
226932_at	SSPN	7,809518224	8,970256485
204573_at	CROT	8,728392321	10,02268429
212390_at	NA	7,054499082	8,099190333
1554915_a_at	PDE12	6,244285119	7,168955138
234941_s_at	GPHN	6,947145713	7,975891492
228074_at	ITPR1L2	5,987456946	6,873965606
44783_s_at	HEY1	10,31657337	11,84403
205846_at	PTPRB	3,632178701	4,169846763
241459_at	NA	5,69971	6,543343611
225660_at	SEMA6A	10,07784413	11,56182227
227103_s_at	ECE2	5,261299496	6,03593537
226520_at	LCOR	7,148986761	8,200349592
228731_at	GUCY1A2	7,116105038	8,162389109
216711_s_at	TAF1	6,423944815	7,367987722
204686_at	IRS1	6,979631242	8,00491643
201124_at	ITGB5	5,546356382	6,360195555
232478_at	MIR181A2H G	6,819277953	7,81890001
237680_at	NA	4,453741711	5,105067902
219853_at	FKRP	6,119822254	7,014560632
220334_at	RGS17	8,543392569	9,792262274
228471_at	ANKRD44	6,519591864	7,472055628

233587_s_at	SIPA1L2	8,767061306	10,04717495
210756_s_at	NOTCH2	7,863488709	9,010073427
207265_s_at	KDEL3	7,401574134	8,476119191
235655_at	NA	5,975543682	6,840846163
239991_at	NA	5,937537831	6,794922966
238466_at	NA	7,11721614	8,142645763
235369_at	C14orf28	6,767999055	7,73977135
242405_at	NA	6,244983291	7,140262057
236458_at	NA	6,209339414	7,098745752
226754_at	ZNF251	6,887494383	7,873122737
216682_s_at	SUPT20H	5,684438675	6,497858482
219632_s_at	NA	5,389465281	6,157956873
228948_at	EPHA4	6,585561265	7,523338339
238647_at	C14orf28	5,80754295	6,634127415
209909_s_at	TGFB2	8,711896265	9,950608097
221986_s_at	KLHL24	7,243541845	8,272863616
242056_at	TRIM45	7,099996467	8,108189696
218113_at	TMEM2	9,828509025	11,2231942
219367_s_at	NRP2	6,201168741	7,080527794
226784_at	TWISTNB	8,812553479	10,06152033
226109_at	C21orf91	8,948808966	10,21540536
219592_at	MCPH1	5,573882217	6,361619721
201367_s_at	ZFP36L2	5,942709875	6,782226415
236600_at	SPG20	6,036229268	6,888377677
214130_s_at	NA	5,538539363	6,320315851
205841_at	JAK2	5,788973707	6,604791689
212400_at	FAM102A	7,53925798	8,599559828
1552455_at	PRUNE2	5,996040258	6,838161872
243068_at	NA	4,393676341	5,010331604
219540_at	ZNF267	6,843542029	7,803770965
201847_at	LIPA	9,040704823	10,30821118
223063_at	C1orf198	8,728988856	9,952297516
213082_s_at	SLC35D2	6,811594474	7,76604165
217097_s_at	PHTF2	6,693865285	7,63179244
201939_at	PLK2	10,19773007	11,62248279
212488_at	COL5A1	7,868503902	8,966745684
220954_s_at	NA	7,383366421	8,413707122
201108_s_at	THBS1	5,079588642	5,788436505
235664_at	NA	5,63250333	6,418461938
230707_at	SORL1	5,069532268	5,776399061
205097_at	SLC26A2	7,786754158	8,872452287
225658_at	SPOPL	8,078333931	9,2039771
223695_s_at	ARSD	6,22306456	7,090099872
238568_s_at	NPC1	5,235277964	5,963974581
238617_at	KIF26B	7,519506737	8,566059343
210510_s_at	NRP1	6,331160631	7,21095627
227409_at	PPP1R3E	6,188482031	7,047853087
204017_at	KDEL3	7,977523113	9,085066197
212806_at	PRUNE2	6,611476113	7,529342816
231838_at	PABPC1L	6,607321398	7,524249824
227816_at	NTN1	7,904711307	9,001322529
212307_s_at	OGT	8,583413277	9,771619169
215920_s_at	NA	5,589098356	6,36244642
226122_at	PLEKHG1	8,515699957	9,693283173
204624_at	ATP7B	5,455296705	6,209514786
1567706_at	NA	4,982076121	5,670775505



203974_at	PUDP	8,449766498	9,616587294
205933_at	SETBP1	6,93479059	7,891468445
214841_at	CNIH3	9,632802979	10,96103264
242250_at	NA	3,286592612	3,73896021
225159_s_at	ELK4	8,680897952	9,875472235
206022_at	NDP	9,219351078	10,48784634
238918_at	NA	5,172556965	5,884217104
221039_s_at	ASAP1	9,47301086	10,77615005
212812_at	SERINC5	8,43270339	9,592194493
240867_at	NA	6,054672853	6,887152781
239431_at	NA	6,545693395	7,445276738
228369_at	CNPY3	6,49832172	7,390372352
212703_at	TLN2	5,57383676	6,337751592
225780_at	NA	8,185446231	9,305429704
236835_at	FUT8-AS1	3,127743756	3,555276526
219740_at	VASH2	6,057770464	6,885731799
226069_at	PRICKLE1	6,030579941	6,85475913
214913_at	ADAMTS3	8,309509648	9,443664998
202063_s_at	SEL1L	4,285280351	4,869676036
226742_at	SAR1B	9,642835366	10,95759889
214831_at	ELK4	6,048557718	6,872943862
232001_at	PRKCQ-AS1	5,830320779	6,624921549
1559691_at	NA	4,163998143	4,731014058
235012_at	LRCH1	6,39670764	7,267737082
243023_at	NA	5,871048231	6,669645229
236090_at	NA	6,435422777	7,310297508
242722_at	LMO7	6,716418735	7,628925722
230152_at	CFAP44	6,831952211	7,759633117
238823_at	FMNL3	4,830427286	5,486307738
227973_at	C2orf69	8,559564235	9,720997393
238929_at	SRSF8	6,206075835	7,047954203
242751_at	NA	5,889299869	6,6852874
1559134_a_at	NA	3,939672529	4,472068908
206172_at	IL13RA2	9,471612922	10,75152148
213737_x_at	GOLGA8N	8,448948219	9,58978228
226694_at	NA	7,851050131	8,91074694
213930_at	ATG12	7,450415959	8,456023766
222094_at	NA	5,17568519	5,87407236
204156_at	SIK3	7,251520422	8,228611817
238825_at	ACRC	6,130201941	6,955232858
1559412_at	MIR99AHG	6,458564449	7,326775956
206380_s_at	CFP	3,982400989	4,517733692
218168_s_at	ADCK3	6,927140209	7,858221484
219042_at	LZTS1	8,448618432	9,583509841
205258_at	INHBB	7,722789305	8,760126237
232235_at	DSEL	9,782914764	11,09615941
202158_s_at	CELF2	8,966037499	10,16891271
228305_at	ZNF565	6,879155601	7,801405924
230719_at	ING3	5,751706197	6,522495379
213126_at	MED8	7,704467819	8,734982562
205399_at	DCLK1	9,692546363	10,98840539
1557521_a_at	NA	5,674193369	6,431392117
205530_at	ETFDH	7,282052455	8,253215868
209506_s_at	NA	7,882300883	8,933277817
232967_at	NA	4,12290416	4,672424752
227022_at	GNPDA2	7,700669429	8,726668665
211965_at	ZFP36L1	6,283071955	7,119923331
208733_at	RAB2A	5,394828516	6,11310908
244533_at	PTPN14	6,641384294	7,52563138
204700_x_at	DIEXF	6,911389209	7,830550752
225056_at	SIPA1L2	9,586795971	10,86044028
217279_x_at	MMP14	7,932103997	8,985896696
227351_at	NA	8,119945799	9,198378462
242825_at	LPPR5	6,89702072	7,813013539
213435_at	SATB2	9,601535301	10,8766145
1568611_at	NA	7,058589757	7,993976931
228661_s_at	LOC102606465	7,650784981	8,660174006
227688_at	LRCH2	7,474231263	8,460144279
213278_at	MTMR9	7,941529713	8,988104066
242738_s_at	ZFH3	7,81103248	8,839203568
222802_at	EDN1	4,107939546	4,648459525
212829_at	PIP4K2A	7,636982673	8,640241387
205020_s_at	ARL4A	8,887229235	10,05351247
226322_at	TMTC1	7,85887113	8,888143076
236908_at	NA	5,563585076	6,291025761
1555372_at	BCL2L11	6,806583977	7,696436159
202341_s_at	TRIM2	9,461391337	10,69787181
1560297_at	NA	6,926963239	7,829923582
233490_at	DCTN4	4,014985811	4,538344841
219514_at	ANGPTL2	5,472199457	6,184052704
220301_at	CCDC102B	6,601748529	7,459411037
205294_at	BAIAP2	7,070096512	7,98770573
224790_at	ASAP1	9,467735843	10,69214059
1569464_at	PPF1BP1	4,421327251	4,992988826
213247_at	SVEP1	5,152537282	5,816916597
33494_at	ETFDH	8,022970252	9,057082591
226492_at	SEMA6D	11,50813518	12,991111144
217875_s_at	PMEPA1	8,398666585	9,48073422
244786_at	NA	6,030544736	6,806524868
210858_x_at	ATM	7,108828411	8,02205735
209201_x_at	CXCR4	10,22646567	11,53997919
202375_at	SEC24D	7,377007328	8,323613402
244687_at	DBT	7,031454371	7,932988652
227080_at	ZNF697	7,787677865	8,785978093
236640_at	NA	6,283829333	7,088651609
225942_at	NLN	7,071243886	7,976096177
228482_at	NA	5,681311497	6,4075184
242380_at	NA	5,188670665	5,851691311
239038_at	C1orf52	6,076208271	6,852536377
240216_at	NA	6,472468829	7,298985317
209147_s_at	PPAP2A	8,602620707	9,695425938
228656_at	PROX1	8,739471239	9,848644489
218972_at	TTC17	7,345606339	8,275171562
243462_s_at	NA	7,202010533	8,113311011
204157_s_at	SIK3	7,50705167	8,456792743
220941_s_at	C21orf91	6,167097502	6,947125541
207826_s_at	ID3	11,22331045	12,64239911
61734_at	RCN3	6,536855316	7,363255147
201929_s_at	PKP4	7,203606434	8,114273743
213197_at	ASTN1	7,647433537	8,61364299
232615_at	NA	6,287949826	7,081657913
204360_s_at	NAGLU	7,713313866	8,686704355

230496_at	AMER2	9,21301801	10,37450037
235328_at	PLXNC1	4,470059855	5,033269675
205000_at	DDX3Y	9,75841126	10,98730082
237833_s_at	SNCAIP	6,659587778	7,497290306
238760_at	YARS	5,514731021	6,207851477
211919_s_at	CXCR4	10,33619432	11,63514922
221185_s_at	IQCG	8,426338803	9,485173098
205001_s_at	DDX3Y	9,437249808	10,62210516
230480_at	PIWIL4	5,42909549	6,110136722
204837_at	MTMR9	8,731343828	9,825560106
211488_s_at	ITGB8	7,400340195	8,325624944
230987_at	NA	4,7884074	5,386128101
222688_at	ACER3	7,948862793	8,934898142
220407_s_at	TGFB2	8,161410353	9,173748835
216611_s_at	SLC6A2	5,879829885	6,609055734
201369_s_at	ZFP36L2	6,974459438	7,838800669
49485_at	PRDM4	7,749119088	8,70846728
243303_at	NA	5,669506552	6,371353245
220319_s_at	MYLIP	6,181006208	6,945641403
202565_s_at	SVIL	9,662505044	10,85657716
207390_s_at	SMTN	5,476894546	6,15235389
238002_at	GOLIM4	8,945427866	10,04661626
228218_at	LSAMP	10,14356043	11,39165381
228284_at	TLE1	9,206140147	10,33801647
202946_s_at	BTBD3	10,69091711	12,0032914
230144_at	GRIA3	9,248126847	10,38098461
232825_s_at	DSEL	6,951750394	7,80286159
1558569_at	LOC100131541	5,887742249	6,608456673
242119_at	PROX1	5,862532838	6,579775782
1570227_at	NA	4,451354934	4,995479849
204094_s_at	TSC22D2	9,263367125	10,39560815
206320_s_at	SMAD9	5,248100019	5,889546014
212902_at	SEC24A	6,066770328	6,807757822
216733_s_at	GATM	9,290908301	10,42541812
229962_at	LRRC37A3	6,138717371	6,88826132
228718_at	ZNF44	6,810360517	7,64152438
226938_at	DCAF4	7,162782736	8,036772017
57516_at	ZNF764	7,440416772	8,347316938
227504_s_at	MED28	6,667211275	7,47983176
230885_at	NA	7,201266129	8,078614632
225528_at	IPO8	10,12106063	11,35376607
1553720_a_at	AMER2	7,979592333	8,95034247
1563881_at	MAGI1	5,289721087	5,932110081
223506_at	ZC3H8	7,845326548	8,797644457
222449_at	PMEPA1	9,174125748	10,28769139
203184_at	FBN2	10,96907503	12,29993412
213341_at	FEM1C	8,40440089	9,421569853
232274_at	CCNL2	6,214134634	6,966159136
229549_at	CALU	8,620711229	9,66210881
242550_at	EIF3B	6,573197453	7,366022161
219240_s_at	C10orf88	7,549326384	8,459315594
235250_at	FLCN	5,813920261	6,513422441
226211_at	MEG3	8,216134686	9,203517934
228594_at	NADK2	8,838335721	9,900429655
226384_at	PPAPDC1B	8,327580556	9,327049808
226773_at	PPM1K	7,488684693	8,386756572
218590_at	C10orf2	7,162333764	8,019616228
239794_at	NA	5,139123014	5,753190081
37079_at	NUS1P3	5,577144999	6,243392812
228904_at	HOXB3	8,891810937	9,953618936
222690_s_at	TMEM39A	7,232881237	8,095904462
226354_at	LACTB	7,530460037	8,427754084
230906_at	GALNT10	5,355398103	5,993458689
210946_at	PPAP2A	8,559827918	9,577131042
226208_at	ZSWIM6	9,652610697	10,79953698
214952_at	NCAM1	5,629028189	6,297799785
205371_s_at	DBT	6,45581867	7,222789995
233482_at	C15orf59	6,365703313	7,121488003
205283_at	FKTN	7,76640064	8,686740432
241342_at	TMEM65	7,793005657	8,714293329
231940_at	ZNF529	8,21283477	9,18154588
218501_at	ARHGEF3	8,137900964	9,097093568
229228_at	NA	8,617581043	9,630005004
214772_at	KIAA1549L	8,20261373	9,16496059
229299_at	NADK2	8,11008621	9,061186298
219284_at	HSPBAP1	7,061651632	7,889625977
203178_at	GATM	9,368131838	10,46633117
226345_at	ARL5B	8,482277759	9,475779367
218740_s_at	CDK5RAP3	9,082645203	10,14399926
44790_s_at	KIAA0226L	7,470527393	8,343445323
242753_x_at	APIAR	3,9792771	4,443896626
226795_at	LRCH1	7,944732082	8,869006037
209286_at	CDC42EP3	7,790678567	8,696493328
213127_s_at	MED8	8,237015729	9,194225055
227708_at	EEF1A1	8,113390454	9,050509826
228973_at	DLG2	4,643301742	5,181388082
226017_at	CMTM7	8,261641663	9,218825023
212693_at	MDN1	7,967568738	8,89062488
238642_at	ANKRD13D	7,001128553	7,811925831
203365_s_at	MMP15	6,964502655	7,770663696
224015_s_at	MRPS25	6,612341841	7,376821203
244354_at	STRN	7,286012076	8,128252305
204435_at	NUP58	8,097092905	9,032031112
204589_at	NUAK1	9,181798822	10,24050078
223482_at	TMEM120A	8,089722615	9,019829096
221605_s_at	PIPOX	8,468402422	9,441933993
225640_at	EBLN3	7,948011518	8,861522752
210357_s_at	SMOX	8,30555579	9,259640351
227764_at	LYPD6	6,64470986	7,407974105
213116_at	NEK3	7,116470312	7,93196835
226065_at	PRICKLE1	7,247297961	8,077182068
214761_at	ZNF423	10,62225997	11,83784066
239834_at	NA	5,806741343	6,470551344
228104_at	PLXNA4	8,657934061	9,646278877
219917_at	ZCCHC4	5,931275779	6,608254221
202723_s_at	FOXO1	7,652805076	8,526263185
1555680_a_at	SMOX	6,117875438	6,815042375
230384_at	ANKRD23	5,689541725	6,337781206
225635_s_at	EBLN3	7,044821871	7,846978369
235127_at	PMP2	10,16608084	11,32246311
219102_at	RCN3	6,061856021	6,751038926
220735_s_at	SENP7	6,463007995	7,197482229

224692_at	PPP1R15B	8,719837866	9,710243981
204518_s_at	PPIC	9,014779927	10,03861777
225381_at	MIR100HG	9,77694238	10,88691887
203220_s_at	TLE1	6,160296021	6,859614582
204807_at	TMEM5	7,514947698	8,367522098
225537_at	TRAPPC6B	8,393352238	9,345360157
209184_s_at	IRS2	8,781245852	9,776385544
235320_at	ARL6	6,962523702	7,751511489
1553743_at	METTL21A	7,971643673	8,874749178
232626_at	NA	4,270584914	4,75351394
65588_at	SNHG17	8,040885423	8,949887106
203222_s_at	TLE1	7,914654731	8,809256613
225899_x_at	NA	7,476684181	8,319927154
227036_at	RASAL2	8,254083984	9,184188472
226419_s_at	SRSF1	7,830843041	8,713029973
1555970_at	FBXO28	6,941996795	7,722132711
226352_at	JMY	8,81741592	9,804550321
1556227_at	VCPIP1	5,22278284	5,807375425
206303_s_at	NA	7,197452298	8,002873894
228950_s_at	WLS	8,709277905	9,683330954
227776_at	ACER3	9,389242273	10,43592283
223325_at	TXNDC11	6,500479599	7,224548248
202897_at	SIRPA	8,700931541	9,669917057
242506_at	NA	4,837882388	5,375640578
1555938_x_at	VIM	6,491018233	7,211813859
226137_at	ZFH3	8,630047768	9,587836357
219182_at	NA	7,383576243	8,202640194
236706_at	LYG1	6,13366228	6,813848201
219522_at	FJX1	9,233094658	10,2558027
227135_at	NAAA	7,075438885	7,858721429
229319_at	NA	7,730388294	8,586080003
210091_s_at	DTNA	7,170026061	7,962829239
227520_at	TXLNG	7,962028012	8,840365118
215364_s_at	SZT2	6,663321332	7,396912914
209457_at	DUSP5	7,201266902	7,994066931
206302_s_at	NA	8,144901194	9,041356248
225752_at	NIPA1	7,658326342	8,500732083
227875_at	KLHL13	8,276568043	9,185876072
201344_at	UBE2D2	7,662715698	8,504175423
1554450_s_at	MIER3	8,220510242	9,12195476
218329_at	PRDM4	8,746989739	9,706029108
224796_at	ASAP1	10,56913121	11,72769331
214803_at	CDH6	7,256257692	8,051144243
213517_at	PCBP2	8,077122744	8,961868899
213459_at	RPL37A	6,721883383	7,457658041
243365_s_at	AUTS2	4,693608095	5,20662258
226946_at	NADK2	8,493983043	9,422013447
227599_at	MB21D2	6,572820317	7,289738365
220943_s_at	NDUFAF7	7,133856433	7,909960798
1561749_at	NA	6,133537981	6,800316318
216199_s_at	MAP3K4	8,87437375	9,838420279
217921_at	MAN1A2	6,050722654	6,707724702
205931_s_at	NA	8,378871423	9,287830203
225366_at	PGM2	7,53640274	8,353579451
212327_at	LIMCH1	8,987423882	9,961611652
1553612_at	ZNF354B	6,323656763	7,008673117

238948_at	TM9SF1	6,393212919	7,085362896
214696_at	NA	7,852225905	8,701649653
227805_at	METAP1D	7,566501006	8,384018225
219118_at	FKBP11	6,386209684	7,075297839
223569_at	PPAPDC1B	7,601414694	8,421413934
226635_at	EBLN3	8,485781149	9,400286766
232910_at	BBIP1	3,764167779	4,169717301
202057_at	KPNA1	6,9444596	7,690931786
226463_at	ATP6V1C1	8,359892606	9,257894716
209383_at	DDIT3	8,322297275	9,216027056
228569_at	PAPOLA	8,336947705	9,232053317
218193_s_at	GOLT1B	8,615954399	9,540530341
231823_s_at	SH3PXD2B	9,270300315	10,26497008
1554774_at	MINA	6,555545474	7,25877055
228172_at	TTL11	6,178170684	6,839889483
238172_at	NA	5,55369789	6,148344258
234734_s_at	TNRC6A	8,79310496	9,733635234
1556555_at	LOC100129461	5,441978097	6,02403679
223580_at	SPSB2	6,62741652	7,335900015
203123_s_at	SLC11A2	8,335202313	9,224526073
218678_at	NES	10,48536614	11,60161705
202370_s_at	CBFB	10,11551961	11,19222165
217028_at	CXCR4	11,26274162	12,46115877
239872_at	NA	4,552104266	5,036468455
230209_at	ZXDC	5,731647154	6,341236136
203124_s_at	SLC11A2	8,717211698	9,644153721
204089_x_at	MAP3K4	8,05464552	8,908291729
219397_at	COQ10B	9,081814574	10,04418289
244414_at	NA	6,851832011	7,577444494
213960_at	NTRK3	5,996447574	6,631407539
1569054_at	SLC1A3	6,64447628	7,347607059
227354_at	PAG1	7,92768253	8,766073837
222258_s_at	SH3BP4	10,64270479	11,76768812
227001_at	NIPAL2	5,987424343	6,61997992
218998_at	FAM206A	8,088761229	8,943099257
233264_at	NA	4,721586337	5,21936494
239544_at	NA	5,162660351	5,706046972
243816_at	ZNF70	6,671492075	7,373443855
224932_at	CHCHD10	9,158593247	10,12208716
226542_at	RNF24	8,333508842	9,20879064
226410_at	CTU2	6,339328197	7,005109054
1558292_s_at	PIGW	7,369131591	8,142428151
225869_s_at	UNC93B1	5,101342646	5,635972946
223594_at	TMEM117	7,678860713	8,482956501
223233_s_at	CGN	5,914634253	6,533090658
203637_s_at	MID1	9,12503748	10,07901133
221427_s_at	CCNL2	9,142907489	10,09836922
214331_at	TSFM	6,100647948	6,737145266
214722_at	NOTCH2NL	9,117335498	10,06787033
226870_at	COMTD1	5,664045886	6,2527954
243256_at	MKNK1	6,348737435	7,007952049
229713_at	PIP4K2A	6,960378031	7,682446667
226344_at	ZMAT1	7,463573095	8,23580993
206481_s_at	LDB2	9,334842434	10,29935639
213455_at	FAM114A1	8,800529089	9,709451681
200661_at	CTSA	10,12196685	11,16731894

225857	s at	SNHG17	8,396619505	9,263734068	219801	at	ZNF34	6,377240845	7,007559503
1557954	at	TXLNG	6,965064106	7,682522081	222450	at	PMEPA1	10,04212542	11,03307698
210123	s at	NA	6,203107383	6,841365292	226766	at	ROBO2	8,661018832	9,515473854
226782	at	SLC25A30	8,820134675	9,727264676	224791	at	ASAP1	11,17415025	12,27549615
1558458	at	LOC401320	6,174323231	6,809257505	212328	at	LIMCH1	9,145288195	10,04647435
214683	s at	CLK1	9,845913402	10,85574374	232852	at	NA	5,902043731	6,483628574
211467	s at	NFIB	9,253054855	10,20082777	238540	at	LOC401320	6,678486914	7,335706787
239283	at	TMED5	5,914644188	6,519375121	227517	s at	NA	9,104061609	9,999857672
204307	at	TECPR2	6,465544379	7,126488858	235486	at	KIAA1549L	8,828814141	9,69634867
228797	at	NLN	8,186956765	9,023758787	220750	s at	P3H1	8,338778124	9,157733265
203988	s at	FUT8	9,247880391	10,19310566	219218	at	BAHCC1	6,71552125	7,374315205
212695	at	CRY2	7,022067903	7,739116195	234993	at	ABHD13	6,291936966	6,909160888
230296	at	NA	9,039520043	9,960981955	227129	x at	LINC01000	7,510866869	8,247547114
204568	at	ATG14	8,075764475	8,898961251	227126	at	PTPRG	10,59288779	11,63151779
227037	at	NA	7,561225092	8,331087276	220974	x at	SFXN3	9,078677939	9,968180612
244433	at	NA	6,427006159	7,080694026	227889	at	LPCAT2	7,911916911	8,686195542
217226	s at	SFXN3	9,040641319	9,958858951	200766	at	CTSD	7,25944066	7,969255619
209711	at	SLC35D1	8,30017426	9,141651318	229001	at	PPP1R3E	7,241544581	7,949541614
206183	s at	NA	5,270227094	5,804507704	1552287	s at	AFG3LIP	8,388029862	9,207824681
226210	s at	MEG3	9,21506721	10,14924084	240452	at	GSPT1	6,370822514	6,991840816
207564	x at	OGT	8,566114297	9,434331921	229366	at	NA	7,407868398	8,129688032
219351	at	TRAPPC2	8,470016849	9,328346671	209501	at	NA	8,156615089	8,951340259
212377	s at	NOTCH2	9,971633375	10,98163281	230492	s at	GPCPD1	7,91460076	8,685179804
224911	s at	DCBLD2	10,20027883	11,23287156	228716	at	THRB	6,489675017	7,121197564
201219	at	CTBP2	7,284778567	8,022164166	221974	at	NA	8,962059811	9,834039292
47550	at	LZTS1	9,374948559	10,32368413	228216	at	ZBTB37	6,937931297	7,61236507
1558027	s at	PRKAB2	7,318528897	8,057267734	212325	at	LIMCH1	7,746969819	8,49983893
228611	s at	NA	7,160604885	7,882879964	225704	at	FBRSL1	6,956080701	7,63173122
214703	s at	MAN2B2	7,958776026	8,7615026	207373	at	HOXD10	7,453306422	8,176849465
232278	s at	DEPDC1	7,999843061	8,806437642	232489	at	TRMT13	7,671992693	8,416420421
203623	at	PLXNA3	6,518691411	7,175874322	209712	at	SLC35D1	8,657731285	9,495385507
225861	at	FAM195A	7,387530815	8,132287665	244007	at	ZNF462	8,42632103	9,241423558
241700	at	ZFHX4	8,265793009	9,098828889	204493	at	BID	9,68100724	10,61622484
206788	s at	CBFB	7,989555273	8,794058065	222453	at	CYBRD1	9,000041682	9,869278838
239313	at	LOC401320	6,661216093	7,33136578	216264	s at	LAMB2	7,735237628	8,482129472
204082	at	PBX3	9,538280681	10,49770768	213624	at	SMPDL3A	9,088777446	9,963715948
238565	at	NA	6,247145614	6,875064363	212194	s at	TM9SF4	8,316517682	9,1169516
226203	at	MYO9A	7,929372613	8,726293116	214895	s at	ADAM10	7,903205495	8,662683454
1554455	at	LINS1	6,764287015	7,443643549	212593	s at	NA	7,650167842	8,384903549
208070	s at	REV3L	10,46497852	11,51577218	218204	s at	FYCO1	7,947695729	8,710901965
227594	at	ZMYM6	7,317221105	8,051445619	235410	at	NPHP3	8,108366033	8,885593731
224221	s at	VAV3	4,771672027	5,250221094	234317	s at	STOX2	7,073431918	7,751260318
220500	s at	NA	5,909759384	6,501266899	227143	s at	BID	10,30787663	11,29529797
231923	at	TMEM150C	5,813327112	6,395156647	229164	s at	ABTB1	5,883830551	6,447313598
210469	at	DLG5	5,127739777	5,640521391	220476	s at	NA	7,849158596	8,600343705
235414	at	ZNF383	6,215481536	6,836722253	238974	at	C2orf69	10,12390318	11,09192732
212946	at	VWA8	8,205207388	9,024837321	237449	at	SP8	10,50111919	11,50462632
238656	at	RAD50	6,725498894	7,396943109	235713	at	ALKBH8	6,524628058	7,147975381
228032	s at	DENND1B	6,169134185	6,784263402	212192	at	KCTD12	9,547221447	10,45898204
235361	at	STAMPB	6,205994645	6,82421743	240616	at	NA	7,139891576	7,821447833
203199	s at	MTRR	7,248214763	7,968934003	214668	at	SPRYD7	6,213933125	6,80696131
201075	s at	SMARCC1	8,329099638	9,156206321	229253	at	THEM4	7,315176287	8,012787731
235926	at	ANAPC5	6,553333924	7,20365092	231975	s at	MIER3	8,322525275	9,116185295
212356	at	KHNYN	7,975837775	8,765583779	211725	s at	BID	9,95159046	10,89798157
235692	at	SH3KBP1	7,313790699	8,036904008	201928	at	PKP4	8,515275657	9,323394614
228476	at	KIAA1407	7,016055386	7,709631235	231969	at	STOX2	7,490293509	8,200979364

227109_at	CYP2R1	7,472365669	8,181167592
1554479_a_at	CARD8	8,49693678	9,301353057
227264_at	TRAF6	7,289913707	7,979799711
211219_s_at	LHX2	8,506026755	9,310862416
202443_x_at	NOTCH2	10,60496491	11,60817647
202156_s_at	CELF2	8,57664119	9,387962276
230097_at	GART	6,624411353	7,250694696
212805_at	PRUNE2	9,962619001	10,90417754
219837_s_at	CYTL1	8,814859957	9,647695995
203224_at	RFK	9,39674056	10,28372016
1554863_s_at	DOK5	9,902272965	10,83647176
228961_at	MIER3	9,2094288	10,07762979
222653_at	PNPO	7,571622194	8,284048374
204027_s_at	METTL1	6,945874424	7,597597856
222696_at	AXIN2	7,057426021	7,719259455
226975_at	RNPC3	7,617570592	8,331033042
222235_s_at	CSGALNAC T2	7,852024149	8,586628177
224414_s_at	CARD6	6,251940735	6,835754108
222720_x_at	C1orf27	5,197229088	5,682422072
242919_at	NA	7,831089849	8,562096593
226104_at	RNF170	8,709724507	9,522536059
209196_at	WDR46	7,740011929	8,462035066
233082_at	ZNF630	7,453090599	8,148192225
1554341_a_at	HELQ	6,55611455	7,166736504
1553113_s_at	CDK8	7,869564845	8,601729094
214933_at	CACNA1A	9,562885454	10,4511205
201797_s_at	VARS	7,520754115	8,218881268
231837_at	USP28	6,850508685	7,486316461
204699_s_at	DIEXF	7,005888768	7,655694496
222999_s_at	CCNL2	10,62328564	11,60496391
232212_at	PLEKHA8	5,944092315	6,493346935
213124_at	ZNF473	7,344844847	8,022967803
202087_s_at	CTSL	8,611512127	9,406519352
202782_s_at	INPP5K	7,816600411	8,537856456
231087_at	NA	5,667950045	6,19033174
222518_at	ARFGEF2	7,945377184	8,677330472
219401_at	XYLT2	7,1935086	7,855833408
238847_at	HOXD10	9,003001536	9,831889433
219249_s_at	FKBP10	8,061847203	8,803895271
224233_s_at	MSTO1	6,897553842	7,530795922
213189_at	MINA	8,408809172	9,179321707
221867_at	N4BP1	7,454069342	8,136174643
228751_at	CLK4	8,538338145	9,318684508
1553725_s_at	ZNF644	7,167315707	7,821494124
235429_at	EIF3E	7,142236957	7,793989828
236436_at	SLC25A45	6,898489191	7,527811638
230294_at	RALY-AS1	5,777014604	6,304014163
222156_x_at	NA	7,36868395	8,040687234
203245_s_at	LINC00094	8,515054667	9,291477435
207417_s_at	NA	8,391064798	9,156133114
225321_s_at	NA	9,2563666	10,09953098
203119_at	CCDC86	7,958791822	8,681423379
244321_at	PGAP1	6,338972276	6,91429751
209294_x_at	TNFRSF10B	7,611575994	8,301115144
228029_at	ZNF721	8,801106394	9,597615853
213152_s_at	SRSF8	8,651204115	9,433509692

224162_s_at	FBXO31	7,748774243	8,445078833
202177_at	GAS6	7,034724105	7,666818037
201409_s_at	PPP1CB	10,8392831	11,81252428
1555562_a_at	ZCCHC7	6,048410792	6,590796571
228433_at	NFYA	7,555765111	8,232028742
217721_at	SEPT7	8,173624645	8,904980416
218456_at	CAPRIN2	9,758935697	10,63046656
229981_at	SNX5	6,562204591	7,148099346
227332_at	PXN-AS1	7,03384065	7,661513322
215207_x_at	NA	6,566494008	7,150760395
232406_at	NA	7,197491658	7,837606385
226261_at	ZNRF2	6,480003054	7,054757699
212915_at	PDZRN3	8,830675594	9,613638181
224826_at	GPCPD1	9,687426566	10,54574602
211475_s_at	BAG1	8,02051452	8,730770423
235413_at	GGCX	7,276812851	7,919854018
212672_at	ATM	8,643849743	9,407689515
227917_at	LOC10050699 0	8,246911662	8,974528279
213418_at	HSPA6	5,957948751	6,482369579
227055_at	METTL7B	7,71403748	8,391825472
225765_at	TNPO1	9,403939638	10,2283211
1553112_s_at	CDK8	7,026779514	7,642717672
228760_at	SRSF8	7,887817985	8,576384683
239377_at	EIF1AD	8,060557611	8,763168418
221958_s_at	WLS	10,32339094	11,22313655
1554456_a_at	LINS1	7,037333681	7,650382821
226885_at	RNF217	7,122258714	7,741430158
213188_s_at	MINA	8,718268414	9,475146587
201967_at	RBM6	8,962887436	9,740977152
239043_at	ZNF404	7,916057622	8,60240212
230637_at	SFXN4	6,298267824	6,844120578
226575_at	ZNF462	9,84061948	10,69216023
208999_at	SEPT8	9,547293585	10,37317027
211596_s_at	LRIG1	10,3253005	11,21798684
227882_at	FKRP	8,112871024	8,813735552
229373_at	NA	5,941858358	6,454906654
201393_s_at	IGF2R	10,47022085	11,37355572
212342_at	YIPF6	7,315772061	7,946876421
213034_at	SIK3	8,811608823	9,57174841
202781_s_at	INPP5K	7,445324731	8,086970373
219415_at	TTYH1	8,511285212	9,244379791
233487_s_at	LRRC8A	9,031282387	9,808907026
201408_at	PPP1CB	10,73525707	11,65854111
228013_at	PPP2R2A	7,983726435	8,669723324
200931_s_at	VCL	9,130830106	9,915355052
218587_s_at	POGLUT1	9,119648804	9,90310993
227191_at	ITFG1	8,194249206	8,897622333
226058_at	B3GNT9	7,478391735	8,119975054
235352_at	MR1	7,278194557	7,902336285
232113_at	NA	9,955437122	10,80795032
226628_at	THOC2	8,430412535	9,151773104
229654_at	NA	7,977034742	8,658905686
225766_s_at	TNPO1	9,718284113	10,54890833
225162_at	SH3D19	9,534878467	10,3493977
222681_at	POGLUT1	8,79771122	9,547749264
218706_s_at	GRAMD3	8,177008431	8,873649041

227465_at	MAU2	9,075850779	9,848442684
201041_s_at	DUSP1	8,26521669	8,968664451
222149_x_at	NA	6,991423339	7,585689459
208782_at	FSTL1	11,78955155	12,79140711
1563549_a_at	ANO8	7,49888526	8,135844167
212422_at	PDCD11	6,826135953	7,404581575
202368_s_at	TRAM2	9,334338633	10,12486375
239482_x_at	ZNF708	7,154502225	7,759426181
212732_at	MEG3	9,676077579	10,49364511
203221_at	TLE1	10,18781959	11,04750376
203878_s_at	MMP11	7,205772564	7,813397512
224615_x_at	HM13	8,656052149	9,385965951
1554547_at	FAM13C	7,299369676	7,914675669
234343_s_at	RASAL2	6,740829662	7,307464882
206826_at	PMP2	11,83542221	12,82870275
219779_at	ZFHx4	8,935181971	9,683970921
226615_at	XPR1	7,596306125	8,232496301
209704_at	MTF2	7,462980266	8,087801599
212341_at	YIPF6	10,05130874	10,89260629
201392_s_at	IGF2R	9,955701189	10,78842718
203286_at	RNF44	8,428720285	9,133297649
203502_at	BPGM	9,307344089	10,08427037
229608_at	NA	7,561847669	8,192758718
202724_s_at	FOXO1	8,051624163	8,723134485
235436_at	DDX31	6,00534071	6,505756914
204085_s_at	CLN5	9,125688557	9,884398652
221992_at	NPIP15	5,612628265	6,079113908
203944_x_at	BTN2A1	9,134719801	9,893914495
219802_at	PYROXD1	7,830162641	8,480869184
209815_at	PTCH1	8,647552035	9,365853957
202536_at	CHMP2B	8,234480765	8,917665626
223740_at	AGPAT4-IT1	6,841475827	7,408975479
209781_s_at	KHDRBS3	8,825466064	9,55710918
220235_s_at	LRIF1	8,703215539	9,42439867
226653_at	MARK1	8,051355359	8,718430883
225071_at	NUS1	9,134212343	9,890068969
210139_s_at	PMP22	11,48553437	12,43489568
219188_s_at	MACROD1	6,997087958	7,574766366
219027_s_at	MYO9A	7,852732628	8,501029438
212599_at	AUTS2	10,87512598	11,77271651
217627_at	ZNF573	8,613486592	9,32419011
243790_at	ZNF585A	7,069734016	7,652324669
225278_at	PRKAB2	8,466965363	9,163783097
204950_at	CARD8	6,845030022	7,406024976
233364_s_at	NA	9,543525809	10,3248492
209705_at	MTF2	7,59961434	8,220933462
212257_s_at	SMARCA2	7,934371297	8,582205215
204517_at	PPIC	10,51593416	11,37356749
219248_at	THUMP2	7,160065292	7,743269768
239289_x_at	FAN1	8,412039833	9,097179145
211038_s_at	CROCCP2	9,35249512	10,11371043
235195_at	FBXW2	7,925348042	8,569826018
230151_at	SPRYD7	6,943897112	7,50850089
36566_at	CTNS	7,215899142	7,802358265
1552508_at	KCNE4	8,913003891	9,636202058
227984_at	LMF1	8,360173521	9,037254482

214070_s_at	ATP10B	7,733536226	8,358476774
230012_at	LINC00324	6,061983711	6,551808481
227855_at	NA	5,28640227	5,712838691
223560_s_at	NDUFAF7	8,403281588	9,080869593
241825_at	TYW5	6,573741584	7,103590307
225286_at	ARSD	7,891686318	8,526510343
235233_s_at	GMEB1	6,81773087	7,365859681
202584_at	NFX1	6,891833418	7,444883808
217850_at	NA	9,643828711	10,41488396
218294_s_at	NUP50	8,983990296	9,701812471
202148_s_at	PYCR1	7,485880364	8,083823037
218826_at	SLC35F2	6,913338144	7,465434426
203280_at	SAFB2	6,401663879	6,912707764
213510_x_at	USP32P2	9,261778498	10,00072148
203231_s_at	ATXN1	8,2155092	8,8690516
228543_at	PET117	8,577457767	9,258929557
230741_at	P2RX7	7,171120798	7,739989961
204937_s_at	ZNF274	7,732070019	8,345400804
209185_s_at	IRS2	10,71320553	11,56243205
227401_at	IL17D	7,718044618	8,329737411
228960_at	ICE2	7,711949035	8,322613846
236989_at	NA	6,937347153	7,485903203
239225_at	NA	6,79358034	7,330417717
221194_s_at	NA	7,424722126	8,010682771
206544_x_at	SMARCA2	9,198725836	9,923428311
209105_at	NCOA1	7,584252168	8,181756747
222942_s_at	NA	9,280355828	10,01090357
224634_at	GPATCH4	8,184212156	8,827482132
213262_at	SACS	9,649853327	10,40804854
228571_at	RBAK	9,543398699	10,29320775
238087_at	RTCA	7,219193329	7,785687525
219247_s_at	ZDHHC14	7,079919482	7,634870969
225247_at	TMEM259	7,952361465	8,575382271
236194_at	NA	7,544369926	8,134819679
202278_s_at	SPTLC1	8,528275957	9,195526155
235077_at	MEG3	9,962310172	10,74141087
230176_at	UEVLD	8,624529104	9,298956029
218282_at	EDEM2	7,92655749	8,545392925
222550_at	ARMC1	10,21395719	11,00962328
229400_at	HOXD10	10,18087789	10,97337951
201074_at	SMARCC1	9,609579855	10,35720236
229303_at	SF3B1	8,001073796	8,62300191
226713_at	CCDC50	8,796094197	9,479612671
201944_at	HEXB	11,58061366	12,4794779
225997_at	MOB1B	9,527926156	10,26742409
223547_at	JKAMP	9,16898684	9,87976619
213785_at	IPO9	7,709051317	8,306571159
230185_at	THAP9	7,133102093	7,685900928
227122_at	ZNF791	7,627701749	8,218250224
229623_at	TMEM150C	7,233063776	7,79297869
227719_at	SMAD9	8,549799569	9,21088531
205613_at	SYT17	8,998348434	9,694055518
204472_at	GEM	9,265569853	9,981096457
235956_at	CEP126	7,58434925	8,169807579
212635_at	TNPO1	10,12321248	10,90452839
231779_at	IRAK2	7,522891821	8,10311471

204137_at	GPR137B	9,334856675	10,05368826	221727_at	SUB1	10,66398607	11,43121387
212181_s_at	NA	9,91610633	10,67869942	223124_s_at	PITHD1	9,884133676	10,59519656
212333_at	FAM98A	9,564883057	10,29948662	222478_at	VPS36	9,308123086	9,977314059
209295_at	TNFRSF10B	11,2783408	12,14446327	208937_s_at	ID1	11,42659838	12,24678561
1554234_at	KATNAL2	6,7642013	7,282880149	202923_s_at	GCLC	7,981317706	8,554191829
209585_s_at	MINPP1	8,699959604	9,366711071	219882_at	TTL7	7,659957682	8,2095386
236814_at	MDM4	8,871633684	9,549986268	213004_at	ANGPTL2	7,680590253	8,23085681
225957_at	CREBRF	7,694183741	8,281550257	203594_at	RTCA	9,7537592	10,45051602
229210_at	RNASEH2B	6,101892289	6,567634089	207876_s_at	FLNC	8,694870407	9,315830358
211962_s_at	ZFP36L1	9,200216102	9,901768552	208290_s_at	EIF5	10,0546137	10,77167714
212920_at	REST	8,648176356	9,307598321	219132_at	PEL12	8,686631935	9,304794229
222136_x_at	NA	8,683166023	9,344969876	227823_at	RGAG4	6,972682569	7,468732811
201069_at	MMP2	11,74737729	12,6427142	203423_at	RBP1	9,244392398	9,902026762
211212_s_at	ORC5	8,141762943	8,76067021	227268_at	RNFT1	8,388750345	8,985196538
1553118_at	THEM4	7,84672784	8,442512733	226409_at	TBC1D20	9,502206551	10,17667701
222444_at	ARMCX3	9,966380362	10,72229475	235647_at	AP4S1	7,637649977	8,179630049
202387_at	BAG1	8,260261995	8,886664753	226508_at	PHC3	9,71088014	10,39976858
221511_x_at	NA	8,139304644	8,755944302	231964_at	BICD1	9,403292029	10,07005252
206900_x_at	ZNF253	7,762347023	8,350114048	227301_at	NA	8,548528283	9,154509709
205437_at	ZNF211	8,529972687	9,175308508	226399_at	DNAJB14	9,015466646	9,65429528
209336_at	PWP2	7,95682203	8,55585295	213001_at	ANGPTL2	8,366826568	8,959202501
202202_s_at	LAMA4	8,431793132	9,065462638	217989_at	HSD17B11	8,240971879	8,824115729
215399_s_at	OS9	9,422010681	10,12982294	218818_at	FHL3	7,177967376	7,68572288
205991_s_at	PRRX1	9,032455404	9,709966592	238477_at	KIF1C	7,442441483	7,968418751
232333_at	NA	6,399443067	6,87925719	229053_at	SYT17	9,291866221	9,948366616
237864_at	NA	5,387139892	5,790619628	206542_s_at	SMARCA2	9,33550256	9,993578815
225191_at	CIRBP	7,908479007	8,499546746	227853_at	PLBD2	8,682463546	9,294067874
213046_at	PABPN1	8,16280834	8,772764459	202919_at	MOB4	9,761119294	10,44862393
204862_s_at	NME3	8,867481662	9,529633514	222120_at	ZNF764	6,561067694	7,02223909
1563331_at	NA	5,752315685	6,181174755	229742_at	C15orf61	9,11874337	9,759586902
211084_x_at	PRKD3	7,662698985	8,233975958	227335_at	DIDO1	7,703875359	8,244539107
225251_at	RAB24	9,017136155	9,687395394	214252_s_at	CLN5	9,016883415	9,64950235
212299_at	NEK9	9,665232367	10,38354827	206700_s_at	KDM5D	8,953072457	9,581088567
1553704_x_at	ZNF791	8,677971136	9,322494044	224632_at	GPATCH4	8,508775972	9,105039644
224881_at	VKORC1L1	8,700601736	9,345348279	202922_at	GCLC	7,822956416	8,370963723
218453_s_at	TMEM242	7,237205444	7,772564425	224714_at	NIFK	9,509127675	10,17439475
203232_s_at	ATXN1	9,169576372	9,846380266	210425_x_at	NA	9,360254862	10,01255021
222565_s_at	PRKD3	8,808990314	9,457511097	203519_s_at	UPF2	8,084257519	8,647438351
219125_s_at	SLC50A1	7,260303853	7,794315794	208798_x_at	GOLGA8A	8,982922222	9,608643438
201175_at	TMX2	10,67642851	11,46146232	205646_s_at	PAX6	8,677434466	9,280710677
213743_at	CCNT2	8,471258871	9,093983724	218100_s_at	IFT57	8,744028242	9,351671441
204831_at	CDK8	8,620119059	9,253761671	201368_at	ZFP36L2	9,606207098	10,27341713
209537_at	EXTL2	9,938559234	10,66803451	203253_s_at	PPIP5K2	9,498774891	10,15730204
222710_at	NA	6,192621524	6,646766894	224934_at	YIPF5	10,11643231	10,81745941
229574_at	TRA2A	8,829595675	9,474529011	214496_x_at	KAT6B	7,387624424	7,899012467
204925_at	CTNS	7,582045151	8,134520437	222754_at	TRNT1	9,025639565	9,650354652
233919_s_at	HABP4	6,99002088	7,499352984	221899_at	N4BP2L2	9,749800507	10,423926
204669_s_at	RNF24	9,117165482	9,780737935	224953_at	YIPF5	9,171192042	9,804463782
1557302_at	ZNF585B	8,942996444	9,593351284	210346_s_at	CLK4	9,480305492	10,13440988
208706_s_at	EIF5	10,53867173	11,30444127	1552625_a_at	TRNT1	7,852200255	8,39389587
224858_at	ZDHC5	8,758347166	9,394712358	235408_x_at	ZNF117	8,253141604	8,822425635
230056_at	BPTF	6,760782995	7,250418965	225740_x_at	MDM4	9,096979302	9,724388076
221016_s_at	TCF7L1	7,680735372	8,236167177	203569_s_at	OFD1	9,061713344	9,686561996
234341_x_at	LOC91548	8,284933231	8,88373269	221645_s_at	ZNF83	9,249395682	9,886800583
212345_s_at	CREB3L2	8,994521841	9,642332547	217707_x_at	SMARCA2	9,427820505	10,07690123
227255_at	PDIK1L	8,836193744	9,471984499	217937_s_at	HDAC7	6,920127876	7,395200278

226189_at	ITGB8	12,15415907	12,98825202	214151_s at	NA	7,809243232	8,3070192
227991_x at	ZBTB43	7,331466693	7,834517288	206695_x at	ZNF43	9,063835984	9,640447242
209717_at	EVI5	9,020149441	9,638759944	212119_at	RHOQ	9,936495533	10,56790045
238465_at	SETD9	9,008568057	9,626300522	203707_at	NA	8,373088163	8,90504733
224741_x at	NA	10,61957604	11,34702998	223071_at	IER3IP1	10,40358913	11,064158
235088_at	C4orf46	7,405534462	7,911984612	213500_at	NA	8,933148319	9,499232377
212486_s at	FYN	9,246561981	9,878772396	1553678_a at	ITGB1	10,66763785	11,34235809
227628_at	GPX8	9,493270454	10,14104821	213878_at	PYROXD1	8,780122907	9,33503143
203635_at	DSCR3	8,405841712	8,978741675	212766_s at	ISG20L2	8,837929877	9,395585969
225760_at	MYSM1	8,845462874	9,447740761	214844_s at	DOK5	11,66876755	12,40394323
224841_x at	NA	10,60856864	11,33085064	203092_at	TIMM44	7,368990585	7,832915297
209902_at	ATR	8,048040194	8,595413905	209149_s at	TM9SF1	8,752773984	9,302990563
201263_at	TARS	10,39443235	11,10050457	214741_at	NA	9,173778506	9,749645801
218135_at	ERGIC2	10,12263614	10,80927395	218890_x at	MRPL35	8,904501271	9,460354326
1553703_at	ZNF791	9,254369454	9,881682124	201576_s at	NA	9,766349542	10,37592379
226005_at	UBE2G1	8,906140078	9,509783264	218296_x at	NA	8,041828715	8,54371327
206707_x at	FAM65B	7,350862244	7,849065114	225916_at	NA	7,388176483	7,849227149
203359_s at	NA	8,124640625	8,675231464	229557_at	MEG3	7,413440581	7,875208024
221011_s at	LBH	8,67858704	9,264950348	213033_s at	NFIB	10,35908349	11,00407299
235716_at	NA	9,615098339	10,26457657	224774_s at	NAV1	7,93239667	8,42623518
226294_x at	FAM91A1	8,925360682	9,527923489	213480_at	VAMP4	8,800380626	9,346772793
216033_s at	FYN	9,569103769	10,21488528	213626_at	CBR4	9,576254242	10,17062918
213029_at	NFIB	11,32165937	12,08136968	225943_at	NLN	8,25411058	8,76542333
226893_at	ABL2	7,89289093	8,421405292	211996_s at	NA	9,609782366	10,20233055
218532_s at	FAM134B	8,064718713	8,604273046	208708_x at	EIF5	10,18378758	10,81068089
229958_at	CLN8	6,864179567	7,322991636	207809_s at	ATP6AP1	10,71496896	11,37338037
242455_at	POU3F2	11,02930372	11,76481345	230712_at	NA	8,166028092	8,667810654
236635_at	ZNF667	8,46471112	9,028743701	225445_at	UBN2	7,963791522	8,451349359
223148_at	PIGS	8,623808602	9,196651436	232347_x at	NA	6,854513292	7,273973426
202414_at	ERCC5	8,208326741	8,753008088	222212_s at	CERS2	10,36823111	11,00258469
235405_at	GSTA4	8,694906762	9,270946874	218093_s at	ANKRD10	10,00223411	10,61412321
1553959_a at	B3GALT6	10,02474836	10,68844472	223268_at	C11orf54	9,223640367	9,786273032
208174_x at	ZRSR2	7,368686287	7,855673139	224509_s at	RTN4IP1	7,217428798	7,657353067
204706_at	INPP5E	7,928876374	8,452728119	227374_at	EARS2	8,370297852	8,880480724
209649_at	STAM2	8,838172874	9,421406519	225593_at	LSM10	9,540263161	10,12135368
218721_s at	C1orf27	8,820254859	9,399092619	210312_s at	IFT20	9,652036154	10,23988682
201067_at	PSMC2	9,405990364	10,02293715	229828_at	CDC73	7,896167584	8,375593034
221825_at	ANGEL2	9,338239687	9,95015618	224713_at	NIFK	9,222092871	9,781568866
210706_s at	RNF24	8,837244887	9,416017626	229532_at	ZNF502	8,02811399	8,515036351
214870_x at	NA	9,979963878	10,63143619	218497_s at	RNASEH1	9,263138928	9,824446392
235388_at	CHD9	7,794653693	8,302015656	202451_at	GTF2H1	9,644744624	10,22916692
221829_s at	TNPO1	11,3706541	12,11032804	233952_s at	ZBTB21	9,129454831	9,682627607
1553530_a at	ITGB1	10,79233221	11,49331923	204284_at	PPP1R3C	8,185916942	8,681433406
228835_at	NA	8,526957771	9,080331082	203840_at	BLZF1	7,417683693	7,866536146
213686_at	VPS13A	7,812731607	8,315279762	224624_at	LRRC8A	11,58472921	12,28303311
214430_at	GLA	9,066584228	9,649669712	208114_s at	ISG20L2	8,392201612	8,89801549
221689_s at	PIGP	9,879124346	10,5138547	218379_at	RBM7	9,024135098	9,567782783
203651_at	ZFYVE16	8,876569926	9,44685389	1569872_a at	LMF1	9,570099687	10,14519721
211536_x at	MAP3K7	8,36720396	8,904281441	214152_at	NA	7,82738213	8,296410499
213478_at	KAZN	8,590658907	9,141953999	225698_at	EPB41L4A-AS1	8,926890939	9,460942058
209903_s at	ATR	9,047525211	9,628092675	202360_at	MAML1	9,455484263	10,02045421
208705_s at	EIF5	11,2160483	11,93454745	235196_at	CDC73	8,247950879	8,740014726
230588_s at	NA	7,658399771	8,147947822	202603_at	ADAM10	10,95676448	11,61030224
212615_at	CHD9	9,312158025	9,907398981	225963_at	KLHL42	7,432897153	7,876108151
229710_at	ERCC6L2	8,140683725	8,660681691	223186_at	NA	8,769495641	9,292375314
230178_s at	ELP2	7,842090184	8,342493578	205895_s at	NOLC1	8,01554511	8,491836055



244411_at	MINCR	6,666238718	7,061596798
202838_at	FUCA1	8,083524917	8,562859482
204065_at	CHST10	9,121161303	9,661698793
218684_at	LRRC8D	9,837452872	10,42025521
204283_at	FARS2	8,332466469	8,825743309
231899_at	ZC3H12C	8,167100859	8,650404977
202157_s at	CELF2	10,8913463	11,53511136
204426_at	TMED2	9,739682098	10,31533411
221842_s at	NA	8,920895869	9,4480172
206140_at	LHX2	10,82471797	11,46426365
202453_s at	GTF2H1	8,136274429	8,616569538
226605_at	DGKQ	7,69876741	8,152687001
1556629_a at	SNAP25	6,941554861	7,350380217
217820_s at	ENAH	11,31439099	11,97989485
31799_at	NA	8,182413896	8,662012573
204529_s at	TOX	11,07623521	11,72431399
223176_at	KCTD20	9,582617049	10,14214435
1557303_at	NT5C	7,332038783	7,75804588
202373_s at	NA	9,897518003	10,47213606
224206_x at	MYNN	8,139321337	8,610391832
209824_s at	ARNTL	8,779945911	9,287558972
224413_s at	TM2D2	10,59518652	11,20755695
224601_at	NA	9,402417597	9,944927248
212124_at	ZMIZ1	10,25672692	10,84823636
228519_x at	CIRBP	7,679098734	8,121300568
225505_s at	PCED1A	9,470342327	10,01412148
221895_at	MOSPD2	8,577119449	9,069601252
202800_at	SLC1A3	12,83807378	13,57280683
202196_s at	DKK3	11,23528946	11,87797802
225644_at	CCDC117	8,970702311	9,483632332
222616_s at	USP16	9,186214445	9,711262232
201878_at	ARIH1	8,031985591	8,490953549
238850_at	NA	11,4113041	12,06296845
220980_s at	ADPGK	9,426582988	9,964454836
230229_at	DLG1	7,971802993	8,426163269
230272_at	NA	11,50055312	12,15587362
220985_s at	RNF170	8,222571095	8,690935466
228299_at	KCTD20	10,48757457	11,08445251
217168_s at	HERPUD1	9,796628946	10,35358968
200899_s at	MGEA5	10,41027137	11,00166069
228822_s at	USP16	9,727481717	10,27871718
214035_x at	NA	9,834079253	10,39126073
225732_at	KLHL42	9,571098104	10,11223701
212399_s at	VGLL4	10,79376964	11,40271439
201960_s at	MYCBP2	9,570831672	10,10982157
201050_at	PLD3	9,136450942	9,650683773
201959_s at	MYCBP2	8,608566029	9,091370498
213128_s at	UBE3A	9,41680046	9,944791214
202372_at	NA	9,439897168	9,969065402
202069_s at	IDH3A	8,588326964	9,06852901
226695_at	PRRX1	11,64761479	12,29790233
208985_s at	EIF3J	9,810089957	10,35715195
200761_s at	ARL6IP5	11,5228548	12,16521405
216268_s at	JAG1	11,07472435	11,69059719
202277_at	SPTLC1	10,78219854	11,38033096
238877_at	EYA4	9,430062885	9,952534899

204847_at	ZBTB11	9,119484995	9,622217328
32099_at	SAFB2	9,637884896	10,16834917
209737_at	MAGI2	10,19987019	10,7606697
212120_at	RHOQ	10,25113961	10,81201537
215030_at	GRSF1	7,620235173	8,036032974
209297_at	ITSN1	8,708879512	9,183971669
211009_s at	ZNF271P	9,238292883	9,741293425
203427_at	ASF1A	9,881311988	10,41874841
214016_s at	SFPQ	10,59219078	11,1680391
204538_x at	NPIPA1	10,37212025	10,93179455
209290_s at	NFIB	11,84386354	12,48184083
203044_at	CHSY1	10,14468859	10,68969106
204744_s at	IARS	10,72755115	11,29699928
218333_at	DERL2	9,5733408	10,07923695
225220_at	NA	9,418449677	9,916047766
223287_s at	FOXP1	9,211414469	9,696999758
209567_at	RRS1	8,555611532	9,006369928
208907_s at	MRPS18B	9,153479075	9,635736185
227052_at	SMIM14	9,779296732	10,29173653
217317_s at	NA	10,43191182	10,97808526
212721_at	SREK1	10,70323135	11,26296785
214280_x at	HNRNPA1	10,7056807	11,26423998
203355_s at	PSD3	10,77076327	11,32918657
201197_at	AMD1	9,565134042	10,0610057
229523_at	TMEM200C	8,726994213	9,179162556
204879_at	PDPN	9,735374393	10,23978862
202491_s at	IKBKAP	9,530664759	10,02434844
235812_at	CNEPIR1	9,146347721	9,618568859
204808_s at	TMEM5	8,910047672	9,369882493
214789_x at	SRSF8	10,16586926	10,68954439
200945_s at	SEC31A	10,73097299	11,28337042
203632_s at	GPRC5B	10,58274039	11,1270887
222416_at	ALDH18A1	9,002091038	9,464634546
218545_at	CCDC91	8,945433338	9,404542177
221656_s at	ARHGEF10L	7,873642186	8,277640175
213212_x at	NA	8,993964769	9,454571408
224694_at	ANTXR1	10,56752534	11,10760898
226235_at	LINC00667	8,432382555	8,862519413
200760_s at	ARL6IP5	11,76410968	12,36376834
205348_s at	DYNC1H1	9,691278778	10,18471215
203586_s at	ARL4D	8,509736674	8,941669843
211537_x at	MAP3K7	9,05930925	9,516110979
223213_s at	ZHX1	9,89342675	10,38855721
201722_s at	GALNT1	10,34953653	10,8673797
202418_at	YIF1A	9,150019224	9,606811976
219002_at	FASTKD1	9,158026029	9,614119244
209289_at	NFIB	11,97915452	12,57449065
225917_at	ATF7IP	9,613765482	10,09094368
226298_at	RUNDC1	8,113330348	8,515914097
1552575_a at	C6orf141	10,09421286	10,59351364
202537_s at	CHMP2B	7,99908665	8,392646929
218386_x at	USP16	9,914681181	10,40196965
224838_at	FOXP1	9,649409712	10,12350531
37549_g at	BBS9	8,051200557	8,446547222
201572_x at	DCTD	9,636416413	10,10897929
1569607_s at	NA	8,718107888	9,144476195

210835_s_at	CTBP2	9,920263782	10,40541233	226529_at	TMEM106B	11,36665204	11,77887913
225163_at	FRMD4A	9,313164476	9,768052762	202857_at	CNPY2	11,44671	11,84828042
211951_at	NOLC1	10,65981655	11,18040933	221482_s_at	ARPP19	10,61490417	10,98668062
225313_at	FAM217B	9,279172107	9,731935604	213086_s_at	CSNK1A1	11,52433971	11,90735905
203320_at	SH2B3	8,921759937	9,3565017	221729_at	COL5A2	11,9510695	12,34377709
223214_s_at	ZHX1	10,24341667	10,74240028	227394_at	NCAM1	11,44085729	11,8008105
204944_at	PTPRG	10,01813989	10,50507105	211072_x_at	TUBA1B	14,22195016	13,83539582
1555226_s_at	C1orf43	10,79620953	11,31939922	201090_x_at	TUBA1B	14,17992302	13,77187509
221501_x_at	NA	10,95346745	11,48281393	212372_at	MYH10	11,4060013	11,02784753
212685_s_at	TBL2	10,36291473	10,8634212	217733_s_at	TMSB10	14,13049403	13,65570323
218236_s_at	PRKD3	10,56425135	11,07173459	225053_at	CNOT7	11,31358211	10,91878039
201095_at	DAP	9,461602646	9,913609397	218146_at	GLT8D1	10,81225454	10,42972038
222433_at	ENAH	11,596502	12,14762873	200043_at	ERH	12,56478832	12,11384891
218088_s_at	RRAGC	9,76827128	10,23147609	208847_s_at	ADH5	11,24680167	10,84173997
225197_at	NA	9,231930645	9,66935583	213699_s_at	YWHAQ	13,42130128	12,93316361
204427_s_at	TMED2	10,59284228	11,09306978	200792_at	XRCC6	11,98710596	11,55084126
210830_s_at	PON2	11,19654134	11,72443536	216526_x_at	HLA-C	12,56637696	12,10797027
225062_at	NA	10,1175953	10,591938	200026_at	RPL34	12,63271698	12,16050884
201630_s_at	ACP1	9,351355883	9,78863801	200773_x_at	PTMA	12,81546231	12,33411483
226505_x_at	USP32	9,814790758	10,27185487	210211_s_at	HSP90AA1	13,42295076	12,91544135
211945_s_at	ITGB1	12,47239425	13,0511363	217963_s_at	NGFRAP1	13,12727176	12,62849211
227116_at	MON1B	9,366263176	9,798410056	230264_s_at	AP1S2	12,07691605	11,61338953
226594_at	ENTPD5	8,40958993	8,797046495	209043_at	PAPSS1	11,79023715	11,33610871
226677_at	ZNF521	9,271064692	9,695602317	201540_at	FHL1	11,62732501	11,15992353
223081_at	PHF23	9,73455414	10,18030895	228155_at	FAM213A	10,83053159	10,39473739
222140_s_at	NA	9,042850886	9,454040925	200772_x_at	NA	12,75973015	12,24014417
220755_s_at	C6orf48	11,36563979	11,88023914	213508_at	SPTSSA	9,125798684	8,752524308
216713_at	KRIT1	9,229501186	9,645667568	234863_x_at	FBXO5	9,678385156	9,282325993
225046_at	NA	10,68442455	11,16472164	217845_x_at	HIGD1A	12,08295298	11,58739623
213682_at	NUP50	9,991851965	10,43885229	222602_at	UBA6	9,546922762	9,15537546
218056_at	BFAR	9,475690999	9,897028902	214328_s_at	HSP90AA1	13,47037537	12,90956194
201096_s_at	ARF4	11,21919038	11,71615685	203581_at	NA	9,942142042	9,526805031
221933_at	NLGN4X	11,09193962	11,57769113	202088_at	SLC39A6	12,25304975	11,74068389
211980_at	COL4A1	9,903833876	10,3371923	202299_s_at	LAMTOR5	11,24358573	10,7698672
226740_x_at	NA	11,44039938	11,93580796	211954_s_at	IPO5	10,46528571	10,02335986
202718_at	IGFBP2	13,13942	13,70560598	202386_s_at	KIAA0430	9,573839688	9,168150431
202522_at	PITPNB	10,8844374	11,35106967	218323_at	RHOT1	10,71878714	10,26445044
208905_at	CYCS	12,41096954	12,94276639	226627_at	SEPT8	9,107598613	8,720300842
222423_at	NDFIP1	10,3669314	10,80952782	223191_at	COX16	11,03914541	10,56968716
210105_s_at	FYN	11,54643254	12,03864423	212426_s_at	YWHAQ	12,45178413	11,91892682
222108_at	AMIGO2	11,35868149	11,8419094	200603_at	PRKAR1A	12,23345904	11,70991877
205358_at	GRIA2	11,20460204	11,68080543	202615_at	GNAQ	11,01015375	10,5386428
1568618_a_at	GALNT1	10,71066383	11,16556703	211921_x_at	NA	12,58709623	12,04773541
201765_s_at	HEXA	9,970595827	10,39338132	201272_at	AKR1B1	11,79290363	11,28275961
223892_s_at	TMBIM4	11,23322247	11,70698862	204031_s_at	PCBP2	11,73523029	11,22704193
209796_s_at	CNPY2	10,50522487	10,94628138	212154_at	SDC2	12,04520155	11,52348405
211423_s_at	SC5D	10,23817684	10,6673586	217720_at	CHCHD2	13,00291014	12,43611712
222495_at	TMEM167B	10,42861844	10,8512193	210559_s_at	CDK1	9,780146276	9,352873473
209377_s_at	HMGN3	12,2423403	12,7378173	209329_x_at	HIGD2A	10,59991069	10,13621013
203956_at	MORC2	9,429252086	9,809274831	234000_s_at	HACD3	11,59399128	11,08509994
201519_at	TOMM70A	9,803498575	10,19225424	218009_s_at	PRC1	10,96648396	10,48316099
225221_at	ZKSCAN1	11,01217764	11,448344	225350_s_at	ZYG11B	9,76073389	9,330064295
225945_at	ZNF655	10,66624565	11,08091982	221676_s_at	CORO1C	10,80068782	10,32169413
217776_at	RDH11	11,58519615	12,02233942	204496_at	STRN3	9,607224435	9,179924342
201084_s_at	BCLAF1	11,6541115	12,08776669	209522_s_at	CRAT	9,115952086	8,709340707
204159_at	CDKN2C	11,64412766	12,06690622	216384_x_at	NA	10,42718283	9,961470839

211318_s_at	RAE1	10,03723521	9,587468529
204028_s_at	RABGAP1	10,25884121	9,798840381
221523_s_at	RRAGD	9,409969923	8,987982076
230435_at	FAM228B	8,68689283	8,295322172
211969_at	HSP90AA1	13,65584225	13,0399579
212199_at	MRFAP1L1	10,63956069	10,15449177
226482_s_at	TSTD1	9,342901916	8,91578422
206102_at	GINS1	10,38041308	9,903137998
224729_s_at	ATPAF1	10,41934421	9,937528186
222404_x_at	HACD3	11,52888962	10,9956266
200640_at	YWHAZ	11,87293177	11,3204485
204173_at	MYL6B	11,44671882	10,91121491
202749_at	WRB	11,57780749	11,0338668
201477_s_at	RRM1	11,56458567	11,01926533
215568_x_at	LYPLA2	8,164301715	7,77927613
212646_at	RFTN1	10,44107775	9,948286798
225771_at	AP1G1	9,516850599	9,067610499
219649_at	ALG6	9,582532377	9,12930201
200639_s_at	YWHAZ	11,90587247	11,34097021
37384_at	PPM1F	9,138211056	8,702827596
226563_at	SMAD2	8,714850743	8,299419692
226581_at	RBSN	9,772607273	9,305797833
212628_at	PKN2	9,385465194	8,932620684
220607_x_at	NELFCD	11,30056835	10,7543663
213313_at	RABGAP1	10,91902538	10,39041521
201541_s_at	ZNHIT1	10,64562449	10,12930313
200978_at	MDH1	11,55894619	10,99669127
222405_at	HACD3	11,89628215	11,31627986
202300_at	LAMTOR5	11,29109789	10,73843541
203790_s_at	HRSP12	9,483443761	9,017378445
203076_s_at	SMAD2	10,05912419	9,564310916
232676_x_at	MYEF2	10,48027839	9,963066268
208839_s_at	CAND1	9,961634671	9,469794599
208647_at	FDFT1	11,64024489	11,06540753
227407_at	TAPT1	10,68189821	10,15378265
225083_at	GTF3C6	11,57634802	11,00321692
218788_s_at	SMYD3	9,074248575	8,623239478
200604_s_at	PRKAR1A	10,51672663	9,993439612
219013_at	GALNT11	10,50366826	9,979888607
212038_s_at	VDAC1	11,68443564	11,10147682
200832_s_at	SCD	12,10117924	11,49611075
201306_s_at	ANP32B	12,07854366	11,47453052
208095_s_at	NA	10,86406082	10,32066421
203077_s_at	SMAD2	9,340339481	8,872667618
217874_at	SUCLG1	11,02500806	10,47170672
203606_at	NDUFS6	11,48488561	10,90709543
203875_at	SMARCA1	10,80399788	10,2595402
223675_s_at	VEZT	9,551840932	9,070283943
202529_at	PRPSAP1	10,15903599	9,646768781
205201_at	GLI3	8,614564867	8,177942389
213088_s_at	DNAJC9	9,633228468	9,143297607
200605_s_at	PRKAR1A	11,93095154	11,32285904
212155_at	RNF187	10,66181684	10,1183627
205956_x_at	PSMC3IP	8,207255359	7,787460806
213971_s_at	NA	10,12345264	9,604621764
224862_at	GNAQ	9,868708639	9,362873728

219485_s_at	PSMD10	10,97349543	10,40968329
200982_s_at	ANXA6	9,945064866	9,433917795
218592_s_at	CECR5	10,06450711	9,543868216
202218_s_at	FADS2	8,666656109	8,217646833
208977_x_at	TUBB4B	12,47723731	11,82980337
229860_x_at	C4orf48	9,921772953	9,404087752
222457_s_at	LIMA1	11,40505553	10,80989866
225261_x_at	NELFCD	11,04436727	10,46797569
226343_at	DPP8	9,520512926	9,022991069
223100_s_at	NUDT5	9,061003019	8,587287208
212546_s_at	FRYL	9,8818767	9,364797213
225865_x_at	NELFCD	10,96502056	10,39078857
202089_s_at	SLC39A6	11,01485813	10,43649199
201193_at	IDH1	12,08938128	11,45455347
216515_x_at	MIR1244-3	11,11414043	10,53040081
221896_s_at	HIGD1A	11,86906123	11,24530045
221007_s_at	FIP1L1	9,964801385	9,44065239
202478_at	TRIB2	13,01736127	12,3318999
200638_s_at	YWHAZ	12,36265288	11,71155833
203970_s_at	PEX3	8,166726178	7,735252039
201574_at	ETF1	10,56160605	10,00301932
1555037_a_at	IDH1	11,85073538	11,22148515
208091_s_at	VOPP1	11,62533754	11,00594165
221685_s_at	SPDL1	9,423515472	8,920894972
200932_s_at	DCTN2	10,90176526	10,31959125
227003_at	RAB28	9,883903804	9,355869546
203130_s_at	KIF5C	12,30526868	11,64691917
202460_s_at	LPIN2	8,827878085	8,355362733
201403_s_at	MGST3	10,87127522	10,28744876
225029_at	LINC01420	9,849204329	9,320250982
222036_s_at	MCM4	9,443761074	8,93268936
212548_s_at	FRYL	10,01517215	9,472256927
234672_s_at	NDC1	9,869760823	9,331121961
200905_x_at	HLA-E	10,03368248	9,485679946
234978_at	SLC36A4	7,808368492	7,38155578
217968_at	TSSC1	8,977064732	8,483315836
221873_at	ZNF143	8,852897876	8,365694829
200956_s_at	SSRP1	10,39832083	9,825862754
201227_s_at	NDUFB8	10,53231606	9,950656528
224919_at	MRPS6	11,33308444	10,70378214
221743_at	CELF1	11,57378405	10,93108362
217456_x_at	HLA-E	9,92932974	9,377653831
217892_s_at	LIMA1	11,48232475	10,84392734
217140_s_at	VDAC1	11,18648319	10,56282375
208549_x_at	PTMA	10,48177989	9,897392075
1556283_s_at	FGFR1OP2	8,367721043	7,901095793
202767_at	ACP2	8,450136854	7,978628564
213726_x_at	TUBB4B	12,52895784	11,82946202
213504_at	COPS6	9,71907522	9,175801327
226003_at	KIF21A	10,73426806	10,13409864
212930_at	ATP2B1	8,38074418	7,909605837
217955_at	BCL2L13	8,999771642	8,49223991
209191_at	TUBB6	10,69521338	10,09022287
226236_at	LINC00493	11,04473376	10,41981576
227630_at	PPP2R5E	8,784675778	8,287530982
223993_s_at	CNIH4	11,44648998	10,79658003

205079_s at	MPDZ	9,903442559	9,340992479
201128_s at	ACLY	11,31128288	10,66814321
200693_at	YWHAQ	12,76156789	12,0350351
202154_x at	TUBB3	12,72799248	12,0032902
204332_s at	AGA	8,758111286	8,258476678
217819_at	GOLGA7	11,42468046	10,77167079
209258_s at	SMC3	9,094511686	8,57427853
1053_at	RFC2	8,902139612	8,392630522
1554577_a at	PSMD10	10,55947519	9,954415445
227249_at	NDE1	10,46989122	9,868748395
228762_at	LFNG	9,651279972	9,096390951
222575_at	SETD5	8,339813016	7,86013724
203350_at	APIG1	8,831511171	8,323201573
202573_at	CSNK1G2	9,755034813	9,191871703
59697_at	RAB15	8,694651838	8,192654772
225006_x at	NELFCD	10,99431797	10,35877104
205347_s at	NA	10,39073847	9,789920925
218461_at	GPN3	9,231787834	8,69776785
213735_s at	COX5B	11,5697241	10,89707448
220770_s at	ZBED8	8,752892933	8,24260385
223378_at	GLIS2	8,981194487	8,456798198
200645_at	GABARAP	12,20383066	11,4905472
239525_at	CTTNBP2NL	7,238760783	6,814665463
201816_s at	GBAS	11,93339218	11,23330765
564_at	GNA11	9,879531511	9,297716695
202427_s at	MPC2	9,948025694	9,361559383
217957_at	CFAP20	10,69201218	10,06153741
210495_x at	FN1	10,51757853	9,897108291
203299_s at	AP1S2	9,80636163	9,22771797
213070_at	PIK3C2A	11,0243031	10,37268985
208002_s at	ACOT7	10,23849783	9,632579055
214075_at	NENF	8,533819841	8,027530705
201375_s at	PPP2CB	12,46511681	11,72519718
209139_s at	PRKRA	10,05019872	9,453429615
213306_at	MPDZ	10,30168069	9,689678859
227099_s at	C11orf96	9,458692715	8,896680804
201554_x at	GYG1	9,914597339	9,325350581
200641_s at	YWHAZ	11,83002599	11,12683336
201555_at	MCM3	10,07494865	9,473012128
204386_s at	MRPL57	10,90936403	10,25742287
239047_at	FAM122C	6,850766039	6,440369293
201476_s at	RRM1	9,989993758	9,389966732
227696_at	EXOSC6	10,05324459	9,446265884
212774_at	ZBTB18	11,69393286	10,98651845
204336_s at	RGS19	8,936287028	8,39430037
213616_at	TPGS2	8,254054448	7,753399105
203620_s at	FCHSD2	8,541617561	8,023258918
201768_s at	CLINT1	8,809630537	8,272409785
226293_at	MED19	8,924764264	8,38030196
224878_at	UBFD1	10,09353253	9,477110172
212094_at	PEG10	13,45269073	12,63096129
209628_at	NXT2	8,622865926	8,095550134
204979_s at	SH3BGR	8,183045001	7,68225806
204387_x at	MRPL57	8,866484117	8,322841971
1555460_a at	SLC39A6	9,452908611	8,872020203
210950_s at	FDFT1	11,0618595	10,38197358

224948_at	NA	11,17295565	10,48445158
202503_s at	KIAA0101	12,09184838	11,34585975
228831_s at	GNG7	9,205348604	8,637217724
201612_at	ALDH9A1	11,49085237	10,77930368
228170_at	OLIG1	10,20415431	9,571905415
209300_s at	NECAP1	9,174473604	8,604184783
215499_at	NA	8,432788682	7,908421757
223626_x at	IFI27L2	8,538333005	8,00665341
223475_at	CRISPLD1	9,639210576	9,038368924
226151_x at	CRYZL1	9,242334079	8,665493829
223302_s at	ZNF655	7,391605728	6,930205272
225637_at	DEF8	8,618997593	8,080587824
238936_at	TMEM178B	8,060506262	7,55675779
226300_at	MED19	9,196777889	8,621424166
203447_at	PSMD5	9,083326324	8,514913244
226013_at	TRAK1	6,920917601	6,487271605
202074_s at	OPTN	7,678551738	7,197178598
226024_at	COMMD1	9,448450009	8,854546487
228899_at	NA	8,451853333	7,919950214
214259_s at	AKR7A2	9,895437048	9,272598505
218809_at	PANK2	10,33038256	9,680001888
206363_at	MAF	7,362174422	6,898536632
222978_at	SURF4	10,298462	9,648981373
224863_at	GNAQ	9,395757403	8,802618215
203656_at	FIG4	8,875589792	8,315064179
230305_at	DNAJC15	7,920554248	7,42001425
225338_at	ZYG11B	9,987977541	9,356034174
202343_x at	COX5B	11,19429287	10,48556339
225689_at	POMGNT2	9,417846982	8,821382639
233571_x at	PPDPF	10,32711918	9,673050244
206949_s at	RUSC1	9,151869384	8,571721418
222581_at	XPR1	9,456510552	8,856572323
203094_at	MAD2L1BP	9,280710914	8,691847567
221810_at	RAB15	7,69922684	7,206419001
213766_x at	GNA11	10,19722122	9,543808717
213283_s at	SALL2	9,27771882	8,682966743
224914_s at	SARNP	10,31661643	9,653689307
211025_x at	COX5B	11,14701817	10,43058159
202596_at	ENSA	10,71423644	10,02468285
205543_at	HSPA4L	8,548269555	7,997900115
224415_s at	HINT2	9,308053064	8,708486723
1556551_s at	SLC39A6	9,570906255	8,954228841
225031_at	CHD6	8,911524725	8,335528828
200824_at	GSTP1	11,45580862	10,71235895
217419_x at	AGRN	7,523436458	7,033809634
227722_at	RPS23	8,263533757	7,725452125
202986_at	ARNT2	9,553983744	8,931714707
225723_at	CCDC167	9,926606098	9,279814016
203275_at	IRF2	8,711612645	8,143042046
224896_s at	TTL	9,650333278	9,020165078
203764_at	DLGAP5	10,16718961	9,502317396
216064_s at	AGA	7,827011183	7,314740344
202316_x at	UBE4B	7,23093904	6,75541684
223248_at	HSDL1	8,846302653	8,263980767
225352_at	SEC62	9,261728247	8,650930586
207268_x at	ABI2	8,970462562	8,378081304

211065_x_at	PFKL	8,836406569	8,250402935	204105_s_at	NRCAM	12,09477082	11,23816371
235550_at	MAP9	6,991549501	6,527835864	211275_s_at	GYG1	10,20328076	9,480072418
212727_at	DLG3	7,34197166	6,854912153	203733_at	DEXI	8,614019817	8,002582194
225436_at	ABHD17C	9,580371681	8,943392388	225440_at	AGPAT3	9,19130814	8,536682174
203445_s_at	CTDSP2	10,52266673	9,822482874	221742_at	CELF1	8,376930911	7,780188383
208881_x_at	ID11	10,0341716	9,366280321	227497_at	SOX6	8,920762224	8,285275604
222785_x_at	C11orf1	7,936202305	7,40670011	217729_s_at	AES	9,730478232	9,036496375
218883_s_at	CENPU	10,261512	9,57648639	224682_at	ANKIB1	10,77066325	10,00202019
235792_x_at	PIK3C2A	8,606915239	8,032057485	211162_x_at	SCD	7,424190921	6,894322427
219066_at	PPCDC	7,448555591	6,950653794	229741_at	MAVS	7,748354563	7,194677631
230326_s_at	C11orf73	10,63058736	9,919259495	238695_s_at	RAB39B	7,424105574	6,893329073
203874_s_at	SMARCA1	10,21568748	9,531839512	208776_at	PSMD11	8,289860589	7,6966321
226319_s_at	ALYREF	10,83780827	10,11138202	200653_s_at	NA	12,46624784	11,5735259
200746_s_at	GNB1	11,78370289	10,99384249	234915_s_at	DENR	8,2296526	7,64004281
235507_at	PCMTD1	7,613329115	7,101582737	209507_at	RPA3	10,42304173	9,67595814
235177_at	METTL21A	8,263142519	7,707389944	242560_at	FANCD2	8,956523778	8,31280738
201215_at	PLS3	11,29630812	10,53580191	222627_at	VPS54	8,585492033	7,967669697
205053_at	PRIM1	8,646039803	8,063613992	228264_at	ACCS	6,832748506	6,340887726
201002_s_at	NA	11,23665292	10,47893072	204615_x_at	ID11	10,17912949	9,445728922
201841_s_at	HSPB1	10,90264034	10,1660895	225105_at	C12orf75	10,27699321	9,536503593
226826_at	LSM11	7,082480089	6,602996144	219596_at	THAP10	8,48243849	7,870849848
203300_x_at	AP1S2	11,57121884	10,78760402	206584_at	LY96	9,407587111	8,728587901
225515_s_at	NA	9,955266186	9,280651635	206258_at	ST8SIA5	10,47140118	9,714506803
208832_at	ATXN10	8,721872203	8,129506626	227164_at	SRSF1	8,309054952	7,708378349
211047_x_at	AP2S1	10,6916024	9,965364098	222589_at	NLK	8,997539629	8,346999592
200662_s_at	TOMM20	11,83605108	11,03096343	1560477_a_at	SAMD11	6,225619738	5,774569467
225850_at	SFT2D1	9,209555631	8,580851948	202825_at	SLC25A4	9,502834249	8,814192239
231772_x_at	CENPH	8,934786932	8,324018672	223065_s_at	STARD3NL	11,87468081	11,01382149
225068_at	KLHL12	10,55105081	9,829303501	203925_at	GCLM	8,488685085	7,87263555
200799_at	NA	10,26472097	9,559594149	226696_at	RBBP9	9,504618361	8,814492424
209517_s_at	ASH2L	9,411826603	8,765271751	211160_x_at	ACTN1	8,922747386	8,274758926
239891_x_at	RAB12	8,285100325	7,7159303	211985_s_at	NA	11,77679356	10,9213353
221516_s_at	MIEF1	8,718047638	8,118396798	208620_at	PCBP1	11,07574744	10,27116768
236321_at	FAM200B	7,635098535	7,109835258	220099_s_at	NA	10,37886774	9,62375368
202260_s_at	STXBP1	9,909641035	9,227592734	202949_s_at	FHL2	7,778166925	7,210709858
225490_at	ARID2	8,443518638	7,861188621	239307_at	MYH11	8,004832109	7,420570003
212288_at	FNBP1	9,183709127	8,549713814	215716_s_at	ATP2B1	8,595812138	7,967027784
223144_s_at	AKIRIN2	9,959691693	9,272001415	221677_s_at	DONSON	8,990817088	8,333056233
200655_s_at	NA	12,63502121	11,76120904	201850_at	CAPG	9,067920683	8,404365907
210337_s_at	ACLY	9,722532025	9,049285222	218208_at	PQLC1	8,470029858	7,849403171
208092_s_at	FAM49A	7,628601319	7,099191768	214083_at	PPP2R5C	6,612416008	6,127050809
220975_s_at	C1QTNF1	7,393704827	6,879829689	212492_s_at	KDM4B	9,643751771	8,934570939
225331_at	CCDC50	9,971973017	9,278627785	209015_s_at	DNAJB6	8,857732965	8,205912865
209563_x_at	NA	12,49468164	11,62581223	223808_s_at	NA	8,979133127	8,318023283
201303_at	EIF4A3	9,947428673	9,255404425	208074_s_at	AP2S1	10,91005312	10,10638829
226094_at	PIK3C2A	9,154657209	8,517044973	202043_s_at	SMS	10,71103279	9,921891013
200738_s_at	PGK1	13,16962021	12,24827654	219321_at	MPP5	8,131031527	7,531683977
226320_at	ALYREF	10,53440913	9,797277874	227456_s_at	C6orf136	8,487554757	7,861914196
218728_s_at	CNIH4	9,821167935	9,131611443	209044_x_at	SF3B4	8,775894372	8,128983489
204252_at	CDK2	9,654463229	8,976294365	224861_at	GNAQ	9,968247042	9,231350646
211708_s_at	SCD	7,640075387	7,103322611	212312_at	BCL2L1	8,962556184	8,299905673
213706_at	GPD1	11,41857815	10,61577356	203540_at	GFAP	11,68029679	10,81640758
228214_at	SOX6	8,86664738	8,241717401	222553_x_at	OXR1	10,1893095	9,434867839
211968_s_at	HSP90AA1	13,18459225	12,25504911	206500_s_at	MIS18BP1	8,830938552	8,176457477
203859_s_at	PALM	6,870522978	6,385920979	210933_s_at	FSCN1	9,465759478	8,764007679
225923_at	VAPB	9,870970636	9,173967757	211984_at	NA	11,74139484	10,87055642

224689_at	MANBAL	10,21154066	9,453838895	201849_at	BNIP3	12,28752185	11,33010892
218020_s_at	ZFAND3	9,059149875	8,386741893	203545_at	ALG8	9,54655661	8,802617261
225569_at	NA	9,019065887	8,348509941	222443_s_at	RBM8A	10,05395148	9,270243219
224945_at	BTBD7	8,787988445	8,134096963	223274_at	TCF19	8,718178435	8,037737968
1554977_at	LKAAEAR1	6,609121434	6,115901598	217645_at	NA	8,117602188	7,483996941
215206_at	NA	5,765608332	5,335255187	218973_at	EFTUD1	8,712063036	8,031603797
212136_at	ATP2B4	8,499895837	7,864243009	213008_at	FANCI	9,233003765	8,511835271
226510_at	HEATR5A	8,182241983	7,570040686	227376_at	GLI3	9,938649587	9,161957771
221142_s_at	PECR	7,32566204	6,777053425	201845_s_at	RYBP	10,27559608	9,47199441
209629_s_at	NXT2	6,953405501	6,431966791	238612_at	BRD4	8,847728998	8,155657492
204127_at	RFC3	9,278073334	8,581948067	204997_at	GPD1	9,691724984	8,933155915
213104_at	TSR3	8,731565165	8,0761375	219204_s_at	SRR	9,423996731	8,685564558
216941_s_at	TAF1B	8,051070405	7,446103236	200774_at	FAM120A	11,2694282	10,38630474
212287_at	SUZ12	10,63710212	9,836680538	211729_x_at	BLVRA	10,39864412	9,583031606
225089_at	USP40	8,233281737	7,61277409	208158_s_at	OSBPL1A	9,163444195	8,443979519
212993_at	NACC2	10,16450813	9,398381065	209306_s_at	SWAP70	8,575243157	7,90083117
203189_s_at	NA	9,314880739	8,61168772	210685_s_at	UBE4B	7,792808422	7,179375344
207761_s_at	METTL7A	10,71488709	9,905620427	218480_at	AGBL5	8,123822956	7,48318271
201794_s_at	SMG7	8,996538407	8,316526837	204836_at	GLDC	9,860392839	9,082636008
209487_at	RBPMS	8,588013963	7,937869199	206397_x_at	NA	9,261432456	8,527164471
212197_x_at	MPRIP	10,43274946	9,642203123	222777_s_at	WHSC1	7,833937015	7,212029995
222844_s_at	SRR	8,696712385	8,036705033	212331_at	RBL2	9,865065788	9,081769847
220526_s_at	MRPL20	11,21194363	10,36011044	202500_at	DNAJB2	8,48105948	7,807164417
227772_at	LATS1	8,783791367	8,115973355	213666_at	SEPT6	6,944157646	6,392014079
218802_at	CCDC109B	10,1355625	9,364740945	200678_x_at	GRN	9,467595341	8,714779666
225754_at	APIG1	7,581827534	7,005129758	201953_at	CIB1	8,747086504	8,050848607
217367_s_at	ZHX3	8,463716872	7,81976046	37966_at	PARVB	7,271221338	6,691814774
225915_at	CAB39L	7,805879458	7,211903743	239153_at	HOTAIR	7,56036914	6,95759925
231720_s_at	JAM3	8,084759229	7,468833363	203190_at	NA	9,89659914	9,107388701
224844_at	SLAIN2	9,308409123	8,599163395	203755_at	BUB1B	10,34035378	9,515707471
225433_at	GTF2A1	9,580963683	8,848334355	219979_s_at	C11orf73	8,992207728	8,274676033
211042_x_at	NA	9,988616898	9,224621204	221311_x_at	LYRM2	9,943048862	9,149342106
217946_s_at	SAE1	9,410325427	8,689710193	204916_at	RAMP1	8,956937671	8,241837336
209947_at	UBAP2L	7,938538477	7,329813797	201931_at	ETFA	10,87803165	10,00825797
201706_s_at	PEX19	8,728817609	8,05850055	202207_at	ARL4C	10,80847568	9,944082303
220150_s_at	FAM184A	7,763902017	7,167393076	1555514_a_at	PIAS2	8,386487211	7,711863717
202673_at	DPM1	11,17147941	10,31313162	205210_at	TGFBRAP1	7,497464255	6,894303151
218318_s_at	NLK	8,027222375	7,410267798	201102_s_at	PFKL	8,101499282	7,449602048
223299_at	SEC11C	10,50120612	9,692886915	226744_at	NA	9,288697193	8,53991283
217842_at	NA	9,498523655	8,766854461	208921_s_at	SRI	11,98373581	11,01719935
217780_at	WDR83OS	10,68340591	9,859252527	203162_s_at	KATNB1	8,073504617	7,422314025
204200_s_at	PDGFB	8,717861147	8,04493924	50400_at	PAOX	5,554528607	5,106064004
214771_x_at	MPRIP	10,53513331	9,721902169	203526_s_at	APC	7,953197217	7,310891493
218050_at	UFM1	10,68991416	9,864613493	205245_at	PARD6A	7,211953879	6,629418411
225108_at	AGPS	8,114015693	7,487057076	202483_s_at	RANBP1	11,65058136	10,70854344
218662_s_at	NCAPG	9,679707945	8,931292186	225901_at	PTPMT1	8,257834015	7,590058006
226188_at	LGALS1	9,174750452	8,465047046	222039_at	KIF18B	9,208122537	8,46335866
209980_s_at	NA	6,964309067	6,425351817	204603_at	EXO1	7,473076781	6,868461722
224462_s_at	CHCHD6	7,978560565	7,360812517	202530_at	MAPK14	9,171130449	8,425223055
213110_s_at	COL4A5	10,13003572	9,345556267	231897_at	PTGR1	8,848896443	8,127513684
223155_at	HDHD2	11,06936681	10,21198479	209856_x_at	ABI2	7,757678198	7,124601502
208789_at	PTRF	9,10453257	8,399023413	210621_s_at	RASA1	9,450038671	8,678770464
202120_x_at	AP2S1	9,281502141	8,560717093	227641_at	FBXL16	10,30986437	9,467806425
218152_at	HMG20A	9,535440327	8,793894732	203209_at	RFC5	8,752830018	8,037645596
228889_at	ARHGAP5-AS1	6,836531516	6,304102862	216041_x_at	GRN	9,288389927	8,528418046
218127_at	NFYB	9,70993925	8,95367273	225125_at	MMGT1	9,522801822	8,742085126

218094_s at	NA	9,06132273	8,318435146
212277_at	MTMR4	9,006012611	8,266841138
204424_s at	LMO3	8,862046544	8,134434891
227908_at	TBC1D24	9,160493723	8,407051921
221235_s at	TGFBRAP1	7,650692252	7,021323665
219205_at	SRR	9,650269677	8,855436393
212412_at	PDLIM5	11,42607848	10,48472976
228190_at	ATG4C	8,37020527	7,68034937
215566_x at	LYPLA2	8,492616838	7,792649476
212692_s at	LRBA	9,560715394	8,772713782
203773_x at	BLVRA	10,49829999	9,63251725
203742_s at	TDG	7,753110899	7,112670558
203525_s at	APC	10,11370485	9,278258477
203743_s at	TDG	10,2196044	9,374939003
209529_at	PPAP2C	7,437784391	6,821027059
1554348_s at	CDKN2AIPN L	5,346684777	4,902596181
1558706_a at	ATOH8	7,061211848	6,474532196
231034_s at	NHSL1	8,171194291	7,491762857
224583_at	COTL1	10,44347533	9,574920476
203310_at	STXBP3	9,890568136	9,067908888
218047_at	OSBPL9	10,08608002	9,247055112
223879_s at	OXR1	9,094699277	8,337889053
32837_at	AGPAT2	7,939512508	7,278818272
205413_at	MPPE2	10,3193643	9,459677592
226406_at	C18orf25	9,379834823	8,598310402
220964_s at	RAB1B	9,536017405	8,741332492
219526_at	C14orf169	7,76903117	7,120693143
226082_s at	SCAF4	9,046168618	8,291096646
203210_s at	RFC5	7,700357042	7,057593361
213630_at	NACAD	8,184922291	7,501572366
225643_at	MAPK1IP1L	9,94785309	9,117071514
225087_at	FOPNL	10,05622884	9,21402081
221693_s at	MRPS18A	9,533057075	8,733222799
218197_s at	OXR1	10,26561363	9,402797155
213940_s at	FNBP1	8,603807577	7,880418532
201769_at	CLINT1	10,16100477	9,306522902
213772_s at	GGA2	7,77614152	7,122133133
227617_at	TMEM201	8,675943523	7,945745189
239407_at	PAXBP1-AS1	6,296900882	5,766777742
212450_at	SECISBP2L	9,264243207	8,483659227
44040_at	FBXO41	7,104799675	6,505127163
212862_at	CDS2	9,014631117	8,252029541
203379_at	RPS6KA1	5,775658889	5,286759798
227124_at	SMIM13	9,998077128	9,150858827
221507_at	TNPO2	9,192871629	8,411561716
214268_s at	MTMR4	9,44336539	8,640179084
219787_s at	ECT2	10,33495999	9,450458609
201710_at	MYBL2	8,342994383	7,628971455
1553991_s at	NA	6,887696249	6,298100773
222863_at	ZBTB10	5,840384997	5,340111459
226428_at	TNPO2	8,540553422	7,808575181
234465_at	EME1	7,445050624	6,806752996
219003_s at	MANEA	7,141985807	6,529449163
224822_at	DLC1	7,106296937	6,496465013
203344_s at	RBBP8	9,871956807	9,024710893
201704_at	ENTPD6	8,776671871	8,022810555

1553694_a at	PIK3C2A	7,683786723	7,02352476
204735_at	PDE4A	6,913897	6,31969848
235588_at	ESCO2	8,489781995	7,759615011
235131_at	RHOJ	9,427507705	8,615829853
226582_at	LOC400043	9,193627272	8,401792011
219931_s at	KLHL12	8,433018438	7,706595634
203185_at	RASSF2	11,75436832	10,74168027
1555500_s at	SLC2A4RG	7,983683784	7,294857364
218355_at	KIF4A	9,297382941	8,495128504
205077_s at	PIGF	10,06161239	9,193407011
200745_s at	GNB1	11,63260204	10,62819607
223184_s at	AGPAT3	8,503339709	7,768472654
225170_at	WDR5	8,255067861	7,540180995
203771_s at	BLVRA	8,619128582	7,872649019
226152_at	TTC7B	8,394426059	7,667288357
204205_at	APOBEC3G	7,608689666	6,949463357
207559_s at	ZMYM3	7,878160205	7,195529105
1555618_s at	SAE1	8,94223051	8,167379934
227013_at	LATS2	9,131414813	8,339719279
218776_s at	TMEM62	6,863727634	6,268499914
204653_at	TFAP2A	8,945475961	8,169162012
221059_s at	NA	10,9223399	9,974378664
204268_at	S100A2	6,436261223	5,876971463
202518_at	BCL7B	8,453166447	7,71851368
214051_at	NA	10,05251492	9,178611363
226651_at	HOMER1	9,227749295	8,424792837
215084_s at	LRRRC42	9,07513363	8,285256465
235399_at	ERCC2	6,886107024	6,286654314
209030_s at	CADM1	11,82309443	10,79373104
227498_at	SOX6	9,383697754	8,566391379
204887_s at	PLK4	8,322708507	7,59748732
227580_s at	TECPR1	9,280350232	8,470404694
205148_s at	CLCN4	6,412842254	5,853042986
227625_s at	STUB1	11,89848431	10,85956715
209608_s at	ACAT2	9,950668404	9,081146121
200904_at	HLA-E	8,243617958	7,523085946
226048_at	MAPK8	7,932079541	7,238726646
226271_at	GDAP1	9,484134224	8,653352522
227370_at	FAM171B	10,93627726	9,978148571
221521_s at	GINS2	9,246369204	8,435723207
203919_at	TCEA2	10,1281491	9,239818326
218979_at	RMI1	9,340530023	8,520886145
229289_at	FAM71E1	6,301556301	5,748558973
202533_s at	DHFR	8,050088539	7,343509831
241505_at	NA	8,203194763	7,482979867
1557315_a at	NA	7,161325968	6,531851256
208632_at	RNF10	7,971716411	7,270403005
210380_s at	CACNA1G	6,229544863	5,680981266
220147_s at	FAM60A	9,962599081	9,084828404
37590_g at	NA	7,197919793	6,562583782
213587_s at	ATP6V0E2	11,2573837	10,2634916
231809_x at	PDCD7	9,509834793	8,669787387
226224_at	FOXK2	8,551114966	7,795147677
213186_at	DZIP3	9,170700784	8,359945911
232751_at	RBBP9	7,330658538	6,681749596
217356_s at	PGK1	12,67091571	11,54926009

226710	at	C8orf82	9,283305912	8,461523691
231918	s at	GFM2	8,664359257	7,897199232
210963	s at	GYG2	6,250300828	5,696418348
201342	at	SNRPC	10,51313357	9,58114732
203968	s at	CDC6	8,302590435	7,566307097
203527	s at	APC	7,771138115	7,081424029
209224	s at	NDUFA2	11,24815392	10,24794197
200788	s at	PEA15	12,23258152	11,14374457
1555948	s at	FAM120A	8,792896829	8,010074135
226177	at	GLTP	11,36292939	10,35028697
202677	at	RASA1	10,49759347	9,561570211
226008	at	NDNL2	8,694432393	7,918622276
229305	at	CENPU	6,658181997	6,063528827
210115	at	RPL39L	7,202564825	6,558757777
218663	at	NCAPG	9,440622966	8,596683827
204126	s at	CDC45	8,035709176	7,317282834
218385	at	MRPS18A	8,539330226	7,775568062
231399	at	RAB3IP	6,674202462	6,077136122
1557119	a at	ZNF575	6,455244306	5,877633468
239034	at	LINC01560	7,166956282	6,524509155
214442	s at	PIAS2	8,461370681	7,702875529
241727	x at	DHFRL1	7,955844186	7,24170858
219865	at	LINC00339	8,600468068	7,828401549
221506	s at	TNPO2	10,79363858	9,824229944
203531	at	CUL5	10,24631108	9,325984345
205733	at	BLM	8,493005272	7,72998606
223022	s at	VTA1	9,604112878	8,741256221
204340	at	TMEM187	7,437292898	6,768709069
210144	at	TBC1D22A	6,384048679	5,809203757
219269	at	HMBOX1	8,975447742	8,166996726
226016	at	CD47	10,37629451	9,441346493
212856	at	GRAMD4	9,003415342	8,189550896
206381	at	SCN2A	6,486743638	5,899975466
204542	at	ST6GALNAC 2	5,722985256	5,204785839
201387	s at	UCHL1	11,87226098	10,79709042
201003	x at	NA	9,031512847	8,213313347
225024	at	RPRD1B	8,631198586	7,848367504
236110	at	ST8SIA5	10,8184511	9,837074315
202479	s at	TRIB2	11,3375979	10,30887727
229864	at	ELP6	6,87164874	6,247718286
244166	at	APLN	5,638914424	5,126561854
209514	s at	RAB27A	5,09134999	4,628234195
218383	at	NA	8,260395587	7,508278455
223153	x at	TMUB1	7,428572276	6,75132817
227607	at	STAMBPL1	7,39593347	6,720643931
223729	at	CECR2	6,178121389	5,613437868
223228	at	LDOC1L	10,44423743	9,488738248
218573	at	MAGEH1	9,441400256	8,577131779
202047	s at	CBX6	9,390681704	8,530878278
206039	at	RAB33A	7,765504174	7,054446248
1555281	x at	ARMC8	6,711078725	6,096015013
224698	at	ESYT2	10,11221614	9,184837398
47560	at	ADGRL1	8,823608197	8,014369202
223367	at	DNAJC30	9,167694803	8,326270266
204908	s at	NA	6,684026805	6,070331631
227712	at	LYRM2	9,637231719	8,750784297

201793	x at	SMG7	6,976157619	6,334059995
228257	at	ANKRD52	8,516631886	7,732006133
218272	at	TTC38	7,645301426	6,94041188
226277	at	COL4A3BP	9,872347042	8,961448205
203928	x at	MAPT	8,023670507	7,282947287
203843	at	RPS6KA3	7,957269779	7,221720362
213201	s at	TNNT1	4,716567881	4,280486109
224715	at	WDR34	8,876278401	8,055569708
243603	at	NA	6,141223655	5,573251644
208838	at	CAND1	10,18076379	9,238912032
209234	at	KIF1B	10,28543303	9,332839652
227453	at	UNC13A	5,902505718	5,355702058
1555234	a at	RHOJ	8,458336417	7,674245366
207232	s at	DZIP3	7,580150697	6,877245567
221908	at	RNFT2	8,723475401	7,913723773
227943	at	NA	7,10639504	6,446001205
1554411	at	CTNNB1	8,843738183	8,019688041
208796	s at	CCNG1	11,40809815	10,34455074
229181	s at	HAUS2	8,458084282	7,669501481
218010	x at	PPDPF	6,868366416	6,227294877
214043	at	PTPRD	8,957703212	8,120969482
226272	at	RCAN3	10,20863862	9,253817522
236701	at	NA	7,248307086	6,570324389
225902	at	PPIG	8,41881604	7,631060223
213007	at	FANCI	9,926389489	8,995727532
201573	s at	ETF1	8,979057804	8,137024796
203729	at	EMP3	10,22696101	9,267743968
202777	at	SHOC2	8,741113467	7,920669048
228415	at	API52	8,681565642	7,86628103
228922	at	SHF	6,410845197	5,807257215
204763	s at	GNAO1	6,063961352	5,49239353
235542	at	TET3	9,113288911	8,253101494
214695	at	UBAP2L	7,30552906	6,615614998
222778	s at	WHSC1	8,736256513	7,910541198
231875	at	KIF21A	8,943505185	8,097757589
212264	s at	WAPL	7,770664068	7,035316973
212157	at	SDC2	10,21592714	9,248786187
211561	x at	MAPK14	7,341794493	6,646110461
205034	at	CCNE2	9,690485852	8,772092931
222412	s at	SSR3	8,74530351	7,916138842
209276	s at	GLRX	8,072135162	7,305970945
219785	s at	NA	7,618241459	6,894679172
229504	at	RAB23	8,069990915	7,30227871
218820	at	C14orf132	9,745960776	8,8172607
213175	s at	SNRPB	11,16299902	10,09720452
229649	at	NRXN3	7,703322223	6,966671996
208270	s at	RNPEP	9,522300617	8,611576177
225458	at	PP7080	7,879259704	7,125240778
239413	at	CEP152	8,426290008	7,618886958
203786	s at	TPD52L1	8,30861963	7,512365122
201848	s at	BNIP3	10,90666973	9,860115873
226001	at	KLHL5	9,801708226	8,860954107
211953	s at	IPO5	10,09073341	9,122181835
227197	at	ARHGEF26	9,53845545	8,622707921
225344	at	NCOA7	8,469794105	7,656332361
217960	s at	TOMM22	9,893663932	8,940882404



229064	s at	RCAN3	5,994691909	5,417218043
205379	at	CBR3	8,454440511	7,639732925
218117	at	RBX1	11,40625571	10,30524022
204767	s at	FEN1	10,45696486	9,446937447
213105	s at	TSR3	8,360896355	7,553169854
200739	s at	SUMO3	7,993658456	7,221348018
218585	s at	DTL	9,997638361	9,031527866
203131	at	PDGFRA	12,7050181	11,47482368
206176	at	BMP6	4,406425018	3,979413296
203642	s at	COBLL1	7,141107764	6,448624106
213551	x at	NA	8,092915808	7,307768584
231721	at	JAM3	7,935648244	7,164954486
239128	at	TMEM221	6,43757589	5,811988366
207458	at	RHPN1-AS1	6,579510956	5,940014097
239466	at	DUBR	7,613296496	6,87222612
205691	at	SYNGR3	8,942906369	8,072059352
224761	at	GNA13	10,93387296	9,869074625
209054	s at	WHSC1	9,623847396	8,686496895
205024	s at	RAD51	8,065629466	7,279416531
221843	s at	TLDC1	7,468993768	6,740794362
209686	at	S100B	12,1507471	10,96550891
204128	s at	RFC3	8,114494768	7,321917682
209764	at	MGAT3	6,06577028	5,472979356
201208	s at	TNFAIP1	6,921347919	6,244814769
204766	s at	NUDT1	8,266775519	7,458096321
224656	s at	NA	12,24206101	11,04109507
202306	at	POLR2G	11,42848251	10,30677777
242082	at	MMAB	6,837397392	6,166224609
229889	at	LRRK75A	7,804525823	7,038358557
225552	x at	AURKAIPI	9,993846037	9,011616147
228606	at	TCTEX1D2	8,985489561	8,101754704
208637	x at	ACTN1	9,172099617	8,269520265
218477	at	TMEM14A	10,61505649	9,570460584
201243	s at	ATP1B1	11,27088601	10,16152213
231877	at	TRMT10A	4,752117117	4,2843651
219267	at	GLTP	9,740220327	8,781131369
1555233	at	RHOJ	8,885569663	8,010563342
238700	at	PIAS2	8,345595213	7,523541356
202549	at	VAPB	8,236234409	7,424587444
228843	at	ARL10	10,44500185	9,413686431
225623	at	CIPC	9,388714075	8,461670815
215557	at	NA	4,985080681	4,492592368
1556195	a at	LOC10537679 6	6,963591283	6,273933456
222474	s at	TOMM22	10,35010956	9,3250284
203455	s at	SAT1	10,63464597	9,580086494
224660	at	NA	11,42523144	10,29129108
226712	at	SSR1	8,869765893	7,986862135
226644	at	MIB2	8,139416889	7,32873032
204768	s at	FEN1	9,95795994	8,965903307
217934	x at	STUB1	10,17661013	9,161726036
223466	x at	COL4A3BP	9,34204249	8,409154666
1316	at	THRA	7,386831745	6,64895387
226741	at	SLC12A6	8,921419498	8,02983
234998	at	RAB11A	8,065523664	7,259262668
40020	at	CELSR3	8,32636119	7,493809356
210592	s at	SAT1	11,00058698	9,900570035
209058	at	EDF1	10,68118556	9,612875033
1555279	at	ARMC8	7,013426813	6,311667609
208821	at	SNRPB	10,63762418	9,572013147
225466	at	PATL1	8,50573748	7,653003184
44696	at	TBC1D13	8,49595819	7,642906635
214097	at	RPS21	9,207470356	8,281583537
203880	at	NA	10,33997907	9,299798019
1556301	at	LOC10028701 5	5,09406793	4,581115888
218625	at	NRN1	10,87430991	9,77929244
223413	s at	LYAR	8,579155471	7,713992622
202440	s at	ST5	8,539815267	7,678251462
227479	at	NA	8,253690125	7,420622717
225914	s at	CAB39L	6,583428333	5,918917047
1562012	at	LOC10050673 0	5,976091075	5,372794133
216804	s at	PDLIM5	9,471258701	8,514920515
219706	at	AP5S1	7,548858732	6,786440665
1555370	a at	CAMTA1	8,832877374	7,940698662
207030	s at	CSRP2	12,74168403	11,45353592
238762	at	MTHFD2L	8,539003386	7,675515766
203851	at	IGFBP6	6,945411171	6,242750099
209479	at	CCDC28A	8,161703472	7,335968747
238646	at	NA	7,019134223	6,308385733
228802	at	RBPM5	7,885506192	7,08499823
218005	at	ZNF22	9,183592246	8,251208333
213793	s at	HOMER1	9,903955023	8,89797405
223803	s at	ZCCHC10	7,746331229	6,9581012
233049	x at	STUB1	10,42162628	9,360533694
209420	s at	SMPD1	8,802056761	7,905364099
221923	s at	NPM1	9,838033155	8,835059447
35846	at	THRA	8,282102719	7,437741304
213223	at	NA	8,195827503	7,359799598
213245	at	ADCY1	7,680063504	6,89526634
242317	at	HIGD1A	8,087112343	7,260224993
200744	s at	GNB1	10,47938811	9,40755016
227165	at	SKA3	8,004702884	7,185416735
232183	at	SERAC1	7,350488047	6,596208714
219077	s at	WVVOX	7,151263137	6,417327783
225499	at	RALGAPA2	8,437935126	7,571753597
242358	at	RASSF8-AS1	8,344304982	7,487725778
226092	at	MPP5	9,787384116	8,781114128
208636	at	ACTN1	11,06513857	9,92723279
217942	at	MRPS35	9,678921585	8,682878697
200903	s at	AHCY	10,54723443	9,461004244
204510	at	CDC7	8,913429553	7,995396192
235709	at	GAS2L3	8,045432988	7,216636234
225259	at	RAB6B	7,758621911	6,958705349
209163	at	CYB561	7,559407028	6,779811511
229872	s at	LOC10099674 0	9,318084375	8,356917028
235740	at	MCTP1	7,909693452	7,093523829
203128	at	SPTLC2	7,295856834	6,542736221
1562013	a at	LOC10050673 0	7,727562561	6,929849615
219354	at	KLHL26	6,924266289	6,208653456
236359	at	SCN4B	8,495339059	7,616623432
207668	x at	PDIA6	11,78596338	10,56514672

218128	at	NFYB	8,579559223	7,690656658
243840	at	CLSPN	5,962657114	5,344288495
225693	s at	CAMTA1	10,44071543	9,357640958
205078	at	PIGF	9,776590689	8,762180814
209031	at	CADM1	11,82175088	10,59431853
229838	at	NUCB2	7,74191867	6,935676294
226030	at	ACADSB	7,911764759	7,087344251
203967	at	CDC6	7,837478225	7,020567302
223021	x at	VTA1	9,571658793	8,573665322
235609	at	BRIP1	7,864805595	7,044331239
228562	at	ZBTB10	8,761336557	7,847221001
213988	s at	SAT1	10,16220676	9,101154005
207801	s at	RNF10	9,724124184	8,708559869
203879	at	PIK3CD	6,810894876	6,099423252
239624	at	LOC10272468 9	7,83886608	7,019727537
205489	at	CRYM	7,925032918	7,095946134
235672	at	MAP6	7,864793241	7,039611603
234331	s at	FAM84A	9,182940532	8,218579503
1553978	at	BORCS8	7,525185334	6,734531896
226278	at	SVIP	7,382529755	6,60670515
202073	at	OPTN	7,593802637	6,795645492
228457	at	PPM1L	5,542286145	4,959323735
230508	at	DKK3	8,4549414	7,564932362
223409	at	FOXK2	5,624486432	5,032377576
210449	x at	MAPK14	7,310962226	6,54091777
212332	at	RBL2	8,015902028	7,170592516
239752	at	CECR2	8,044164096	7,195325265
212985	at	APBB2	9,232456629	8,257978
222392	x at	PERP	10,56657633	9,451222906
226987	at	RBM15B	8,013701397	7,16585449
219723	x at	AGPAT3	6,348165317	5,675933422
209059	s at	EDF1	10,97465325	9,812238619
200787	s at	PEA15	10,30168375	9,210339847
217930	s at	TOLLIP	7,98845951	7,141576435
218845	at	DUSP22	9,023364125	8,066430619
228448	at	MAP6	7,347821455	6,568090163
242723	at	NA	6,174518362	5,518790498
206789	s at	POU2F1	7,787847759	6,960608381
219288	at	C3orf14	9,929186775	8,873621686
224564	s at	RTN3	11,06981319	9,891980292
218580	x at	AURKAIP1	9,876128103	8,824230443
214801	at	TOR1AIP2	8,441200546	7,541685606
208639	x at	PDIA6	11,77468996	10,51764446
213279	at	DHRS1	8,086206534	7,222515375
213242	x at	CEP170B	8,992067754	8,031541966
225574	at	RWDD4	9,65065282	8,61933168
205417	s at	DAG1	10,53105268	9,405407836
230706	s at	CAMK2N2	8,30997434	7,421082925
241471	at	NA	4,750776464	4,242560158
218163	at	MCTS1	9,78410696	8,737251733
202234	s at	SLC16A1	9,411694246	8,404510357
207124	s at	GNB5	8,004584502	7,147466267
226993	at	TRIP12	9,190115902	8,206032881
1553974	at	C22orf39	7,778628279	6,94438912
223303	at	FERMT3	5,735037366	5,119736554
219215	s at	SLC39A4	7,12663231	6,361158094

235037	at	TMEM41A	7,487578804	6,682846614
223173	at	SPNS1	8,094142628	7,223977641
212128	s at	DAG1	7,487051369	6,681997869
214239	x at	NA	8,989075344	8,021753405
216069	at	PRMT2	6,792285226	6,06035661
206743	s at	ASGR1	5,811151475	5,184839564
227176	at	SLC2A13	8,658498995	7,724585258
202484	s at	MBD2	9,713467548	8,664499649
226918	at	NA	8,08944669	7,215144844
201135	at	ECHS1	9,902575449	8,831895701
218988	at	SLC35E3	8,757660483	7,810697925
213710	s at	CALM1	8,839070437	7,882753759
217894	at	KCTD3	9,445473863	8,421163987
221524	s at	RRAGD	10,045792	8,955554646
227761	at	MYO5A	9,288757481	8,280323042
224522	s at	DCAKD	8,320959509	7,416299495
213657	s at	NA	7,668340361	6,834609421
210201	x at	BIN1	8,184660872	7,292221838
223038	s at	FAM60A	8,588272161	7,650478389
214441	at	STX6	7,169826518	6,3857187
201860	s at	PLAT	9,700665351	8,637744766
222680	s at	DTL	7,905410469	7,038069741
219034	at	PARP16	7,379346236	6,56954911
238520	at	TRERF1	7,379051833	6,568199441
203566	s at	AGL	8,935876395	7,953697529
224954	at	NA	8,823938088	7,853967019
219625	s at	COL4A3BP	9,499743098	8,45547643
202204	s at	AMFR	8,687160533	7,731285566
234992	x at	ECT2	7,687058479	6,841196151
226871	s at	ATG4D	6,96596244	6,199142203
231599	x at	DPF1	7,085570523	6,303768472
230497	at	CELF5	7,948792167	7,071134632
221593	s at	RPL31	8,141209834	7,24223059
1558626	at	NA	6,720288829	5,977901077
218176	at	MAGEF1	8,633534348	7,679464218
232224	at	MASP1	6,680013935	5,941106036
223320	s at	ABCB10	8,824615904	7,848191733
219703	at	MNS1	8,469018142	7,531739481
219006	at	NDUFAF4	9,243853561	8,220820391
218725	at	SLC25A22	6,957066939	6,187111775
231912	s at	TECPR1	7,960849577	7,079582989
204022	at	WWP2	7,358996568	6,543845251
214365	at	TPM3	6,615107303	5,882146889
204040	at	RNF144A	8,023184142	7,134091109
218032	at	SNN	11,00989383	9,789589812
204823	at	NAV3	9,161978276	8,145216776
218006	s at	ZNF22	8,485880378	7,541681786
205893	at	NLGN1	9,253707653	8,22317377
218483	s at	IFT46	8,466015276	7,522208224
220466	at	CCDC15	7,624746251	6,77443077
201207	at	TNFAIP1	9,134950047	8,116096163
244080	at	NA	4,799938625	4,264290479
203550	s at	FAM189B	9,140576781	8,119442477
216640	s at	PDIA6	11,27226704	10,01267168
1555945	s at	FAM120A	9,581591853	8,508542947
209621	s at	PDLIM3	7,60842006	6,755817063

210102_at	VWA5A	7,867788477	6,985672268
202846_s_at	PIGC	9,489930122	8,423937776
225679_at	NAA30	9,171578492	8,140654102
1556047_s_at	MAGEE1	8,013610488	7,112394806
233401_at	NA	7,682604253	6,817597506
225214_at	LOC10012903 4	8,855803637	7,858481318
1567222_x_at	ELOVL5	5,247554788	4,656447132
203927_at	NFKBIE	6,907250872	6,129102606
229057_at	SCN2A	7,471448789	6,627781462
209794_at	SRGAP3	8,250403721	7,317944904
223465_at	COL4A3BP	9,282159122	8,232993066
202223_at	STT3A	9,96865444	8,841552071
226146_at	HEIH	9,280269064	8,229620644
219545_at	NA	8,362655081	7,415772844
211088_s_at	PLK4	5,026289433	4,457095385
209146_at	MSMO1	11,38845454	10,09736416
203081_at	CTNBP1	9,555860995	8,472054397
227259_at	CD47	7,883544884	6,988908243
203532_x_at	CUL5	7,845523518	6,953431408
242486_at	NA	6,01623046	5,330531384
228003_at	RAB30	6,416887818	5,685478194
219236_at	PAQR6	8,708421736	7,71493746
207847_s_at	MUC1	4,919560317	4,357455276
239913_at	SLC10A4	9,216276937	8,160798427
58916_at	NA	8,124147375	7,192853895
1556043_a_at	TTN-AS1	5,342915952	4,729329963
201247_at	SREBF2	8,361199471	7,400609228
209643_s_at	PLD2	7,031944576	6,223258203
230871_at	DHX30	8,767028133	7,758723307
227572_at	USP30	8,86016399	7,841125735
224707_at	CYSYM1	9,492132681	8,39977659
235219_at	EXOC3-AS1	6,908820001	6,113693903
205888_s_at	JAKMIP2	8,511333953	7,530587782
223652_at	AS3MT	8,024884306	7,099350044
217220_at	LOC10028738 7	4,193207997	3,709448099
218283_at	SSI1L2	9,612958729	8,501527368
240407_at	LOC10012678 4	6,067844034	5,365904223
228880_at	NAT8L	6,613815404	5,848643519
227424_x_at	URB1-AS1	7,295821573	6,451728513
209334_s_at	PSMD9	6,175545386	5,461058271
207010_at	GABRB1	7,779283274	6,877700869
241360_at	CCDC15	7,148496958	6,319613782
203242_s_at	PDLIM5	8,780136762	7,761649936
65630_at	TMEM80	7,472704539	6,604774437
213847_at	PRPH	8,107721089	7,165992109
218741_at	CENPM	8,627481464	7,624964642
1557070_at	TFAP2A-AS1	6,60700217	5,839219062
231952_at	NA	7,94458167	7,02117941
211499_s_at	MAPK11	7,540351766	6,663614185
222976_s_at	TPM3	11,78762623	10,41552112
1561485_at	IQCA1	4,457110091	3,938218853
202048_s_at	CBX6	9,345529816	8,256981277
225095_at	SPTLC2	8,062132649	7,120960557
224888_at	EPT1	7,893974925	6,970301365

204886_at	PLK4	7,974429718	7,039906048
216593_s_at	PIGC	8,349946279	7,371099903
211126_s_at	CSRP2	12,20381889	10,77138959
227658_s_at	PLEKHA3	7,559860116	6,670628312
230118_at	GEMIN6	6,630084839	5,849727809
217744_s_at	PERP	9,411214065	8,303378351
227838_at	UNC5C	7,78582969	6,868544383
203349_s_at	ETV5	11,5260641	10,16744245
223182_s_at	AGPAT3	9,011245992	7,947548948
202403_s_at	COL1A2	7,452881073	6,57277099
223471_at	RAB3IP	9,330519998	8,228436755
210416_s_at	CHEK2	7,360242418	6,490682455
218170_at	ISOC1	9,204510306	8,11663167
204279_at	PSMB9	9,802709421	8,643856095
203147_s_at	TRIM14	8,315300658	7,330852469
227539_at	GNA13	8,605733371	7,583355133
230314_at	NA	6,485327433	5,714056072
225447_at	GPD2	9,206803501	8,111420047
239295_at	SRSF12	6,904556552	6,08149545
201897_s_at	CKS1B	10,66044942	9,387622243
206401_s_at	MAPT	7,714493133	6,792821684
242762_s_at	FAM171B	8,015058243	7,056308402
224653_at	EIF4EBP2	9,624148342	8,470898169
227283_at	EFR3B	8,327759834	7,329851747
208206_s_at	RASGRP2	5,305219722	4,669211701
205475_at	SCRG1	12,4603398	10,96546679
1563687_a_at	FRYL	6,188949889	5,444985417
224661_at	NA	9,194415738	8,088910696
208669_s_at	EID1	11,01931733	9,693056891
214036_at	EFNA5	7,463502284	6,565193364
218055_s_at	WDR41	9,825903909	8,641370957
213172_at	TTC9	5,96360001	5,244294636
241710_at	C1GALT1C1 L	6,539275919	5,750518315
205452_at	PIGB	7,751318289	6,815657309
227603_at	NA	8,398582351	7,384453996
222986_s_at	SHISA5	9,676310933	8,507799626
210585_s_at	TNPO2	5,988679506	5,265194396
231420_at	GGN	5,288139853	4,649021929
214436_at	FBXL2	7,304734131	6,421500716
1555565_s_at	TAPBP	6,6735224	5,866175599
201010_s_at	TXNIP	12,29489201	10,80743357
223046_at	EGLN1	11,30729792	9,936283779
242447_at	C3orf70	9,39038788	8,251493559
224608_s_at	VPS25	9,951908413	8,744232638
202205_at	VASP	7,613234313	6,689305074
201526_at	ARF5	10,33144281	9,076705607
239730_at	NA	4,951836576	4,350249677
201886_at	DCAF11	7,642505403	6,71359061
215481_s_at	PEX5	5,55162119	4,876793298
225536_at	TMEM54	8,347698643	7,332890678
211495_x_at	NA	5,914807492	5,195447262
222301_at	C1orf61	8,89791226	7,815603061
1554017_at	NA	6,4790477	5,690333839
209137_s_at	USP10	9,306415712	8,173314755
229274_at	GNAS	7,990107438	7,016876212
217080_s_at	HOMER2	6,836012956	6,002612992

206601_s at	NA	5,99233536	5,261072287
240528_s at	EXOC4	6,757040759	5,9308108
242655_at	BARD1	7,601530875	6,671313159
201242_s at	ATP1B1	11,40631221	10,00843442
205011_at	VWA5A	7,039228161	6,17558809
218101_s at	NA	11,56652618	10,1457963
219294_at	CENPQ	7,520587771	6,596328977
1560339_s at	NAP1L4	9,811786146	8,605639423
231097_at	NA	5,80893181	5,094749951
214439_x at	BIN1	7,959544228	6,979386498
217765_at	NRBP1	8,59118854	7,533053012
207738_s at	NCKAP1	11,25180527	9,864787688
242774_at	SYNE2	7,215809076	6,325124741
228725_x at	PRMT2	9,955752819	8,726432927
1556190_s at	LOC100507516	3,389887445	2,971232846
226925_at	PXYLP1	10,97057136	9,613326637
211935_at	ARL6IP1	12,95882888	11,35441445
213375_s at	N4BP2L1	6,785232959	5,944985776
223785_at	FANCI	6,602980773	5,785276547
214157_at	GNAS	8,618168583	7,550395695
208692_at	RPS3	12,71865117	11,14018666
209308_s at	BNIP2	9,432465929	8,261655244
224962_at	C9orf69	8,761865489	7,674091474
205162_at	ERCC8	8,161039231	7,147760664
217938_s at	KCMF1	10,16191558	8,899998101
201079_at	SYNGR2	7,880288783	6,901380263
209143_s at	CLNS1A	10,59399478	9,27772794
209136_s at	USP10	8,52781142	7,467632772
235456_at	NA	8,445741122	7,395744079
223408_s at	FOXK2	7,165992685	6,272491702
227254_at	POU2F1	8,336382726	7,293784761
200020_at	TARDBP	10,76903008	9,421862656
212533_at	WEE1	10,43370823	9,128271353
221951_at	TMEM80	7,175345298	6,276410006
223434_at	GBP3	9,273634478	8,110318325
1556346_at	COTL1	5,572807153	4,873224227
241998_at	C2orf80	9,246800953	8,085653466
201248_s at	SREBF2	7,853421164	6,866410598
216389_s at	DCAF11	6,618206765	5,785897161
1552618_at	STX6	8,330097063	7,282015598
230574_at	NA	5,956724774	5,206992443
209841_s at	LRRN3	11,7160576	10,24056367
213351_s at	TMCC1	9,685960137	8,466039766
222297_x at	RPL18	4,452169413	3,89132149
236852_at	FBXO43	6,37992412	5,576204462
224437_s at	VTA1	10,09660037	8,82293483
1568873_at	ZNF519	5,039005505	4,402281688
238965_at	C21orf2	6,284974751	5,490502282
203348_s at	ETV5	10,89349754	9,515371636
223556_at	HELLS	6,875838628	6,00491422
220233_at	FBXO17	8,635719716	7,541559779
238975_at	MMAB	6,095897362	5,322508938
236718_at	MYO10	6,772225985	5,91193741
223249_at	CLDN12	9,668026972	8,438936802
1554883_a at	ERCC8	7,555614389	6,594682238
227476_at	LPGAT1	7,609013178	6,640634234

211814_s at	CCNE2	8,435872905	7,361244258
209840_s at	LRRN3	11,57024422	10,09553093
203929_s at	MAPT	7,243981894	6,320652997
205268_s at	ADD2	6,681259497	5,829516219
224981_at	TMEM219	9,701767564	8,464207269
231313_at	NA	5,020003709	4,379264111
225227_at	SKIL	7,868749165	6,863181278
1556646_at	DCTN5	9,298960573	8,110097437
205166_at	CAPN5	6,962004239	6,07187955
209032_s at	CADM1	11,61603666	10,13061682
202598_at	S100A13	9,671648397	8,433599307
225512_at	ZBTB38	9,185691734	8,009621373
220387_s at	HHLA3	7,156811185	6,240267149
211698_at	EID1	10,36733228	9,03918897
238654_at	VSIG10L	3,780769624	3,296214106
235046_at	INPP4B	8,598021078	7,49565912
208398_s at	TBPL1	9,2370611	8,051810736
224960_at	SCYL2	10,00579189	8,721899641
218309_at	CAMK2N1	10,78044055	9,396913553
230241_at	TOR1AIP2	6,333539762	5,520238041
225692_at	CAMTA1	10,55588156	9,20028015
226388_at	TCEA3	8,308865201	7,239311027
218021_at	NA	8,411499816	7,327676748
210964_s at	GYG2	7,044404235	6,135820191
223005_s at	TMEM245	8,660737439	7,543660259
223414_s at	LYAR	7,022130548	6,116385481
228722_at	PRMT2	7,859118076	6,844454087
217790_s at	SSR3	6,811825881	5,931839502
220797_at	NA	6,990699122	6,086940892
221279_at	GDAP1	6,767906894	5,892147358
216959_x at	NRCAM	9,009686889	7,840496088
228565_at	KIAA1804	5,958697829	5,185352857
1552579_a at	ADAM21	4,770077267	4,150265536
211087_x at	MAPK14	6,083679557	5,293121641
228560_at	CHDH	6,037143443	5,252456786
228646_at	PPP1R1C	7,367729668	6,409509256
222609_s at	EXOSC1	8,17747218	7,111281288
205152_at	SLC6A1	7,646717158	6,649131446
212970_at	APBB2	8,545016019	7,427200273
225376_at	GID8	10,22115074	8,883440887
218980_at	FHOD3	7,819097448	6,794422154
225435_at	SSR1	9,828792834	8,540035232
222396_at	HN1	11,10498799	9,648797099
223340_at	ATL1	8,910602424	7,74207335
218537_at	HCFC1R1	8,537260887	7,417578955
1564883_a at	TAS1R1	4,710879574	4,092998673
210508_s at	KCNQ2	10,7115159	9,305017089
208670_s at	EID1	11,12053086	9,66025931
237270_at	NA	8,101315073	7,036223733
206582_s at	ADGRG1	6,461883726	5,610768669
204594_s at	MIEF1	8,692781047	7,547176491
213745_at	ATRNL1	7,13346461	6,192354309
242624_at	ABLIM2	5,94194062	5,157044874
238758_at	NA	5,69894162	4,946027804
218187_s at	C8orf33	9,808583901	8,511809994
226088_at	ZDHHC12	7,175592888	6,22670404

236174_at	NA	5,437971614	4,717045151
220140_s_at	SNX11	8,099057337	7,024965399
229584_at	LRRK2	6,578164644	5,704711596
211975_at	ARFGAP2	8,901699082	7,718111237
228721_at	KRBOX1	8,329900469	7,221989111
227112_at	TMCC1	10,3758148	8,995584555
202564_x_at	ARL2	8,473840888	7,345672536
219211_at	USP18	7,455139284	6,462543792
224734_at	HMGB1	9,941083596	8,615077661
227890_at	TMEM198	7,952686869	6,891702342
211056_s_at	SRD5A1	7,824592962	6,77986461
204825_at	MELK	9,438316043	8,177405774
244704_at	NFYB	4,18094714	3,621377321
209237_s_at	SLC23A2	7,052059886	6,108148988
213253_at	SMC2	7,468243165	6,467354771
218857_s_at	ASRGL1	9,063604322	7,848527763
224100_s_at	DPYSL5	7,129027874	6,1728129
235562_at	C3orf70	7,883558995	6,82593138
213852_at	NA	10,55680101	9,140005698
217978_s_at	UBE2Q1	10,28360062	8,903282159
202472_at	MPI	7,401167212	6,405051171
228302_x_at	CAMK2N1	8,197976135	7,094416535
205120_s_at	SGCB	10,46733048	9,057278162
200083_at	USP22	11,13946468	9,637395359
221265_s_at	VWA9	8,839508091	7,64666917
230109_at	PDE7B	7,828186252	6,770602367
239326_at	NA	4,768634453	4,124159489
225991_at	TMEM41A	7,266893391	6,284781288
243405_at	NA	7,006511053	6,059060208
202931_x_at	BIN1	8,131090781	7,031246105
240357_at	NA	5,547873679	4,797433475
220651_s_at	MCM10	6,773006015	5,855425119
219170_at	FSD1	7,785934895	6,73071358
203593_at	CD2AP	8,738579999	7,553817428
228033_at	E2F7	10,04069143	8,672474149
207836_s_at	RBPMS	7,461128229	6,44429074
232416_at	CELF5	7,176394971	6,194474645
201490_s_at	PPIF	7,755314414	6,69417626
217514_at	ST8SIA5	8,228426472	7,102290641
224671_at	MRPL10	9,217594506	7,955574165
218561_s_at	LYRM4	9,762803835	8,425334409
223362_s_at	SEPT3	7,390309822	6,377805068
1554408_a_at	TK1	7,897411838	6,812725944
235117_at	CHAC2	7,734122127	6,670724481
231723_at	SNX12	7,193013384	6,203983683
239854_at	SYCE3	6,097807365	5,258606326
209230_s_at	NUPR1	6,797408111	5,861004893
208609_s_at	NA	6,103785872	5,262297773
236270_at	NFATC4	6,373843668	5,495124429
238504_at	SDHAF4	8,526520523	7,347023622
226785_at	ATP11C	8,125174554	7,000892821
221193_s_at	ZCCHC10	8,302751383	7,153559063
224613_s_at	DNAJC5	7,233097808	6,231948762
211276_at	TCEAL2	8,738322276	7,527701429
39966_at	CSPG5	9,506976158	8,188481205
208788_at	ELOVL5	11,43158056	9,845787597

204392_at	CAMK1	7,525219346	6,480854832
232547_at	SRCIN1	6,972280519	6,003809432
202764_at	STIM1	6,691910363	5,761790314
241355_at	HR	7,784714965	6,70165398
1555775_a_at	ZAR1	5,830137198	5,018265295
201414_s_at	NAP1L4	9,381096909	8,074210523
217726_at	COPZ1	9,988370012	8,595230903
241905_at	PIK3C2A	8,024594869	6,905044871
206045_s_at	NOL4	7,513780636	6,463721939
205889_s_at	JAKMIP2	6,389756139	5,496477232
235685_at	NA	6,883024679	5,918751281
242975_s_at	NA	7,370635219	6,33802059
238574_at	SLC25A51	6,519981263	5,606193548
1558225_at	NA	2,924340864	2,514332399
225283_at	ARRDC4	10,42355837	8,961788866
217499_x_at	NA	7,048146132	6,059530228
238605_at	NOL4	6,947674444	5,972620067
200740_s_at	SUMO3	11,22714889	9,6491414
215518_at	STXBP5L	4,537184605	3,898984014
209513_s_at	HSDL2	9,547933559	8,204527467
210127_at	RAB6B	6,40765857	5,505731522
202670_at	MAP2K1	10,43249732	8,962675655
204421_s_at	FGF2	6,523277185	5,603095873
241416_at	NA	5,452197761	4,682100492
1553479_at	TMEM145	6,078472944	5,219394145
226572_at	SOCS7	8,539175565	7,331681395
225817_at	CGNL1	7,840007858	6,730464853
212669_at	CAMK2G	7,123440156	6,114137363
222139_at	ERV3-2	5,716925999	4,905738881
223854_at	NA	8,753355312	7,511226287
200999_s_at	CKAP4	11,18234189	9,594251446
201397_at	PHGDH	7,955795973	6,824129267
212301_at	RTF1	10,10769462	8,668823549
205412_at	ACAT1	10,54927073	9,047402354
213264_at	PCBP2	6,655021042	5,705153461
212092_at	PEG10	11,67629369	10,0061451
226852_at	MTA3	6,922601231	5,931096449
213923_at	RAP2B	9,797917385	8,393749904
225489_at	TMEM18	8,466159823	7,252737248
200974_at	ACTA2	8,762599105	7,506205725
207074_s_at	SLC18A1	9,148770998	7,832940983
211926_s_at	MYH9	8,053819929	6,894366894
200998_s_at	CKAP4	10,40512057	8,907145015
229822_at	PARVB	7,49090127	6,411555651
242001_at	NA	4,535506392	3,880652312
200028_s_at	STARD7	11,098742	9,494936037
205344_at	CSPG5	6,986508419	5,976668756
1569796_s_at	ATRNL1	7,097779466	6,069031352
215170_s_at	CEP152	5,78027284	4,942468774
208978_at	CRIP2	9,621300248	8,226131021
202203_s_at	AMFR	9,122066282	7,797599591
216945_x_at	PASK	6,196457215	5,295472994
205376_at	INPP4B	7,732798742	6,607430894
225001_at	RAB3D	7,834497631	6,693591157
230502_s_at	NA	6,576163139	5,618040759
205698_s_at	MAP2K6	8,176360148	6,984213269

213362_at	PTPRD	7,638506887	6,523807281
37433_at	PIAS2	7,841248638	6,695670215
205050_s_at	MAPK8IP2	6,010788856	5,132326316
207525_s_at	GIPC1	8,937873806	7,625430298
213352_at	TMCC1	8,628592857	7,358523744
1556789_a_at	PAXBPI-AS1	4,7230317	4,026431401
206093_x_at	NA	7,262891058	6,19122877
222730_s_at	ZDHC2	7,358132229	6,271977518
242760_x_at	PIGB	6,755470492	5,757012541
236311_at	LOH12CR2	7,023384167	5,984661726
214087_s_at	MYBPC1	6,492500103	5,532064972
203619_s_at	FAIM2	6,857895997	5,84339272
208877_at	PAK2	9,942779532	8,469039427
214373_at	NA	6,823687185	5,812062918
225876_at	NIPAL3	10,01608139	8,525797566
213272_s_at	TMEM159	6,946135146	5,912476041
202338_at	TK1	7,188091726	6,118118425
201009_s_at	TXNIP	11,65440214	9,919464607
224684_at	SNX12	8,887311091	7,563654278
214121_x_at	PDLIM7	6,144258117	5,228509609
229111_at	NA	8,189428647	6,968058965
202235_at	SLC16A1	8,623701816	7,336644411
228773_at	LOC100506100	7,117553375	6,055127066
1555852_at	PSMB8-AS1	7,163943187	6,093394129
217993_s_at	MAT2B	10,66318285	9,069608881
224931_at	SLC41A3	7,571584519	6,438340082
229264_at	NA	6,238480907	5,303270989
224611_s_at	DNAJC5	9,323525306	7,924802483
223007_s_at	TMEM245	9,929003596	8,438792942
223749_at	C1QTNF2	7,049720347	5,991513952
225198_at	VAPA	9,783587416	8,313128253
212297_at	ATP13A3	9,342216999	7,937291605
224612_s_at	DNAJC5	8,856401873	7,521476307
236761_at	LHFPL3	12,40976332	10,53824837
1569022_a_at	PIK3C2A	6,926291509	5,881313712
235572_at	SPC24	8,433477136	7,160548364
230942_at	CMTM5	6,761560344	5,739981521
213535_s_at	UBE2I	10,94202967	9,285951303
203007_x_at	LYPLA1	9,633967828	8,174910581
228338_at	COLCA2	6,455451228	5,477774941
205712_at	PTPRD	7,022355269	5,958812022
213256_at	MARCH3	7,111650286	6,032507025
201771_at	SCAMP3	9,540201613	8,09173895
201933_at	CHMP1A	8,792413562	7,454798925
220231_at	PPP1R17	4,547956485	3,855238861
218711_s_at	SDPR	5,126422934	4,345125655
221613_s_at	ZFAND6	11,43655514	9,692213385
202912_at	ADM	10,83474866	9,180824569
200695_at	PPP2R1A	10,07671024	8,536464258
204730_at	RIMS3	7,718280913	6,538313715
1556269_at	MYT1	4,845326706	4,104427782
228792_at	MYEF2	6,503122232	5,508335932
231828_at	PSMD5-AS1	7,511614902	6,361246544
220486_x_at	NA	7,398480426	6,264494472
223008_s_at	TMEM245	10,43783065	8,837651322

219791_s_at	HAND2-AS1	4,454567707	3,771020938
214744_s_at	NA	5,808132271	4,916708652
202330_s_at	UNG	8,522862755	7,212598294
201008_s_at	TXNIP	11,14990671	9,434015548
206051_at	ELAVL4	8,232437451	6,964241366
226183_at	GSK3B	8,419938018	7,121347416
216375_s_at	ETV5	8,827064563	7,465640845
209078_s_at	TXN2	9,631250744	8,145157878
236834_at	SCFD2	9,439574887	7,982651878
200011_s_at	ARF3	10,02815023	8,479658871
240857_at	DNAH9	4,578142014	3,871129589
217289_s_at	SLC37A4	7,27622435	6,151919326
224753_at	CDCA5	9,124768248	7,713947021
201870_at	TOMM34	9,670372698	8,175053021
225487_at	TMEM18	6,80945003	5,755587556
201087_at	PXN	7,749559028	6,54998677
218102_at	DERA	9,731026954	8,224713465
235072_s_at	KIF13A	9,124510899	7,711956557
235785_at	NA	6,184140253	5,226653141
202464_s_at	PFKFB3	9,548474552	8,070067917
1552947_x_at	ZNF114	5,544540425	4,684616928
213174_at	TTC9	6,065477349	5,123774189
222857_s_at	KCNMB4	8,857899419	7,482516194
226029_at	VANGL2	9,123656947	7,706661858
226112_at	SGCB	10,86710484	9,179026816
226923_at	SCFD2	11,25461981	9,505601269
212449_s_at	LYPLA1	9,84368831	8,312604958
227153_at	IMMP2L	9,756830942	8,238593363
235422_at	NA	7,60972426	6,424648232
227731_at	CNBP	8,090024061	6,82963788
217856_at	RBM8A	9,720318092	8,20528413
1553288_a_at	NYAP1	6,637396236	5,601706043
211613_s_at	GPD2	5,13873672	4,33676591
202269_x_at	GBP1	8,19703189	6,917533926
204081_at	NRGN	7,384664626	6,230033437
235697_at	NA	5,347168439	4,51091769
228861_at	CDS2	6,196238591	5,226470283
213534_s_at	PASK	6,493433757	5,476170686
45714_at	HCFC1R1	8,969141053	7,563161738
213424_at	KIAA0895	7,927252304	6,68310984
213712_at	ELOVL2	10,0353965	8,456994978
228096_at	MINOS1	7,070793002	5,955844388
227107_at	PANX1	9,878740629	8,318847547
222376_at	NA	6,441506516	5,424254265
1554027_a_at	SLC4A4	5,148797418	4,335535201
219172_at	UBTD1	6,466905715	5,443906063
205234_at	SLC16A4	9,127880855	7,683660462
215711_s_at	WEE1	8,923502702	7,51160245
212180_at	CRKL	10,55848411	8,887275227
226748_at	LYSMD2	9,146564524	7,697343622
226117_at	TIFA	7,286552454	6,130571916
202270_at	GBP1	8,343698386	7,018990803
204070_at	RARRES3	7,959373346	6,693392268
222805_at	MANEA	8,608489408	7,238117931
238073_at	ELAVL4	8,398963143	7,061433534
210202_s_at	BINI	6,496811018	5,462184085

219010_at	C1orf106	8,853069542	7,442759213
225098_at	ABI2	10,74101265	9,028845115
208992_s_at	STAT3	10,10250265	8,491895842
223276_at	SMIM3	11,35280337	9,539174002
216105_x_at	PPP2R4	8,068178576	6,778862036
203362_s_at	MAD2L1	10,76710182	9,04610214
218190_s_at	UQCR10	12,1976852	10,24798195
236207_at	SSFA2	7,942813394	6,670462132
223006_s_at	TMEM245	9,782846037	8,214891652
206452_x_at	PPP2R4	8,218744535	6,895652093
243287_s_at	OSTM1	4,880569808	4,093808077
223868_s_at	WVOX	5,078333833	4,259124547
204000_at	GNB5	7,896430538	6,621100326
206857_s_at	FKBP1B	9,192744706	7,707264903
213050_at	COBL	7,953214294	6,666858508
209965_s_at	RAD51D	6,97473467	5,845912611
210959_s_at	SRD5A1	8,470129363	7,097926129
223707_at	NA	4,409951612	3,694451771
222764_at	ASRGL1	8,342321119	6,987963507
209512_at	HSDL2	8,519122042	7,134755334
212800_at	STX6	8,32036469	6,966118056
208424_s_at	CIAPIN1	9,532141497	7,978487954
1555900_at	DCTN5	7,845226532	6,565537148
226292_at	CAPN5	8,683963815	7,267452238
220532_s_at	TMEM176B	7,141576781	5,973217553
225864_at	FAM84B	9,639188699	8,061306479
232230_at	OLMALINC	6,804911071	5,68917731
209077_at	TXN2	9,506517759	7,947562377
207231_at	DZIP3	6,950513739	5,810393973
211366_x_at	CASP1	6,616596228	5,530927449
205141_at	ANG	6,336670631	5,296605234
207012_at	MMP16	7,842411227	6,553010548
225112_at	ABI2	10,78047984	9,004797636
228662_at	SOCS7	9,146267595	7,636958202
213131_at	OLFM1	9,63230443	8,040554536
206502_s_at	INSM1	10,87072667	9,074317022
217188_s_at	C14orf1	8,959481743	7,477880744
223784_at	TMEM27	4,741570979	3,956299583
233437_at	GABRA4	5,117633638	4,270033876
227897_at	NA	9,293077847	7,753053151
203854_at	CFI	8,31234116	6,933832625
213280_at	RAP1GAP2	5,444883262	4,541639185
222797_at	DPYSL5	8,816198223	7,353237005
213009_s_at	TRIM37	10,75494947	8,968944531
212757_s_at	CAMK2G	8,254992185	6,883557324
219461_at	PAK6	5,089063695	4,243441582
219175_s_at	SLC41A3	7,598696892	6,333145883
236170_x_at	NA	7,298492511	6,082609251
211622_s_at	ARF3	8,074160877	6,728092989
212973_at	RPIA	8,957720409	7,464103426
1553633_s_at	NA	5,486192157	4,570621613
236372_at	PANX1	6,215361717	5,176006699
205586_x_at	VGF	5,678129842	4,727719033
1554768_a_at	MAD2L1	10,09913024	8,407684723
1557038_s_at	UBAC2-AS1	6,915947039	5,757518646
205303_at	KCNJ8	7,295854209	6,073422474

203908_at	SLC4A4	8,549883212	7,11652432
227998_at	S100A16	11,58679909	9,642263625
226350_at	CHML	8,005679274	6,66160285
228274_at	SDSL	7,808726669	6,497433766
218332_at	BEX1	11,79220492	9,811193454
235024_at	JADE1	6,129530844	5,099432986
202357_s_at	CFB	4,754961724	3,953635792
230625_s_at	TSPAN12	6,954089658	5,780962102
203148_s_at	TRIM14	9,273470716	7,706012556
211503_s_at	RAB14	9,740972905	8,0941882
233230_s_at	SLAIN2	6,161657758	5,11856773
228456_s_at	CDS2	10,41646076	8,652167068
226431_at	FAM117B	8,339872562	6,927122289
205894_at	ARSE	5,952511311	4,943215383
221497_x_at	EGLN1	8,729510944	7,245905204
202830_s_at	SLC37A4	7,850707534	6,514300749
1553207_at	ARL10	6,046521513	5,016113753
220914_at	NA	4,558924404	3,781477264
219549_s_at	RTN3	11,81014674	9,790257248
219201_s_at	TWSG1	7,607022291	6,305878244
231579_s_at	TIMP2	12,54418957	10,39816789
228051_at	ARFGEF3	7,294530778	6,042415705
201678_s_at	HMCES	8,035505466	6,655910186
37793_r_at	RAD51D	5,79592588	4,79946555
219274_at	TSPAN12	9,791322235	8,10723732
232682_at	MREG	7,518965924	6,224757201
231577_s_at	GBP1	8,143242275	6,740274434
223201_s_at	NA	6,820770541	5,644383526
229733_s_at	NA	7,54668125	6,243017426
235543_at	LOC10272377 9	6,231873359	5,154399001
230201_at	FXR1	7,334740158	6,064632751
229866_at	STK32A	8,553759104	7,072096369
202009_at	TWF2	8,039323647	6,645774252
229321_s_at	NA	8,332065867	6,882861355
235224_s_at	CAND1	6,650243846	5,489772585
202562_s_at	C14orf1	9,556694773	7,888875277
235295_at	PANX1	8,183337732	6,754204178
208874_x_at	PPP2R4	8,285235408	6,835606385
231558_at	INSM1	4,867867512	4,01554418
208078_s_at	NA	8,506321022	7,01613425
204519_s_at	PLLP	7,027856313	5,796644398
219648_at	MREG	9,350685603	7,710327061
228584_at	SGCB	9,452699538	7,791505948
200734_s_at	ARF3	10,39092383	8,564359733
235309_at	RPS15A	8,64069515	7,119751293
225119_at	CHMP4B	8,574261289	7,06340568
222386_s_at	COPZ1	10,32557458	8,503176991
1556213_a_at	BTG3	5,887575595	4,848104632
204723_at	SCN3B	5,030235067	4,141844389
218976_at	DNAJC12	6,405322037	5,272499425
220029_at	ELOVL2	7,952579927	6,540252141
204306_s_at	CD151	9,993307077	8,218085148
235948_at	RIMKLA	7,068780629	5,811645038
228142_at	UQCR10	8,154003287	6,702916198
230393_at	CUL5	5,307460011	4,361950354
1555464_at	IFIH1	4,204873898	3,455738844

224735_at	CYB561A3	7,655768773	6,2912187	208991_at	STAT3	10,7001501	8,615519705
209983_s_at	NRXN2	7,493011558	6,156933506	202656_s_at	SERTAD2	8,551016209	6,883206431
203528_at	SEMA4D	5,504714375	4,521584687	230104_s_at	TPPP	6,944200485	5,588724496
200927_s_at	RAB14	10,20114521	8,378978926	221581_s_at	LAT2	6,087287589	4,898261033
224314_s_at	EGLN1	7,999489673	6,569689663	208829_at	TAPBP	9,139923751	7,345156121
225048_at	PHF10	9,628838333	7,905425183	1553392_at	NA	5,156910288	4,143104292
231925_at	NA	7,410405156	6,083202335	220915_s_at	NA	5,90656316	4,743726308
223614_at	MMP16	9,52595905	7,817324253	229656_s_at	EML6	8,930145402	7,17089972
1555892_s_at	PSMD5-AS1	6,794076827	5,575202999	205375_at	MDF1	7,626695994	6,12357662
236283_x_at	LOC646214	7,369472326	6,045233772	204365_s_at	REEP1	7,563297935	6,070268836
225498_at	CHMP4B	10,7587157	8,819030871	210334_x_at	BIRC5	8,93064795	7,166301144
203180_at	ALDH1A3	4,029750912	3,301838265	205715_at	BST1	6,001974135	4,815849186
205006_s_at	NMT2	7,234915949	5,928019945	236838_at	SRCIN1	6,714598188	5,387242469
236278_at	HIST1H3E	6,731899748	5,515305752	36499_at	CELSR2	9,693058052	7,776663294
212070_at	ADGRG1	11,18861883	9,166484886	1560023_x_at	NA	5,15427875	4,134253587
201883_s_at	B4GALT1	6,229763831	5,103617921	1555310_a_at	PAK6	6,089464002	4,884357104
224638_at	SPPL3	6,860781328	5,619941479	223570_at	MCM10	6,528164025	5,235781278
208968_s_at	CIAPIN1	10,29050281	8,42716861	242294_at	FBXO45	6,931546049	5,550051214
225406_at	TWSG1	10,33572707	8,448040832	224345_x_at	FAM162A	11,45989055	9,173916868
34408_at	RTN2	7,026771296	5,743334564	221236_s_at	STMN4	8,214911198	6,572985198
208760_at	UBE2I	9,062141345	7,402422583	235719_at	CYP4V2	5,696025972	4,554666955
223183_at	AGPAT3	8,278372295	6,75979194	229582_at	INO80C	9,218734594	7,367266843
221220_s_at	SCYL2	8,088720524	6,601874362	204029_at	CELSR2	8,947369398	7,149613092
205227_at	IL1RAP	7,685046509	6,271931628	209323_at	PRKRIR	10,33135628	8,253463309
204437_s_at	FOLR1	6,410175756	5,231412172	209452_s_at	VTIIB	10,25484491	8,183559909
1560503_a_at	TFAP2A-AS1	6,514281878	5,314834919	226576_at	ARHGAP26	5,98639774	4,776874757
214113_s_at	RBM8A	10,90415443	8,886443317	239688_at	SMCIA	5,039794718	4,020865278
238066_at	RBP7	6,152481487	5,006612095	1555867_at	GNG4	7,91937225	6,315150364
203439_s_at	STC2	7,276165344	5,92069169	204364_s_at	REEP1	7,453696542	5,941781133
210007_s_at	GPD2	6,981877981	5,676452882	227547_at	NA	9,188839432	7,324916117
204260_at	CHGB	5,681691527	4,617307303	205304_s_at	KCNJ8	6,708733271	5,346304733
236037_at	ARFGEF3	4,284777482	3,481585238	1555141_a_at	NA	4,535141613	3,611255004
243301_at	COL22A1	3,970631957	3,226116736	225289_at	STAT3	9,873096249	7,84965689
220942_x_at	FAM162A	11,60698601	9,430342137	232553_at	PCYT1B	7,174797314	5,704054153
205440_s_at	NPY1R	8,870822163	7,207246987	201677_at	HMCES	6,691024422	5,319113676
40148_at	APBB2	8,210179494	6,666048764	200782_at	ANXA5	12,25912	9,73119285
225928_at	VTIIB	8,125821529	6,593055131	237365_at	ELOVL2-AS1	6,491970185	5,15317855
223193_x_at	FAM162A	11,5448832	9,3654289	212647_at	RRAS	6,138222564	4,872123116
228811_at	NA	6,19145622	5,022207355	226456_at	RMI2	8,552216223	6,782338491
235346_at	FUNDC1	9,343517408	7,578395937	227997_at	IL17RD	9,580197237	7,593889092
205737_at	KCNQ2	7,784250065	6,309582915	213552_at	GLCE	5,869186254	4,651475594
239202_at	RAB3B	4,717340389	3,821177391	207183_at	GPR19	8,129399438	6,436200998
224560_at	TIMP2	12,11484412	9,810120877	213927_at	MAP3K9	5,990640171	4,739511256
205700_at	HSD17B6	5,568264558	4,508144654	227396_at	PTPRJ	9,998586674	7,907273679
209970_x_at	CASP1	6,440986432	5,208831476	1555826_at	BIRC5	6,797649454	5,375158238
235205_at	OXR1	8,926338139	7,215128218	242785_at	EML6	7,334547839	5,797586362
223925_s_at	MTPN	7,691888088	6,21730984	204995_at	CDK5R1	8,23980874	6,512770036
213419_at	APBB2	8,334667352	6,735307356	1555602_a_at	ELAVL3	7,333880043	5,791956996
202095_s_at	BIRC5	10,15355717	8,202795773	222557_at	STMN3	11,27226807	8,901789831
236721_at	ALKBH1	5,169265364	4,175383593	226579_at	NA	8,847574977	6,97930114
217383_at	PGK1	6,046213964	4,882422576	201998_at	ST6GAL1	7,595531753	5,991075056
233814_at	EFNA5	5,800880672	4,683898394	239729_at	NA	6,294693393	4,964027622
214006_s_at	GGCX	8,195172093	6,615796007	211572_s_at	SLC23A2	5,476599271	4,317856608
1554095_at	RBM33	4,676975153	3,771100435	219645_at	CASQ1	4,291596612	3,383528938
243156_at	NA	5,580462241	4,498003434	1555765_a_at	GNG4	7,840409598	6,181408933
210560_at	GBX2	5,507347442	4,438309731	1554897_s_at	RHBDL2	4,725451053	3,724728327



236312	at	MAD2L1	6,965718254	5,490248533
222391	at	TMEM30A	10,36419142	8,157139728
216247	at	NA	6,235083869	4,905678065
1562736	at	LHX9	3,36094655	2,642389923
205190	at	PLS1	5,814060692	4,556798829
204035	at	SCG2	8,352124064	6,541582498
221564	at	PRMT2	10,52478385	8,241527921
242326	at	COL22A1	7,209077809	5,642917254
213599	at	OIP5	9,22260384	7,216820856
222456	s at	LIMA1	5,648299254	4,419339071
225556	at	VMA21	11,12594136	8,705030445
1554102	a at	TMTC4	9,1139942	7,128589665
217857	s at	RBM8A	8,98037559	7,02382342
229590	at	NA	6,293901419	4,920102327
244088	at	NA	6,410221152	5,005524223
244362	at	NA	5,447116327	4,253363146
239209	at	NA	4,697872656	3,665642245
230163	at	GFRA1	6,45666362	5,035035365
229579	s at	DISP2	7,868420911	6,132818953
225926	at	VTIB	8,747951754	6,816250927
240236	at	STXBPL	6,372717973	4,96428193
215273	s at	TADA3	9,906033418	7,71398442
214949	at	NA	9,665515633	7,524354081
226632	at	CYGB	5,748599196	4,46889419
214948	s at	TMF1	9,813996885	7,628448623
225666	at	TMTC4	10,95852562	8,518007704
229208	at	HAUS2	6,905868488	5,36492135
236369	at	TSPY26P	8,724576068	6,776058876
232523	at	MEGF10	8,139373152	6,317220431
211421	s at	RET	4,763915821	3,696232904
203000	at	STMN2	11,18694719	8,678977377
205368	at	FAM131B	8,17237045	6,337487706
204777	s at	MAL	7,64529942	5,92391273
202657	s at	SERTAD2	8,959462302	6,935681406
205121	at	SGCB	7,902182688	6,116285194
206693	at	IL7	7,790713086	6,027161356
227612	at	ELAVL3	9,165280505	7,089101006
1565951	s at	CHML	5,088685602	3,93517011
218115	at	ASF1B	8,911549653	6,882801016
213150	at	HOXA10	6,685357386	5,161134632
1553938	a at	STK32A	5,523385445	4,262900308
226847	at	FST	7,268160499	5,607261545
240629	at	NA	4,042904668	3,116493609
206751	s at	PCYT1B	4,563809955	3,518017972
212690	at	DDHD2	9,175808543	7,064846388
221932	s at	GLRX5	10,29319039	7,924354643
210255	at	RAD51B	5,777594734	4,444455511
1554101	a at	TMTC4	9,086912824	6,981450756
203001	s at	STMN2	10,81260259	8,291691018
205184	at	GNG4	8,184188192	6,267805052
224926	at	EXOC4	9,801999273	7,502548507
227550	at	GFRA1	8,468427791	6,474577864
235198	at	OSTM1	8,48724871	6,487193286
236550	s at	ZNF311	5,611768261	4,289103572
211782	at	IDS	4,377849606	3,345061657
217757	at	A2M	8,749250544	6,677078284
1553670	at	INTS4	4,505423056	3,435660978
235947	at	LOC101930067	3,723472714	2,83396977
209982	s at	NRXN2	7,849047088	5,972214705
207345	at	FST	5,67292692	4,312398104
224985	at	NRAS	10,38219655	7,861147062
203438	at	STC2	8,956761782	6,777283785
208784	s at	KLHDC3	7,503034856	5,649763275
37512	at	HSD17B6	4,394456501	3,298157895
223095	at	MARVELD1	8,534867971	6,402943517
219763	at	DENND1A	6,801844074	5,102323511
205678	at	AP3B2	6,540721656	4,903208268
206440	at	LIN7A	5,568483015	4,173359325
236551	at	ZNF311	6,386118755	4,78131136
242086	at	SPATA6	8,921854393	6,6768187
223530	at	TDRKH	6,912186461	5,16021225
225004	at	TMEM101	8,253254298	6,156958884
212864	at	CDS2	9,104398662	6,780078503
1569342	at	GLI3	5,929280445	4,403002435
205204	at	NMB	8,410086601	6,238412791
232591	s at	TMEM30A	8,186033428	6,066050492
207400	at	NPY5R	7,030246975	5,207293832
230547	at	KCNC1	7,657417466	5,667620369
206271	at	TLR3	5,658985617	4,188372409
204458	at	PLA2G15	7,719522384	5,704958956
1552502	s at	RHBDL2	4,50251646	3,325223072
231098	at	NA	6,005138057	4,432891623
218196	at	OSTM1	9,985563465	7,338758849
204612	at	PKIA	11,22884001	8,247174299
223500	at	CPLX1	5,092921945	3,7401659
229160	at	MUM1L1	6,000219202	4,404201726
222480	at	UBE2Q1	6,522248019	4,785812529
219196	at	SCG3	4,887788202	3,585211748
202094	at	BIRC5	8,85126371	6,484392971
200887	s at	STAT1	10,30289605	7,54755732
232422	at	GGACT	5,507185656	4,018988069
1555022	at	RGS12	6,84352203	4,97074116
203662	s at	TMOD1	8,852659613	6,428389563
235197	s at	OSTM1	7,765691813	5,633612678
214383	x at	KLHDC3	7,957921714	5,768665572
227196	at	RHPN2	8,252931919	5,958210736
206110	at	NA	6,087293581	4,392235554
211368	s at	CASP1	6,075450313	4,375727699
AFFX-HUMISGF3A/M97935	3 at	STAT1	9,882095897	7,109633789
226864	at	PKIA	9,031280331	6,490801278
239587	at	TLR3	5,367575457	3,853105308
203661	s at	TMOD1	8,87950209	6,328853069
217743	s at	TMEM30A	9,432162614	6,720990141
207455	at	P2RY1	5,700334287	4,053018944
205590	at	RASGRP1	7,888334706	5,591199406
207093	s at	NA	6,889771823	4,867808936
202454	s at	ERBB3	6,050601238	4,271340047
206101	at	ECM2	6,216435718	4,379608039
209875	s at	SPP1	9,812272234	6,900304123
231817	at	USP53	4,296455064	3,015053375

206011_at	CASP1	5,957615828	4,158356168
227132_at	ZNF706	8,157622839	5,687699246
234103_at	KCNT2	5,732226168	3,991594204
205696_s_at	GFRA1	5,820245145	4,036849362
238459_x_at	SPATA6	6,530439216	4,523681101
203650_at	PROCR	5,991611607	4,137068436
205675_at	MTPP	5,420773875	3,70152415
1552703_s_at	NA	5,621819932	3,836782711
204929_s_at	VAMP5	8,544956597	5,820706498
226213_at	ERBB3	6,166365317	4,116929779
215388_s_at	NA	4,717256375	3,140300178
203285_s_at	HS2ST1	8,315735138	5,484387714

205128_x_at	PTGS1	8,145666466	5,345101078
218207_s_at	STMN3	6,998914139	4,570756656
223836_at	FGFBP2	7,505435776	4,87815603
223599_at	TRIM6	5,695811698	3,70007826
214005_at	GGCX	8,474563838	5,480402053
203697_at	FRZB	5,71568871	3,669669278
236517_at	MEGF10	5,95570663	3,778679217
203284_s_at	HS2ST1	9,53199598	6,001417633
206718_at	LMO1	10,61146829	6,674247121
203283_s_at	HS2ST1	9,046275921	5,406649606
1552701_a_at	CARD16	5,645517013	3,337163282

## 11.8 Antibodies used in this study.

<i>Antibody (Clone)</i>	<i>Host</i>	<i>Use</i>	<i>Dilution</i>	<i>Producer</i>	<i>Catalog #</i>
<b>Annexin II (5/Annexin II)</b>	mouse	IHC	1:2000	BD Bioscience	610068
<b>Annexin II (C-10)</b>	mouse	IF <i>In vitro</i> neutralization <i>In vivo</i> neutralization	1:100 5-20µg/ml 2µg/egg	Santa Cruz Biotechnology	sc-28385
<b>β-actin (AC-74)</b>	mouse	WB	1:20000	Sigma-Aldrich	A5316
<b>CD133-PE (AC133/1)</b>	mouse	FC	1:25	Miltenyi Biotec	130-080-801
<b>GFAP</b>	rabbit	IF	1:1000	Dako	Z0334
<b>Ki67 (MIB-1)</b>	mouse	IF	1:100	Dako	M7240
<b>MAP2 (AP-20)</b>	mouse	IF	1:100	Sigma-Aldrich	M1406
<b>Nestin (10C2)</b>	mouse	IF	1:200	Millipore	MAB5326
<b>OSP</b>	rabbit	IF	1:200	Abcam	ab53041
<b>S100</b>	rabbit	IF	1:400	Dako	Z0311
<b>Sox2 (D6D9)</b>	rabbit	IF	1:200	Cell Signaling Technology	3579
<b>anti-mouse-Alexa594</b>	goat	IF	1:1000	Life Technologies	A11005
<b>anti-mouse-Alexa488</b>	goat	IF	1:1000	Life Technologies	A11001
<b>anti-rabbit-Alexa488</b>	goat	IF	1:1000	Life Technologies	A11008
<b>Anti-rabbit-Alexa594</b>	goat	IF	1:1000	Life Technologies	A11012
<b>anti-mouse-HRP</b>	goat	WB	1:50000	Perkin Elmer	NEF822001 EA

IHC: Immunohistochemistry; IF: immunofluorescence; WB: western blot; FC: flow cytometry.

## 11.9 Sequence of primers used in this study.

<i>Gene</i>	<i>Sequence (5'-3')</i>
ANXA2 forward	GGGGACGCGAGATAAAGGTCC
ANXA2 reverse	CGCTTTCTGGTAGTCGCCCT
ANXA2_CDS forward	ATGGGCCCGCCAGCTAGCG
ANXA2_CDS reverse	TCAGTCATCTCCACCACACAGGTAC
ANXA2_BamHI-5'	ACTGGGATCCATGGGCCCGCCAGCTAGCG
ANXA2_XhoI-3'	ACTGCTCGAGTCAGTCATCTCCACCACACAGGT AC
ADAM12 forward	CATCGGCATGGCCCCAATCA
ADAM12 reverse	GGCTGCACCAAGGGGATTGT
COL5A1 forward	CCCTGACAAGAAGTCCGAAGGG
COL5A1 reverse	GCAGCCGCAGGAAGGTCAT
DNAH9 forward	GGCCCGACCGGATGACCTAT
DNAH9 reverse	TCCACCCCTGGAGACAGGATG
FBN1 forward	GCTGCGAGTGTCCCTTTGGT
FBN1 reverse	GGGCTCAAATCCCTCCTCGC
HMMR forward	GGAGTGCCAGTCACCTTCAGT
HMMR reverse	ACATCATAAGCACCTGGAGATGG
PLAT forward	GCCCGATTGAGAAGAGGAGCC
PLAT reverse	ACTGTGCCCTGCCACTGTTG
SDK2 forward	CCGTCAACGACGTGGGGAAA
SDK2 reverse	ACTGGTTGGTTCGACCGCTG
SEMA5A forward	CCCAGGCGCTGGATGACTG
SEMA5A reverse	GTGTGGAAAGTGCCAAGGAGAGAG
COCH forward	AAGGGAGAGCCCCAACAAGAAC
COCH reverse	AGGTCATCCAGAGGTGCCCAA
MYO1B forward	GGGTGGAAATGCCGCACACA
MYO1B reverse	CGAGCCTTCCAACCCCGGATA
MYL5 forward	GTACCGACGCGAGGAGACC
MYL5 reverse	CGATGGAGGCCGAACCTGGAACA
CCNA2 forward	CGTGAAGATGCCCTGGCTTTTA
CCNA2 reverse	TGGTACTTCATTAACACTCACTGGC
MKI67 forward	GCCTGCTCGACCCTACAGAG
MKI67 reverse	ACTGCGGTTGCTCCTTCACTG
CDCA3 forward	GGACTCAGATCCCCGCTCTC
CDCA3 reverse	GGTACCCAGAGGCAAGTCCAA
CDK1 forward	AAGCCGGGATCTACCATACCC
CDK1 reverse	GCAGTACTAGGAACCCCTTCTCT
KIF14 forward	CCTCTGCAGGAAAAGACCCCT
KIF14 reverse	CGTGTGAGGGTGTTCACAGTT
KIF20A forward	GAACGAACGCAGCGCGTAAT
KIF20A reverse	GCCTAGGTCCGAAGACGTGC
GUSB forward	GAAAATACGTGGTTGGAGAGCTCATT
GUSB reverse	CCGAGTGAAGATCCCCTTTTAA

## 12. ABBREVIATIONS USED IN THE TEXT

5-ALA: 5-aminolevulinic acid

ANXA2: annexin 2A

BBB: blood brain barrier

BCNU: 1,3-bis[2-chloroethyl]-1-nitrosourea

bFGF: basic fibroblast growth factor

BME: basal membrane extract

BV: bevacizumab

CAM: chick embryo chorioallantoic membrane

CNS: central nervous system

CSCs: cancer stem cells

DAB: 3,3'-diaminobenzidine

DAPI: 4',6-diamidino-2-phenylindole

Down: down-regulated

DSS: disease-specific survival

ECM: extracellular matrix

ECs: endothelial cells

EGF: epidermal growth factor

EGFP: enhanced green fluorescent protein

EGFR: epidermal growth factor receptor

EMT: epithelial to mesenchymal transition

FAs: focal adhesions

FFPE: formalin-fixed and paraffin embedded

FITC: fluorescein isothiocyanate

GBM: glioblastoma multiforme

GEO: gene expression omnibus

GFAP: glial fibrillary acidic protein

GO: gene ontology

GSCs: glioma stem cells

GSEA: gene set enrichment analysis

Hi: high

Hif-1 $\alpha$ : hypoxia-inducible factor 1, alpha subunit  
IHC: immunohistochemistry  
IFDR: local false discovery rate  
Lo: low  
MET: mesenchymal to epithelial transition  
MGMT: O(6)-methylguanine-DNA methyltransferase  
miRNAs: micro RNAs  
MMPs: matrix metalloproteinases  
MR: maximal resection  
MRI: magnetic resonance imaging  
mRNAs: messenger RNAs  
MTT: 3-(4,5-dimethylthiazol-2-yl)-2,5-diphenyltetrazolium bromide  
NES: nuclear export signal  
OS: overall survival  
PFS: progression free survival  
PVDF: polyvinylidene difluoride immobilon-p membrane  
RFS: relapse-free survival  
RT: radiation therapy  
siNEG: non targeting siRNA  
siRNA: small interfering RNA  
TGCA: the cancer genome atlas  
TMZ: temozolomide  
tPA: plasminogen activator  
US: united states  
UTRs: untranslated regions  
VEGF: vascular endothelial growth factor  
WB: western blot  
WHO: world health organization